



HAL
open science

Efficacité et durabilité des restrictions à grande échelle contre la pandémie de COVID-19 en France en 2020-2021

Chiara Sabbatini

► **To cite this version:**

Chiara Sabbatini. Efficacité et durabilité des restrictions à grande échelle contre la pandémie de COVID-19 en France en 2020-2021. Médecine humaine et pathologie. Sorbonne Université, 2023. Français. NNT : 2023SORUS533 . tel-04529785

HAL Id: tel-04529785

<https://theses.hal.science/tel-04529785>

Submitted on 2 Apr 2024

HAL is a multi-disciplinary open access archive for the deposit and dissemination of scientific research documents, whether they are published or not. The documents may come from teaching and research institutions in France or abroad, or from public or private research centers.

L'archive ouverte pluridisciplinaire **HAL**, est destinée au dépôt et à la diffusion de documents scientifiques de niveau recherche, publiés ou non, émanant des établissements d'enseignement et de recherche français ou étrangers, des laboratoires publics ou privés.

Sorbonne Université

École Doctorale Pierre Louis de Santé Publique:
Épidémiologie et Sciences de l'Information Biomédicale

Équipe SUMO, IPLESP UMRS-1136, INSERM

Efficacité et durabilité des restrictions à grande échelle contre la pandémie de COVID-19 en France en 2020-2021

par

Chiara Elisa SABBATINI

Thèse de doctorat de Biostatistique et Biomathématique

dirigée par

Vittoria COLIZZA

Présentée et soutenue publiquement le 18 Décembre 2023

Devant un jury composé de :

Leo FERRES

Birgitte FREIESLEBEN DE BLASIO

Nicola PERRA

Vittoria COLIZZA

Rapporteur

Rapporteure

Examineur

Directrice de thèse

Ph.D. Thesis

**Effectiveness and sustainability of large-scale
restrictions against the COVID-19 pandemic in
France in 2020-2021**

Chiara Elisa Sabbatini

18/12/2023

Fortunately for me, I know well enough what I want, and am basically utterly indifferent to the criticism that I work to hurriedly. In answer to that, I have done some things even more hurriedly theses last few days.

– Vincent Van Gogh

Effacité et durabilité des restrictions à grande échelle contre la pandémie de COVID-19 en France en 2020-2021

Chiara Elisa Sabbatini

Résumé de la these en français

Introduction

L'année 2020 restera gravée dans notre mémoire comme l'année où le monde entier a été confronté à une pandémie mondiale sans précédent. La COVID-19, causée par le virus SARS-CoV-2, est apparue pour la première fois en Chine en décembre 2019 et s'est rapidement propagée dans le monde entier [1]. L'Organisation mondiale de la santé l'a déclarée pandémie en mars 2020 [1]. La nouveauté de l'agent pathogène, associée aux incertitudes initiales concernant ses modes de transmissions, sa pathogénicité et ses conséquences graves, a posé un défi sans précédent aux systèmes de santé publique du monde entier, entraînant une crise sanitaire sans précédent. En conséquence, des mesures strictes telles que des formes de distanciation sociale, notamment des confinements et des couvre-feux, ont été rapidement mises en place pour contenir la propagation du virus [2]. Avant la disponibilité généralisée des vaccins, la mise en œuvre de restrictions à grande échelle est devenue une stratégie cruciale utilisée par les gouvernements pour atténuer l'impact de l'épidémie sur la santé publique et le bien-être de la société. À la suite de la deuxième vague (fin année 2021), l'Europe a connu des changements significatifs avec le lancement de campagnes de vaccination et l'émergence de nouveaux variants. Bien que la vaccination soit avérée très efficace pour protéger contre les infections et réduire les conséquences graves [3, 4], la mise en œuvre d'interventions non pharmacologiques a joué un rôle vital dans le contrôle de la propagation du virus jusqu'à ce que des niveaux élevés d'immunité de la population puissent être atteints [5].

Les modèles mathématiques ont été essentiels pour guider les politiques publiques en évaluant l'efficacité des mesures de distanciation sociale [6, 7]. Cependant, avant l'avènement de la science des données, le manque de données sur les interactions humaines limitait l'applicabilité pratique de ces modèles aux scénarios réels. La nature mondiale de la crise sanitaire de la COVID-19, associée à la collecte et au partage généralisé de données provenant de sources multiples, ainsi qu'à l'augmentation des ressources informatiques, a facilité l'utilisation de modèles mathématiques en temps réel pour informer la prise de décision basée sur les données. Cela s'est produit à une échelle sans précédent par rapport aux épidémies précédentes. Par conséquent, la communauté de la santé publique a de plus en plus reconnu l'importance de l'utilisation de la modélisation mathématique pour le contrôle des maladies, car elle est devenue un outil indispensable.

L'objectif de cette thèse est de réaliser une analyse approfondie de l'efficacité des restrictions à grande échelle mises en place pour lutter contre l'épidémie de COVID-19 en France. En nous appuyant sur diverses sources de données disponibles, notamment des données épidémiologiques et comportementales, cette recherche vise à fournir des informations précieuses sur les résultats et les implications de ces restrictions. Elle évalue l'impact des interventions non pharmacologiques sur le contrôle de la transmission du virus, l'allègement de la pression sur le système de

santé et l'évaluation des atteintes potentielles à la liberté individuelle. Cette thèse présente deux modèles mathématiques de la transmission de la maladie. Le premier modèle, désigné comme **modèle #1**, est un modèle compartimental structuré par âge utilisé pour évaluer la situation épidémique en temps réel et réaliser une analyse de scénarios tout au long de la pandémie. Le deuxième modèle discuté dans cette thèse, désigné comme **modèle #2**, est un modèle de métapopulation compartimental qui intègre la connectivité spatiale pour évaluer rétrospectivement l'efficacité des stratégies mises en œuvre et de certaines alternatives.

Epidémie de COVID-19 en France

En France, le premier cas de COVID-19 a été confirmé en Janvier 2020 [8]. Au cours des deux premières années de la pandémie de COVID-19, la majorité des pays ont mis en place différentes formes de restriction afin d'endiguer les vagues de COVID-19. En France, trois confinements nationales ont été appliquées au cours de cette période en réponse aux trois premières vagues : une première confinement strict en mars-mai 2020 (première vague) [9], une deuxième confinement modéré avec ouverture des écoles en octobre-décembre 2020 (deuxième vague)[10], et une troisième confinement léger autorisant plus de temps à l'extérieur en mars-mai 2021, avec un assouplissement progressif des restrictions s'achevant en juin (troisième vague, en raison du variant Alpha) [11]. Entre le deuxième et le troisième confinement, la population française a passé plusieurs mois sous couvre-feu nocturne (see **Figure**) [12]. Toutes les fermetures ont été appliquées à l'échelle nationale. Toutefois, avant les deuxième et troisième confinements, les autorités françaises ont temporairement opté pour des restrictions plus localisées au niveau départemental afin de cibler localement l'augmentation des taux de transmission.

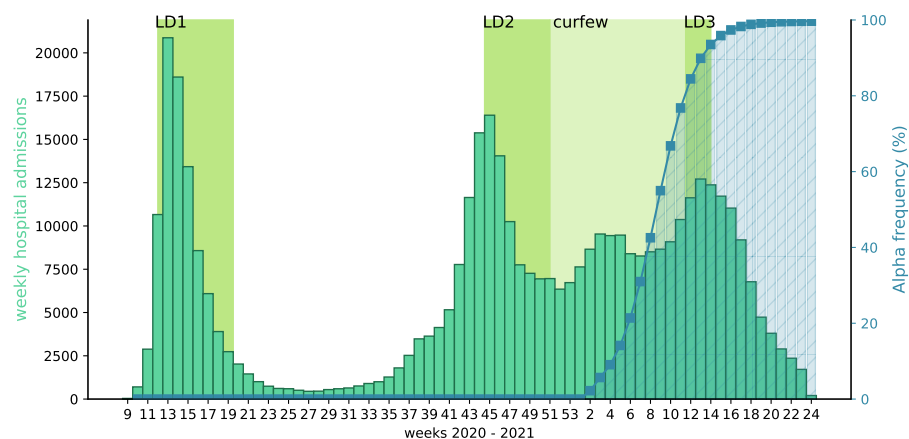


Figure. Pandémie de COVID-19 en France entre Mars 2020 et Juin 2021 Le panneau montre le nombre d'admissions hebdomadaires à l'hôpital (histogramme vert) et le pourcentage du variant Alpha au fil du temps (histogramme bleu, axe des ordonnées de droite). Les zones indiquées en vert font référence aux mesures de distanciation sociale : confinement pendant la première vague, confinement pendant la deuxième vague, confinement pendant la troisième vague (vert foncé), et couvre-feu entre les deux (vert clair).

Modélisation de la propagation du COVID-19

Pour simuler la propagation du virus SARS-CoV-2, j'ai utilisé deux approches différentes : la première est un modèle compartimental [13] basé sur l'âge (**modèle #1**), tandis que la seconde est un modèle de métapopulation (**modèle #2**) [14]. Les deux sont destinés à répondre à différentes questions.

Dans le **modèle #1**, j'ai divisé la population en quatre groupes d'âge : 0-10 ans, 11-18 ans, 19-64 ans et 65 ans et plus, afin de tenir compte des variations de gravité de la maladie et des contacts entre les différents groupes d'âge [15]. La matrice des contacts, qui régit les interactions entre les groupes d'âge, a été modélisée en tenant compte à la fois du stade d'infection et du temps, afin de simuler les changements de comportement liés à l'apparition des symptômes, à la perception du risque et aux mesures telles que la distanciation sociale [16, 17, 18]. De plus, le modèle a pris en compte le variant Alpha et les effets de la vaccination, en évaluant l'efficacité du vaccin contre l'infection, les symptômes graves et la transmission conditionnelle à l'infection.

Le **modèle #2**, était basé sur une structure de métapopulation à l'échelle régionale, en divisant la population suivantes les 12 régions de la France métropolitaine. Ce modèle a pris en compte la force quotidienne d'infection en tenant compte de différentes sources de transmission, notamment les résidents infectés qui ne se déplacent pas, les visiteurs infectés en provenance d'autres régions et les résidents qui reviennent après avoir été précédemment infectés dans d'autres régions [19]. Le modèle a utilisé un schéma compartimental similaire à SEIR (SEIHR), avec des sous-populations pour différents états de vaccination, et a intégré toutes les données disponibles, y compris celles sur la saisonnalité et la pénétration du variant Alpha, au niveau régional.

Les paramètres des modèles (à l'exception du taux de transmission) ont été obtenus à partir des données disponibles. Le taux de transmission a été estimé en calibrant les modèles sur les données d'admissions à l'hôpital.

Résultats et discussion

L'application de mesures restrictives à grande échelle au sein d'une population a un impact significatif sur la propagation d'une maladie [20, 21, 22, 23, 24, 25]. Dans cette thèse, deux nouveaux modèles ont été développés pour quantifier l'efficacité et la durabilité de certaines interventions, dans le but de fournir des stratégies d'évaluation applicables à différents contextes et scénarios.

L'analyse met en évidence le rôle crucial joué par la mise en place de restrictions à grande échelle, notamment les confinements et les couvre-feux, dans la maîtrise de la propagation de la COVID-19 en France. Ces mesures ont contribué de manière significative à réduire les taux d'infection et à soulager la pression sur les systèmes de santé. Cependant, elles n'ont pas été sans défis ni effets indésirables, tels que difficultés économiques, problèmes de santé mentale et une fatigue générale de la population.

Pour faire face aux défis actuels et futurs posés par les pandémies, il est essentiel d'adopter diverses approches et modèles [26, 27]. Le choix d'un cadre de modélisation doit être adapté aux questions spécifiques et aux données disponibles. Les études présentées dans cette thèse se sont principalement concentrées sur l'évaluation de l'efficacité des interventions à l'échelle de la population de régions spécifiques ou à l'échelle nationale.

Dans l'**article #1**, nous avons analysé l'efficacité de différentes mesures de confinement pour contrôler la propagation du COVID-19, en comparant plusieurs scénarios de confinement sévère et modéré, en utilisant la perte d'adhésion observée empiriquement. Nous avons confirmé que les confinements courts de haute intensité seraient plus efficaces pour contrôler l'épidémie que les confinements modérés, mais surtout: (i) nous avons montré que les interventions modérées seraient plus largement affectées par la perte d'adhésion, avec le

risque de compromettre le contrôle de l'épidémie si elles étaient maintenues pendant une longue période. (ii) Nous avons introduit un "indice de détresse" basé sur des données pour comparer l'impact des différentes interventions sur la qualité de vie de la population. (iii) Nous avons constaté que pour des valeurs intermédiaires de l'indice de détresse, les enfermements stricts plus courts (4 semaines) sont largement plus efficaces que les enfermements modérés plus longs (6 semaines). Le concept d'acceptabilité a souvent été considéré comme un argument potentiel contre la mise en œuvre d'interventions précoces et strictes [28, 29]. Cependant, les résultats de notre recherche remettent en question cette notion et suggèrent que le fait d'opter pour des interventions plus douces au lieu de politiques strictes peut avoir des conséquences négatives à long terme, en particulier lorsqu'elles sont prolongées dans le temps et que l'adhésion à ces mesures diminue.

De nombreuses études ont exploré les effets des interventions non pharmaceutiques dans la gestion de la pandémie de COVID-19 [5, 30, 31, 32, 33, 22, 20, 34], y compris les mesures locales dans des régions spécifiques. Cependant, ces études traitaient souvent les régions de manière indépendante, négligeant l'impact de la mobilité interrégionale sur la transmission de la maladie. Dans l'article #2, il a été constaté que les effets de débordement dus à la mobilité influençaient considérablement l'efficacité des interventions locales, entraînant des écarts dans les réductions estimées du nombre de reproduction pouvant aller jusqu'à 40%. Les principales conclusions sont : (i) le troisième confinement au printemps 2021 était tout aussi efficace que le deuxième confinement à l'automne 2020, malgré les différences entre les deux mandats. (ii) Le couvre-feu nocturne à partir de 18 heures était considérablement efficace lorsqu'il était associé à la fermeture du secteur de la gastronomie. Même s'il était maintenu longtemps, cette stratégie pourrait préserver l'activité d'un plus grand nombre de secteurs d'emploi. (iii) Des confinements répétés (au lieu du couvre-feu) pourraient réduire à la fois les impacts sur la santé et sociaux, mais cette stratégie doit être mise en œuvre de manière proactive, lorsque le nombre d'hospitalisations est encore faible.

Des questions importantes restent à explorer, telles que l'efficacité des interventions à différentes échelles spatiales, la gestion des autres variants du virus et la prise en compte de la fatigue de la population face aux mesures répétées.

Avec la crise de la pandémie derrière nous, nos découvertes offrent une compréhension exhaustive et plus précise des mesures de contrôle nécessaires à la phase à moyen terme d'une pandémie de virus respiratoire, de l'alerte initiale à la campagne de vaccination de masse. L'expérience spécifique de la France, où différentes interventions ont été mises en œuvre, alimente un éventail d'options ainsi que leur évaluation pour informer les plans de préparation à la pandémie contre les menaces futures.

Enfin, l'intégration de la modélisation dans la prise de décision politique devrait devenir une pratique courante pour mieux gérer les pandémies et autres crises.

Bibliographie

[1] WHO announces COVID-19 outbreak a pandemic, March 2020. Library Catalog: www.euro.who.int
Publisher: World Health Organization.

[2] Epicentre. COVID-19 Epi Dashboard. Library Catalog: reports.msf.net.

[3] Vaccine efficacy, effectiveness and protection.

[4] Ibrahim Mohammed, Areej Nauman, Pradipta Paul, Sanjith Ganesan, Kuan-Han Chen, Syed Muhammad Saad Jalil, Shahd H. Jaouni, Hussam Kawas, Wafa A. Khan, Ahamed Lazim Vattoth, Yasmeen Alavi Al-Hashimi, Ahmed Fares, Rached Zeghlache, and Dalia Zakaria. The efficacy and effectiveness of the COVID-19 vaccines in reducing infection, severity, hospitalization, and mortality: a systematic review. *Human Vaccines Immunotherapeutics*, 18(1):2027160.

- [5] Sam Moore, Edward M. Hill, Michael J. Tildesley, Louise Dyson, and Matt J. Keeling. Vaccination and non-pharmaceutical interventions for COVID-19: a mathematical modelling study. *The Lancet Infectious Diseases*, 21(6):793–802, June 2021. Publisher: Elsevier.
- [6] ANIRUDDHAADIGA,DEVDATDUBHASHI,BRYANLEWIS,MADHAVMARATHE,SRINIVASAN VENKATRAMANAN, and ANIL VULLIKANTI. MATHEMATICAL MODELS FOR COVID-19 PANDEMIC: A COMPARATIVE ANALYSIS. ArXiv, page arXiv:2009.10014v1, September 2020.
- [7] JasminaPanovska-Griffiths.CanmathematicalmodellingsolvethethecurrentCovid-19crisis? *BMC Public Health*, 20(1):551, April 2020.
- [8] Etienne Jacob. Coronavirus: trois premiers cas confirmés en France, deux d’entre eux vont bien, January 2020. Library Catalog: www.lefigaro.fr Section: Sciences Environnement.
- [9] Le Monde. « Nous sommes en guerre » : le verbatim du discours d’Emmanuel Macron. [Le Monde.fr](http://LeMonde.fr), March 2020.
- [10] LOI n ° 2020-1379 du 14 novembre 2020 autorisant la prorogation de l’état d’urgence sanitaire et portant diverses mesures de gestion de la crise sanitaire (1), November 2020.
- [11] Décret n° 2021-384 du 2 avril 2021 modifiant les décrets n° 2020-1262 du 16 octobre 2020 et n° 2020-1310 du 29 octobre 2020 prescrivant les mesures générales nécessaires pour faire face à l’épidémie de covid-19 dans le cadre de l’état d’urgence sanitaire - Légifrance.
- [12] Décret n° 2021-217 du 25 février 2021 modifiant les décrets n° 2020-1262 du 16 octobre 2020 et n° 2020-1310 du 29 octobre 2020 prescrivant les mesures générales nécessaires pour faire face à l’épidémie de covid-19 dans le cadre de l’état d’urgence sanitaire - Légifrance.
- [13] William Kermack and A.G. McKendrick. A contribution to the mathematical theory of epidemics | *Proceedings of the Royal Society of London. Series A, Containing Papers of a Mathematical and Physical Character*.
- [14] Vittoria Colizza, Alain Barrat, Marc Barthélemy, and Alessandro Vespignani. The role of the airline transportation network in the prediction and predictability of global epidemics. *Proceedings of the National Academy of Sciences*, 103(7):2015–2020, February 2006. Publisher: *Proceedings of the National Academy of Sciences*.
- [15] Guillaume Béraud, Sabine Kazmerczak, Philippe Beutels, Daniel Levy-Bruhl, Xavier Lenne, Nathalie Mielcarek, Yazdan Yazdanpanah, Pierre-Yves Boëlle, Niel Hens, and Benoit Dervaux. The French Connection: The First Large Population-Based Contact Survey in France Relevant for the Spread of Infectious Diseases. *PLOS ONE*, 10(7):e0133203, 2015. Publisher: *Public Library of Science*.
- [16] Ruiyun Li, Sen Pei, Bin Chen, Yimeng Song, Tao Zhang, Wan Yang, and Jeffrey Shaman. Substantial undocumented infection facilitates the rapid dissemination of novel coronavirus (SARS-CoV2). *Science*, 368(6490):489–493, March 2020. Publisher: *American Association for the Advancement of Science* Section: *Research Article*.
- [17] Nicholas G. Davies, Petra Klepac, Yang Liu, Kiesha Prem, Mark Jit, and Rosalind M. Eggo. Age-dependent effects in the transmission and control of COVID-19 epidemics. *Nature Medicine*, 26(8):1205–1211, June 2020. Publisher: *Nature Publishing Group*.
- [18] Kim Van Kerckhove, Niel Hens, W. John Edmunds, and Ken T. D. Eames. The impact of illness on social networks: implications for transmission and control of influenza. *American Journal of Epidemiology*, 178(11):1655–1662, December 2013.
- [19] Giulia Pullano. Human mobility and epidemics. phdthesis, Sorbonne Université, September 2021.
- [20] Laura Di Domenico, Giulia Pullano, Chiara E. Sabbatini, Pierre-Yves Boëlle, and Vittoria Colizza. Impact of lockdown on COVID-19 epidemic in île-de-France and possible exit strategies. *BMC Medicine*, 18(1):240, July 2020.

- [21] Giulia Pullano, Laura Di Domenico, Chiara E. Sabbatini, Eugenio Valdano, Clément Turbelin, Marion Debin, Caroline Guerrisi, Charly Kengne-Kuetche, Cécile Souty, Thomas Hanslik, Thierry Blanchon, Pierre-Yves Boëlle, Julie Figoni, SophieVaux, Christine Campèse, Sibylle Bernard-Stoecklin, and Vittoria Colizza. Underdetection of cases of COVID-19 in France threatens epidemic control. *Nature*, December 2020.
- [22] Laura Di Domenico, Chiara E. Sabbatini, Giulia Pullano, Daniel Lévy-Bruhl, and Vittoria Colizza. Impact of January 2021 curfew measures on SARS-CoV-2 B.1.1.7 circulation in France. *Eurosurveillance*, 26(15):2100272, April 2021. Publisher: European Centre for Disease Prevention and Control.
- [23] Seth Flaxman, Swapnil Mishra, Axel Gandy, H. Juliette T. Unwin, Thomas A. Mellan, Helen Coupland, Charles Whittaker, Harrison Zhu, Tresnia Berah, Jeffrey W. Eaton, Mélodie Monod, Azra C. Ghani, Christl A. Donnelly, Steven Riley, Michaela A. C. Vollmer, Neil M. Ferguson, Lucy C. Okell, and Samir Bhatt. Estimating the effects of non-pharmaceutical interventions on COVID-19 in Europe. *Nature*, 584(7820):257–261, August 2020. Number: 7820 Publisher: Nature Publishing Group.
- [24] Nicholas G. Davies, Adam J. Kucharski, Rosalind M. Eggo, Amy Gimma, W. John Edmunds, Thibaut Jombart, Kathleen O'Reilly, Akira Endo, Joel Hellewell, Emily S. Nightingale, Billy J. Quilty, Christopher I. Jarvis, Timothy W. Russell, Petra Klepac, Nikos I. Bosse, Sebastian Funk, Sam Abbott, Graham F. Medley, Hamish Gibbs, Carl A. B. Pearson, Stefan Flasche, Mark Jit, Samuel Clifford, Kiesha Prem, Charlie Diamond, Jon Emery, Arminder K. Deol, Simon R. Procter, Kevin van Zandvoort, Yueqian Fiona Sun, James D. Munday, Alicia Rosello, Megan Auzenbergs, Gwen Knight, Rein M. G. J. Houben, and Yang Liu. Effects of non-pharmaceutical interventions on COVID-19 cases, deaths, and demand for hospital services in the UK: a modelling study. *The Lancet Public Health*, 5(7):e375–e385, July 2020. Publisher: Elsevier.
- [25] Nikolaos Askitas, Konstantinos Tatsiramos, and Bertrand Verheyden. Estimating worldwide effects of non-pharmaceutical interventions on COVID-19 incidence and population mobility patterns using a multiple-event study. *Scientific Reports*, 11(1):1972, January 2021. Number: 1 Publisher: Nature Publishing Group.
- [26] Glenn Marion, Liza Hadley, Valerie Isham, Denis Mollison, Jasmina Panovska-Griffiths, Lorenzo Pellis, Gianpaolo Scalia Tomba, Francesca Scarabel, Ben Swallow, Pieter Trapman, and Daniel Villela. Modelling: Understanding pandemics and how to control them. *Epidemics*, 39:100588, June 2022.
- [27] Pascal Crépey, Harold Noël, and Samuel Alizon. Challenges for mathematical epidemiological modelling. *Anaesthesia, Critical Care Pain Medicine*, 41(2):101053, April 2022.
- [28] Jonathan A. Polonsky, Sangeeta Bhatia, Keith Fraser, Arran Hamlet, Janetta Skarp, Isaac J. Stopard, Stéphane Hugonnet, Laurent Kaiser, Christian Lengeler, Karl Blanchet, and Paul Spiegel. Feasibility, acceptability, and effectiveness of non-pharmaceutical interventions against infectious diseases among crisis-affected populations: a scoping review. *Infectious Diseases of Poverty*, 11(1):14, January 2022.
- [29] Marlena Klaic, Suzanne Kapp, Peter Hudson, Wendy Chapman, Linda Denehy, David Story, and Jill J. Francis. Implementability of healthcare interventions: an overview of reviews and development of a conceptual framework. *Implementation Science : IS*, 17:10, January 2022.
- [30] Jonathan Stokes, Alex James Turner, Laura Anselmi, Marcello Morciano, and Thomas Hone. The relative effects of non-pharmaceutical interventions on wave one Covid-19 mortality: natural experiment in 130 countries. *BMC Public Health*, 22(1):1113, June 2022.
- [31] Francisco Pozo-Martin, HeideWeishaar, Florin Cristea, Johanna Hanefeld, Thurid Bahr, Lars Schaade, and Charbel El Bcheraoui. The impact of non-pharmaceutical interventions

on COVID-19 epidemic growth in the 37 OECD member states. *European Journal of Epidemiology*, 36(6):629–640, 2021.

[32] Yang Liu, Christian Morgenstern, James Kelly, Rachel Lowe, James Munday, C. Julian Villabona-Arenas, Hamish Gibbs, Carl A. B. Pearson, Kiesha Prem, Quentin J. Leclerc, Sophie R. Meakin, W. John Edmunds, Christopher I. Jarvis, Amy Gimma, Sebastian Funk, Matthew Quaife, Timothy W. Russell, Jon C. Emory, Sam Abbott, Joel Hellewell, Damien C. Tully, Rein M. G. J. Houben, Kathleen O'Reilly, Georgia R. Gore-Langton, Adam J. Kucharski, Megan Auzenberg, Billy J. Quilty, Thibaut Jombart, Alicia Rosello, Oliver Brady, Katherine E. Atkins, Kevin van Zandvoort, James W. Rudge, Akira Endo, Kaja Abbas, Fiona Yueqian Sun, Simon R. Procter, Samuel Clifford, Anna M. Foss, Nicholas G. Davies, Yung-Wai Desmond Chan, Charlie Diamond, Rosanna C. Barnard, Rosalind M. Eggo, Arminder K. Deol, Emily S. Nightingale, David Simons, Katharine Sherratt, Graham Medley, Stéphane Hué, Gwenan M. Knight, Stefan Flasche, Nikos I. Bosse, Petra Klepac, Mark Jit, and CMMID COVID-19 Working Group. The impact of non-pharmaceutical interventions on SARS-CoV-2 transmission across 130 countries and territories. *BMC Medicine*, 19(1):40, February 2021.

[33] Paul R Hunter, Felipe J Colón-González, Julii Brainard, and Steven Rushton. Impact of nonpharmaceutical interventions against COVID-19 in Europe in 2020: a quasi-experimental non-equivalent group and time series design study. *Eurosurveillance*, 26(28):2001401, July 2021.

[34] Impact of non-pharmaceutical interventions, weather, vaccination, and variants on COVID-19 transmission across departments in France | *BMC Infectious Diseases* | Full Text.

Abstract

After one year of COVID-19 mitigation, in the spring of 2021, European countries faced sustained viral circulation of the Alpha variant. As vaccination campaigns advanced, the challenge persisted: finding a balance between the effectiveness of long-lasting interventions and their impact on quality of life. This thesis combines insights drawn from two studies conducted in France, with the aim of evaluating the efficacy and sustainability of the interventions employed between 2020 and 2021, while also proposing more sustainable alternatives preserving their effectiveness.

We first employed an age-structured compartmental model to assess the real-time epidemic situation and conducted scenario analyses. Optimal scenarios were identified by the integration of intervention efficacy and a data-driven index accounting for the intensity and duration of social distancing measures. Our findings indicate that shorter and strict lockdowns tend to be considerably more effective than prolonged and moderate ones, all while maintaining a similar level of public discomfort and individual freedoms.

Subsequently, we employed a regionally-based metapopulation model to retrospectively evaluate the effectiveness of the implemented strategies and potential alternatives, taking into account the interconnectivity between regions in France. The results revealed that the spatial interplay between regions significantly influenced the outcomes of nationwide interventions, particularly in regions characterized by high mobility rates. Moreover, our analysis showed that implementing stop-and-go lockdowns early enough, instead of a prolonged curfew period, could have substantially reduced both the healthcare and societal burdens.

Our results contribute to characterize the success and failures of implemented strategies, highlighting the complexity of balancing effectiveness and sustainability. These findings also highlight the importance of considering geographical connectivity in the implementation and evaluation of public health policies. Results can inform policymakers and health authorities in designing targeted interventions, thus enhancing the overall effectiveness of management strategies.

Resumé

Après un an de lutte contre la COVID-19, au printemps 2021, les pays européens ont dû faire face à une circulation virale soutenue avec le variant Alpha. Alors que les campagnes de vaccination progressaient, le défi persistait: trouver un équilibre entre l'efficacité des mesures à long terme et leur impact sur la qualité de vie. Cette thèse combine les enseignements de deux études menées en France, dans le but d'évaluer l'efficacité et la durabilité des interventions mises en œuvre entre 2020 et 2021, tout en proposant des alternatives plus durables préservant leur efficacité.

Dans un premier temps, nous avons utilisé un modèle compartimental structuré par âge pour évaluer la situation épidémique en temps réel et réalisé des analyses de scénarios. Les scénarios optimaux ont été identifiés en intégrant l'efficacité des interventions à un indice basé sur les données tenant compte de l'intensité et de la durée des mesures de distanciation sociale. Nos résultats indiquent que les confinements courts et stricts sont nettement plus efficaces que les confinements prolongés et modérés, tout en maintenant un niveau similaire d'inconfort public et de libertés individuelles.

Par la suite, nous avons utilisé un modèle de métapopulation basé sur les régions pour évaluer rétrospectivement l'efficacité des stratégies mises en œuvre et des alternatives potentielles, en tenant compte de l'interconnexion entre les régions françaises. Les résultats ont révélé que l'interaction spatiale entre les régions influençait significativement les effets des interventions nationales, en particulier dans les régions caractérisées par des taux de mobilité élevés. De plus, notre analyse a montré que la mise en place de confinements intermittents, au lieu d'une période de couvre-feu prolongée, aurait pu réduire considérablement à la fois la charge sanitaire et sociétale.

Nos résultats contribuent à caractériser le succès et les échecs des stratégies mises en œuvre, mettant en évidence la complexité de trouver un équilibre entre l'efficacité et la durabilité. Ces conclusions soulignent également l'importance de prendre en compte la connectivité géographique dans la mise en œuvre et l'évaluation des politiques de santé publique. Ces résultats peuvent informer les autorités sanitaires dans la conception d'interventions ciblées, renforçant ainsi l'efficacité globale des stratégies de gestion.

Contents

Contents	xix
1 Introduction	1
2 COVID-19 epidemic in France	5
2.1 Timeline and type of interventions	5
2.2 Mathematical modeling for outbreak response	7
2.3 Model parametrization and validation	9
2.4 Challenges	12
3 Epidemic models for COVID-19	15
3.1 Age structured compartmental model	15
3.1.1 Parametrization of contact matrices and adaptive behavior	17
3.1.2 Modeling two-strains	19
3.1.3 Modeling vaccination	20
3.1.4 Calibration, validation and reproductive numbers	21
3.1.5 Behavioral indicators, counterfactual scenarios	22
3.2 Metapopulation model	23
3.2.1 Mobility	24
3.2.2 Effective modeling of variants and seasonality	25
3.2.3 Inference framework and validation	26
3.2.4 Behavioral indicators, counterfactual scenarios	27
4 Can we strike a balance between the effectiveness and sustainability of interventions?	29
4.1 Introduction	29
4.2 Article #1: Adherence and sustainability of interventions informing optimal control against the COVID-19 pandemic	30
4.3 Discussion	46
5 Evaluating the effectiveness of COVID-19 interventions: a spatial perspective	49
5.1 Introduction	49
5.2 Article #2: The impact of spatial connectivity on NPIs effectiveness	50
5.3 Discussion	76
6 Conclusions and perspectives	79
 SUPPLEMENTARY MATERIALS	 83
 Bibliography	 135
 ACKNOWLEDGEMENTS	 149

The year 2020 will remain etched in our memory as the year when the entire world faced an unprecedented global pandemic. COVID-19, caused by the SARS-CoV-2 virus, first appeared in China in December 2019 and quickly spread around the globe [1]. The World Health Organization declared it a pandemic in March 2020 [1]. The novelty of the pathogen, coupled with initial uncertainties regarding its modes of transmission, pathogenicity, and severe outcomes, posed an unprecedented challenge to public health systems worldwide, leading to an overwhelming health crisis. As a result, stringent measures such as strict forms of social distancing, including lockdowns and curfews, were swiftly implemented to contain the virus's spread [2]. In France, the government announced the first nationwide lockdown starting March 17, 2020 [3].

Similar to many other countries, France was ill-prepared when the pandemic struck, experiencing shortages of masks and tests [4]. Additionally, numerous public hospitals were on strike [4]. Prior to the widespread availability of vaccines, implementing large-scale restrictions became a crucial strategy employed by governments to mitigate the epidemic's impact on public health and societal well-being. As the year 2021 began, following the second wave, Europe witnessed significant changes as vaccination campaigns were initiated simultaneously with the emergence of new variants. While vaccination has proven highly effective in protecting from infections and in reducing severe outcomes [5, 6], the implementation of non-pharmaceutical interventions (NPIs) played a vital role in controlling the spread of the virus until high levels of population immunity could be achieved [7].

Mathematical models have played a pivotal role in addressing the crisis in this challenging landscape, serving as valuable tools to inform public policies [8, 9]. They have played a central role in estimating the effectiveness of various social distancing measures.

Epidemiological models have been employed since their introduction in 1927 [10], operating under the assumption that the transmission and progression of diseases can be explained by a relatively simple set of rules adaptable to different pathogens. However, until the advent of data science, the lack of data on human interactions limited the practical applicability of these models to real-world scenarios. The global nature of the COVID-19 health crisis, along with the widespread collection and sharing of data from multiple sources, combined with increased computational resources, has facilitated the use of real-time mathematical models to inform data-driven decision-making on an unprecedented scale compared to previous epidemics. Consequently, the public health community has increasingly recognized the importance of employing mathematical modeling for disease control, as it has become an indispensable tool in addressing this problem [8, 11].

This dissertation aims to conduct a comprehensive analysis of the effectiveness of large-scale restrictions implemented against the COVID-19 outbreak in France. Our assessment encompassed both the real-time efficacy of interventions and the potential consequences of alternative governmental decisions. Throughout the pandemic timeline, we employed different models that we developed. Drawing on various

available data sources, including epidemiological and behavioral data, this research seeks to provide valuable insights into the outcomes and implications of these restrictions. It evaluates the impact of NPIs in curbing virus transmission, alleviating pressure on the healthcare system, and assessing potential infringements on personal freedom.

This thesis introduces two mathematical models of disease transmission. The first model presented, referred to as **model #1**, is an age-structured compartmental model employed to assess the real-time epidemic situation and perform scenario analysis throughout the pandemic. The second model discussed in this thesis, referred to as **model #2**, is a compartmental metapopulation model that incorporates spatial connectivity to retrospectively evaluate the effectiveness of implemented or alternative strategies. The thesis is organized as follows. **Chapter 2** provides an overview of the management of the COVID-19 pandemic in France, outlining the research context and the challenges encountered during the parameterization of the models. **Chapter 3** details the mathematical framework used to construct the COVID-19 transmission models.

Chapter 4 (article #1, model #1) focuses on the modeling work conducted immediately after the emergence of the Alpha variant. It identifies optimal control strategies against the third wave by considering effectiveness, sustainability, and adherence to social distancing interventions through a data-driven stress index. **Chapter 5 (article #2, model #2)** presents a study evaluating France's response to COVID-19 accounting for the spatial connectivity of time-varying inter-regional mobility. In the list below I also provide a list of additional articles on COVID-19 pandemic that I co-authored, and which are related to the works presented in this thesis. The last chapter of this thesis (**Chapter 6**) contains a summary of the results and a discussion of their reliability, assumptions, limitations, as well as the potential future research directions. The models were designed in Python and C++, while data analysis, pre-post data processing and graphing were performed in Python.

Research articles published as first author contained in this thesis

Laura Di Domenico*, **Chiara E. Sabbatini***, Pierre-Yves Boëlle et al.
Adherence and sustainability of interventions informing optimal control against the COVID-19 pandemic.
 Communications Medicine, 1 (1), 57, 2021.
 Cited in this thesis as **article #1** [12]. (*co-first)

Research articles submitted as first author contained in this thesis

Chiara E. Sabbatini, Giulia Pullano, Laura Di Domenico et al.
The impact of spatial connectivity on NPIs effectiveness.
 BMC infectious diseases, under review.
 Cited in this thesis as **article #2**.

Research articles published and related to this thesis

Laura Di Domenico, Giulia Pullano, **Chiara E. Sabbatini**, Pierre-Yves Boëlle, Vittoria Colizza.

Impact of lockdown in Île-de-France and possible exit strategies.

BMC Medicine, 18, 240 (2020).

Cited in this thesis as [13].

Laura Di Domenico, Giulia Pullano, **Chiara E. Sabbatini**, Pierre-Yves Boëlle, Vittoria Colizza.

Modeling safe protocols for reopening schools during the COVID-19 pandemic in France.

Nature Communications, 12,1073 (2021).

Cited in this thesis as [14].

Laura Di Domenico*, Giulia Pullano*, **Chiara E. Sabbatini** et al.

Underdetection of COVID-19 cases in France threatens epidemic control.

Nature, 590, 134-139(2021).

Cited in this thesis as [15].

Laura Di Domenico, **Chiara E. Sabbatini**, Giulia Pullano, Daniel Lévy-Bruhl, Vittoria Colizza.

Impact of January 2021 curfew measures on SARS-CoV-2 B.1.1.7 scirculation in France.

Eurosurveillance, 26, 2100272 (2021).

Cited in this thesis as [16].

The COVID-19 pandemic presented an unparalleled global challenge, demanding swift and efficient actions to mitigate its impact. Within this chapter, I provide an exhaustive overview of the elements needed to assess the efficacy of these restrictive measures. We will delve into multiple aspects, including the timeline and nature of implemented interventions, the use of mathematical models in shaping epidemic responses, the parameterization and validation of these models, as well as the encountered challenges throughout this process. Our analysis covers the period from early 2020 to June 2021 and not the entirety of the pandemic.

2.1 Timeline and type of interventions

Having a clear timeline of events is crucial for understanding the actions that were undertaken. The COVID-19 pandemic caused by the SARS-CoV-2 virus originated in China in December 2019 and swiftly became a global threat. The World Health Organization (WHO) officially declared it a pandemic on March 11, 2020 [1]. Consequently, strict forms of social distancing measures were implemented in numerous countries, including France. In this context, assessments of intervention effectiveness offer important tools to facilitate the real-time sharing of insights regarding efficacy, ineffectiveness, potential strategies, and their suitability for specific groups.

On January 24, 2020, the first case of COVID-19 in both Europe and France was confirmed in Bordeaux, then, a cluster of cases was detected in Haute Savoie on February 8, 2020 [17]. As the epidemic rose in the country, the French government ordered a national lockdown on March 17, 2020 [18]. The aim of these measures was to increase social distancing between individuals and break the chains of transmission to prevent the healthcare system from being overwhelmed. As the pandemic unfolded, various European countries responded to the crisis by enacting their own strategies and measures. Each country tailored its approach based on its specific circumstances, healthcare systems, and socio-economic factors. For instance, Sweden adopted a milder approach with a focus on voluntary measures [19], while countries like Austria and Italy implemented testing strategies coupled with strict lockdown measures [20].

Lockdowns in France required people to stay at home except for essential reasons such as buying food or seeking medical attention. All non-essential businesses, including restaurants and cafes, were closed, and public gatherings were prohibited. Schools and universities were also closed. After eight weeks of lockdown, as rates of infection started to fall, the French government exited lockdown on May 11, 2020 [21].

Restrictive measures were gradually relaxed [15]. From May 2020, testing capabilities (Test Treat Isolate (TTI)) were progressively increased, enabling the implementation of a strategy based on identifying and isolating infected individuals and tracing their contacts. However, due to the limited level of immunity acquired by the population during the first wave and following the easing of measures, an increase in cases and hospitalizations was observed by the end of summer 2020 [15]. As a result, in September 2020 [22], targeted restrictions were implemented in areas with a high

incidence of the virus, such as closing bars and restaurants and banning gatherings of more than 10 people. On October 17, 2020, night-time curfew measures were enforced in several areas with degrading indicators. Due to the rapid surge in the number of infections, a second national lockdown was put in place starting October 30, 2020 [23]. The restrictions imposed were less stringent compared with the first national lockdown in the spring 2020 (**Figure 2.1**, stringency index [24], presented in **Chapter 3.1.5**), as schools and a larger number of job sectors were allowed to remain open. Short trips were limited to a maximum radius of one kilometer from home. Bars, restaurants, gyms and other non-essential services were closed, and then reopened on November 28, 2020, while maintaining strict sanitary protocols and limiting the number of customers. The lockdown was lifted on December 15, 2020, with the application of a night-time curfew (8pm to 6am) [25].

Soon after the appearance of the Alpha variant in France, curfew hours were anticipated nationally between 6pm and 6am on January 16, 2021 [26]. Following the rise in cases due to the Alpha epidemic, on March 20, 2021 localized lockdowns were implemented in the regions of Île-de-France, Haute-de-France and other French departments. The lockdown was then extended to the whole country on April 3, 2021, with the closure of all non-essential activities [27].

Differently from the second lockdown, the third lockdown included mobility restrictions only for trips exceeding 10 km from the place of residence. The stringent stay-at-home mandates imposed during the other lockdowns turned into endorsing outdoor activities as a preventive measure against transmission in enclosed settings. This third nationwide lockdown ended on May 3, 2021. Then the government began to gradually ease other restrictions, including lifting the night-time curfew and allowing some businesses to reopen [28].

In June 2021, as vaccination rates increased and cases continued to decline, the government lifted most remaining restrictions, including the requirement to wear masks outdoors. All these measures are summarized in **Table 2.1**.

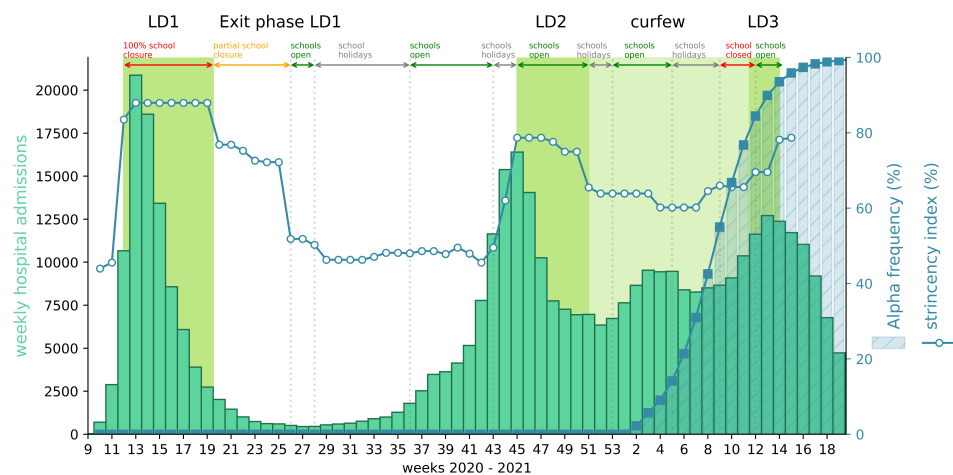


Figure 2.1: Timeline of the COVID-19 pandemic in France from March 2020 to June 2021. Left y-axis: weekly hospital admissions observed in metropolitan France. Right y-axis: frequency of Alpha variant in the country (%) (stucked plot) and stringency index [24] (%) (dotted plot). Shades green bands in the plot indicate periods of restrictions, the lockdowns (dark green) and the night-time curfew period (light green). Vertical dotted lines and horizontal arrows indicate different periods of school closure.

Table 1. Description of the restrictions applied in France between September 2020 and June 2021.

Period	Brief description of the applied NPIs	Abbreviation
March 17 – May 10	First nationwide lockdown. Closure of schools levels. Ban on non-work-related travel, authorized only essential purchases for grocery and health reasons.	LD1
October 17– October 29	Night-time curfew (9pm to 6am) in several French departments.	-
October 30 – December 14	Second nationwide lockdown. Primary and secondary schools remained open, subject to strict health protocols. Grocery shops and factories continued to operate, medical-related appointments remained possible. Bars, restaurants, gyms and other non-essential services were closed. Displacements were limited to a maximum radius of one kilometer from home.	LD2
December 15 – January 15	Night-time curfew in place between 8pm and 6am every day.	Curfew 8pm
January 16 – March 19	Night-time curfew hours extended to between 6pm and 6am every day.	Curfew 6pm pre-holidays / holidays / post-holidays*
March 20 – May 2	Third lockdown imposed on March 20 in 16 departments at high incidence (including the whole of Île-de-France, Hauts-de-France, one department of Normandy and one department of Provence-Alpes-Côte d'Azur). The lockdown was then extended nationwide on April 3. Schools remained closed for an extended duration, with the planned holiday closure being prolonged of an additional one or two weeks (for primary and middle/high schools, respectively). Non-essential activities were closed. A declaration was required for travel beyond 10 km of one's place of residence. Stay-at-home orders were replaced with recommendations to encourage spending time outdoors, aiming to reduce transmission in closed spaces.	LD3

*We splitted the period of curfew 6pm into three distinct phases: before school holidays, during school holidays, and after school holidays. These three phases vary by region because the two-week school breaks are applied at different times in France (see Table S2).

Table 2.1: Description of the restrictions applied in France between March 2020 and June 2021.

2.2 Mathematical modeling for outbreak response

Epidemic modeling involves a range of approaches that use mathematical, statistical, and computational tools to investigate the transmission of infectious diseases in host populations. Mathematical models are employed to capture the intricate dynamics of disease transmission and they offer a framework that allows to formalize assumptions regarding the processes we aim to comprehend [29, 30].

There are many reasons for employing modeling techniques. For example, the nonlinear nature of epidemic dynamics [31, 32]. Modeling also allows for the consideration of uncertainty related to all the parameters that describe the disease and its spread [33, 34, 35]. In addition, models offer valuable insights into various aspects of epidemic response, such as the estimation of pathogen spread parameters (through fitting procedures, mathematical models can help identify key parameters that govern pathogen spread, e.g. the transmission rate), exploring future scenarios or retrospectively assessing the efficacy of interventions. Furthermore, the models allow us to disentangle the temporal and spatial factors at play, thus enabling us to better understand the dynamics of spread.

While a single model may address multiple questions, it often requires significant adaptations to account for different temporal and spatial scales, as well as changes in the environment and human behaviors. This flexibility became evident during the COVID-19 pandemic, where different models were extensively used to tackle various policy issues [36, 37]. As the pandemic unfolded and new challenges arose, also the questions that needed to be answered evolved. Consequently, the models we developed tracked, from the pandemic onset, the inherent characteristics of the virus and adapted to simulate the ongoing social distancing interventions in place, following the timeline.

During the initial phase of the epidemic, models played a crucial role in real-time risk assessment. When the first cases of SARS-CoV-2 were reported in Wuhan, China, the extent of community spread remained uncertain. A modeling study [38] estimated that there were between 400 and 4,000 cases with symptoms appearing before January 12, 2020, indicating a much higher disease incidence compared to the officially reported 41 cases in Wuhan by January 16, 2020. Another study [39] focused on the detection rate and revealed that, by mid-February, only 4 out of 10 imported cases worldwide had been identified through surveillance systems. Even with travel restrictions and border controls in place, the disease rapidly spread to nearly every corner of the world within a matter of weeks [40]. Among European countries, France emerged as one particularly vulnerable to the importation of cases from China [41].

Shortly thereafter, as the virus had already spread extensively in France, authorities implemented a lockdown, prompting the need to swiftly evaluate the expected impact on disease transmission. It was also crucial to devise safe exit strategies to prevent a rapid resurgence once the lockdown measures were lifted. In this context, our compartmental model (**model #1**), described in **Chapter 3** was developed [13]. The model was fitted using hospital admission data to estimate key parameters such as the basic reproduction number (R_0) and the proportion of the population infected. Furthermore, the model was also parameterized with available mobility reduction data [42], to mimic the social distancing interventions by reconstructing the associated changes of contacts engaged.

Through simulations incorporating various durations of lockdown and gradually relaxed social interventions, potential strategies were identified to effectively control the epidemic while preventing healthcare system overload during the reopening phase. Our analysis assessed also the impact of reopening schools [14]. In addition, in another work [15], we integrated the transmission model with virological and participatory surveillance data to quantitatively assess spatial and temporal detection rates. This allowed us to evaluate the performance of the testing system, identify limitations, and propose practical improvements. As the situation progressed, the compartmental model was further extended to incorporate multiple strains and the progress of the vaccination campaign. A two-strain mathematical model was employed to assess the differential effects of night-time curfew measures on the Alpha variant and previous strains, providing projections for various scenarios involving social distancing and vaccination rates in anticipation of the third wave in March 2021 [16].

The first article discussed in this thesis, **article #1**, uses the two-strain compartmental model (**model #1**) to analyze optimal intervention strategies for controlling the third wave. By incorporating historical mobility data and model-derived estimates, we simulated interventions of varying intensities and durations, taking into account the potential decline in adherence over time. Additionally, a distress index was introduced to quantitatively compare the sustainability and effectiveness of different social distancing measures. In this work the focus was on assessing the effectiveness of interventions at the population level within a specific region (Île-de-France), and the spatial structure was not included in the model.

On the other hand, the second article presented in this thesis, **article #2**, aimed to retrospectively evaluate the effectiveness of adopted or alternative strategies, accounting also for connectivity between regions. To enable the evaluation of intervention scenarios at the regional level, a spatially structured metapopulation

model (**model #2**) was introduced. We underlined the importance of considering spatial connectivity between regions, through mobility, when evaluating intervention strategies. Additionally, the study analyzes alternative policy decisions alongside the evaluation of implemented interventions.

The selection of a modeling framework depends on the specific questions to be addressed and the available data [35]. In this thesis, the primary objectives revolved around evaluating the effectiveness of interventions at different scales. In the following sections I address the challenges, obstacles, and limitations we have encountered in using these models.

2.3 Model parametrization and validation

One of the essential requirements for all modeling processes is data [43, 44]. Mathematical models prove valuable as they enable the integration of different data sources. However, it is important to underline that the effectiveness of the modeling process is strongly tied to the accuracy, completeness, and timeliness of the data used [45]. In the context of an emerging disease, data availability is not only limited but also prone to biases due to its reliance on uncertain information [46].

In the following subsections, I will present several datasets that have been used. In the methods section (**Chapter 3**) I describe in detail how these data were integrated into our models (see also **Figure 2.2**).

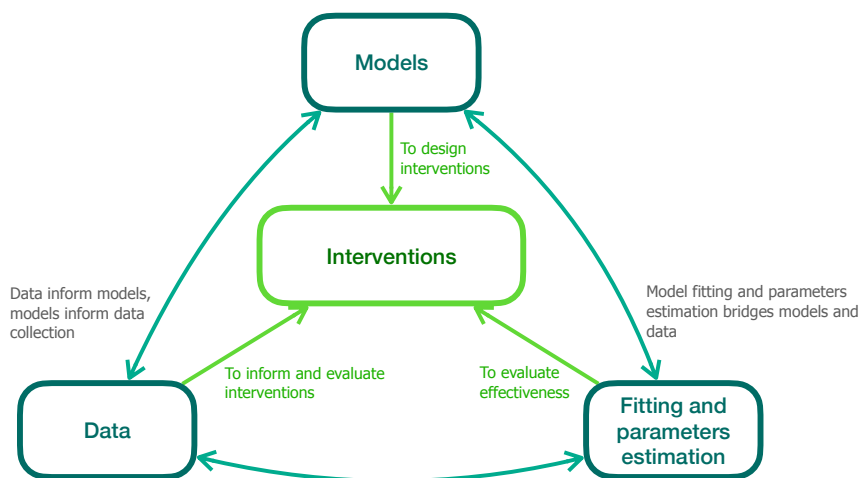


Figure 2.2: Relationships between interventions, models and data, inspired from ref. [46].

Hospital surveillance data

These data are in general less biased due to their reduced proneness to underreporting. Unlike the number of detected cases, the hospital data remains overall consistent in terms of detection and sampling. Consequently, they are extensively employed in modeling studies [47, 15, 13, 48, 49]. Nonetheless, they do present with the drawback of inherent delays, attributed to the latency, incubation, and infection stages of

the disease. All our models were fitted to daily hospitalization data to capture the trajectory of the epidemic over time. We used regional or national data obtained from the SIVIC database [50], which tracks daily hospital admissions of patients for COVID-19 in public or private hospitals. Originally established in 2016, the SIVIC database was modified to specifically monitor the number of admissions in both regular hospitals and intensive care units.

Seroprevalence data

In situations where pathogens involve a significant number of unreported infections (for instance, due to asymptomatic cases), relying solely on surveillance data may not yield accurate estimations of the actual incidence and prevalence. Seroprevalence data play a central role in validating model calibration. All of our models have been validated against these data. We compared the projections of our models for individuals testing positive for antibodies (AB+) with the independent serological surveys conducted in 2020-2021 (prior to the start of the vaccination campaign) [51, 52].

Biological and epidemiological data

Biological parameters are also important to parametrize a transmission model, such as the duration of the infectious period, the infectivity of symptomatic and asymptomatic cases, hospitalization probabilities, etc. During the initial stages of the epidemic, uncertainty surrounding these parameters highlights the need to perform numerous sensitivity analyses to explore how changes to these model parameters could affect future epidemic trajectories. For instance, in our work Ref. [13], assumptions and sensitivity analyses about the fraction of asymptomatic infections were necessary and were revised as more evidence became available.

Virological and genomic surveillance data

Genetic sequencing plays a crucial role in tracking the emergence of novel variants, providing deeper insights into the epidemic's dynamics and its propagation. Some SARS-CoV-2 variants disappeared immediately, while others, characterized by several key mutations, adapted well, such as the Alpha variant. Within our models, detailing the spatial and frequency distribution of variant dissemination is important, as is quantifying its advantages over historical strains. The Alpha variant, initially detected in the United Kingdom [53], quickly spread to all European countries [54] and a large-scale genome sequencing initiative was conducted in France on Jan. 7-8 (Flash #1 survey [55], the first in a series of surveys). Starting from week 6 of 2021, a new virological surveillance protocol was introduced to provide estimates of the weekly frequency of viruses carrying specific mutations. This protocol involved the use of second-line RT-PCR tests with specific primers that allowed to detect the key mutations associated with the variants of interest [55, 56]. We use data from these surveys to describe the spread of variants in France. To model the variant, we have also considered both its transmission advantage compared to historical variants and the heightened risk of hospitalization. Both of these parameters have been estimated from the literature (see **Chapter 3**).

Vaccination data and vaccine effectiveness

Vaccinations and treatments are key interventions for epidemic management. In France the vaccination campaign's progress was tracked through available data on the administration of vaccine doses [57], which provided information at both the regional level and by vaccination stage (first or second dose) and by age. We have considered the impact of vaccination on various aspects: effectiveness in preventing infection, reducing the risk of contracting the disease for vaccinated individuals compared to those unvaccinated; effectiveness in preventing severe symptoms, reducing the likelihood that vaccinated individuals develop severe symptoms in case of infection; and effectiveness in reducing transmission, decreasing the risk that vaccinated individuals who are infected transmit the disease to others compared to the unvaccinated.

Seasonality data

In our studies, we also took into account the influence of seasonal factors. A number of studies have suggested that SARS-CoV-2 transmission is seasonally varying, modulated by environmental variables and environmentally-mediated social behavior [58, 59, 60, 61]. We integrated seasonality by using the estimates provided in Ref.[62] based on daily data from the National Oceanic and Atmospheric Administration

Contact data

Another key ingredient in epidemic models is the interaction between individuals. These interactions are encoded through contact rates (which can be age-specific) that quantify the frequency and duration of contacts between individuals [63]. Our models incorporate data on social contacts, which have been adjusted over time to account for behavioral changes during the implementation of different NPIs. The pre-pandemic contact data (i.e., when no interventions are in place) are taken from a study conducted by Beraud in 2012 [63].

Mobility data

Human mobility assumes a twofold role within epidemic contexts. On one hand, mobility data can be integrated into a model to simulate the spatial propagation of the epidemic, as the act of moving from one place to another can either facilitate or impede the transmission of infections [64, 65]. On the other hand, it is notable that mobility restrictions have played a central role in responding to the COVID-19 epidemic [66, 67, 13] since social distancing measures primarily hinge on movement limitations. Mobility reductions can thus be incorporated into models to simulate the effects of social distancing interventions.

The mobility data used were extracted from two different data sources. One comes from mobile telephony data provided by Orange Business Service Flux Vision [67]. The data include origin-destination travel flows of mobile phone users. Origin-destination matrices were aggregated at the regional level to compute coupling probabilities between regions. The other was derived from the estimated presence

at workplaces obtained from Google Mobility Reports [68]. This dataset provides the relative change in the number of daily visitors in workplaces compared to a pre-pandemic baseline.

2.4 Challenges

The use of mathematical models to provide assessments of implemented interventions faces numerous obstacles, both in modeling the interventions themselves and in evaluating their effectiveness. These challenges include uncertainties in model parameters, the complexity of real-world epidemics, limitations in data availability, underlying assumptions, prediction complexities, and difficulties in effective communication. Moreover, this complexity is enhanced by the context of an ongoing epidemic, characterized by rapidly evolving situations and the need for constant updates in both model structures (such as with the emergence of new variants or the beginning of vaccination campaigns) and parameter values (for instance, in response to emerging evidence).

During lockdown periods, a specific challenge emerged concerning understanding the changes in social contacts adopted by the population. In our modeling works [13, 15], we wanted to simulate the implemented social distancing measures, using only pre-pandemic contact data, mobility reductions, and various behavioral indicators extracted from studies. Our approach involved reconstructing a synthetic contact matrix and adjusting the contacts made by different age classes based on the available data (see **Chapter 3**). After generating distinct contact matrices for various lockdown interventions, all of which are capable of capturing epidemic dynamics, it became crucial to assess whether the reduced effectiveness of one intervention compared to another (e.g., the first lockdown versus the second) was inherent to the intervention itself or resulted from a lack of adherence by the population. In **article #1**, we analyzed the effectiveness of various social distancing strategies, considering the level of adherence as well.

Not only can adherence to an intervention modify its effectiveness, but also numerous other factors that change over time. The reason mathematical models are used is because they allow distinguishing the factors that contribute to epidemic dynamics by explicitly modeling them. For example, by explicitly including factors such as seasonality, the presence of vaccines, and the existence of multiple viral strains, it becomes possible to quantify the impact of each of them in relation to the intervention, as done in **article #2** and described in **Chapter 3**.

Moreover, the definition of intervention effectiveness can be based on various epidemiological and health indicators. In both works presented in this thesis, we evaluated hospital-related indicators combined with indices that measure the restrictions on personal freedom induced by an intervention.

All these factors have contributed to the intricacy of effective communication with both public health authorities and the general public. The complexity of epidemic dynamics has posed challenges in communicating risks and facilitating informed decision-making. For instance, after the 2020 Christmas holidays, hospitalization rates began rising, resulting in a plateau by early February. Our multi-strain model (**model #1**) explained this plateau as the result of two opposing dynamics: a decline in viral circulation for the historical strains, and a continued rise of the Alpha variant.

The overall trajectory masked the true impact of the variant; the flattened dynamics indicated no immediate threat to authorities and the public. However, it was essential to communicate that reinforcing the existing NPIs would be necessary to avert a substantial resurgence in cases (this was addressed in a press conference with the Ministry of Health [69] on February 18, 2021).

Within this chapter, I present two of the mathematical models we used to simulate the transmission of COVID-19 (**model #1** and **model #2**). Both models simulate the early stages of the epidemic and then take into account the spread of the Alpha variant and the introduction of vaccines. I introduce the different behavioural data sources and how they were incorporated into the models. I present the inference frameworks used to fit them, and finally I introduce different behavioral indicators that have been created during the pandemic.

3.1 Age structured compartmental model

The first modelling approach we used, lied on compartmental model [70]. Let N , be the number of people within the population under consideration - we do not consider any demographic process (natural births, natural deaths, etc.) and we assume that the size of the population is large and does not change over time. We first categorize individuals into mutually exclusive groups, called compartments, based on disease status. A simple example is the so called *SEIR* model, where individuals are divided into:

- Susceptible (S): individuals that can contract the infection.
- Exposed (E): individuals who have been exposed to the disease but are not yet infectious.
- Infected (I): individuals who carry the disease that can transmit it to susceptible individuals.
- Recovered (R): individuals who have recovered from the disease and are no longer infectious.

The SEIR model consists of these four compartments. Alternative models can be created by adjusting the underlying assumptions or by adding supplementary compartments. To trace the evolution of the SEIR model over time, the variables $S(t)$, $E(t)$, $I(t)$, and $R(t)$ are employed to represent the number of susceptible, exposed, infected, and recovered individuals. To describe how these variables change with time, we can build a system of differential equations; where only transitions of the following type are allowed: $S \rightarrow E$: *exposure*, $E \rightarrow I$: *infection*, $I \rightarrow R$: *recovery*

Now, we have to establish the rates (probabilities per unit time) at which the transitions can occur:

- β : rate of infection per contact (called *transmission rate*).
- ϵ : rate at which an exposed person becomes infectious.
- μ : recovery rate.

The rate at which susceptible individuals (S) enter the infected compartment can be calculated as the product of the infection rate β and the number of contacts with infectious individuals.

At this stage, the *homogeneous mixing approximation* [71] is commonly used, meaning that individuals have an equal chance of interacting with each other. By calling C the number of contacts per person, a fraction of these contacts, $C \frac{I(t)}{N}$, will be established with infected individuals.

Ultimately, the rate for the $S \rightarrow E$ transition is defined as $\lambda(t) = \beta C \frac{I(t)}{N}$, which is also known as the *force of infection*.

Compartments in compartmental models can also be expanded to include spatially or age stratified conditions, where individuals are grouped by location or age. In the latter case, the population is divided into n age groups. This allows for more detailed analysis of disease transmission, as parameters such as susceptibility, transmissibility, and mixing patterns can vary by age. Each individual in compartment S_i , i.e. a susceptible individual of age i , experiences an age-specific force of infection λ_i , which is driven by the normalized per capita number of contacts $C_{i,j}$ [72] that an individual of age i has with an individual of age j , the likelihood of contacting every infectious individual from every age group j , and the transmissibility per contact β :

$$\lambda_i(t) = \beta \sum_j C_{ij}(t) \frac{I_j(t)}{N} \quad (3.1)$$

with $j \in \{1, 2, \dots, n\}$. I will explore more in detail the role of the entries C_{ij} of the matrix C in Sec. 3.1.1.

To model the outbreak of COVID-19 (in **article #1**), we used a compartmental model that follows the transmission dynamics outlined in **Figure 3.1a**. The model incorporates four age classes: young children (yc - [0, 10 y.o.]); adolescents (t - [11, 18 y.o.]); adults (a - [19, 64 y.o.]); and the elderly (s - [65, 100+ y.o.] or older. We based our model on demographic and age profile data **Figure 3.1b** and generalized the classic SEIR model.

It is worth noting that evidence suggested that individuals with coronavirus may be infectious even before manifesting symptoms [73]. Thus, we divided the incubation period into two stages: the first stage is the exposed (E) compartment, where individuals are infected but not yet infectious, and the second stage is the prodromic phase (I_p), during which individuals become capable of transmitting the virus. At the end of the prodromic phase, individuals may either remain asymptomatic (I_{as}) or develop symptoms.

For those who develop symptoms, our model considers different degrees of severity, ranging from paucisymptomatic individuals (I_{ps}) to individuals with mild (I_{ms}) or severe symptoms (I_{ss}). We have incorporated knowledge from various studies indicating that children have a lower propensity to show clinical symptoms and are either asymptomatic or paucisymptomatic once infected. Also, children in both classes (yc and t) are less susceptible than adults (**Table 3.1**). Hospitalization rates, were informed by data from SIVIC dataset [50]. The force of infection can then be rewritten:

$$\lambda_i(t) = s_i \beta \sum_k \sum_j r_\beta(k, j) C_{ij}(k, t) \frac{I_{k,j}(t)}{N} \quad (3.2)$$

Incubation period	5.2 days	[74]
Duration of prodromal phase	1.5 days, computed as the fraction of pre-symptomatic transmission events out of pre-symptomatic plus symptomatic transmission events.	[75]
Latency period	3.7 days (incubation period - prodromal phase)	-
Probability of being asymptomatic	0.4	[76]
If symptomatic, probability of being paucisymptomatic	1 for children, adolescents. 0.2 for adults, seniors	[45]
If symptomatic, probability of developing mild symptoms	0 for children, adolescents. 0.7704 for adults. 0.546 seniors	[45, 77, 47]
If symptomatic, probability of developing severe symptoms	0 for children, adolescents. 0.0296 for adults. 0.254 seniors	[77, 47]
Mean generation time	6.6 days	[78]
Infectious period	2.3 days (to match the generation time)	-
Relative infectiousness of I_p, I_{as}, I_{ps}	0.25 for children. 0.55 for adolescents, adults, seniors	[79]
Relative susceptibility	0.5 for children, adolescents. 1 for adults, seniors	[80]

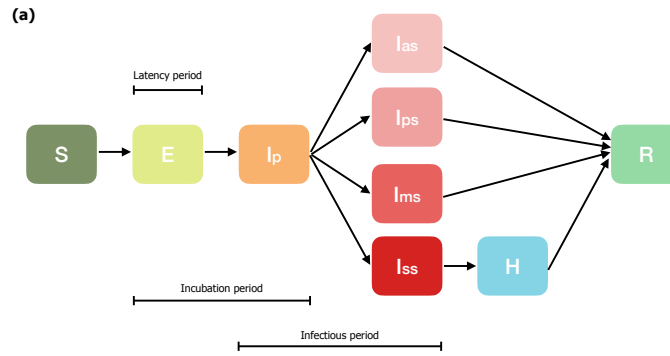
Table 3.1: Parameters, values, and sources used to define the COVID-19 compartmental model.

where k indicates the infectious compartments, i.e. $I_k = I_p, I_{as}, I_{ps}, I_{ms}, I_{ss}$, and the indexes i, j indicate the corresponding age group. The parameter $s_i \in [0, 1]$ represents the age-dependent susceptibility profile. The parameter $r_\beta \in [0, 1]$ modulates the infectiousness, according to both age and type of symptoms developed. All model parameters (except the transmission rate) were informed from evidence available (See Table 3.1).

3.1.1 Parametrization of contact matrices and adaptive behavior

The patterns of contact between individuals and groups play a crucial role in determining the risk of infection, and are therefore key components in modeling outcomes. In 2012, Beraud et al. [63] conducted a study in France to gather data on social contacts through surveys. Participants were randomly assigned a day of the week to document every person they came in contact with. Contacts were categorized as either skin-to-skin (physical contacts - e.g. a hug, $C^{physical}$), or no-skin-to-skin (nonphysical contacts - e.g. a conversation, $C^{non-physical}$). The setting where the contact occurred (home, work, school, leisure, transport, or other, $C_{location}$, with $location \in \{home, work, school, leisure, transport, other\}$) was specified for each contact. We have $C_{location} = C_{location}^{physical} + C_{location}^{non-physical}$; thus the baseline contact matrix is the result of different contributions (Figure 3.2). And it represents the mixing in a pre-pandemic scenario, without any NPI put in place.

Modifications were made to the baseline contact matrix to model changes in behavior. In simpler terms, our approach consisted in predicting how the baseline contact matrix modifies according to the adaptive behavior induced by NPIs in place. We modify contacts not only in specific settings but also for specific age groups, more precisely:



(b)

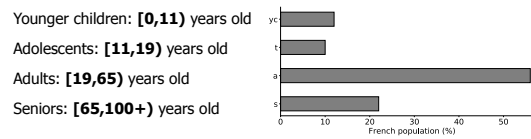


Figure 3.1: Compartmental scheme and demography. (a) S=Susceptible, E=Exposed, Ip=Infectious in the prodromic phase, Ias=Asymptomatic Infectious, Ips=Paucysymptomatic Infectious, Ims=Symptomatic Infectious with mild symptoms, Iss=Symptomatic Infectious with severe symptoms, H=severe case admitted to the hospital, R=Recovered. (b) Age profile in France corresponding to younger children, teenagers, adults, seniors.

- *School closure* : During full school closures, the contact matrix for schools was removed [81]. During partial attendance periods, the number of contacts at school for children and adolescents was reduced based on their attendance [82]. A modified school matrix was constructed with reduced elements, considering the proportion of students not attending school ($\hat{C}_{i,j,school} = C_{i,j,school} \cdot (1 - p_i) \cdot (1 - p_j)$ where p_i is the age-specific proportion of children/adolescents not attending school). This framework was used to parameterize contact matrices during the exit phase from the first lockdown (Figure 2.1) and simulate scenarios of school reopening [13, 14].
- *Remote working* : Contacts at work were adjusted based on the percentage of workers not going to work, using estimates from mobile phone location data provided by Google Mobility Reports [68]. These data capture changes in the number of people visiting workplaces compared to pre-pandemic levels. The work contact matrix was modified accordingly, considering the reduction percentage ($\hat{C}_{i,j,work} = C_{i,j,work} \cdot (1 - p)^2$, where $p_i = p$ is the percentage of workers not going to work. Data are not available by age-group). For contacts on transport, the percentage of workers not going to work was combined with the fraction of workers within each age group (considering that contacts on transport are not solely engaged in relation to work). Household contacts were increased proportionally [63].
- *Other activities* : To take into account the full (or partial) closure of non-essential activities, restrictions on mass gatherings, or similar measures, we decreased the number of contacts in the matrices "leisure" and "other" [68].
- *Avoidance of physical contacts* : After the first lockdown, public health authorities persisted in recommending preventive measures like avoiding close physical contact and maintaining social distancing. A survey conducted by Santé publique France gathered data on the adoption of these measures [83]. To incorporate this information into the contact matrices, we decreased the

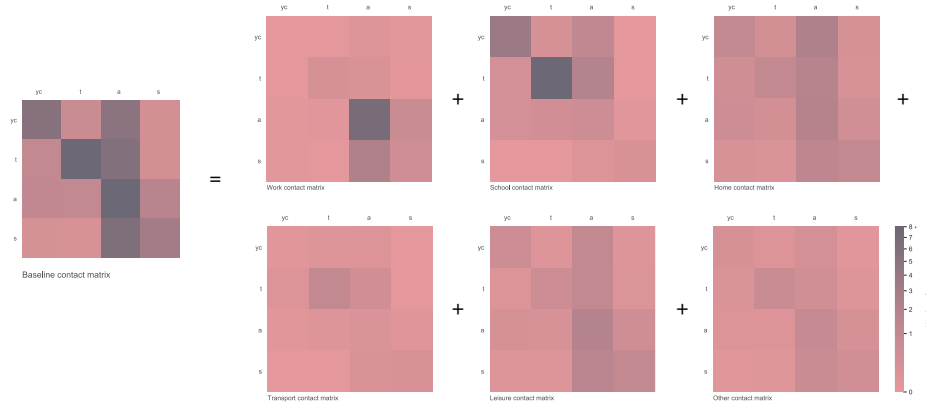


Figure 3.2: Contact matrix in the baseline scenario (no intervention), obtained as the sum of different "location matrices". Each "location matrix" accounts for physical and non-physical contacts.

number of physical contacts in all settings except households, taking into account the proportion of the population that reported avoiding physical contact ($\hat{C}_{location} = C_{location}^{non-physical} + (1 - k) \cdot C_{location}^{physical}$, being k the proportion of individuals adopting physical distancing).

- *Heightened risk aversion* : Additionally, we took into account the potential reduction in contacts among seniors by a specific percentage. This reduction could reflect the implementation of a targeted social distancing strategy for age groups at higher risk, or it could be a result of increased risk perception. In France, during the phase following the initial lockdown, data from the CoviPrev survey [83] showed evidence of this behavior. Therefore, when parameterizing the contact matrix, we considered a reduction in the elements associated with the senior age group.

Furthermore, the change in behaviour due to illness has been taken into account. We made the assumption that individuals with severe symptoms (I_{ss}) would self-isolate and voluntarily reduce their number of contacts by 75%, based on observations from the 2009 H1N1 pandemic [84]. Thus, the contact matrix associated with the infectious compartment I_{ss} in the force of infection was defined as 0.25 times the baseline contact matrix. To simulate the effects of the test, trace, and isolate (TTI) strategy [85], we did not explicitly create a separate compartment for it. Instead, we incorporated its impact by assuming that a certain percentage of infectious individuals would reduce their contacts by 90% and self-isolate upon testing positive. This reduction was applied directly to the contact matrix. To accommodate any delays in testing and self-isolation, individuals in their prodromic stage (I_p) were assumed to maintain their contacts as in the baseline.

3.1.2 Modeling two-strains

Genomic surveillance data [55] indicates that the Alpha variant of SARS-CoV-2 began circulating in France towards the end of 2020 and replaced previous strains by February 2021 [16]. A large-scale genome sequencing initiative called Flash surveys [56] was implemented in January, which showed that the Alpha variant was responsible for 3.3% of detected COVID-19 cases in France on January 8, 2021, with significant regional variations ranging from 0.2% to 6.9%. The Alpha variant has been

associated with increased transmissibility [55, 86, 87] and severity [86, 88] compared to the previous strain. With this information, we can construct a two-strain model to simulate the co-circulation of the Alpha variant and the previous strain. We can extend the compartmental model of **Figure 3.1a** to explicitly differentiate individuals infected with the Alpha variant. Practically we divide all the compartments of our model (except for of the susceptible one) in two: one that takes into account the infections due to the historical strains, the other considers those due to the Alpha variant. The force of infection is also split into two and take the form:

$$\lambda_i(t) = s_i \beta^{historical} \sum_k \sum_j r_\beta(k, j) C_{ij}(k, t) \frac{I_{k,j}^{historical}(t)}{N} + s_i \beta^{Alpha} \sum_k \sum_j r_\beta(k, j) C_{ij}(k, t) \frac{I_{k,j}^{Alpha}(t)}{N} \quad (3.3)$$

The transmission rate of the Alpha variant is expressed as $\beta^{Alpha} = z\beta^{historical}$, where $z = 1.59$ denotes the factor representing the Alpha transmission advantage [55, 86, 87]. Upon entering the $E^{historical}$ or E^{Alpha} compartments, individuals will undergo disease progression. Complete cross-immunity is assumed, meaning that those who were infected with one strain cannot be infected by the other strain. To account for the higher risk of hospitalization associated with the Alpha variant [86, 88], the probability of developing severe symptoms is increased (increased hospital risk equal to 1.64).

3.1.3 Modeling vaccination

Starting from December 27, 2020, a massive vaccination campaign started in France, prioritizing individuals at higher risk, including the elderly, vulnerable individuals, and healthcare workers. The campaign's progress was tracked through available data on the administration of vaccine doses, which provided information at both the regional level and by vaccination stage (first or second dose) and by age [57]. To incorporate the impact of vaccination, the compartmental model was stratified based on vaccination status, distinguishing between individuals who were unvaccinated, those who received one dose, and those who received two doses. The administration of first and second doses was modeled taking into account the reported vaccination rate [57]. We considered the impact of vaccination on the following factors: (i) effectiveness against infection, lowering the risk of contracting the disease for vaccinated individuals compared to those who were not vaccinated VE_{inf} ; (ii) effectiveness against severe symptoms, reducing the likelihood of vaccinated individuals developing severe symptoms that require hospitalization if they do become infected $VE_{hosp|inf}$; and (iii) effectiveness against transmission, decreasing the risk of vaccinated infected individuals transmitting the disease to others compared to unvaccinated individuals VE_{transm} .

Let VE_{hosp} be the efficacy against severe symptomatic infection, not conditional to infection, as the estimates reported in clinical trials. We can retrieve the corresponding conditional effects $VE_{hosp|sympt}$, knowing that:

$$1 - VE_{hosp} = (1 - VE_{inf}) \cdot (1 - VE_{hosp|inf})$$

The force of infection on S_i^w , susceptible individuals of age group i with vaccination status w is:

$$\lambda_i^w(t) = s_i(1 - VE_{inf}^w) \sum_v \sum_{strain} \sum_k \sum_j r_{\beta}(x, j) \beta_{strain}(1 - VE_{transm}^v) C_{ij}(k, t) \frac{I_{k,j}^{strain,v}(t)}{N}$$

where $strain = historical, Alpha$ indicates the strain of the infected compartment, and w, v represent the vaccination status of the susceptible and the infectious compartment respectively. The efficacy against hospitalization further reduces the probability of developing severe symptoms. It was assumed that the vaccines would become effective 14 days after injection.

3.1.4 Calibration, validation and reproductive numbers

The compartmental model used in this study is a stochastic model with discrete time steps, each representing one day. The epidemic was initialized with a group of infectious individuals in the adult compartment, and simulations were conducted for the entire period of 2020 - 2021. Multiple independent stochastic runs were performed so that results included median values and 95% probability ranges. The model was fitted against daily hospital admission data, obtained from the SIVIC database [50]. The model was fitted by estimating the transmission rate per contact (β) in subsequent time windows. Each time window corresponds to a specific phase of the pandemic, characterized by the NPI implemented.

In the pre-pandemic phase (January-March 2020), we estimated $\{\beta_{pre-LD}, t_0\}$, where β_{pre-LD} represents the transmission rate per contact and t_0 is the starting date of the simulation. For each subsequent phase (e.g. first lockdown, exit from lockdown, second lockdown, etc.), we estimated $\alpha(phase)$, which is a scaling factor for the phase-specific transmission rate per contact. This means that the previously mentioned transmission rate per contact β , is a time-dependent parameter that varies for each phase, multiplied by the scaling factor $\alpha(phase)$. This scaling factor captures temporal variations in the transmission rate that are not captured through the parameterization of contact matrices, such as mask usage.

A Poisson likelihood function was maximized to obtain the parameter estimates:

$$\mathcal{L}(Data|\Theta) = \prod_{t=t_1}^{t_n} Poiss(H_{obs}(t)|H_{pred}(t, \Theta)) \quad (3.4)$$

Θ is the set of parameters that we want to evaluate. $H_{obs}(t)$ is the empirical number of hospital admissions on day t . $H_{pred}(t)$ is the number of hospital admissions foreseen by the model on day t . $Poiss(\cdot|H_{pred}(t))$ is the mass function of a Poisson distribution with mean $H_{pred}(t)$ and $[t_1, t_n]$ is the time interval considered for the fit.

The parameter space was explored using grid-search to find the maximum likelihood estimator (MLE), which was determined by evaluating the log-likelihood function.

The transmissibility per contact is a crucial parameter for calculating the basic reproductive number (R_0). R_0 represents the growth factor of consecutive generations in an epidemic and can be derived from a matrix known as the next generation matrix (NGM), denoted as K [89]. To calculate R_0 , we can construct two matrices: F , which describes the generation of new infections, and V , which represents transitions within infected individuals (e.g. recovery). The entry $-V_{ij}^{-1}$ denotes the expected time an individual in compartment j spends in infected compartment i , while the entry F_{ij} represents the rate at which an infected individual in compartment j generates individuals in infected compartment i . Thus, the entry $-FV_{ij}^{-1}$ represents the expected number of infected offspring in state i produced by an individual currently in infected state j . By defining K as $-FV^{-1}$, the basic reproduction number (R_0) can be determined as its largest eigenvalue. Additionally, the effective reproductive number $R(t)$ at a specific time t can be calculated by considering the effective susceptible population at that time, rather than using the total population size.

3.1.5 Behavioral indicators, counterfactual scenarios

In this paragraph, I present behavioral indicators that we used in **article #1 (Chapter 4)**.

Loss of adherence. In **article #1**, we examined how mobility levels, based on mobile phone data [67], changed during the implementation of the same measure in order to understand how adherence to policies evolved over time. For instance, during the first lockdown, mobility levels remained relatively stable over the weeks. However, during the second lockdown, a significant increase in mobility was observed after 3 weeks from the beginning, indicating a spontaneous decline in adherence to the imposed policies.

We fit the model to hospital admission data during the second wave, we calculated the relative increase in the reproduction number after the initial three weeks of the lockdown compared to its start. This computation provided an estimate of the loss of adherence and was employed to inform counterfactual lockdown scenarios.

Distress index. When analyzing different lockdown scenarios, we need to evaluate their intensity, duration, adherence, and their impact on quality of life. To address this, we introduced a distress index based on mobility data [67]. This index was calculated by considering weekly mobility reductions, as social distancing measures primarily rely on restricting movement, and the reduction in mobility can be seen as a measure of the perceived limitations on individual freedom due to imposed restrictions.

In calculating the distress index, we took into account the overall reduction in mobility, assessing the relative variation in the number of origin-destination displacements compared to a pre-pandemic baseline. Origin-destination travel flows were obtained from Orange mobile phone records [67]. The distress index represents the sum of the absolute values of weekly mobility reductions during the period when each restriction was in place. The index was normalized to a scale from 0 to 10 (with 10 representing a strict 8-weeks lockdown and 0 indicating absence of restrictions).

Stringency index. The stringency index [24] is a composite measure that takes into account various indicators such as restrictions on public gatherings, stay-at-home requirements, school closures, and travel bans. It quantifies the intensity of

government policies on a scale from 0 to 100, with a higher value indicating a stricter response. It is shown in **Figure 2.1**.

Lockdown scenarios. Starting in March 2021 (week 11, 2021), we compared the impact of various COVID-19 control measures. We compared scenarios assuming curfew conditions with those involving lockdowns lasting 2 to 8 weeks. Our analysis considered strict and moderate lockdowns, based on mobility changes and transmissibility during the first and second lockdowns. We also explored different starting dates for lockdowns, from week 11 to week 15 in 2021. For lockdowns exceeding 2 weeks, we examined scenarios with full adherence and those with decreasing adherence. Adherence decline was modeled as an increase in the reproductive number.

3.2 Metapopulation model

In the context of disease transmission, mobility fluxes can substantially impact the likelihood of encounters, exposure patterns, and the probability of transmission [90, 91, 92]. The metapopulation approach offers a natural framework for examining the interplay between mobility, spatial structure, and epidemic transmission. This structured approach integrates compartmental models into a system that explicitly accounts for individual movements and space. The model assumes that the population is spatially fragmented into sub-populations, or patches, that represent distinct entities. Each patch undergoes local disease transmission, while also interacting with other patches through mobility. The metapopulation model has a multiscale structure that includes individual patches, each containing a population of individuals whose health status is modeled by a compartmental model. The dynamics of each compartment account for the possibility of contact between individuals and changes in their health status based on the infection dynamics. By using this approach, it is possible to capture the spatial heterogeneity of disease transmission, including local outbreaks and their potential spread to other regions (**Figure 3.3a**). The metapopulation model has a network structure where subpopulations are nodes connected by individual movements; mobility fluxes between patches can be: explicit or effective. The explicit approach defines mechanistic individual movements [93, 94], while the effective approach accounts for mobility patterns through force of infection generated by infectious individuals [95, 96]. With this effective approach, individuals residing in patch i are subjected to a force of infection that is proportionate to the coupling between subpopulations, even if they do not explicitly move from one patch to another. Both methods are informed by mobility data such as mobile phone, commuting, or air traffic data.

We used an effective stochastic non-Markovian (as it has memory of the home location of individuals [97, 98]) transmission model with a structure at the regional level. The population was divided in the 12 regions of mainland France (excluding Corsica). In each region, the model accounted for disease transmission due to (i) infected residents not moving (ii) infected visitors coming from other regions and (iii) returning residents previously infected in other regions. These three terms were embedded in the force of infection $\lambda_i(t)$ as follows:

$$\lambda_i(t) = \lambda_{ii}(t) + \sum_{j \neq i} \lambda_{ji}^v(t) + \sum_{j \neq i} \lambda_{ij}^r(t)$$

$$\begin{cases} \lambda_{ii}(t) = \beta_i(t) p_{ii}^2(t) \frac{I_i(t)}{\hat{N}_i(t)} \\ \lambda_{ji}^v(t) = \beta_i(t) p_{ii}(t) p_{ji} \frac{I_j(t)}{\hat{N}_i(t)} \\ \lambda_{ij}^r(t) = \beta_j(t) p_{ij}(t) \frac{\hat{I}_j(t)}{\hat{N}_j(t)} \end{cases}$$

where $\beta_i(t)$ was the transmission rate of region i at time t , $p_{ij}(t)$ the coupling probability between regions i and j inferred from mobility data (**Chapter 3.2.1**), and $\hat{N}_i(t) = p_{ii}(t)N_i + \sum_{j \neq i} p_{ji}(t)N_j$ and $\hat{I}_i(t) = p_{ii}(t)I_i(t) + \sum_{j \neq i} p_{ji}(t)I_j(t)$, were the effective population and the effective number of infections in region i , respectively [99].

Transmission dynamics followed a SEIR-like compartmental scheme (**Figure 3.3b**), in which individuals were divided into 5 health status: susceptible, exposed, infectious, hospitalized and recovered. Thus we simplified the scheme of **Figure 3.1** for the sake of different the research questions, also because these simplifications align with the common practice in metapopulation models, where the primary focus is mobility [100, 101]. We did not consider the age structure of the population, similarly to what commonly done in COVID-19 metapopulation models [100, 102]. Age-specific mixing is absorbed in the estimate of the regional transmissibility.

Hospital admission rate was informed from French hospital data for patient trajectories (SIVIC database [50]); parameters, values, and sources used to define the compartmental model are listed in **Table 3.2**.

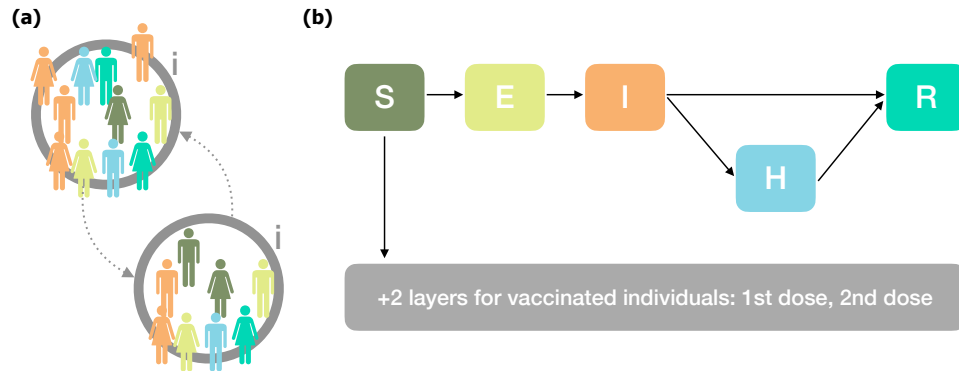


Figure 3.3: Metapopulation model, compartmental scheme with vaccination. (a) Scheme of metapopulation model. (b) Compartments (top) account for infections due to historical strains for non-vaccinated people. Analogous compartments are considered for vaccinated individuals (not shown for the sake of visualization). S=Susceptible, E=Exposed, I= Infectious, H=severe case admitted to the hospital, R=Recovered.

3.2.1 Mobility

Individual trajectories captured from mobile phones can offer valuable insights for developing epidemic models. Anonymized aggregated mobility fluxes extracted from mobile phone signaling data were provided by the Orange business service Flux Vision [67]. Specifically, we had access to aggregated, de-identified origin-destination matrices reporting the daily number of user displacements among 1,436 geographical areas of mainland France. Geographical areas are defined according to

Incubation period	5.2 days	[74]
Duration of prodromal phase	1.5 days, computed as the fraction of pre-symptomatic transmission events out of pre-symptomatic plus symptomatic transmission events.	[75]
Latency period	3.7 days (incubation period - prodromal phase)	-
Mean generation time	6.6 days	[78]
Infectious period	2.9 days (to match the generation time)	-
Time from infection to hospital	10.2 days	-
Time from symptoms onset to hospitalization	5 days	[103]
If infected, probability of going to hospital	2.1%	[104]

Table 3.2: Parameters, values, and sources used to define the COVID-19 compartmental model.

the 2018 EPCI level (Établissements Publics de Coopération Intercommunale). The anonymization procedure was approved by the French data protection authority CNIL (Commission Nationale de l'Informatique et des Libertés). Origin-destination matrices were aggregated at regional level to compute weekly coupling probabilities p_{ij} between regions and were used to inform the metapopulation model.

The coupling probability between i and j for a given week p_{ij} is defined as the probability that a resident in i visits j due to his mobility trajectory:

$$p_{ij} = \frac{w_{ij}}{\sum_k w_{ik}}$$

Where w_{ij} is the average number of daily trips between i and j for a given week.

3.2.2 Effective modeling of variants and seasonality

To model how the Alpha variant spread over time and across different regions, we modulate transmissibility accordingly to the variant penetration, transmission advantage. In this context, we also decided to explicitly include seasonality when modeling the transmission.

The penetration of the variant was estimated by analyzing Flash surveys data [55] and by fitting them with a logistic function, resulting in a modulating factor that varies daily by regions (Equation 3.6).

The transmission advantage was estimated by calculating the daily effective reproductive numbers independently for each strain (wildtype or Alpha) and fitting the daily ratio $\frac{R_{Alpha}}{R_{wildtype}}$ with a zero-degree and a second-degree polynomial over time. The magnitude of the transmission advantage varied over time, decreasing from 1.58 in week 5, 2021 to 1.42 in week 22, 2021, similarly to what observed in United Kingdom [105]. These effects could be associated with vaccination, as vaccines may reduce outward transmission by reducing viral loads [105, 106]. To model the increased severity with respect to the historical strains, we considered a 64% increase in hospitalization rates, following Ref.[88].

Several studies have investigated the relationship between SARS-CoV-2 transmission and weather factors, recognizing climate as a driver in the coronavirus SARS-CoV-2 spread. To integrate seasonality into our model we used the estimates provided in the Ref. [107]. The variable allows us to estimate the variation in transmission rate induced by climatic factors. To have a smooth variable over time, we assumed that seasonality behaves sinusoidally over a year. We fitted the estimates with a sinusoidal function with 1-year period, one per each region, in order to obtain daily values of the seasonality factor $\sigma_i(t)$ affecting transmission in region i on day t . $\sigma_i(t)$ is defined between an 18% reduction in summer (on average) and a 23% increase in reverse (on average). We used a least-squares optimization function for the seasonality parameter fit.

$$\beta_i(t) = \beta_i^{intrinsic}(t)[(1 - A_i(t)) + \eta_i(t) \cdot A_i(t)] \cdot \sigma_i(t) \quad (3.6)$$

where i indicates the region. The parameter $A_i \in [0, 1]$ is region-dependent and is used to account for the variant penetration. The parameter $\eta_i(t)$ is used to modulate the transmission advantage of the Alpha variant. The parameter $\sigma_i(t)$ accounts for weather conditions.

3.2.3 Inference framework and validation

Model parameters were estimated in a Bayesian framework by sampling the posterior parameter distribution obtained by updating prior beliefs based on a likelihood function. The likelihood function is evaluated on daily data of regional hospital admissions (**Equation 3.7**). We assumed that observed data followed a Poisson distribution with mean H_{pred} , that is the daily number of hospital admissions predicted by the model. The log-likelihood function is of the form:

$$\log \mathcal{L}(data|\Theta) = \sum_{i=i_1}^{i_{12}} \sum_{t=t_{start}}^{t_{end}} \log Poiss(H_{obs}(t, i)|H_{pred}(t, i, \Theta)) \quad (3.7)$$

where $\Theta = \{\beta_{i_1}, \dots, \beta_{i_{12}}\}$ indicates the regional transmission rates to be estimated. $H_{obs}(t, i)$ is the observed number of hospital admissions on day t in the region i , $H_{pred}(t, i, \Theta)$ is the number of hospital admissions predicted by the model using parameter values Θ , $Poiss(\cdot|H_{pred}(t, i, \Theta))$ is the probability mass function of a Poisson distribution with mean $H_{pred}(t, i, \Theta)$, and $[t_{start}, t_{end}]$ is the time window considered for the fit. The time windows used for the fit were defined based on the interventions applied in France; specifically: pre-second lockdown period (Sept 21, 2020 – region dependent date), second lockdown period (region dependent date - Nov 22, 2020), curfew 8p.m (Dec 15, 2020 – Jan 15, 2021), curfew 6pm pre holidays (Jan 16, 2021 – region dependent date due to school holidays), curfew 6p.m. during holidays (region dependent date due to school holidays), curfew 6p.m. post holidays (region dependent date due to school holidays– region dependent date), third lockdown period (region dependent date – Jun 13, 2021).

We used Markov Chain Monte Carlo (MCMC) to obtain posterior distributions. We used three independent chains, with each chain performing 3000 steps, to approximate the posterior distribution. We used the Metropolis-Hasting algorithm to accept or reject the set of parameters at each step.

To demonstrate that our model was able to estimate the parameters with the proposed inference approach and does not suffer from identifiability issues, we performed the following synthetic experiment. We parameterized the model using as priors the set of parameter values estimated with the first MCMC, and we re-calibrated the model with another MCMC procedure. By retrieving the same set of parameter values, we showed that the model was well identified and could be calibrated without bias.

To initialize the model, we first fitted a stochastic region-independent transmission model (from Ref. [15]) on the 12 French regions. We then fitted through maximum likelihood a Gumbel-r distribution on the prevalence in each compartment predicted by the model on March 1, 2020 (end of week 9). The choice of the Gumbel-r distribution was based in terms of AIC (Akaike Information Criterion) among a set of commonly used distributions.

For each stochastic run of the metapopulation model, the initial condition for each compartment was sampled from the corresponding Gumbel-r distribution. This procedure allowed to initialize the model in March 2020, while maintaining in the model the variability associated with a trajectory seeded at the start of the epidemic (late January 2020).

We validated the model by comparing its predictions of the percentage of antibody-positive people with seroprevalence estimates from multiple studies at different dates [51, 52].

We performed 200 stochastic simulations to compute median values and associated 95% probability ranges for all quantities of interest.

3.2.4 Behavioral indicators, counterfactual scenarios

Normalcy index. The Normalcy index, introduced by The Economist [108], measures changes in human behavior based on a set of daily indicators to evaluate how life has been affected since the onset of the pandemic. The index tracks eight different variables (sports attendance, time at home, traffic congestion, retail footfall, office occupancy, flights, film box office and public transport) to quantify an overall score. The pre-pandemic activity level was set at a normalcy index of 100 to ease comparison. During the second lockdown and curfews, the index for France was computed to be between 38 and 53, indicating that progress toward returning to pre-pandemic life was around halfway.

Counterfactual scenarios. We simulated various alternative policy scenarios regarding the implementation of lockdowns in France. These scenarios included a "stop-and-go" approach, where lockdowns were periodically applied and lifted, in contrast to the nighttime curfew between the second and third lockdowns in France. Since French authorities did not define specific thresholds for imposing restrictions, and for the purpose of comparing different policy choices, we established criteria for initiating and ending lockdowns based on per-capita hospital admissions. As a reference value for triggering lockdowns (T), we used the per-capita hospitalization rate in the region with the highest hospitalization incidence during the second lockdown, namely the Auvergne-Rhône-Alpes region (ARA). This level represented the maximum hospital occupancy that authorities deemed sustainable. For the release threshold (R), we instead considered the average hospitalization incidence across regions at the time the second lockdown was lifted. Unlike the triggering

threshold, the release threshold does not have a maximum capacity constraint, so we used the average value.

We then varied these threshold values to evaluate the impact of interventions triggered or released at different levels. Specifically, a nationwide lockdown was initiated when the first region reached the trigger threshold (region i with $T_i = T$; all others had $T_j < T$), and it was lifted when the last region reached the release threshold ($R_k = R$; $R_j < R$). We systematically varied and examined these thresholds.

For our simulations, we used the transmissibility and inter-regional mobility values from the second lockdown for the first nationwide lockdown in the "stop-and-go" series, and for subsequent simulated lockdowns, we employed values from the third lockdown.

Effective days under restrictions. Given the heterogeneity of the measures implemented in the period under study (second lockdown, curfew, third lockdown), days spent under restriction could not be accounted with equal weights. We thus defined a measure of "effective day D_t " spent under restriction, based on the Normalcy index [108] associated to the interventions, as follows

$$D_t = \frac{N(pre_{LD2}) - N(t)}{N(pre_{LD2}) - N(LD2)}$$

where $N(t)$ is the Normalcy index at time t . Effective days are an output of the type, stringency and duration of restrictions considered in the study (the ones applied in France and the ones considered in the scenarios) and are used for comparison across policies.

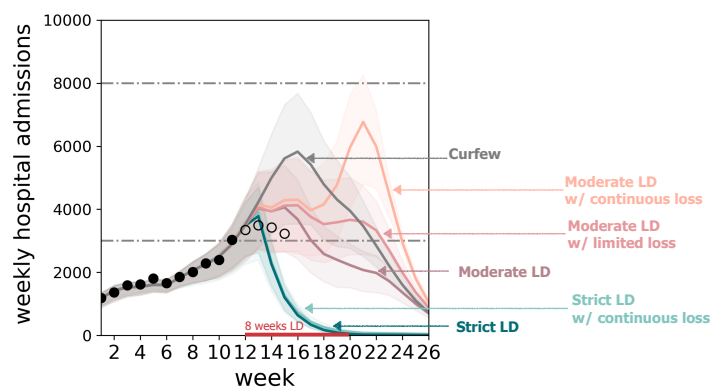
Can we strike a balance between the effectiveness and sustainability of interventions?

4

In this chapter, I present a work that uses the age-structured model (**model #1**, presented in **Chapter 3.1**) to identify optimal intervention strategies for controlling the third wave of the pandemic. We explored the complex interplay between epidemic dynamics, vaccination efforts, societal adherence, and policy sustainability. We conducted simulations considering interventions of different intensities and durations, considering also the possibility of loss of adherence over time. To quantitatively compare the sustainability and effectiveness of different NPIs, we introduced an index called "distress index". The results of this work helped to offer valuable insights into the outcomes of the interventions and their potential consequences in the future. The article was published in *Communications Medicine* [12]. The additional information referred to in **article #1** can be found in the **Supplementary Materials** section of the thesis.

4.1 Introduction

The emergence of the SARS-CoV-2 Alpha variant in December 2020 sent shockwaves through Europe, disrupting the management of the COVID-19 pandemic (**Chapter 2.1**). Just as some governments were easing interventions after the second wave, the variant's alarming spread compelled swift action. A few months later, with vaccination rates lagging behind in continental Europe and the Alpha variant fueling a third wave, a significant challenge emerged. How could countries rely on heavy restrictions once again to reduce viral circulation and improve the epidemic situation?



INTERVENTIONS	DISTRESS INDEX			
	2 weeks	4 weeks	6 weeks	8 weeks
Strict LD	2.50	5.00	7.50	10.00
Strict LD w/ limited loss of adherence	-	4.51	6.53	8.54
Strict LD w/ continuous loss of adherence	-	-	6.14	7.45
Moderate LD	1.55	3.09	4.64	6.19
Moderate LD w/ limited loss of adherence	-	2.79	4.04	5.29
Moderate LD w/ continuous loss of adherence	-	-	3.80	4.61
Curfew	0.92	1.84	2.76	3.67

Figure 4.1: Timecourse of weekly hospital admissions in Île-de-France for lockdown scenarios of varying stringency, duration, and adherence and distress index. Top row: lockdown duration of 8 weeks, vaccination pace accelerated to 300,000 first doses/day since the start of April. Interventions are applied in w12 and assume a delay of one week to the peak in hospital admissions. Dots refer to data; filled dots correspond to the data used to fit the model and to provide the trajectory for the curfew scenario void dots correspond to more recent data. Curves refer to the median trajectory; shaded areas around the curves correspond to the 95% probability range obtained from 250 stochastic simulations. The type of intervention is coded by different line colors. Horizontal dashed lines refer to the peak of the first and second wave in the region. Results for strict lockdown scenarios with full adherence or loss of adherence overlap; for this reason, we do not show the scenario with limited loss of adherence. Bottom row: distress index values according to different scenarios and different duration of lockdowns (expressed in weeks)

The article analyzed the efficacy of different social distancing strategies with a focus on both sustainability and adherence. After one year into the pandemic, characterized by intense restrictions, that were prolonged over time, the NPIs chosen to control the emerging third wave had to consider several crucial aspects. In addition to preventing the healthcare system from collapsing, it was important to assess the impact of these interventions on personal freedom limitations and the potential loss of adherence to the imposed measures. Sustainability of interventions depended on the intensity and duration of restrictions. Long-lasting measures could lead to decreased adherence and potential negative impacts on the population's mental health and quality of life. Over time, there was a risk of decreased adherence to restrictions and adherence to intervention strategies played a key role in limiting virus transmission [109]. However, the level of adherence might vary influenced by factors such as public trust, information dissemination and personal risk perception [110]. Surveys conducted in France have revealed an increase in anxiety among the population since the implementation of long-standing interventions during the pandemic [83]. This suggested that even less severe measures could have a significant impact on quality of life if prolonged over time.

The study used the two-strain transmission model with vaccination (**model #1**) to explore different intervention scenarios. The explored scenarios were analyzed in relation to past implemented measures: both strict lockdowns, like the first one, and more moderate ones, like the second, simulating various durations and potential declines in adherence. The study was applied to the real situation of Île-de-France, where simulations could guide policy decisions, offering a range of options to strike a balance between the sustainability and effectiveness of NPIs. This highlighted how different options would lead to compatible outcomes.

The efficacy of interventions was measured using various epidemiological and healthcare indicators, such as hospital incidence, cumulative hospital admissions, and hospital pressure (which is defined as the number of weeks during which hospital admissions remained above the peak level observed during the second wave). To quantify the sustainability of interventions, a distress index was defined (**Figure 4.1, Chapter 3.1.5**). This index measures the impact of restrictions in terms of limitations on individual freedom, based on mobility changes. Mobility data proves valuable in quantifying the sustainability of the intervention strategies, which encompasses both their duration and intensity. This index takes into account the total duration of the lockdown, the intensity of the interventions, and the level of adherence. We opted for a cumulative measure to enable comparisons between different lockdown strategies that may differ not only in their stringency but also in their acceptance and duration.

The study also conducted a secondary analysis, including testing accelerated vaccination plans, impact of seasonality, and different strategies for phasing out restrictions.

4.2 Article #1: Adherence and sustainability of interventions informing optimal control against the COVID-19 pandemic

BEGINNING

L Di Domenico, CE Sabbatini, PY Boëlle, C Poletto, P Crépey, J Paireau, S Cauchemez, F Beck, H Noel, D Levy-Bruhl, V Colizza

Adherence and sustainability of interventions informing optimal control against the COVID-19 pandemic

Communications Medicine 1, 57 (2021)

Adherence and sustainability of interventions informing optimal control against the COVID-19 pandemic

Laura Di Domenico^{1,6}, Chiara E. Sabbatini^{1,6}, Pierre-Yves Boëlle¹, Chiara Poletto¹, Pascal Crépey², Juliette Paireau^{3,4}, Simon Cauchemez³, François Beck⁴, Harold Noel⁵, Daniel Lévy-Bruhl⁴ & Vittoria Colizza^{1,5}✉

Abstract

Background After one year of stop-and-go COVID-19 mitigation, in the spring of 2021 European countries still experienced sustained viral circulation due to the Alpha variant. As the prospect of entering a new pandemic phase through vaccination was drawing closer, a key challenge remained on how to balance the efficacy of long-lasting interventions and their impact on the quality of life.

Methods Focusing on the third wave in France during spring 2021, we simulate intervention scenarios of varying intensity and duration, with potential waning of adherence over time, based on past mobility data and modeling estimates. We identify optimal strategies by balancing efficacy of interventions with a data-driven “distress” index, integrating intensity and duration of social distancing.

Results We show that moderate interventions would require a much longer time to achieve the same result as high intensity lockdowns, with the additional risk of deteriorating control as adherence wanes. Shorter strict lockdowns are largely more effective than longer moderate lockdowns, for similar intermediate distress and infringement on individual freedom.

Conclusions Our study shows that favoring milder interventions over more stringent short approaches on the basis of perceived acceptability could be detrimental in the long term, especially with waning adherence.

Plain language summary

In the spring of 2021, social distancing measures were strengthened in France to control the third wave of COVID-19 cases. While such measures are needed to slow the spread of the virus, they have a significant impact on the population’s quality of life. Here, we use mathematical modelling based on hospital admission data and behavioural and health data (including data on mobility, indicators of social distancing, risk perception, and mental health) to evaluate optimal COVID-19 control strategies. We look at the effects of interventions, their sustainability and the population’s adherence to them over time. We find that shorter, more stringent measures are likely to have similar effects on viral circulation and healthcare burden to long-lasting, less stringent but less sustainable interventions. Our findings have implications for the design and implementation of public health measures to control future COVID-19 waves.

¹INSERM, Sorbonne Université, Pierre Louis Institute of Epidemiology and Public Health, Paris, France. ²Univ Rennes, EHESP, REPERES « Recherche en Pharmaco-Epidémiologie et Recours aux Soins »—EA 7449, 35043 Rennes, France. ³Mathematical Modelling of Infectious Diseases Unit, Institut Pasteur, UMR2000, CNRS, Paris, France. ⁴Santé Publique France, French National Public Health Agency, Saint-Maurice, France. ⁵Tokyo Tech World Research Hub Initiative, Institute of Innovative Research, Tokyo Institute of Technology, Tokyo, Japan. ⁶These authors contributed equally: Laura Di Domenico, Chiara E. Sabbatini. ✉email: vittoria.colizza@inserm.fr

The emergence of the SARS-CoV-2 Alpha variant in December 2020^{1,2} disrupted the management of COVID-19 pandemic in Europe. The alert arrived as some governments were lifting interventions that had been applied to curb the second wave. Some countries, such as the UK and Ireland, were forced to rapidly implement strict lockdowns to control the explosion of cases due to the variant. Others maintained or strengthened their restrictions because of concerns over the new variant³.

Few months after, with vaccination lagging behind (25% of the population of the European Union with a first dose on May 1, 2021 vs. 44% in the US, 51% in the UK, and 62% in Israel⁴) and a third wave due to the Alpha variant, continental Europe faced the challenge of relying once again on heavy restrictions to reduce sustained viral circulation and improve the epidemic situation approaching the summer. But what is the optimal strategy, given vaccination rollouts, the epidemic conditions, and the sustainability of long-lasting restrictive policies? On one side, limited available options remain beyond high intensity interventions, once milder layers of social distancing have been accumulated, strengthened, and extended over time (e.g., curfew, closure of restaurants and bars, closure of schools). On the other side, the efficacy and long-term sustainability of the adopted policies are potentially threatened by loss of adherence and policy-induced fatigue^{5,6}, affecting the quality of life of the population.

Building on observed adherence waning and introducing a data-driven measure capturing the limitations on individual freedom resulting from restrictions, we compared intervention scenarios of varying intensity and duration, and examined the role of adherence and sustainability on optimal epidemic control. The study is applied to the third wave in Île-de-France—the Paris region, the most populated of France and heavily hit by the pandemic—accounting for vaccination rollout plans, seasonality, and plans for the phasing out of restrictions.

We show that long-lasting interventions of moderate stringency achieve the same reductions in viral circulation and healthcare burden of shorter but higher stringency restriction, but at the expense of a higher distress in the population. This is exacerbated if adherence to policy wanes over time.

Methods

Data

Hospital surveillance data. We used regional daily hospital admission data, collected in the SIVIC database⁷. The database includes the number of admissions of COVID-19 confirmed patients to regular hospital or intensive care units. Hospital data are corrected for notification delays and do not suffer changes in detection or sampling, unlike the number of detected cases. As such, they provide a robust data source and have been used throughout 2020 in France for pandemic assessment and response^{8–11}.

Mobility data. Mobility reductions shown in Fig. 1 were extracted from two different data sources. Overall mobility was reconstructed from mobile phone data provided by Orange Business Service Flux Vision^{12,13}. Data included origin-destination travel flows of mobile phone users among 1436 geographical areas in France. Each area corresponds to a group of municipalities, defined according to the 2018 EPCI level (Établissements Publics de Coopération Intercommunale¹⁴). Mobility reduction in a given week was computed as the relative variation of the number of trips with respect to the pre-pandemic baseline. Estimated presence at workplaces was obtained from Google Mobility Reports¹⁵. This dataset provides the relative change in the daily number of visitors to places of work compared to a pre-pandemic baseline, based on Google location-history data.

Indicators of social distancing, risk perception, mental health. Several initiatives collect data over time through surveys to explore individual behaviours in response to COVID-19 pandemic. Here we use data from YouGov¹⁶ and Santé publique France¹⁷. Surveys gather self-reported data, tracking compliance with preventive measures (e.g., avoiding social gatherings or contacts with other people, frequency of the use of masks), as well as risk perception and mental health indicators (e.g., fear to contract the virus, anxiety, depression). Indicators for specific social distancing behaviors (avoiding gatherings, use of masks) are used in addition to mobility data described above. YouGov surveys cover multiple countries and provide data at least every 2 weeks. Santé publique France polls collect data at the national level at least every month.

Ethics statement. Orange Business Service Flux Vision aggregated mobility travel flows were previously anonymised in compliance with strict privacy requirements, presented to and audited by the French data protection authority (CNIL, Commission Nationale de l'Informatique et des Libertés). They were accessed under license for this study. The study did not require an ethical approval as it involved review of publicly available documents, involved analyses that were based on previously published studies, involved aggregated and anonymous data, did not involve evaluation of experimental or patient data.

SARS-CoV-2 two-strain transmission model. We used a stochastic discrete age-stratified two-strain transmission model, integrating data on demography¹⁸, age profile¹⁸, social contacts¹⁹, mobility¹⁵, and adoption of preventive measures¹⁷. The model accounts for the co-circulation of two strains and vaccination. Four age classes are considered: [0–11], [11–19], [19–65], and 65+ years old (children, adolescents, adults and seniors respectively). Transmission dynamics follows a compartmental scheme specific for COVID-19 (Supplementary Fig. 1) where individuals are divided into susceptible, exposed, infectious, hospitalized, and recovered. The infectious phase is divided into two steps: a prodromic phase (I_p) and a phase where individuals may remain either asymptomatic (I_{as} , with probability $p_a = 40\%$ ²⁰) or develop symptoms. We distinguished between different degrees of severity of symptoms, ranging from pauci-symptomatic (I_{ps}), to individuals with mild symptoms (I_{ms}), or severe symptoms (I_{ss}) requiring hospitalization^{11,21}. The duration of the infectious period was computed from the estimated mean generation time of 6.6 days²² (Supplementary Fig. 2). Prodromic, asymptomatic and pauci-symptomatic individuals have a reduced transmissibility²³. A reduced susceptibility is considered for children and adolescents, along with a reduced relative transmissibility for children, based on available evidence^{24–27}. We assume that infectious individuals with severe symptoms reduce of 75% their number of contacts because of the illness they experience. Parameter values and corresponding sources are reported in the Supplementary Table 1. Sensitivity analysis on the probability of being asymptomatic, the susceptibility of younger age classes and transmissibility of children was performed in previous works^{8,9,28}.

Contact matrices are parametrized over time to account for behavioral response to social distancing interventions and adoption of preventive measures. Contacts at school, work and on transports are considered according to the French school calendar, school closures, and presence at workplaces estimated by Google. Physical contacts are reduced based on data from regular large-scale surveys conducted by Santé Publique France⁸. Contacts engaged by seniors are subject to an additional reduction of 30%,

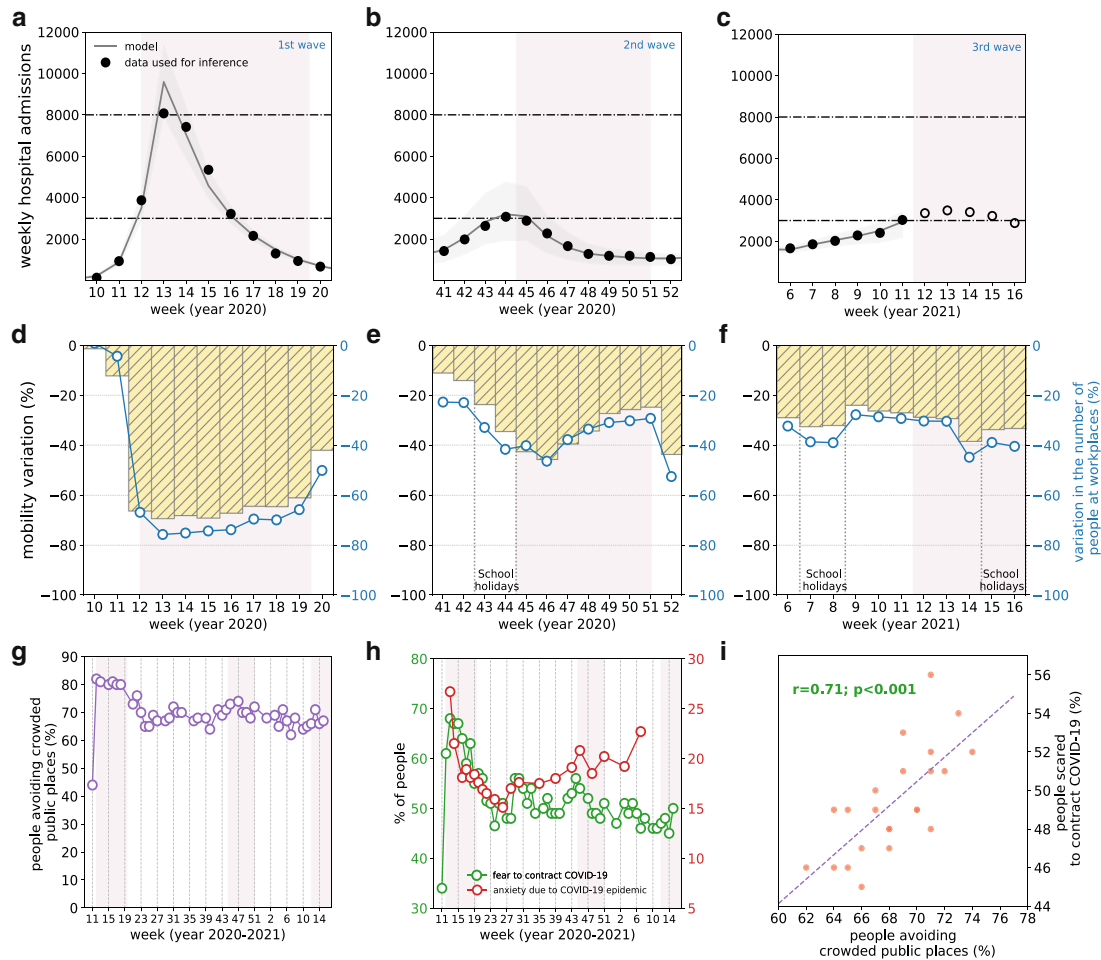


Fig. 1 COVID-19 pandemic waves in Île-de-France, with associated mobility reductions, social distancing, risk perception, and psychosocial burden. **a–c** Weekly hospital admissions in Île-de-France during the first (**a**; weeks 10–20, March 2–May 17, 2020), second (**b**; weeks 41–52, October 5–December 27, 2020), and third (**c**; weeks 6–16, February 8–April 25, 2021) pandemic wave. Dots refer to data; filled dots correspond to the data used to fit the model, void dots correspond to data outside the inference window. Curves and shaded areas correspond to median fitted trajectories and 95% probability ranges, obtained from $n = 250$ independent stochastic runs. Horizontal dashed lines refer to the peak of the first and second wave in the region. **d–f** Mobility reduction in Île-de-France during the first (**d**), second (**e**), and third (**f**) pandemic wave. Yellow histograms represent the variation of mobility with respect to pre-pandemic levels, based on the number of trips extracted from mobile phone data¹². Blue curves show the estimated change in presence at workplace locations over time with respect to pre-pandemic levels based on Google location-history data¹⁵. Shaded rectangles in the plots of the first two rows correspond to social distancing measures (strict lockdown in the first wave, moderate lockdown in the second wave, strengthened measures in the third wave). The second week of the second lockdown and the third week of the strengthened measures against the third wave have lower mobility and presence at workplaces due to bank holidays in the week. Vertical dotted gray lines correspond to school holiday periods. **g–i** Percentage of individuals avoiding crowded public places¹⁶ (**g**), percentage of individuals scared to contract COVID-19¹⁶ and prevalence of anxiety in the context of COVID-19 epidemic (**h**)¹⁷ as functions of time; scattered plot between the percentage of individuals scared to contract COVID-19 and the percentage of individuals avoiding crowded places (**i**) in the time period October 2020–April 2021 (full time period shown in Supplementary Fig. S5), with the results of a Pearson correlation test (effect size 0.71, p -value $< 10^{-3}$). Results for these indicators refer to the national scale. Shaded rectangles in panels **g**, **h** correspond to social distancing measures as in panels **a–f**.

to account for evidence of a higher risk aversion behavior of the older age class compared to other age classes⁸.

Alpha variant. Genomic and virological surveillance to identify specific mutations are in place in France since the start of 2021 to monitor variants over time. The first large-scale genome

sequencing initiative (called Flash1 survey) was conducted on January 7–8 and analyzed all positive samples provided by participating laboratories²⁹. The proportion of the Alpha variant in Île-de-France was estimated to be 6.9%, compared to the national estimate of 3.3%, making Île-de-France the region with the highest penetration registered in the country. Flash surveys are performed on average every two weeks on a sample of sequences.

Starting week 6, 2021 a new protocol for virological surveillance was implemented to provide more timely estimates on the weekly frequency of detected viruses with specific mutations. It was based on second-line RT-PCR tests with specific primers that allow the detection of the main mutations that characterize the variants of concern. They must include at least the N501Y mutation and allow to distinguish the Alpha variant from the Beta or the Gamma variants. The frequency of the Alpha variant over time in Île-de-France is reported in the Supplementary Fig. 3.

We considered the co-circulation of the Alpha variant together with the historical strains, assuming complete cross-immunity. An increase in transmissibility of 59% (95% credible interval: 54–65%)²⁹ was considered for the Alpha variant compared to the historical strains. This early estimate was obtained from the Flash1 and Flash2 survey in France, and it is in line with other estimates^{1,2}. To account for uncertainty in the transmission advantage and possible changes due to restrictions, we also show for sensitivity the results assuming 40% of increase in transmissibility, i.e., the lower estimate provided by ref. ². (Supplementary Fig. 11). We considered a 64% increase in hospitalization rates, following evidence of an increased risk of hospitalization after infection due to the Alpha variant compared with other lineages^{30,31}. The frequency of the Alpha variant was initialized in the model on January 7, 2021 using the estimates of the first large-scale nationwide genomic surveillance survey (Flash1). The model was validated against virological and genomic surveillance data¹⁰ on prevalence of Alpha variant over time. The Alpha variant was estimated to become dominant in the region by mid-February 2021¹⁰ (Supplementary Fig. 3).

Vaccination rollout campaign. Administration of vaccines was included in the model according to the vaccination rhythm adopted in France starting January 2021. We considered the administration of 100,000 doses per day (including first and second doses) at the national level from the end of January (w04), accelerated to 200,000 first doses per day starting the beginning of March (w10), and 300,000 first doses per day starting April (w13). Rollout plans were expressed in terms of first administrations from March on to follow the objectives of authorities, delaying the administration of the second dose to reach a higher coverage in a smaller timeframe. Higher vaccination paces (400,000–800,000 doses/day) were also tested (Supplementary Fig. 9). Paces are defined at the national level, and the number of doses is proportionally distributed to the region according to the population eligible for the vaccine. Vaccination is prioritized to the older age class, assuming 80% coverage, and then shifted to adults considering 50% coverage, according to surveys on vaccine hesitancy³². Vaccination to healthcare personnel and patients in long-term care facilities, performed at the start of the vaccination program, could not be explicitly included.

We considered 75% vaccine efficacy against infection³³ and 65% vaccine efficacy against transmission³⁴, estimated after the first injection. We further considered 80% vaccine efficacy against symptoms given infection, computed from the estimated vaccine reduction of symptomatic disease^{34,35} estimated at 95% after the second dose, and found to be similar after the first dose³⁶. As the landscape for vaccine efficacy rapidly evolves, we also tested vaccine efficacy against transmission equal to 40%³⁷ (Supplementary Fig. 13). We assumed efficacy to start 3 weeks after the first injection, and tested a delay of 2 weeks for sensitivity (Supplementary Fig. 14).

Inference framework. The model is fitted to daily hospital admission data through a maximum likelihood procedure, by estimating the transmission rate in each pandemic phase. More

precisely, prior to the first lockdown and in absence of intervention (period January–March 2020), we estimated $\{\beta, t_0\}$ where β is the transmission rate per contact and t_0 is the date of the start of the simulation. Then, in each phase we estimated α_{phases} , i.e., the scaling factor of the transmission rate per contact specific to the pandemic phase under study (e.g., lockdown, exit from lockdown, summer, start of second wave, second lockdown, etc.). The transmission rate per contact in each phase is then defined as the transmission rate per contact in the pre-lockdown phase β multiplied by the scaling factor α_{phases} . A pandemic phase is defined by the interventions implemented (e.g., lockdown, curfew, and other restrictions) and activity of the population (school holidays, summer holidays, etc.). The effective reproductive number is derived from the estimated transmission rate through the next generation matrix approach³⁸. The likelihood function is of the form

$$L(Data|\Theta) = \prod_{t=t_1}^{t_n} Poiss(H_{obs}(t)|H_{pred}(t, \Theta)) \quad (1)$$

where Θ indicates the set of parameters to be estimated, $H_{obs}(t)$ is the observed number of hospital admissions on day t , $H_{pred}(t, \Theta)$ is the number of hospital admissions predicted by the model on day t using parameter values Θ , $Poiss(\cdot|H_{pred}(t, \Theta))$ is the probability mass function of a Poisson distribution with mean $H_{pred}(t, \Theta)$, and $[t_1, t_n]$ is the time window considered for the fit.

For Île-de-France, we seeded the model with 140 infected individuals to reduce the strong fluctuations associated with fitting the rapid increase and the high peak of hospitalizations observed in the first wave (the region was one of the areas mostly affected by the epidemic in early 2020). Simulations progress throughout 2020 to build immunity in the population. The model was validated against the estimates of three independent serological surveys conducted in France⁸. We used 250 stochastic simulations to compute median values and associated 95% probability range for all quantities of interest.

First lockdown, second lockdown, curfew. French authorities implemented two national lockdowns in 2020 to face the rapid surge of COVID-19 cases observed in the first and second wave. The first lockdown started on March 17, 2020 and lasted 8 weeks. It involved strict mobility restrictions outside home, together with closure of schools and non-essential activities. A less stringent lockdown was implemented for 6 weeks, starting on October 30, 2020. Schools remained open and a larger number of job sectors were allowed to operate. Measures were relaxed in the last two weeks of the lockdown, with the reopening of all retail for Christmas shopping. The second lockdown was lifted in mid-December with the application of a curfew starting at 8 pm, then anticipated in January 2021 to 6 pm to face increasing SARS-CoV-2 spread. Starting March 20, 2021, strengthened measures were additionally put in place in the region of Île-de-France to curb the third wave. These measures included mobility restrictions for trips exceeding 10 km, closure of business and of schools (1 week for primary schools, 2 weeks for middle and high schools in addition to 2-week school holidays in April). Values of the stringency index according to the timeline of interventions applied in France can be found in the Supplementary Fig. 4.

Loss of adherence. We used mobility data during the second lockdown and estimates of mobility reductions over time to assess if adherence to adopted policy waned over time, given unchanged restrictions. Focusing on the second lockdown, we compared the mobility reduction and reproductive number estimated in the first 3 weeks of lockdown implementation (w45–47, November 2–November 22, 2020) with respect to the following week. We

considered the average over the first-3-week period to smooth out the effect of the national holiday on November 11, altering mobility and presence at work with respect to a regular week.

Lockdown scenarios. Starting from week 12, 2021 (March 22, 2021), we compared a scenario assuming unchanged curfew conditions—as estimated in week 11 (*curfew scenario*)—with the trajectories resulting from the application of a lockdown for a duration of 2–8 weeks. We modeled the effect of a strict lockdown and a moderate lockdown based on measured mobility reductions and estimated transmissibility conditions during the first and second lockdowns, respectively, before relaxation emerged. The delay from the date of implementation of lockdown and the peak of hospitalizations was estimated to be 9 days during the first lockdown in the region, and varied between 7 and 12 days across regions⁸. In our scenarios we assumed a 7-day delay, and tested 10 days for sensitivity (Supplementary Fig. 12). We also tested lockdown scenarios with different starting dates, ranging from w11 to w15, 2020 (Supplementary Figs. 6–S7).

For lockdowns longer than 2 weeks, we compared scenarios assuming full adherence with situations characterized by a loss of adherence over time. We modeled the loss of adherence throughout interventions by a relative increase in the reproductive number, according to estimates from the second lockdown. We applied it after 2 weeks from implementation of interventions (to model a faster dynamics of adherence waning compared to the one observed in the second lockdown), and considered it limited in time (one drop) or continuous (repeated drops every two weeks).

Distress index. In order to quantify the infringement on individual freedom associated with lockdowns and provide a measure of the policy impact on the quality of life, we introduced a quantity called distress index. This measure takes into account both the duration and the intensity of restrictions. It is defined as the sum of the absolute values of weekly mobility reductions, over the number of weeks in which each restriction is maintained, and normalized to a scale from 0 to 10 (10 representing a strict 8-weeks lockdown and 0 the absence of restrictions). In case of a strict or moderate lockdown without loss of adherence, we considered the mobility reductions recorded during the two interventions in 2020, respectively, and varied durations from 2 to 8 weeks. Loss of adherence is computed with a variation of the mobility reduction after 2 weeks (limited loss) and repeated every 2 weeks (continuous loss), according to estimates from the second lockdown. We took the end of January 2021 (w04) as reference for the mobility reduction associated with curfew.

Seasonality. Multiple studies have investigated the relationship between SARS-CoV-2 transmission and weather factors, including temperature, humidity, ultraviolet radiation³⁹, suggesting that summer conditions may help in reducing transmission of the virus. Seasonal factors and simultaneous social distancing interventions are difficult to disentangle; however, containment measures are estimated to have a larger impact on the epidemic compared to seasonal effects only. Considering the estimated dependence of the reproductive number on UV radiation⁴⁰ and temperature⁴¹, we extracted data on downward UV radiation at the surface and daily temperature recorded in Paris, in Île-de-France, in the last three years (2018–2020)⁴² to derive an approximate estimate of the reduction in the transmission rate induced by climate factors for the region under study.

Reporting summary. Further information on research design is available in the Nature Research Reporting Summary linked to this article.

Results

Adherence and impact of interventions of varying stringency and duration. During the strict lockdown implemented to curb the first wave (March–May 2020), mobility showed a reduction of 68.9% in the region compared to the prepandemic level (65% reduction at the national level¹²) that remained fairly constant over time (Fig. 1a, d). The associated effective reproductive number was estimated to be 0.73 [95% confidence interval: 0.72, 0.74]. During the second wave (October–December 2020, Fig. 1b), a less stringent lockdown was enforced, corresponding to an effective reproductive number of 0.88 [95% CI: 0.86, 0.90] estimated in the first 3 weeks of implementation (w45–47, November 4–22, 2020), before relaxation occurred. Recorded mobility and estimated presence at work decreased but remained almost two times higher compared to the first lockdown (average mobility reduction of 42.6% in the first 3 weeks compared to prepandemic levels) and showed a rapid and marked increase over time (Fig. 1e). This loss of adherence occurred remarkably faster (after the third week) and more substantially during the second lockdown compared to the first. The mobility reduction with respect to the prepandemic phase went from 42.6% in the first 3 weeks to 34.3% in the fourth week of the lockdown (w48, November 23–29, 2020), corresponding to a relative change of 19%. This was associated to an estimated relative increase of 10.9% in the effective reproductive number. Higher mobility was registered later, in the last 2 weeks of the lockdown (w49–50, November 30–December 13, 2020), due to the reopening of shops. The second lockdown was lifted with the application of an 8 pm curfew, then anticipated to 6 pm in January. The resulting effective reproductive number was estimated to be 0.90 [95% CI: 0.86–0.93] for the historical strains and 1.43 [95% CI: 1.37–1.48] for the Alpha variant at the end of January¹⁰.

Indicators obtained from surveys report that fear of contracting COVID-19 showed an overall decrease over time after the second wave in France, whereas prevalence of anxiety in the population showed an increasing tendency, despite the lower stringency of restrictions. Performing a linear regression in this time window (i.e., October 2020–April 2021), we found a weekly average reduction of -0.31% for individuals scared to contract the virus, and -0.39% for individuals avoiding crowded places. In the same time window, we found an average weekly increase of $+0.13\%$ in the prevalence of anxiety in the population (Fig. 1h). Fear of contracting COVID-19 showed a positive correlation with the behavior of avoiding crowded places (Pearson $r = 0.71$, $p < 10^{-4}$, in the time period from w40 (September 28–October 4, 2020) to w15 (April 12–18, 2021), shown in Fig. 1g; results are robust when extending the timeframe of analysis). We observed a non-significant association between the prevalence of anxiety in the population and adoption of social distancing (Pearson $r = 0.2$, $p = 0.46$, in the time period from w11 in 2020 (March 9–15, 2020) to w11 in 2021 (March 15–21, 2021) (Supplementary Fig. 5).

Starting mid-February 2021, the region witnessed a sustained rise in hospitalizations leading to the start of the third wave (Fig. 1c). We fitted the model up to week 11 (March 15–21, 2021), when the region was still under curfew before strengthened measures were applied on March 20 to control the third wave. We then simulated intervention scenarios starting week 12, 2021, with stringency, efficacy and potential loss of adherence informed by past mobility data¹² and modeling estimates^{8,9}.

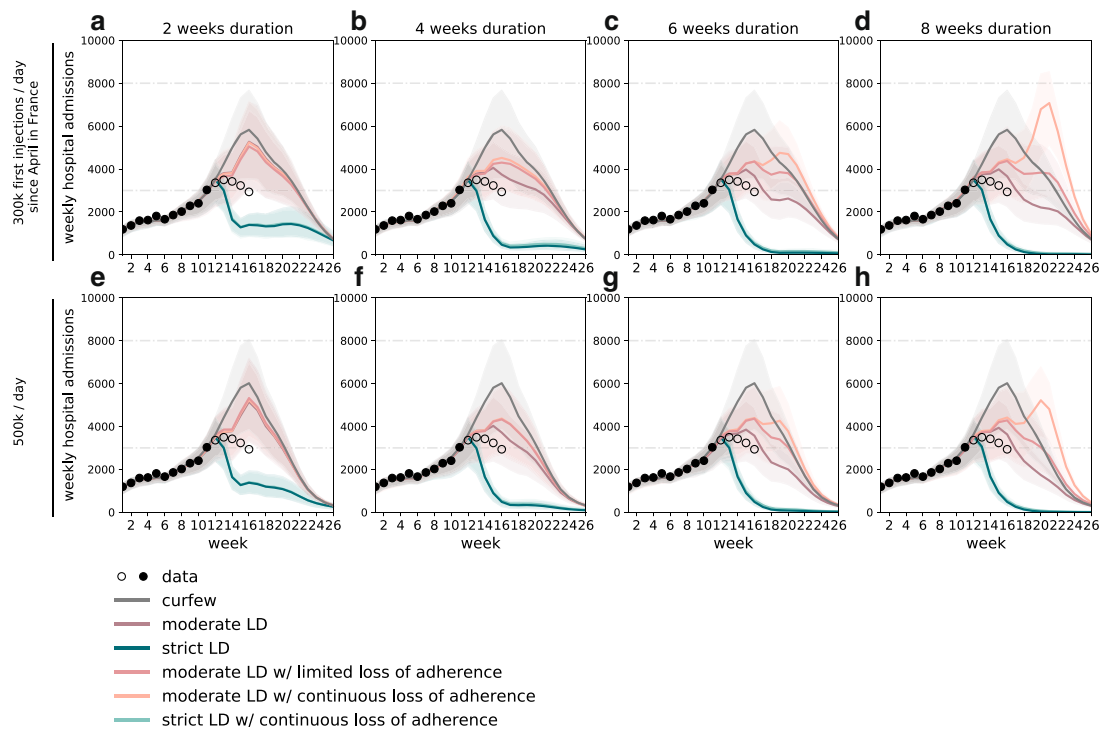


Fig. 2 Timecourse of weekly hospital admissions in Île-de-France for lockdown scenarios of varying stringency, duration, and adherence. **a-d**: vaccination pace accelerated to 300,000 first doses/day since the start of April, lockdown duration of two (**a**), four (**b**), six (**c**), or eight (**d**) weeks; **e-h**: as in **a-d**, but assuming 500,000 first doses/day. Interventions are applied in w12 and assume a delay of one week to the peak in hospital admissions. Dots refer to data; filled dots correspond to the data used to fit the model and to provide the trajectory for the curfew scenario; void dots correspond to more recent data. Curves refer to the median trajectory; shaded areas around the curves correspond to the 95% probability ranges obtained from $n = 250$ independent stochastic simulations. The type of intervention is coded by different line colors; the abbreviation LD stands for lockdown. Horizontal dashed lines refer to the peak of the first and second wave in the region. Results for 2 weeks lockdown scenarios with or without loss of adherence overlap, as loss of adherence occurs in the third week. Results for strict lockdown scenarios with full adherence or loss of adherence overlap; for this reason, we do not show the scenario with limited loss of adherence.

Regardless of adherence, the strict lockdown was predicted to be the only measure able to achieve a rapid decrease of the epidemic trajectories (Figs. 2 and 3), in line with observations in the UK and Ireland following similar interventions. It would outperform moderate lockdowns of any duration, on both short- and longer-term epidemic impacts. Starting from about 3000 weekly hospitalizations at the time measures were applied, admissions would be reduced to less than 400 when exiting a strict lockdown of at least 1 month vs. more than 2000 after a moderate lockdown (Fig. 3a). Even with adherence waning, a strict lockdown would reduce the epidemic to the levels recorded at the exit of the first lockdown in May 2020 (670 weekly admissions in w20, 433 in w21, 330 in w22 in 2020), and it would be maintained low by increasing immunization rates. These levels would also enable a better control of viral circulation through test-trace-isolate when partially alleviating restrictions^{8,43}. Importantly, a short circuit-breaker⁴⁴ of 2 weeks, after which curfew was restored, was predicted to be already enough to rapidly reduce hospitalizations to levels below the ones of February 2021. Rebounds at the end of the short lockdown would be prevented by maintaining a certain degree of social distancing (curfew) and increasing immunization, with stronger reductions over time for increasing vaccination rhythms (from 300,000 to 500,000 first doses/day since April; Fig. 2).

Obtaining results equivalent to a short strict lockdown would require moderate interventions to last longer than 2 months, and could potentially be compromised by loss of adherence to restrictions (Fig. 3a). This could slowdown and stop the decrease in hospitalizations, leading to a plateau or a rise in hospitalizations after several weeks of moderate lockdown, potentially higher than the peak of the third wave (Figs. 2 and 3a). This occurs in our scenarios as repeated drops in adherence over time may reduce the efficacy of a lockdown to values lower than a simple curfew after a few weeks, because of the small difference between the estimated efficacies of the second lockdown (before relaxation) and curfew conditions. Since moderate lockdowns would not be able to considerably reduce viral circulation, they would entail a larger impact on the hospital system (median hospitalizations in the period w12–w26 around 38,000–50,000 compared to 10,000–23,000 for strict lockdowns, Fig. 3c) for a longer time (median 6–10 weeks with hospitalization incidence above the peak of the second wave compared to at most 2 weeks for a strict lockdown of any duration, Fig. 3d). This impact would be more substantial if adherence waned, leaving the hospital system under high pressure for twice the amount of time (median 12 weeks above the peak of the second wave assuming continuous adherence loss, compared to 6 weeks for full adherence, corresponding to 80% of the time period under study).

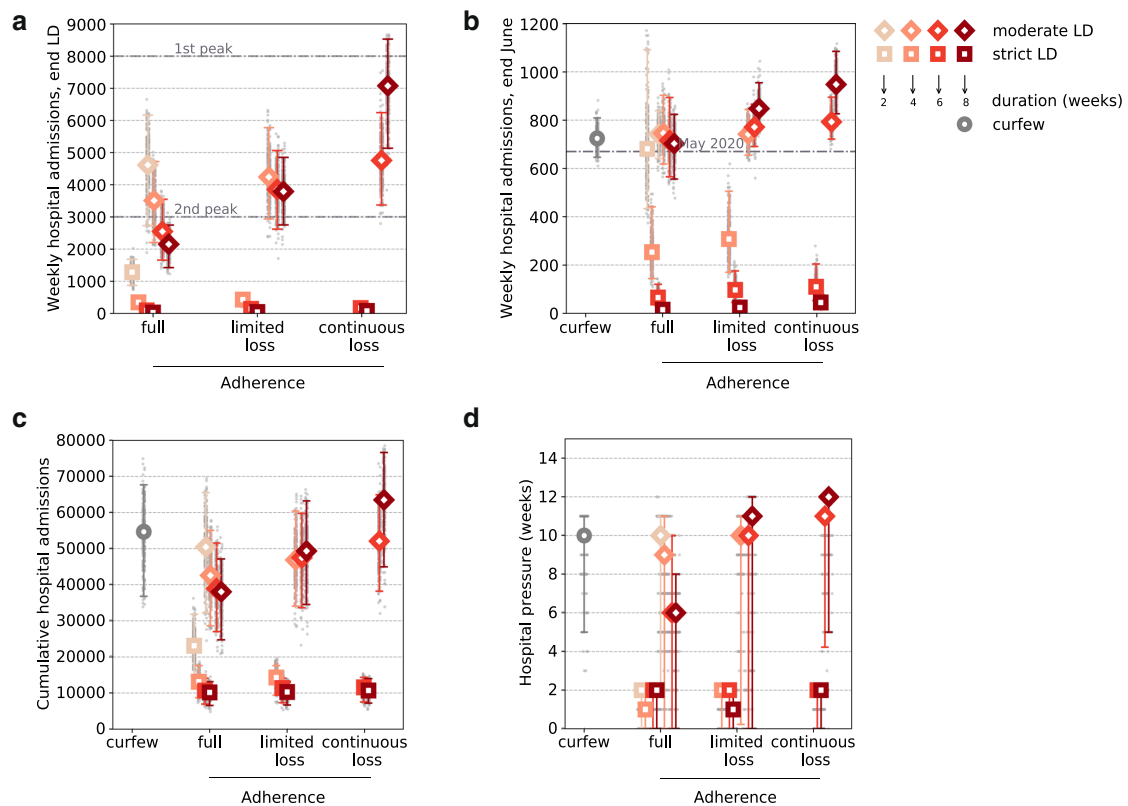


Fig. 3 Impact of loss of adherence on intervention efficacy, for varying stringency and duration of interventions. Weekly hospital admissions at the end of the lockdown (a), weekly hospital admissions at the end of June (w26) (b), cumulative hospital admissions computed over the time period w12–w26 (c), hospital pressure, defined as the number of weeks in which hospital admissions remain above the peak level achieved during the second wave, in the period w12–w26 (d) as functions of the adherence level—full adherence over time, limited loss of adherence, continuous loss of adherence over time. The point with the curfew (gray circle) represents the estimate under the curfew scenario with no additional intervention, and is shown for comparison. Results refer to a vaccination rhythm accelerated to 300,000 first doses/day since April. Symbol types refer to the stringency of intervention (squares representing a strict lockdown scenario, diamonds representing a moderate lockdown scenario). Color shades of the symbol contour refer to the duration (weeks) of the lockdown intervention (from the lightest shade corresponding to 2 weeks, to the darkest one corresponding to 8 weeks); the abbreviation LD in the legend stands for lockdown. Plots show median values; error bars represent 95% probability ranges, obtained from $n = 250$ independent stochastic runs (gray points). Horizontal dashed lines in panel (a) refer to the peak of the first and second wave in the region; horizontal dashed line in panel (b) refers to the level of mid-May 2020 at the exit of the first lockdown.

Despite different trajectories, our model anticipates that moderate lockdowns could reach at the end of June the hospitalization levels measured in May 2020 (670 weekly admissions) if adherence was maintained over time, similarly to a short strict lockdown, and with no advantage compared to curfew measures at this stage (Fig. 3b). Adherence loss would lead to higher hospital admission levels.

Removing contacts at schools, we found that the two weeks of school closure for spring holidays (w15–16) would have a marked impact on the efficacy of moderate lockdowns, otherwise with schools open. They would allow flattening the curve and avoiding even longer plateaus in critical conditions before the accrued effect of immunization would decrease the epidemic (Supplementary Fig. 8).

Optimizing interventions’ sustainability by minimizing policy-induced distress. Another critical dimension associated with the nature of interventions—besides their stringency, duration, and adherence—is their sustainability over time, which is a

combination of intensity of restrictions and how long they last. To account for this aspect, we introduced a distress index, integrating the intensity, duration, and adherence level in each scenario, and providing a quantitative measure of the policy-induced distress perceived on average by an individual. The higher the distress index and the lower is the sustainability of the measure.

Moderate lockdowns of less than 6 weeks are all characterized by low levels of distress (<4), similar to those of a curfew and of a 2-week strict lockdown (Fig. 4; estimated values of the distress index are reported in the Supplementary Table 2). In this range of distress values, a net advantage was observed for the short strict lockdown that substantially reduced the total number of hospitalizations (23,000 vs. an average of 47,000) and hospital pressure (2 weeks vs. more than 8 weeks). High values of the distress index (>7) were associated exclusively to strict and long lockdowns (of 6 weeks, with full adherence, or longer, also with adherence waning over time), which correspond to the most effective measures in suppressing viral circulation and reducing the healthcare impact, but also the least sustainable.

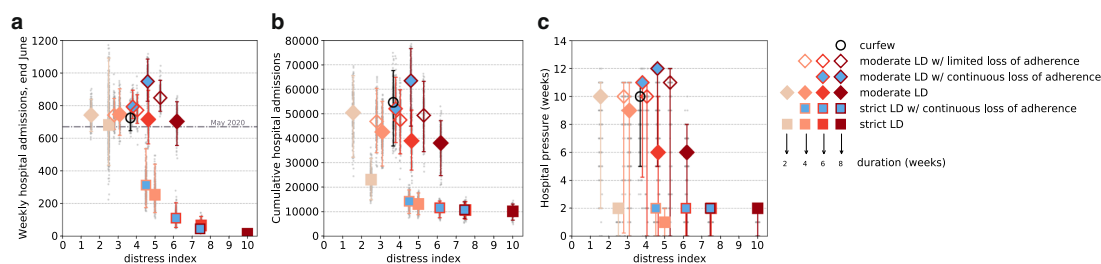


Fig. 4 Intervention efficacy vs. associated policy-induced distress. Weekly hospital admissions at the end of June (w26) (**a**), cumulative hospital admissions (computed in the time period w12–w26) (**b**), hospital pressure, defined as the number of weeks in which hospital admissions remain above the peak level achieved during the second wave, in the period w12–w26 (**c**) as functions of the distress index. Results refer to the accelerated vaccination pace of 300,000 first doses/day since April. Symbol types refer to the stringency of intervention (squares representing a strict lockdown scenario, diamonds representing a moderate lockdown scenario, void circle representing the projection under the curfew scenario). Color shades of the symbol contour refer to the duration (weeks) of the lockdown intervention (from the lightest shade corresponding to 2 weeks, to the darkest one corresponding to 8 weeks); the abbreviation LD in the legend stands for lockdown. Adherence to moderate and strict lockdowns is coded with the fill color (filled symbols with the color of the scenario correspond to scenarios with full adherence, void symbols represent scenarios with limited loss of adherence, blue filled-in symbols correspond to scenarios with continuous loss of adherence). Plots show median values; error bars represent 95% probability ranges obtained from $n = 250$ independent stochastic runs (gray points). Horizontal dashed line in panel (**a**) refers to the level of mid-May 2020 at the exit of the first lockdown.

There exists, however, quite a diversified range of intervention options that, for moderate distress (index between 4 and 7), would achieve better control of the epidemic than moderate lockdowns. One-month strict lockdowns would largely outperform moderate interventions in terms of health metrics while inducing similar distress, as the latter must be maintained for a longer duration. Six- or eight-week moderate lockdowns would lead to about three times as many patients hospitalized and about three to six times the hospitalization incidence at the end of June compared to interventions that exhibit a similar distress level as a strict lockdown of 1 month. If moderate lockdown restrictions were less respected over time, epidemiological and healthcare indicators would considerably worsen, for relatively small gains in lowering the policy-induced distress.

Vaccination and seasonality while managing reopening plans.

According to weather data for Île-de-France, an average increase of 23 kJ/m^2 in UV radiation and of 11°C in temperature were registered from March to June in the last three years. Based on the estimated relation between climate factors and the reproductive number^{40,41}, this increase would correspond to a 7.7% and 7.3% reduction in viral transmission, respectively. In the following, we explore values up to 30% reductions of the transmissibility starting from May, to also account for reductions resulting from changes of behaviors associated with the upcoming summer (e.g., more time spent outdoor, increased ventilations of indoor environments, etc.).

Further acceleration of vaccination pace coupled with the potential effect of seasonality may act in synergy to (i) counteract the deterioration of the epidemic due to the waning of adherence over time, or (ii)—if stronger—bring down the epidemic faster than what is expected from moderate interventions. Figure 5 shows the interplay of these factors assuming that seasonality acts on reducing viral transmission starting May. Keeping the planned vaccination rhythm at 300,000 first injections per day since April, a 5–10% reduction of transmission induced by seasonality would be necessary to absorb the potential loss of adherence against moderate interventions by the end of June (label (1)). Without counting on seasonal effects, vaccination rollout should increase by 33% (i.e., from 300,000 to 400,000 first doses per day). Larger seasonality (>20%) or accelerations in vaccination rollouts (up to 800,000 first doses per day) would be able to compensate for the larger cumulated number of patients requiring hospitalization

due to adherence loss (label (2)). Reaching by the start of the summer the weekly admissions achieved by an imperfectly adhered 1-month strict lockdown would require substantial seasonality coupled with large increases in vaccination rhythms (contour line at 300 in the top row of Fig. 5).

In all situations, a certain degree of social distancing is required to accompany the gradual lifting of lockdown to avoid slowdowns or rebounds (bottom row of Fig. 5). Even the summer conditions estimated in mid-July 2020, but considering schools in session, may lead to an epidemic resurgence if incidence is high, despite the growth in population immunity and summer seasonality. Results show that a progressive transition in phasing out restrictions is essential, and they further support the importance to lower the incidence level to better manage potential rebounds while reopening.

Discussion

Managing sustained viral circulation after long periods of social distancing measures of varying intensity faces the challenge to reduce the strain on the healthcare system and to limit long-lasting or stringent interventions affecting the quality of life of the population. Moreover, with accelerating vaccination campaigns and the prospects of reopening the society, adherence waning may represent a threat to phasing out restrictions. Using Île-de-France as a case study, we compared the efficacy of different measures against their sustainability and potential for case resurgence due to imperfect adherence of the population. Given the high incidence levels reached by the epidemic in the region by mid-March 2021, exceeding the peak of the second wave¹⁰, only high intensity interventions would have been able to rapidly curb viral circulation, allowing the region to considerably reduce the burden of hospitalization after only 2 weeks and despite loss of adherence. Once incidence substantially declined, the management of the epidemic could largely benefit from test-trace-isolate strategies^{8,43} and the large-scale availability of self-test kits for iterative screening⁴⁵, while immunization due to vaccination builds up in the population. Hospitals could more rapidly restore routine care beyond COVID-19. Moreover, rapidly reaching low incidence levels would also lower the potential for SARS-CoV-2 evolution conferring fitness advantages, and allow a better control of the possible emergence or importation of variants of concern⁴⁶.

Moderate interventions as the strategy adopted in November–December 2020 to curb the second wave constitute

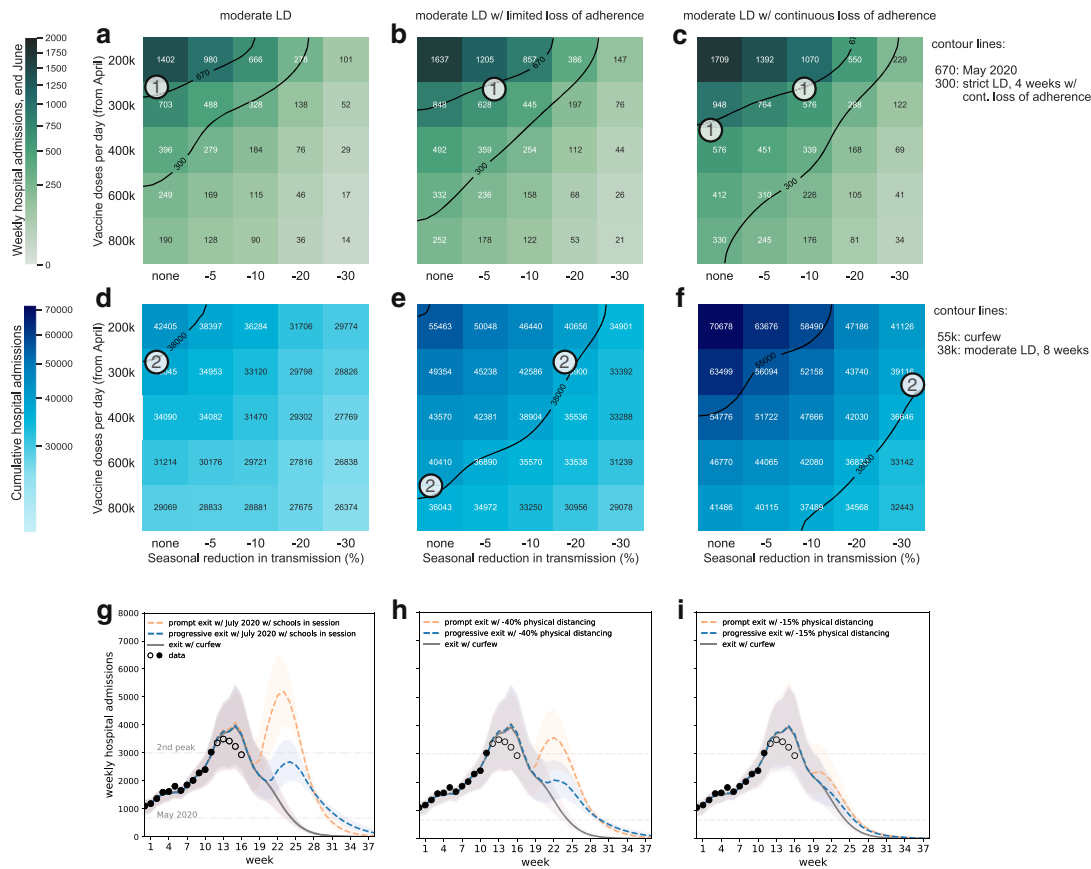


Fig. 5 Impact of vaccination, seasonality, and reopening plans. **a–f** Heatmaps show median values of weekly hospital admissions at the end of June (w26) (**a–c**) and cumulative hospital admissions in the time period w12–w26 (**d–f**), as functions of vaccination rhythm (y-axis) and seasonal reduction in transmission (x-axis) for moderate lockdowns of 8 weeks with full adherence (**a, d**), limited loss of adherence (**b, e**), continuous loss of adherence (**c, f**). The abbreviation LD stands for lockdown, contour lines indicate reference values of specific intervention scenarios defined in the legends. Circled numbers refer to a subset of conditions of interventions (heatmaps from left to right), vaccination and seasonality (variables in the y- and x-axis in each heatmap) achieving the same outcome, identified by the contour lines (see legend) and discussed in the main text. **g–i** Plots show projections of the weekly hospital admissions under different hypotheses for the reopening conditions, assumed right after lifting the moderate lockdown (orange curves), or through a progressive transition (blue curves): conditions experienced in mid-July 2020, but with schools in session (**g**); curfew scenarios with 40% fewer individuals respecting physical distancing (**h**); curfew scenarios with 15% fewer individuals respecting physical distancing (**i**). Curves and shaded areas correspond to median trajectories and 95% probability ranges, obtained from $n = 250$ independent stochastic runs. In all plots, gray continuous line refers to a scenario in which curfew conditions as in week 11 are restored after the moderate lockdown. Dots refer to data; filled dots correspond to the data used to fit the model and to provide the trajectory for the curfew scenario; void dots correspond to data outside the inference time window showing the peak of the third wave. Scenarios assume a 10% reduction in transmissibility due to seasonality (except for the mid-July 2020 conditions that already embed seasonal aspects) and a vaccination rhythm of 300,000 first doses per day starting April. Plots showing projections for the reopening conditions, assumed right after lifting the strict lockdown are shown in Supplementary Fig. 10.

suboptimal options for the management of the epidemic till summer. Their efficacy remains limited because of the Alpha variant’s higher transmissibility^{1,2,29} and still low immunization levels (15.7% population vaccinated with a first dose in the region by April 20). Our results show that these measures should be maintained for much longer to reach incidence values similar to the result of a short and strict circuit-breaker⁴⁴, at the expense of a large number of severe cases requiring hospital care, a continuously high pressure on the hospital system, and high levels of distress cumulated over time. The strengthened measures in place during the spring 2021, based on closure of non-essential businesses, ban on gatherings and recommendations to telework, are

similar in intensity to the moderate scenarios considered in this study, as also confirmed by the similarity of the stringency index⁴⁷ (Supplementary Fig. 4). These were however accompanied by the advanced closure of schools just before the 2 weeks regular school holidays in April that provided an extra break on the epidemic evolution showing in the observed trend.

Despite different trajectories, epidemic conditions by the time summer starts are predicted to be similar across intervention scenarios (with the exception of high intensity interventions lasting 1 month or longer, largely suppressing the epidemic) and close to the curfew scenario in absence of additional restrictions. Differences in how the epidemic is managed throughout spring

are absorbed over time thanks to vaccination. However, large disparities remain for cumulative epidemiological and public health indicators, depending on whether early suppression or mitigation were achieved by the interventions. This would have an impact not only throughout the third wave (by increasing the overall number of hospitalizations, patients requiring critical care, and deaths), but also on the medium-to-long term due to the rising number of individuals who are likely to suffer from long-term health consequences following a COVID-19 infection (long COVID)^{48,49}. Early estimates indicate that about 10% of individuals testing positive for COVID-19 exhibit symptoms after 4 months⁴⁸, and about 3/4 of hospitalized patients report at least one symptom after 6 months⁴⁹—mainly fatigue, muscle weakness, sleep difficulties, anxiety, depression. Choosing a 2-week strict lockdown against an 8-week moderate lockdown would correspond to estimated 30,000 avoided long COVID cases among detected infections from mid-March to the end of June.

The choice of interventions inevitably also impacts the quality of life of the population due to imposed restrictions, leading to possible spontaneous relaxation. The shorter the measure's application, the less likely it is to observe adherence waning over time. Interventions of high intensity but short duration may therefore constitute an optimal approach to reduce both epidemic and healthcare burdens, while minimizing possible loss of adherence as well as policy-induced distress. Evidence from OECD countries after one year of COVID-19 pandemic show that swift lockdown measures were overall less restrictive of civil liberties, thanks to achieved control, compared to recurrent mitigation policies severely impacting individual freedom⁵⁰. Indeed, moderate or mild (curfew) interventions cumulate distress over time, as they need to be implemented for much longer to achieve the reduction of health indicators, with the potential risk of losing population adherence. This would considerably worsen both incidence and cumulative indicators, slowing down or stopping the decrease in incidence obtained with restrictions, thus remaining on a long plateau at sustained viral circulation, as occurred after the second wave. If relaxation against measures is left uncontrolled, epidemic rebounds can also be expected. At the same time, loss of adherence would correspond to a limited gain in personal freedom, when averaged overall individuals (−26% in distress index by continuously losing adherence in moderate lockdowns lasting 8 weeks), compared to interventions of lower stringency (−60% in distress index from an 8-week moderate lockdown to a 2-week strict lockdown).

In our study, loss of adherence occurs over time and is informed from observed increases in mobility during the second lockdown and corresponding estimated impact on the epidemic, during unchanged restrictions and recommendations. We did not consider initial adherence to restrictions different from what was measured in the first and second lockdown. While lower initial adherence may be expected as stringent social distancing measures are being applied for the third time, this may also depend on the acceptability of new measures, clarity of restriction and recommendations. For example, a recent survey showed that about 70% of individuals approved the strengthened measures recently applied in France, however almost half of them planned to disobey the rules⁵¹. Also, adherence loss should not be confused with population response to restrictions induced by socio-economic conditions and life circumstances^{6,12,13,52}. Prior work showed that this response—despite numerical differences depending on the stringency of measures (first lockdown, second lockdown, localized curfew at 8 pm, nationwide curfew at 6 pm)—is associated to the composition of the population, with blue-collar jobs and household crowding emerging as determinants of higher mobility during restrictions in France¹³.

We introduced an index integrating mobility reduction and duration of restrictions to provide a quantitative measure of policy-induced distress along the spectrum of varying stringency. This is meant to integrate the impact of restrictions infringing on individual freedom, as well as psychosocial effects of prolonged measures, linked for example to isolation, uncertainty, loss of purpose, and lack of social contacts^{53,54}. While both distress index and adherence were informed from data, we did not consider an explicit relation between distress and adherence loss, potentially leading to feedback mechanisms reinforcing relaxation for increasingly long durations. Related to “pandemic fatigue”, a concept often introduced as the presumed cause to limited adherence, this relation remains highly debated⁶. Some behavioral scientists warned against an ill-defined concept used to justify avoiding strict and/or early interventions^{6,55}. Different features and origins of fatigue are likely at play—including for example life constraints independent of motivation, as discussed above—that would require a range of definitions, data, and frameworks for analysis. A study on data from 14 countries showed that adherence to physical distancing evolved following a U-shape between March and December 2020⁵. However, in France this drop would correspond to the summer period, between the first two waves, during which restrictions were lifted and only recommendations on the use of personal preventive measures were in place. As such, it does not relate to the adherence loss throughout interventions considered here. Different indicators obtained from surveys show that fear of contracting COVID-19 decreased over time after the second wave in France, while anxiety continued to increase in the population. We found a positive association between fear and social distancing (expressed by the percentage of individuals avoiding crowded places), confirming the role that risk perception has in shaping health-related behaviors⁵⁶. However, we did not find a significant association between increasing anxiety, concurrent with lasting restrictions, and decreasing social distancing (Supplementary Fig. 5). So far there exists little evidence on the mechanisms of action of behavioral interventions that could improve our understanding and be leveraged to boost policy observance.

Available evidence indicates that interventions implemented in 2020 largely reduced the incidence of COVID-19^{9,11,57–60}, in the absence of effective treatments and prior to vaccination. Substantial differences were observed between analyses aiming to assess the efficacy of single social distancing measures (e.g., closure of schools, businesses, all but essential services, ban on mass gatherings and public events, restrictions on movements and stay-at-home orders). Our study did not focus on isolated measures, but considered the estimated efficiency of policy packages that were deployed during the first and second wave in France, along with observed policy compliance and wane in time. A lockdown as strict as the first one is unlikely to reach nowadays the efficiency observed last year, and for this reason we considered reduced adherence, which we show would marginally affect the results. The two lockdowns implemented in 2020 did not differ exclusively for the closure or opening of schools, but also for the mobility levels and presence at workplace estimated from data. Behaviors related to mobility, presence at work and school are not independent and we currently lack enough data to parameterize their relationship. In addition, alternative versions of interventions allowing time outdoor where risk of transmission is reduced⁶¹—such as recommendations in place during the third wave—may reshape mobility, contacts and associated risk in ways different than previously observed, preventing their assessment on the basis of historical data. Open questions remain on the combination and sequence of restrictions to be progressively lifted after the lockdown, as specific measures are too detailed for

mathematical models to quantify (e.g., reopening of restaurants). Strategic prioritization will likely depend on countries' interests.

Vaccination is key to exit the health crisis; however, our numerical evidence shows that epidemic management still needs to rely on social distancing to curb viral transmission, confirming prior work^{62–64}. Increasing vaccination rollout coupled with 5–30% reduction in transmission due to seasonal effects would be able to compensate for the slowdown or rebound effects of adherence waning or fast reopening. Multiple studies have investigated the relationship between SARS-CoV-2 transmission and weather. Results suggest that warm and humid conditions, and high UV radiation levels, are less favorable to disease spread³⁹. Based on previous estimates^{40,41}, we derived that the average increase in UV radiation and temperature reported in Île-de-France from March to June corresponds to ~10% reduction in transmission. Additional mitigating effects are expected due to seasonal behavior, with individuals spending more time outdoor than indoor, and aerating indoor settings more compared to winter time. But misconceptions on seasonality may generate excessive trust in the public altering their risk perception, and in authorities affecting their decision-making⁶⁵. Despite a building literature on the topic, there remain aspects that are difficult to measure and include a strong behavioral component. A large second wave started last year in the United States during summer because of early reopening, and cases started to rise in France from mid-July 2020, paving the way to the second wave in the fall. Lifting restrictions with the conditions experienced in mid-July 2020 is expected to lead to an epidemic rebound if incidence is high. We did not consider here the situation at the end of the first lockdown in spring 2020 because it was characterized by the maintenance of cautious behaviors, and additional levers existed that continued curbing transmission after lockdown was lifted (e.g., the increase in mask use, from 45% in mid-May 2020 to >70% at the end of the summer¹⁷, also due to mask mandates). Managing the epidemic while gradually releasing non-pharmaceutical interventions through the summer should mainly rely on the speed of vaccination rollout.

Our study has a set of limitations. It is applied to a region only, as indicators for France hide a variable situation at the local level, limiting the accuracy of modeling approaches extended to the whole country. Geographical heterogeneity depends on the evolving epidemic situation, population immunity due to natural infection, and variant frequency, so that results are not directly generalizable to other regions. We did not consider waning of immunity⁶⁶ or reinfections over the time frames modeled. We assumed the transmissibility advantage of the Alpha variant from early estimates in France²⁹, in agreement with other studies^{1,2}; however, this may be altered over time by social distancing and competition with other strains. Assuming a smaller transmissibility advantage for the variant would lead to lower incidence projections; however, it would not be able to capture the evolution in time of the Alpha variant's frequency in the region (Supplementary Figs. 3, 11). We did not consider the interaction with other variants, such as the Beta variant or the Gamma variant, that are already present in the country and show so far limited diffusion. If these variants can at least partially escape natural or vaccine-induced immunity⁶⁷, they may pose a challenge for the management of the epidemic as population immunity increases. Our approach is not suited to account for contacts in low-risk and high-risk conditions, e.g., in closed ill aerated settings vs. open settings, but seasonal reductions effectively account for these aspects. Modeled vaccination rhythms according to authorities' plans were slightly faster than observed. By May 4, 23.6% of the population was vaccinated with a first dose in the model, compared to 20.3% according to data; however, this is not expected to affect our findings. We did not

consider slowdowns that were recently observed after the temporary stop of AstraZeneca vaccine administration, undermining demand relatively to other vaccines. We considered 50% coverage in the adult population, following the declared intentions to get vaccinated of this age class in France³², but we did not consider changes in this expected coverage due to a possible reduction in perceived risk in relation to the successful reduction of epidemic incidence⁶⁸ or the application of measures targeting the non-vaccinated population thus incentivizing uptake. Our findings and prior work show that relaxing social distancing with limited immunization may result in epidemic rebounds^{62–64}. We did not consider the economic impact of social distancing measures, as our study focused on the epidemiological, healthcare, and behavioral components. There is increasing evidence, however, that economic growth, public health, and civil liberties do not need to be in opposition in the management of the COVID-19 crisis, with countries aiming for elimination faring largely better than countries adopting mitigation strategies⁵⁰. Also, we did not consider health impacts beyond COVID-19 that can result from a high pressure on the hospital system. Psychosocial impact was instead introduced through a simplified empirically-driven indicator based on restricted mobility, the core of many social distancing measures. However, this indicator is an average, therefore it hides the effects on vulnerable populations who may experience disproportionately higher distress^{6,13,52}. Also, being informed by mobility only, it aims at providing a measure of infringement of personal freedoms, but without explicitly capturing other elements associated with the quality of life⁵⁴. However, the increasing trend in anxiety observed following the second wave and throughout a prolonged application of curfew measures supports the idea of a progressive buildup of distress concurrent with lasting restrictions.

Control of the epidemic in a partially immunized population depends, in non-linear ways, on the interplay between the characteristics of the circulating variants, the stringency of social distancing measures, vaccination rollout plans, and population adherence to measures and vaccination. Mathematical models help to unravel the complexity of these interactions, accounting for the uncertainties characterizing some of these aspects, and to quantitatively inform on the optimal solutions for epidemic control. Our study shows that favoring milder interventions over more stringent approaches limited in time on the basis of perceived acceptability could be detrimental in the long term, especially with waning adherence.

Data availability

The mobility data supporting the findings of this study were available to authors from the Orange Business Service Flux Vision within the framework of the research project ANR EVALCOVID-19 (ANR-20-COVI-0007). Restrictions apply to the availability of these data, which were used under license, and so are not publicly available. Access to the data can be requested from Orange Business Service Flux Vision on a contractual basis. All other indicators used in the study are publicly available online at the links provided in the references. Hospitalization data were obtained from the SIVIC dataset⁷. Presence at workplaces was obtained from Google Mobility Reports¹⁵ specific to Île-de-France region. Indicators of social distancing ("Avoiding crowded public places")⁶⁹ and risk perception ("% people who say they are 'very' or 'somewhat' scared that they will contract COVID-19")⁷⁰ were obtained from YouGov.uk. Data on mental health were obtained from Santé publique France¹⁷, in the section "Santé mentale - Prévalences et évolutions de l'anxiété". Source data for the main figures in the manuscript can be accessed as Supplementary Data 1–5.

Code availability

Analyses were carried out in Python 3.8.5. Code for the transmission model is available on GitHub⁷¹.

Received: 14 May 2021; Accepted: 10 November 2021;

Published online: 06 December 2021

References

- Volz, E. et al. Assessing transmissibility of SARS-CoV-2 lineage B.1.1.7 in England. *Nature* <https://doi.org/10.1038/s41586-021-03470-x> (2021).
- Davies, N. G. et al. Estimated transmissibility and impact of SARS-CoV-2 lineage B.1.1.7 in England. *Science* **372**, eabg3055 (2021).
- ECDC. *Integrated COVID-19 response in the vaccination era*. <https://www.ecdc.europa.eu/sites/default/files/documents/Integrated-COVID-19-response-vaccination-era.pdf> (2021).
- Our World in Data. Coronavirus (COVID-19) Vaccinations—Statistics and Research. *Our World in Data* <https://ourworldindata.org/covid-vaccinations> (2021).
- Petherick, A. et al. A worldwide assessment of changes in adherence to COVID-19 protective behaviours and hypothesized pandemic fatigue. *Nat. Hum. Behav.* <https://doi.org/10.1038/s41562-021-01181-x> (2021).
- Michie, S., West, R. & Harvey, N. The concept of “fatigue” in tackling covid-19. *BMJ* **371**, m4171 (2020).
- data.gouv.fr. *Données hospitalières relatives à l'épidémie de COVID-19*. <https://www.data.gouv.fr/fr/datasets/donnees-hospitalieres-relatives-a-lepidemie-de-covid-19/> (2021).
- Pullano, G. et al. Underdetection of cases of COVID-19 in France threatens epidemic control. *Nature* **590**, 134–139 (2021).
- Di Domenico, L., Pullano, G., Sabbatini, C. E., Boëlle, P.-Y. & Colizza, V. Impact of lockdown on COVID-19 epidemic in Île-de-France and possible exit strategies. *BMC Med.* **18**, 240 (2020).
- Di Domenico, L., Sabbatini, C. E., Pullano, G., Lévy-Bruhl, D. & Colizza, V. Impact of January 2021 curfew measures on SARS-CoV-2 B.1.1.7 circulation in France. *Eurosurveillance* **26**, 2100272 (2021).
- Salje, H. et al. Estimating the burden of SARS-CoV-2 in France. *Science* **369**, 208–211 (2020).
- Pullano, G., Valdano, E., Scarpa, N., Rubrichi, S. & Colizza, V. Evaluating the effect of demographic factors, socioeconomic factors, and risk aversion on mobility during the COVID-19 epidemic in France under lockdown: a population-based study. *Lancet Digit. Health* **2**, e638–e649 (2020).
- Valdano, E., Lee, J., Bansal, S., Rubrichi, S. & Colizza, V. Highlighting socio-economic constraints on mobility reductions during COVID-19 restrictions in France can inform effective and equitable pandemic response. *J. Travel Med.* <https://doi.org/10.1093/jtm/taab045> (2021).
- Gouvernement.fr. *Cartographie des EPCI à fiscalité propre | collectivités-locales*. <https://www.collectivites-locales.gouv.fr/institutions/cartographie-des-epci-fiscalite-propre> (2021).
- Google.com. *COVID-19 Community Mobility Report*. <https://www.google.com/covid19/mobility?hl=fr> (2021).
- YouGov.co.uk. *COVID-19 Public Monitor*. <https://yougov.co.uk/covid-19> (2021).
- Santé Publique France. *CoviPrev: une enquête pour suivre l'évolution des comportements et de la santé mentale pendant l'épidémie de COVID-19*. <https://www.santepubliquefrance.fr/etudes-et-enquetes/coviprev-une-enquete-pour-suivre-l-evolution-des-comportements-et-de-la-sante-mentale-pendant-l-epidemie-de-covid-19> (2020).
- INSEE. *Estimations de population—Pyramide des âges régionales et départementales*. <https://www.insee.fr/fr/statistiques/3696315> (2020).
- Béraud, G. et al. The French Connection: the first large population-based contact survey in France relevant for the spread of infectious diseases. *PLoS ONE* **10**, e0133203 (2015).
- Lavezzo, E. et al. Suppression of a SARS-CoV-2 outbreak in the Italian municipality of Vo'. *Nature* **584**, 425–429 (2020).
- Riccardo, F. et al. Epidemiological characteristics of COVID-19 cases and estimates of the reproductive numbers 1 month into the epidemic, Italy, 28 January to 31 March 2020. *Eurosurveillance* **25**, 2000790 (2020).
- Cereda, D. et al. The early phase of the COVID-19 outbreak in Lombardy, Italy. *arXiv* <http://arxiv.org/abs/2003.09320> (2020).
- Li, R. et al. Substantial undocumented infection facilitates the rapid dissemination of novel coronavirus (SARS-CoV-2). *Science* **368**, 489 (2020).
- Davies, N. G. et al. Age-dependent effects in the transmission and control of COVID-19 epidemics. *Nat. Med.* **26**, 1205–1211 (2020).
- Galmiche, S. et al. *Etude des facteurs sociodémographiques, comportements et pratiques associés à l'infection par le SARS-CoV-2 (ComCor)*. <https://hal-pasteur.archives-ouvertes.fr/pasteur-03155847> (2021).
- Goldstein, E., Lipsitch, M. & Cevik, M. On the effect of age on the transmission of SARS-CoV-2 in households, schools, and the community. *J. Infect. Dis.* **223**, 362–369 (2021).
- Viner, R. M. et al. Susceptibility to SARS-CoV-2 infection among children and adolescents compared with adults: a systematic review and meta-analysis. *JAMA Pediatr.* **175**, 143 (2021).
- Di Domenico, L., Pullano, G., Sabbatini, C. E., Boëlle, P.-Y. & Colizza, V. Modelling safe protocols for reopening schools during the COVID-19 pandemic in France. *Nat. Commun.* <https://doi.org/10.1101/2020.05.08.20095521> (2021).
- Gaymard, A. et al. Early assessment of diffusion and possible expansion of SARS-CoV-2 Lineage 20I/501Y.V1 (B.1.1.7, variant of concern 202012/01) in France, January to March 2021. *Eurosurveillance* **26**, 2100133 (2021).
- Funk, T. et al. Characteristics of SARS-CoV-2 variants of concern B.1.1.7, B.1.351 or P.1: data from seven EU/EEA countries, weeks 38/2020 to 10/2021. *Eurosurveillance* **26**, 2100348 (2021).
- Bager, P. et al. Risk of hospitalisation associated with infection with SARS-CoV-2 lineage B.1.1.7 in Denmark: an observational cohort study. *Lancet Infect. Dis.* [https://doi.org/10.1016/S1473-3099\(21\)00290-5](https://doi.org/10.1016/S1473-3099(21)00290-5) (2021).
- Santé publique France. *COVID-19: point épidémiologique du 1er avril 2021*. <https://www.santepubliquefrance.fr/maladies-et-traumatismes/maladies-et-infections-respiratoires/infection-a-coronavirus/documents/bulletin-national/covid-19-point-epidemiologique-du-1er-avril-2021>.
- Amit, S., Regev-Yochay, G., Afek, A., Kreiss, Y. & Leshem, E. Early rate reductions of SARS-CoV-2 infection and COVID-19 in BNT162b2 vaccine recipients. *Lancet* **397**, 875–877 (2021).
- Lipsitch, M. & Kahn, R. Interpreting vaccine efficacy trial results for infection and transmission. *Vaccine* **39**, 4082–4088 (2021).
- Halloran, M. E., Struchiner, C. J. & Longini, I. M. Jr. Study designs for evaluating different efficacy and effectiveness aspects of vaccines. *Am. J. Epidemiol.* **146**, 789–803 (1997).
- Baden, L. R. et al. Efficacy and safety of the mRNA-1273 SARS-CoV-2 vaccine. *N. Engl. J. Med.* **384**, 403–416 (2021).
- Harris, R. J. et al. Effect of vaccination on household transmission of SARS-CoV-2 in England. *N. Engl. J. Med.* **385**, 759–760 (2021).
- Diekmann, O., Heesterbeek, J. P. & Roberts, M. G. The construction of next-generation matrices for compartmental epidemic models. *J. R. Soc. Interface* **7**, 873–885 (2010).
- Paraskevis, D. et al. A review of the impact of weather and climate variables to COVID-19: In the absence of public health measures high temperatures cannot probably mitigate outbreaks. *Sci. Total Environ.* **768**, 144578 (2021).
- Metelmann, S. et al. Impact of climatic, demographic and disease control factors on the transmission dynamics of COVID-19 in large cities worldwide. *One Health Amst. Neth.* **12**, 100221 (2021).
- Wang, J. et al. Impact of temperature and relative humidity on the transmission of COVID-19: a modelling study in China and the United States. *BMJ Open* **11**, e043863 (2021).
- Copernicus Climate Change Service. *ERA5 monthly averaged data on single levels from 1979 to present*. <https://cds.climate.copernicus.eu/doi/10.24381/cds.f17050d7> (2019).
- Dighe, A. et al. Response to COVID-19 in South Korea and implications for lifting stringent interventions. *BMC Med.* **18**, 321 (2020).
- Keeling, M. J. et al. Precautionary breaks: planned, limited duration circuit breaks to control the prevalence of COVID-19. *medRxiv* <https://www.medrxiv.org/content/10.1101/2020.10.13.20211813v1> (2020).
- Mercer, T. R. & Salit, M. Testing at scale during the COVID-19 pandemic. *Nat. Rev. Genet.* <https://doi.org/10.1038/s41576-021-00360-w> (2021).
- Fontanet, A. et al. SARS-CoV-2 variants and ending the COVID-19 pandemic. *Lancet Lond. Engl.* **397**, 952–954 (2021).
- Hale, T. et al. A global panel database of pandemic policies (Oxford COVID-19 Government Response Tracker). *Nat. Hum. Behav.* **5**, 529–538 (2021).
- ons.gov.uk. *The prevalence of long COVID symptoms and COVID-19 complications—Office for National Statistics*. <https://www.ons.gov.uk/news/statementsandletters/the-prevalenceoflongcovidsymptomsandcovid19complications> (2021).
- Huang, C. et al. 6-month consequences of COVID-19 in patients discharged from hospital: a cohort study. *Lancet* **397**, 220–232 (2021).
- Oliu-Barton, M. et al. SARS-CoV-2 elimination, not mitigation, creates best outcomes for health, the economy, and civil liberties. *Lancet* **397**, 2234–2236 (2021).
- Franceinfo. *Covid-19: sept Français sur dix approuvent les mesures annoncées par Emmanuel Macron, selon un sondage Odoxa Backbone Consulting*. <https://www.francetvinfo.fr/sante/maladie/coronavirus/covid-19-sept-francais-sur-dix-approuvent-les-mesures-annoncees-par-emmanuel-macron-selon-un-sondage-odoxa-backbone-consulting-4355545.html> (2021).
- Garnier, R., Benetka, J. R., Kraemer, J. & Bansal, S. Socioeconomic disparities in social distancing during the COVID-19 pandemic in the United States: observational study. *J. Med. Internet Res.* **23**, e24591 (2021).
- Pfefferbaum, B. & North, C. S. Mental health and the Covid-19 pandemic. *N. Engl. J. Med.* **383**, 510–512 (2020).
- Peretti-Watel, P., Alleaume, C., Léger, D., Beck, F. & Verger, P. Anxiety, depression and sleep problems: a second wave of COVID-19. *Gen. Psychiatry* **33**, e100299 (2020).
- Michie, S. & West, R. Behavioural, environmental, social, and systems interventions against covid-19. *BMJ* **370**, m2982 (2020).
- van der Pligt, J. Risk perception and self-protective behavior. *Eur. Psychol.* **1**, 34–43 (1996).
- Flaxman, S. et al. Estimating the effects of non-pharmaceutical interventions on COVID-19 in Europe. *Nature* **584**, 257–261 (2020).

58. Islam, N. et al. Physical distancing interventions and incidence of coronavirus disease 2019: natural experiment in 149 countries. *BMJ* **370**, m2743 (2020).
59. Li, Y. et al. The temporal association of introducing and lifting non-pharmaceutical interventions with the time-varying reproduction number (R) of SARS-CoV-2: a modelling study across 131 countries. *Lancet Infect. Dis.* **21**, 193–202 (2021).
60. Haug, N. et al. Ranking the effectiveness of worldwide COVID-19 government interventions. *Nat. Hum. Behav.* **4**, 1303–1312 (2020).
61. Qian, H. et al. Indoor transmission of SARS-CoV-2. *Indoor Air* **31**, 639–645 (2021).
62. Giordano, G. et al. Modeling vaccination rollouts, SARS-CoV-2 variants and the requirement for non-pharmaceutical interventions in Italy. *Nat. Med.* <https://doi.org/10.1038/s41591-021-01334-5> (2021).
63. Moore, S., Hill, E. M., Tildesley, M. J., Dyson, L. & Keeling, M. J. Vaccination and non-pharmaceutical interventions for COVID-19: a mathematical modelling study. *Lancet Infect. Dis.* [https://doi.org/10.1016/S1473-3099\(21\)00143-2](https://doi.org/10.1016/S1473-3099(21)00143-2) (2021).
64. Kiem, C. et al. A modelling study investigating short and medium-term challenges for COVID-19 vaccination: From prioritisation to the relaxation of measures. *EClinicalMedicine* **38**, 101001 (2021).
65. Carlson, C. J., Gomez, A. C. R., Bansal, S. & Ryan, S. J. Misconceptions about weather and seasonality must not misguide COVID-19 response. *Nat. Commun.* **11**, 4312 (2020).
66. Hall, V. J. et al. SARS-CoV-2 infection rates of antibody-positive compared with antibody-negative health-care workers in England: a large, multicentre, prospective cohort study (SIREN). *Lancet* **397**, 1459–1469 (2021).
67. Wang, P. et al. Antibody resistance of SARS-CoV-2 variants B.1.351 and B.1.1.7. *Nature* **593**, 130–135 (2021).
68. The New York Times. *As over 100 million people in the U.S. are fully vaccinated, concern grows over reaching those who haven't gotten shots.* <https://www.nytimes.com/2021/04/30/us/politics/us-100-million-vaccinated.html> (2021).
69. YouGov.co.uk. *Personal measures taken to avoid COVID-19.* <https://yougov.co.uk/topics/international/articles-reports/2020/03/17/personal-measures-taken-avoid-covid-19>.
70. YouGov.co.uk. *COVID-19 fear of catching.* <https://yougov.co.uk/topics/international/articles-reports/2020/03/17/fear-catching-covid-19>.
71. EPIcx-lab. *EPIcx-lab/COVID-19: First release.* <https://doi.org/10.5281/zenodo.5603812> (2021).

Acknowledgements

This study is partially funded by: ANR projects DATAREDUX (ANR-19-CE46-0008-03), EVALCOVID-19 (ANR-20-COVI-0007), and SPHINX (ANR-17-CE36-0008-05); EU H2020 grants MOOD (H2020-874850) and RECOVER (H2020-101003589).

Author contributions

V.C. conceived and designed the analysis. L.D.D. and C.E.S. performed the analysis. V.C. wrote the manuscript. L.D.D., C.E.S., P.Y.B., C.P., P.C., J.P., S.C., F.B., H.N., D.L.B. and V.C. critically revised the manuscript and approved its final version.

Competing interests

The authors declare no competing interests.

Additional information

Supplementary information The online version contains supplementary material available at <https://doi.org/10.1038/s43856-021-00057-5>.

Correspondence and requests for materials should be addressed to Vittoria Colizza.

Peer review information *Communications Medicine* thanks the anonymous reviewers for their contribution to the peer review of this work. Peer reviewer reports are available.

Reprints and permission information is available at <http://www.nature.com/reprints>

Publisher's note Springer Nature remains neutral with regard to jurisdictional claims in published maps and institutional affiliations.



Open Access This article is licensed under a Creative Commons Attribution 4.0 International License, which permits use, sharing, adaptation, distribution and reproduction in any medium or format, as long as you give appropriate credit to the original author(s) and the source, provide a link to the Creative Commons license, and indicate if changes were made. The images or other third party material in this article are included in the article's Creative Commons license, unless indicated otherwise in a credit line to the material. If material is not included in the article's Creative Commons license and your intended use is not permitted by statutory regulation or exceeds the permitted use, you will need to obtain permission directly from the copyright holder. To view a copy of this license, visit <http://creativecommons.org/licenses/by/4.0/>.

© The Author(s) 2021

END

L Di Domenico, CE Sabbatini, PY Boëlle, C Poletto, P Crépey, J Paireau, S Cauchemez, F Beck, H Noel, D Levy-Bruhl, V Colizza

Adherence and sustainability of interventions informing optimal control against the COVID-19 pandemic

Communications Medicine 1, 57 (2021)

4.3 Discussion

We analyzed the effectiveness of different lockdown measures in controlling the spread of COVID-19, with a focus on comparing severe and moderate lockdown scenarios, using the empirically observed loss of adherence. We confirmed that high intensity lockdowns would be more efficient in controlling the epidemic in a shorter time compared to moderate lockdowns, but most importantly:

- We showed that moderate interventions would be more largely affected by adhesion loss, with the risk of compromising the control of the epidemic if these were kept for a long time.
- We introduced a data-driven "distress index" to compare the impact of different interventions on the quality of life of the population.
- We found that for intermediate values of the distress index, shorter strict lockdowns (≤ 4 weeks) are largely more effective than longer moderate lockdowns (≥ 6 weeks)

The concept of acceptability was often seen as a potential argument against implementing early and strict interventions [111, 112]. However, our research findings challenge this notion and suggest that opting for milder interventions instead of stringent policies may have negative consequences in the long run, particularly when they are prolonged in time and when adherence to these measures decreases.

Our study revealed that implementing severe lockdown measures had a rapid and significant impact on reducing the spread of the epidemic. This resulted in a swift relief of the burden on hospitals and the resumption of non-COVID medical services. Furthermore, by maintaining low levels of the virus during the gradual exit phase, we were able to achieve better control over viral circulation [15], supported for example by a robust TTI system. Interestingly, we found that a strict two-week closure, followed by the reinstatement of a curfew during the exit phase, could bring about substantial improvements in the epidemic situation within a very short period of time. In contrast, moderate lockdown measures took longer to yield results comparable to those achieved by strict measures. Prolonged interventions resulted in a prolonged plateau in the epidemic, which kept hospitals under pressure for several weeks. Moreover, if adherence to the restrictions declined over time, the effectiveness of moderate interventions decreased significantly. This does not occur for strict interventions.

The global scientific community widely agrees that mass vaccination has proven to be the most effective approach in mitigating the impact of the COVID-19 pandemic [113]. However, during the study period, effective epidemic control still required the implementation of significant social distancing measures [12, 114]. From a public health perspective, social distancing and vaccination are interventions that provide greater benefits when applied simultaneously [115]. Moreover, during the study period, it was crucial to convey the message that vaccination was a complement to social distancing measures and not a substitute [116].

Another factor that has contributed to the alleviation of social distancing measures during the summer, alongside vaccines, was the impact of seasonality. Seasonality encompasses not just climatic factors but also human behavior, given that people tend to spend more time outdoors in the summer. Even during the transition following the first wave, studies were emerging to quantify the seasonal effects on transmissibility.

As the summer of 2021 approached, it was estimated that this seasonal behavior mitigates transmission, resulting in a decrease in transmissibility of approximately 10% [117, 118]. Nevertheless, due to lingering uncertainties linked to this factor, our scenario analysis explored a spectrum of values, ranging from the more cautious "no reduction" to an optimistic 30%.

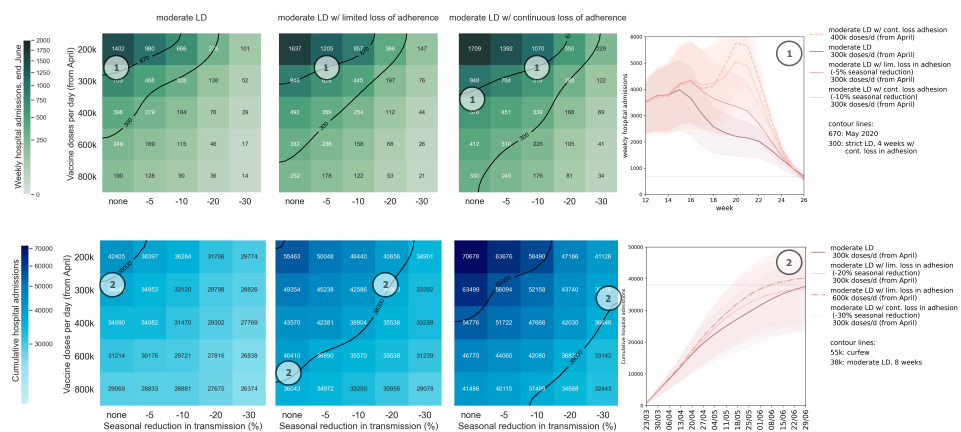
From our simulations, it was observed that doubling the speed of vaccine administration coupled with seasonal effects reducing transmissibility by 5-10% would have been sufficient to compensate for the effects of adherence waning (refer to Figure 6 in the paper (**article #2**) and **Figure 4.2**). Lifting restrictions with the conditions experienced in mid-July 2020 was expected to lead to an epidemic rebound. Managing the epidemic while gradually releasing non-pharmaceutical interventions should have mainly relied on the speed of the vaccination rollout.

It is crucial to acknowledge the limitations of our study. We hypothesized that the loss of adherence would have a similar impact regardless of the intensity of lockdown measures, although various studies on adherence have been conducted in different regions of the world, revealing that adherence varies over time and across different protective behaviors. For instance, there is an increase in adherence to low-cost and habitual behaviors like mask-wearing, while the same is not observed for high-cost and sensitive behaviors such as physical distancing [119]. Another aspect we did not consider in our study was the repetition of implemented restrictive measures. Common sense suggests that adherence might also be related to the number of occurrences, meaning that the same measure could be less effective when implemented for the second or third time. This aspect has not been investigated in France, as the same sequence of interventions has never been repeated, however, it could be an interesting study for countries such as Italy and Chile

The distress index used in our study, which measures policy-induced distress based on mobility data, did not account for specific demographic groups or vulnerable populations disproportionately affected by the measures. Moreover, it cannot be directly compared with other indicators, such as the stringency index or mental health indicators that measure anxiety or disorders. Our study measured adherence overall and not by age group, other studies have shown that younger participants were more likely to make misrepresentations and not adhere [120].

Until now, our discussions have mainly focused on the measures applied from the third wave onwards. However, in order to thoroughly assess the sustainability of these measures, we should also consider a longer time horizon. It is crucial to acknowledge another limitation of the study, which is the absence of analysis regarding alternative options overall time period, such as scenarios where the curfew was never implemented. This lack of evaluation of alternatives could have a considerable impact on the long-term sustainability of the measures adopted. There could have been alternative approaches that were equally effective or even more sustainable from both economic and social perspectives.

Figure 4.2: Impact of accelerated vaccination and seasonality. Heatmaps show median values of weekly hospital admissions at the end of June (w26) (top row) and cumulative hospital admissions in the time period w12-w26 (bottom row), as functions of vaccination rhythm (y axis) and seasonal reduction in transmission (x axis) for moderate lockdowns of 8 weeks with full adherence (left), limited loss of adherence (center), continuous loss of adherence (right). Contour lines indicate values of reference of specific scenarios or situations defined in the legends. Circled numbers refer to conditions of interest discussed above. Plots in the fourth column show hospital admissions over time (weekly admissions, top row; cumulative admissions, bottom row) associated to the conditions labelled by the circled numbers. Curves refer to the median trajectory; shaded areas around the curves correspond to the 95% probability range obtained from 250 stochastic simulations. The type of intervention is coded by different line colors; the vaccination rhythm is coded by different line types; the reduction in transmissibility due to seasonality is coded by different color shades. Horizontal solid lines correspond to the value of the contour line indicated by the circled number in the top right-hand corner.



Evaluating the effectiveness of COVID-19 interventions: a spatial perspective

5

This chapter focuses on analyzing the effectiveness of COVID-19 interventions implemented in France, from September 2020 to June 2021. The central aspect of this investigation has been to quantify the impact of each implemented measure (different lockdowns, nighttime curfews), considering both health and societal indicators. We also considered the spatial connectivity among different regions, emphasizing how the effectiveness of these measures has been influenced by interregional mobility flows. Once we have set all these elements, we analyzed further the effects of NPIs and we proposed alternative scenarios. Scenarios such as early implementation of intermittent lockdowns instead of the prolonged periods of nighttime curfew.

Throughout this chapter, I will examine and analyze the findings presented in **article #2**. The additional information referred to in **article #1** can be found in the **Supplementary Materials** section of the thesis.

5.1 Introduction

Throughout the course of the health crisis, several European nations, including France, Germany, and the UK, implemented national lockdowns. These measures included restricted movement, the closure of non-essential businesses, and limitations on social gatherings [121]. In contrast, countries such as Sweden and the Netherlands adopted more relaxed strategies, primarily relying on voluntary guidelines [121]. Italy, on the other hand, adopted a tiered system to implement targeted and localized measures [121, 122]. Nighttime curfews were imposed in some countries, while others chose not to implement them [121, 123]. Additionally, various factors, such as seasonal conditions and the emergence of more transmissible variants, influenced the effectiveness of NPIs both in terms of timing and geographical location [124, 12, 125, 62].

The diversity of interventions adopted and of the situations across different territories prompted us to ponder the questions: Can we quantify the relative contributions of temporal and spatial factors on NPIs' effectiveness? What if France had implemented different measures? How would the outcomes have been altered, in terms of health and societal indicators? The analysis presented in **article #1** led us to consider an extended time horizon, encompassing evaluations of alternative approaches over a longer duration. For example, this could involve evaluating the feasibility and consequences of implementing intermittent lockdowns throughout the designated period, thus avoiding the prolonged period of moderate measures (e.g. 188 consecutive days under curfew in France) that has proven to be burdensome for the population [12, 126].

To address these questions, a more precise quantification of the measures' impact was necessary, enabling the simulation of alternative scenarios. We evaluated the effectiveness of various implemented NPIs, with a particular focus on nighttime curfews, an aspect that has received limited attention in the existing literature [127, 128, 129, 130]. For every NPI implemented we disentangled the relative contributions of spatial and temporal factors (vaccination efforts, seasonal patterns, new variants seeding, increased variant transmissibility, etc.), so it was possible to

distinguish the role of the drivers that influenced epidemic dynamics and estimate their effectiveness.

Furthermore, observations of spatial spread patterns during various phases of the epidemic [50] (e.g., a second wave with a spatial concentration in the south-east and a third wave was initially shaped by the spread of the Alpha variant in the north and the Marseille region) prompted us to investigate the influence of human mobility on the efficacy of interventions, unveiling insights into the importance of interregional connectivity and its role in introducing an additional layer of complexity to the pandemic dynamics.

We thus introduced a regionally-based spatially-explicit epidemic metapopulation model (**model #2**). Using (**model #2**), informed by mobile phone data in France, we captured the interplay between regional epidemics and provided a more comprehensive understanding of the effectiveness of lockdowns and curfews of various type.

This study underscores the importance of considering geographical connectivity in the formulation and assessment of public health policies. These findings have the potential to guide policymakers and health authorities in crafting targeted interventions, thereby enhancing the overall effectiveness of their management strategies.

5.2 Article #2: The impact of spatial connectivity on NPIs effectiveness

BEGINNING

CE Sabbatini, G Pullano, L Di Domenico, S Rubrichi, S Bansal, V Colizza

The impact of spatial connectivity on NPIs effectiveness

XXXXXX

The impact of spatial connectivity on NPIs effectiveness

Chiara E. Sabbatini¹, Giulia Pullano², Laura Di Domenico¹, Stefania Rubrichi³, Shweta Bansal², Vittoria Colizza^{1,*}

¹Sorbonne Université, INSERM, Pierre Louis Institute of Epidemiology and Public Health, Paris, France. ²Department of Biology, Georgetown University, Washington, DC, USA. ³Orange Labs, Sociology and Economics of Networks and Services (SENSE), Chatillon, France. *corresponding author: vittoria.colizza@inserm.fr

Abstract

Background. France implemented a combination of non-pharmaceutical interventions (NPIs) to manage the COVID-19 pandemic between September 2020 and June 2021. These included a lockdown in the fall 2020 – the second since the start of the pandemic – to counteract the second wave, followed by a long period of nighttime curfew, and by a third lockdown in the spring 2021 against the Alpha wave. Interventions have so far been evaluated in isolation, neglecting the spatial connectivity between regions through mobility that may impact NPI effectiveness.

Methods. Focusing on September 2020 – June 2021, we developed a regionally-based epidemic metapopulation model informed by observed mobility fluxes from daily mobile phone data and fitted the model to regional hospital admissions. The model integrated data on vaccination and variants spread. Scenarios were designed to assess the impact of the Alpha variant, characterized by increased transmissibility and risk of hospitalization, of the vaccination campaign and alternative policy decisions.

Results. The spatial model better captured the heterogeneity observed in the regional dynamics, compared to models neglecting inter-regional mobility. The third lockdown was similarly effective to the second lockdown after discounting for immunity, Alpha, and seasonality (51% vs 52% median regional reduction in the reproductive number R_0 , respectively). The 6pm nighttime curfew with bars and restaurants closed, implemented in January 2021, substantially reduced COVID-19 transmission. It initially led to 49% median regional reduction of R_0 , decreasing to 43% reduction by March 2021. In absence of vaccination, implemented interventions would have been insufficient against the Alpha wave. Counterfactual scenarios proposing a sequence of lockdowns in a stop-and-go fashion would have reduced hospitalizations and restriction days for low enough thresholds triggering and lifting restrictions.

Conclusions. Spatial connectivity induced by mobility impacted the effectiveness of interventions especially in regions with higher mobility rates. Early evening curfew with gastronomy sector closed allowed authorities to delay the third wave. Stop-and-go lockdowns could have substantially lowered both healthcare and societal burdens if implemented early enough, compared to the observed application of lockdown-curfew-lockdown, but likely at the expense of several labor sectors. These findings contribute to characterize the effectiveness of implemented strategies and improve pandemic preparedness.

Keywords. COVID-19, NPIs, modeling, curfew, restrictions.

INTRODUCTION

Non-pharmaceutical interventions (NPIs) represented the primary response to the COVID-19 pandemic in 2020-2021 before mass vaccination campaigns reached a substantial fraction of the population in Europe¹. After the generalized use of strict lockdowns during the first wave²⁻⁹, combinations of NPIs reached finer granularity in the second and third waves¹⁰, occurring in the fall 2020 and in the spring 2021, respectively. These included the closure of certain business sectors (e.g. restaurants, retail and leisure venues), remote education for specific school levels (e.g. high school), bans of gatherings, mobility restrictions, and nighttime curfews at different hours, in addition to less stringent lockdowns. They were meant to manage a rapidly evolving context characterized by the emergence of the first variant of concern^{11,12} and the rollout of vaccination¹, while pandemic fatigue developed in the population¹³⁻¹⁵.

Spatial heterogeneities in COVID-19 resurgence¹⁶ and in the geographic seeding of the Alpha variant further added to the complexity of the pandemic phase between the fall 2020 and the summer 2021. In France, the second wave showed a clear spatial pattern with a resurgence in the south-east of the country (**Figure 1a**), likely fueled by summer displacements to touristic destinations. In contrast, the third wave was initially shaped by the seeding of the Alpha variant in the north and in the region of Marseille (Provence-Alpes-Côte d'Azur; **Figure 1a**) then invading other regions through mobility. Population response to nationwide restrictions varied regionally^{17,18} with the potential to affect the epidemiological impact both locally and in other regions connected through mobility fluxes. Spatial connectivity determines geographic spillover events¹⁹⁻²¹ and source-sink mechanisms^{22,23} that can weaken local control policies. Estimating NPIs' effectiveness and societal burden while accounting for all these elements is key to adequately plan for the medium-term phase of a pandemic, i.e. following the initial emergency and before mass vaccination allows lifting restrictions.

Here, we introduced a regionally-based spatially-explicit epidemic metapopulation model that integrates mobility fluxes estimated from mobile phone data to study the COVID-19 pandemic in France between September 2020 and June 2021. Accounting for spatiotemporal heterogeneities, we estimated the effectiveness of implemented NPIs by disentangling spatial and temporal effects (inter-regional mobility, Alpha variant seeding and penetration, seasonality, vaccination). We also examined alternative policy options to the ones implemented by authorities to best balance the epidemiological and healthcare impacts of interventions with the resulting burden of restrictions. The aim was to improve the guidance of policy decisions for the medium-term management of future pandemic threats.

METHODS

Restrictions

In **Table 1** we describe the main restrictions implemented in France during the study period (September 2020 – June 2021). In response to the second wave, on October 17, 2020, a nighttime curfew from 9pm to 6am was enforced in several areas with degrading indicators. Due to the rapid surge in the number of infections, a national lockdown was put in place starting October 30, 2020. The restrictions imposed were less stringent compared with the first national lockdown in the spring 2020, as schools and a larger number of job sectors were allowed to remain open.

Bars, restaurants, gyms, leisure venues and other non-essential services were closed. Displacements were limited to a maximum radius of one kilometer from home. The lockdown was lifted on December 15, 2020, with the application of a nighttime curfew (8pm – 6am). Soon after the detection of the Alpha variant on the French territory in early 2021, curfew hours were extended nationally between 6pm and 6am on January 16, 2021. Following the rise in cases due to the Alpha epidemic initiating the third wave, on March 20, 2021 localized lockdowns were implemented in the regions of Île-de-France, Haute-de-France and in few other French departments at high incidence. The lockdown was extended to the whole country soon after on April 3, 2021, with the closure of non-essential activities. The gastronomy sector remained closed and the curfew was maintained starting at 7pm. However, differently from the second lockdown, schools were closed for most of the period, extending the planned closure for school holidays of 1 week in the primary schools, and of 2 weeks in the middle and high schools. Movements restrictions were only applied to trips exceeding 10km from the place of residence. Also, stay-at-home orders of the second lockdown were converted into recommendations to spend time outdoor to limit transmission in closed settings in this period. The third lockdown ended on May 3, 2021.

Data

Mobility Anonymized aggregated mobility fluxes extracted from mobile phone signaling data were provided by the Orange business service Flux Vision^{18,24}. Data included de-identified origin-destination matrices reporting the daily number of user displacements among 1,436 EPCI (Établissements Publics de Coopération Intercommunale) areas in mainland France. The anonymization procedure was approved by the French data protection authority CNIL (Commission Nationale de l'Informatique et des Libertés). Origin-destination matrices were aggregated at regional level to compute weekly coupling probabilities p_{ij} between regions i and j and inform our model (see the **Model subsection**). The coupling probability p_{ij} for a given week is defined as the probability that a resident in i visits j due to his mobility trajectory:

$$p_{ij} = \frac{w_{ij}}{\sum_k w_{ik}}$$

where w_{ij} is the average number of daily trips between i and j for a given week. We considered the daily average to avoid daily fluctuations in the weekly pattern. We chose as a pre-pandemic baseline period the week 6, 2020 (February 03, 2020 – February 09, 2020), as in previous work¹⁷.

Seasonality. A number of studies have suggested that SARS-CoV-2 transmission is seasonally varying, modulated by environmental variables and environmentally-mediated social behavior^{25–28}. We integrated seasonality in the regional transmissibility (see **Model subsection**) based on estimates provided in Ref.²⁹. These estimates quantify the impact of seasonal climatic conditions on transmission rate based on daily data from the National Oceanic and Atmospheric Administration (**Figure S12, Supplementary Materials**). We fitted the estimates with a sinusoidal function with 1-year period, one per each region, in order to obtain daily values of the seasonality factor $\sigma_i(t)$ affecting transmission in region i on day t . We used a least-squares optimization function for the fit.

Alpha variant. According to genomic surveillance data³⁰, the Alpha variant started to circulate in France at the end of 2020 and replaced the previous SARS-CoV-2 strains in March 2021³¹. Results of a large-scale genome sequencing initiative launched in January (so-called Flash surveys³⁰) showed that the Alpha variant was responsible for 3.3% of detected COVID-19 cases on January 8, 2021 at the national level, with large spatial heterogeneity, ranging from 0.2% penetration to 6.9%. We modeled the overall virus transmissibility (i.e. wild strain and Alpha variant) by accounting for the regional frequency of Alpha over time and its transmission advantage, to be fitted (**Figure S12**). We modeled the presence of Alpha over time in each region by modulating transmissibility according to the daily variant penetration and its daily transmission advantage (see Model subsection). In agreement with prior estimates³⁰, we found that the SARS-CoV-2 Alpha variant was 58% more transmissible than the wild type in the invasion phase. We also considered a 64% increase in hospitalization rate³².

Vaccination. We modeled three different vaccination strata, i.e. unvaccinated, vaccinated with one dose or with two doses, based on data on the administration of doses by region³³ (**Figure S12**). We assumed vaccines to be effective 14 days after injection. We considered 60% vaccine effectiveness against infection and 15% against transmission after the first injection^{34,35}, increasing to 87.5% and 68%, respectively, after the second injection^{35,36}. We considered 80% vaccine effectiveness against hospitalization after one dose, and 97.2% after two doses^{34,36}. We did not consider waning in vaccine effectiveness in the timeframe under study.

Normalcy index. The Economist's Normalcy index³⁷ is a measure of the impact of the pandemic on human behavior, integrating multiple daily indicators of human activities in a score from 0 to 100, with 100 representing the pre-pandemic level (**Figure S1**). We used the Normalcy index to define the effective days under restrictions (see the corresponding subsection).

Model

Metapopulation model summary. We used a discrete stochastic non-Markovian transmission model with a metapopulation structure at the regional level. The population was divided in the 12 regions of mainland France (excluding Corsica). The daily force of infection λ_i in region i at time t accounts for disease transmission due to (i) infected residents not moving out of the region (λ_{ii}) (ii) infected visitors coming from other regions (λ_{ji}^v) and (iii) returning residents previously infected in other regions (λ_{ij}^r)³⁸:

$$\lambda_i = \lambda_{ii} + \sum_{j \neq i} \lambda_{ji}^v + \sum_{j \neq i} \lambda_{ij}^r$$

Let $\beta_i(t)$ be the transmission rate of region i on day t , $p_{ij}(t)$ the coupling probability between regions i and j estimated from mobility data; let $\hat{N}_i(t) = p_{ii}(t)N_i + \sum_{j \neq i} p_{ji}(t)N_j$ and $\hat{I}_i(t) = p_{ii}(t)I_i(t) + \sum_{j \neq i} p_{ji}(t)I_j(t)$ be the effective population and the effective number of infections in region i on day t , respectively³⁸. Then, the daily force of infection can be written as

$$\begin{cases} \lambda_{ii}(t) = \beta_i(t) p_{ii}^2(t) \frac{I_i(t)}{\hat{N}_i(t)} \\ \lambda_{ji}^v(t) = \beta_i(t) p_{ii}(t) p_{ji} \frac{I_j(t)}{\hat{N}_i(t)} \\ \lambda_{ij}^r(t) = \beta_j(t) p_{ij}(t) \frac{\hat{I}_j(t)}{\hat{N}_j(t)} \end{cases}$$

where $\beta_i(t)$ accounts for both seasonality and the presence of the Alpha variant. All variables in the previous equations depend on daily time t , but we dropped the dependence for the sake of clarity. We indicate with $A_i(t) \in [0, 1]$ the variant's penetration in region i on day t , with $\eta_i(t)$ the transmission advantage of the Alpha variant, and with $\sigma_i(t)$ the seasonality factor. The resulting transmission rate in region i on day t can be written as:

$$\beta_i(t) = \beta_i^{intrinsic}(t) \cdot [(1 - A_i(t) + \eta_i(t) \cdot A_i(t))] \cdot \sigma_i(t)$$

With $\beta_i^{intrinsic}(t)$ being the fitted transmission rate. We considered a SEIHR compartmental scheme (**Figure S2** of the **Supporting Materials, SM**), including susceptible, exposed, infectious, hospitalized and recovered. The model was stratified by three different vaccination status. All the data presented before were integrated in the model at the regional level (**SM**). Parameters, values, and sources used to define the compartmental scheme are listed in **Table S1**. The study period ranges from September 21, 2020 to June 13, 2021 (w39-2020 to w23-2021), to capture the second and third COVID-19 waves.

Inference framework and validation. Model parameters were estimated in a Bayesian framework using Markov Chain Monte Carlo (MCMC) method (**SM**). The likelihood function was evaluated on daily data of regional hospital admissions. The log-likelihood function is of the form:

$$\log \mathcal{L}(data|\Theta) = \sum_{i=1}^{12} \sum_{t=t_{start}}^{t_{end}} \log Poiss(H_{obs}(t, i) | H_{pred}(t, i, \Theta))$$

where $\Theta = \{\beta_1^{intrinsic}, \dots, \beta_{12}^{intrinsic}\}$ indicates the regional transmission rates to be estimated. $H_{obs}(t, i)$ is the observed number of hospital admissions on day t in the region i , $H_{pred}(t, i, \Theta)$ is the number of hospital admissions predicted by the model using parameter values Θ , $Poiss(\cdot | H_{pred}(t, i, \Theta))$ is the probability mass function of a Poisson distribution with mean $H_{pred}(t, i, \Theta)$, and $[t_{start}, t_{end}]$ is the time window considered for the fit. The time windows used for the fit are defined based on the interventions applied in France (**Table 1**). When the time window includes a lockdown, we also fitted the time from lockdown implementation to hospitalization peak for each region, to better capture the peak and the decline of the epidemic curve that may vary regionally based on population response³⁹ (**Table S3**). We validated the model by comparing its predictions of the percentage of antibody-positive people with seroprevalence estimates from multiple studies at different dates^{40,41}. Modeling results were in good agreement with the serological estimates, both at the regional and at the national levels (**Figures S13, S14, SM section 2.4**).

Reproductive numbers. We computed the regional basic reproductive numbers with the next-generation approach⁴² for each time window of the fit. The resulting estimates are obtained from the fitted transmissibility values of the metapopulation model that account for the mobility process. We distinguished between the basic reproductive number R_0 obtained from the fitted transmissibility $\beta_i(t)$ that includes seasonality and the increasing frequency of Alpha, and the intrinsic basic reproductive number $R_0^{intrinsic}$ that discounts for the seasonal and variant effects, in order to compare different time windows. Analogously, we computed the corresponding effective reproductive numbers, R and $R^{intrinsic}$, accounting for immunity.

Counterfactual lockdown scenarios. We modeled alternative policy scenarios with respect to the lockdown-curfew-lockdown policy implemented in France, and considered stop-and-go nationwide lockdowns, i.e. repeated lockdowns intercut by periods with no restrictions. As French authorities did not establish thresholds to apply restrictions, we considered stop-and-go lockdown scenarios triggered and released by a given threshold of per-capita hospital admissions, and then we systematically explored these thresholds. We used as reference value T of the trigger threshold the hospitalizations per capita in the region at the highest hospitalization incidence when the second lockdown was applied, i.e. the Auvergne-Rhône-Alpes region (ARA). This level corresponds effectively to the highest hospital occupation that authorities deemed sustainable. For the release threshold R we considered instead the average hospitalization incidence reported across regions at the moment of lifting the second lockdown. We used the average value because, differently from the triggering threshold, the release threshold is not constrained to a maximum capacity.

We systematically explored different values of trigger and release thresholds, expressed as percentage threshold variations (from T to $T-95\%$, from $R+5\%$ to $R-90\%$). Given a pair of values of trigger and release thresholds, a nationwide lockdown is activated in the stop-and-go lockdown scenarios when a region first reaches T , and it is lifted when the last region reaches R . A table with the threshold values is included in the SM (**Table S5**). In the scenarios we simulate a repetition of lockdowns, triggered and lifted according to the above rules, assuming that their stringency would be equal to the one estimated for the second lockdown applied in France (LD2) for the first lockdown in the stop-and-go series, and to the one estimated for the third lockdown applied in France (LD3) for the following lockdowns simulated in the series. This was done to align with the observed political choice of moving from a lockdown largely imposing at-home restrictions (LD2) to one promoting time spent outdoors (LD3). In each simulated nationwide lockdown in the stop-and-go scenarios, the transmissibility and the inter-regional mobility are set to the estimated values of the corresponding lockdown applied in France in the period under study (LD2 or LD3, **Figure S23**). The phasing out of each lockdown was simulated through a two-week piecewise linear function to capture a progressive return to normality after restrictions⁴³ (**Figure S22**).

Effective days under restrictions. We used the Normalcy index³⁷ to weight the days under restrictions by capturing population response and to compare restriction days across intervention scenarios. We defined an “effective day” \mathcal{D}_t spent under restrictions as

$$\mathcal{D}_t = \frac{\mathcal{N}(\text{pre LD2}) - \mathcal{N}(t)}{\mathcal{N}(\text{pre LD2}) - \mathcal{N}(\text{LD2})}$$

where $\mathcal{N}(t)$ is the Normalcy index at time t . \mathcal{D}_t ranges from 0 to 1, with 0 correspond-

ing to the pre-lockdown situation in early October 2020 and 1 representing a day under the second lockdown. We estimated $\mathcal{D}_t = 0.58$ under curfew (average over all curfew types, applied from December 2020 to April 2021) and $\mathcal{D}_t = 0.77$ in the third lockdown. Effective days are also computed for the counterfactual scenarios, based on the duration of implementation emerging from the choice of the trigger and release thresholds.

Non-spatial model. We tested a non-spatial model, i.e. a model where regions are not coupled by mobility ($p_{ij} = 0$). We fitted the model to the regional hospital admission data (**Figure S15**) and evaluated its performance in comparison to the metapopulation model integrating mobility. We performed a model selection test using the deviance information criterion (DIC) and we evaluated the errors of each model using the mean absolute error (MAE) metric. (**Subsection 2.5 of the SM**).

Role of the funding source. The funders had no role in study design, data collection, data analysis, data interpretation, writing of the manuscript, and decision to submit.

RESULTS

In the fall of 2020, French authorities introduced control measures in response to the growing epidemic (**Figure 1, Table 1**). The nighttime curfew implemented in few departments on October 17 was followed by a national lockdown on October 30, the second since the start of the pandemic. Inter-regional mobility dropped by 43-85% in the first three weeks of lockdown compared to pre-pandemic levels, depending on the region (**Figure 1b**). By fitting the metapopulation model to hospital admission data (**Figure 1c**), we estimated a regional median reduction of the basic reproductive number R_0 of 45% (IQR 42-52%) during the second lockdown compared to the pre-lockdown value in early October 2020 (**Figure 2a**). The 8pm nighttime curfew implemented to phase out the second lockdown in mid-December was not enough to limit community transmission ($R > 1$; **Figure 2b**), due to winter seasonality and Alpha initial spread. Anticipating at 6pm the start of the nighttime curfew on January 16, 2021 resulted in $R < 1$ in all regions except Île-de-France and Hauts-de-France. Such control however deteriorated over time, due to Alpha becoming dominant in the country. Inter-regional mobility remained fairly stable during this time, with a reduction of 23-70% across regions compared to pre-pandemic level, with the exception of the increase registered in February for the school holidays.

Discounting for Alpha and seasonality allows us to compare the effectiveness of the 6pm curfew throughout the period in which the variant was becoming dominant, while entering into the spring season. Little change was estimated during the school holidays ($R_0^{intrinsic}$ reduction of 49% (IQR 46-51%) vs. 48% (IQR 44-52%) in the pre-holiday period), but the effectiveness lowered afterwards ($R_0^{intrinsic}$ reduction of 43% (IQR 40-44%) post-holiday). Effectiveness varied comparably in all regions during these 3 periods with the 6pm curfew (Spearman correlation $r=0.9$, $p<0.01$; **Figure S19**), but less so when comparing 8pm and 6pm curfew periods ($r=0.6$, $p=0.04$). With hospital admissions rapidly increasing (estimated regional median $R=1.14$ (IQR 1.11-1.19)), on March 20 authorities enforced a third lockdown in the highest incidence areas (Île-de-France, Haute-de-France, and few other departments; **Figure 1a**), then extended it nationwide on April 3, till May 3.

The third lockdown resulted in 6% higher Normalcy index compared to the second lockdown (**Figure S1**). A small mobility drop was registered passing from the curfew to the third lockdown (**Figure 1b**). We estimated a 20% (IQR 18-23%) regional median reduction of R_0 during the third lockdown (**Figure 2a**), i.e. less than half the value achieved with the application of the second lockdown. By discounting seasonality and the Alpha variant, our model indicates however that the intrinsic effectiveness of the two lockdowns was rather similar ($R_0^{intrinsic}$ reduction of 52% (IQR 49-59%) in the second lockdown vs. 51% (IQR 48-52%) in the third).

NPI effectiveness varied regionally throughout the period under study (**Figure 2c**, **Figure 3a**). The metapopulation model integrating observed inter-regional mobility was found to be statistically preferable with respect to a non-spatial model neglecting connectivity (**Table S4**), yielding a lower mean absolute error in 64% of the regions (**Figure S16**). Relative deviations on the estimates of R obtained with a non-spatial model compared to the metapopulation approach could be >40% and were found to increase with increasing mobility for a given regional population (Spearman correlation $r=0.46$, $p < 10^{-4}$, **Figure 3b**).

Alpha spread was estimated to be responsible for 129,335 (IQR 112,290-144,396) additional hospitalizations in mainland France, corresponding to 41% of the overall hospitalizations recorded in the study period (**Figure S10**). Our model predicted that Île-de-France, the region of Paris, was the most impacted by the variant (50% of the overall hospitalizations), followed by Hauts-de-France (48%). The least impacted was Nouvelle Aquitaine (29%). This result was not exclusively explained by the geographical seeding of Alpha (**Figure 1a**). Indeed, if Île-de-France reported the largest variant frequency at the start of January 2021 (**Figure S20**), such ranking was rapidly altered by mid-January, despite the same control measures being applied nationwide. Vaccination was estimated to prevent 255,195 (IQR 224,993-279,502) hospitalizations in mainland France in the time period under study, equal to 81% of the hospitalizations that were actually reported (**Figure S20**). An anticipated and faster vaccination rollout, as implemented in the UK, would have prevented additional 122,877 (IQR 107,404-137,971) hospitalizations (i.e. additional 39%). Most importantly, without vaccination, implemented NPIs would have not been sufficient to control the Alpha variant (**Figure S20c**).

The application of nighttime curfew allowed authorities to manage the pandemic between the second and third waves, albeit maintaining a high incidence of cases and hospitalizations. To examine whether additional policies could have been more beneficial, we explored counterfactual scenarios with stop-and-go lockdowns. With the trigger and release thresholds (T and R in **Figure 4** and **Figure 5**; see also **Methods**) computed from the experience of the second lockdown in France in the fall 2020, three lockdowns would have been needed to manage the pandemic between September 2020 and June 2021, reducing by 22% the effective days under restrictions, but increasing hospitalizations by 40%. Also, the impact on regional healthcare would have largely varied, with Bretagne, for example, predictive to have an increase of 190% of its hospitalizations (**Figure 5c**). The second of the three lockdowns foreseen under this scenario would have lasted more than 3 months to control the rise of the Alpha wave (January– April 2021; **Figure 5b**).

Reducing the trigger and release thresholds, i.e. applying and lifting the lockdowns at lower per capita hospital admissions than observed, would have decreased hospitalizations (**Figure 4a**, **Figure 5a**) and increased the effective days under restrictions (**Figure 4b**), through two to four lockdowns (**Figure 4c**). For example,

maintaining the same number of effective days under restriction as observed, our model predicts that it could have been possible to largely reduce national hospitalizations by around 40% through the early application of two (e.g. with $T = 35\%$ and $R = 70\%$ thresholds) or three lockdowns (e.g. with $T = 70\%$ and $R = 35\%$ thresholds). However, this would have been achieved with a long uninterrupted lockdown period (>4 months; **Figure 5b**).

The interface between decreasing hospitalizations and increasing restriction days yields an intermediate region of threshold values where both quantities are reduced compared to observations, thus limiting both the healthcare and societal burdens. Adopting these criteria, a higher benefit would be on average achieved in the reduction of hospital patients (17%, IQR 9-27%; **Figure 4d**) compared to the reduction of effective days under restrictions (6%, IQR 3-10%; **Figure 4e**), and with a benefit for more than 70% of the regions (**Figure S21**). This would be obtained with two lockdowns in most of the cases (59% of the scenarios), whereas higher lifting thresholds would induce three (38% of scenarios) or four (3%) lockdowns (**Figure 4f**).

DISCUSSION

Using an epidemic metapopulation model integrating time-varying inter-regional mobility and spatial effects, we provided a detailed analysis of the impact of different measures applied in France between September 2020 to June 2021. Despite their different nature, we showed that the third lockdown (spring 2021) was similarly effective to the second lockdown (fall 2020), after discounting for the transmissibility of the circulating variants, immunity, and seasonal effects (**Figure 2a**). We found a strong difference in the estimated impact of the nighttime curfew starting at 8pm or 6pm, with the latter being able to considerably reduce community transmission (coupled with gastronomy and leisure sectors closed, **Figure 2b**). Under the observed vaccination campaign and NPIs, Alpha was estimated to be responsible for 41% of observed hospitalizations. Conversely, without vaccines, we found that implemented measures would not have been enough to control the Alpha wave (**Figure S18, S20**). Finally, stop-and-go lockdowns triggered early enough would have resulted in lower hospitalizations and effective days under restrictions compared to the observed lockdown-curfew-lockdown (**Figure 4**).

Our analysis demonstrates that the spatial model better captures the observed regional dynamics compared to non-spatial models that neglect case importations across regions coupling regional epidemics (**Figure S15, Table S4**). This finding highlights the importance of considering mobility and spatial data to better characterize epidemic transmission processes and evaluate interventions. Even if these interventions are applied nationwide, local conditions (e.g. incidence, penetration of a variant of concern, seasonal effects, human response to interventions) can be rather heterogeneous geographically, so that spillover events across different areas have unexpected implications for the local epidemic dynamics and control. We found that reproductive number estimates were largely affected by the spatial connectivity fueling regional epidemics, with relative deviations that may be larger than 40% and generally higher for higher shares of incoming mobility compared to the number of inhabitants (**Figure 3b**). Careful considerations should therefore be given to local estimates neglecting the impact of continuous importations from outside areas.

Our analysis confirms the large effectiveness of lockdowns in controlling transmission, in line with prior works^{5,7,8,44,45}. Despite their difference in the granularity and definition of restrictions (stay-at-home orders with schools open during the second lockdown vs. stay-outdoor recommendations with extended school holidays in the third lockdown), the two lockdowns implemented in France in the period under study had similar impact on the epidemic. They reduced the intrinsic transmissibility by 52% and 51%, respectively (**Figure 2a**), compared to the situation in October 2020 for a rather similar Normalcy index. Our findings therefore suggest that the higher effective reproductive number reached during the third lockdown in France compared to the second ($R=0.89$ vs. $R=0.67$, respectively (**Figure 2b**)) was mainly the result of the Alpha variant spread, characterized by a higher transmissibility, and not of different stringency of restrictions or lower adherence of the population³¹. Similar transmission reductions were estimated for the most stringent tier applied in Italy in the same period (52% reduction)⁴⁶, and corresponding to Normalcy index values close to the ones of the French lockdowns.

We produced new evidence on the effectiveness of intermediate-stringency NPIs, such as nighttime curfews, for which there was little available literature^{31,47,48}. Coupled with the closure of the gastronomy sector, the curfew starting at 6pm was found to be considerably effective, suggesting that a moderate intervention focusing restrictions on certain sectors and times of the day may be a viable control option while ensuring a larger functioning of the economy. Over a longer period of time, however, we found that curfew lost effectiveness in all regions (**Figure 2b**), suggesting that pandemic fatigue¹³⁻¹⁵ likely settled in the population. Maintaining it for a long time (in France it was implemented for a total of 188 consecutive days) should therefore be evaluated in light of expected population adherence¹⁵ and the potential increase in the prevalence of mental health issues¹⁵. Regional responses changed in a similar way to changing NPIs, but to a lesser degree when comparing the nighttime curfew starting at 8pm with the one starting at 6pm. This suggests that anticipating the start of the curfew required different organizations of daily routines which may be specific to the regional contexts. Prior work already pointed out the role of local socio-economic factors and labor structure in driving the response to restrictions^{17,18,49}. This also limits the generalizability of our curfew results to other societal contexts, as it will depend on local social habits involving mixing activities that may be efficiently restricted by the curfew.

The first half of 2021 witnessed a race between the rollout of vaccines and the spread of the Alpha variant. We found that both vaccines and NPIs were key to control the Alpha wave⁵⁰. Specifically, without vaccines, stricter measures should have been adopted to avoid hospital saturation (**Figure S18**).

Other countries opted for different policies, repeating lockdowns. We showed that stop-and-go lockdowns (intercut with periods of no restrictions) could have achieved a substantial reduction of hospitalizations (-40%) for similar number of effective days under restrictions compared to the policy implemented in France, i.e. the application of two lockdowns intercut with a long period of curfew (**Figure 4, Figure 5**). This result would require however acting early, at low hospitalization incidence^{43,51-53}. In the balance between ensuring epidemic control and limiting societal impact, we also found a range of thresholds to trigger and release lockdowns that would reduce both hospitalizations and overall effective days under restrictions. However, in the pandemic phase characterized by a more transmissible and severe variant, this would translate in the implementation of a rather long second lockdown (to

compensate for the absence of the curfew in between lockdowns), raising again issues of sustainability and acceptance^{14, 15} (**Figure 5**).

Our work has a number of limitations due to simplifying assumptions in our analysis. First, we did not consider the age structure of the population, asymptomatic transmission, or changes of travel behavior when infectious, similarly to what commonly done in COVID-19 metapopulation models^{43,54} where the complexity of the model lies in its spatial dimension. Age-specific mixing and the impact of asymptomatic transmission and travel avoidance behavior are effectively absorbed in the estimate of the regional transmissibility and may be a factor behind resulting regional variations^{17,55}. Second, in the stop-and-go lockdown scenarios we considered a 2-week relaxation to phase out restrictions⁴³, reproducing what happened in France. Other countries opted instead for more structured tiered systems to guarantee a better control in lifting interventions^{46,56}. Also, the thresholds considered to trigger and lift interventions in the scenarios are based on per-capita hospital admissions, implicitly assuming equal hospital capacity across regions. While regional variations exist, the crisis also showed a certain flexibility in adjusting such capacity according to needs⁷. Finally, we used the Normalcy index to define the effective days under restrictions and compare interventions of different stringencies. Other indicators can be defined using the mobility data, which was at the core of restrictions, as we did in prior work¹⁵. Different indicators should instead be used for a more comprehensive analysis that may include also economic aspects and the impact on mental health whose prevalence was found to increase substantially throughout the curfew in France¹⁵.

CONCLUSIONS

Our analysis provides a detailed overview of the epidemiological impact of the various NPIs and of the vaccination campaign implemented in France from September 2020 to June 2021. Using a spatially-explicit regional metapopulation model allows us to disentangle the effects of spatial and temporal drivers – seasonality, Alpha variant geographic seeding and penetration over time, vaccination rollout, time-varying inter-regional mobility – in the estimates of the effectiveness of lockdowns and curfews of different type. Our findings help the design of preparedness plans for the medium-term management of respiratory virus pandemics.

ACKNOWLEDGMENTS

We thank Mélanie Prague for sharing the estimates on seasonal transmissibility. We thank Pierre-Yves Boëlle for useful discussions.

AUTHORS' CONTRIBUTORS

VC conceived and designed the study. CES and GP developed the code. CES ran the simulations and analyzed the data. All authors interpreted the results. CES and VC wrote the initial manuscript draft. All authors edited and approved the final version of the Article.

FUNDINGS

This study was partly supported by: Agence Nationale de la Recherche project DATAREDEX (ANR-19-CE46-0008-03) to VC; ANRS–Maladies Infectieuses Émergentes project EMERGEN (ANRS0151) to VC; EU Horizon 2020 grants MOOD (H2020-874850) to VC; Horizon Europe grant ESCAPE (101095619) to VC.

AVAILABILITY OF DATA AND MATERIALS

Mobile phone data are proprietary and confidential. We obtained access to these data from the Orange Business Service Flux Vision within the framework of the research project ANR EVALCOVID-19 (ANR-20-COVI-0007). Access to the mobility data can be requested from Orange on a contractual basis. Hospitalization data were obtained from the SIVIC dataset⁵⁷. Estimates for seasonal transmissibility were obtained from the authors of Ref.29. Vaccination data are available from the French Government data hub (<https://www.data.gouv.fr/en/datasets/donnees-relatives-aux-personnes-vaccinees-contre-la-covid-19-1/>); the normalcy index is available from The Economist (<https://www.economist.com/graphic-detail/tracking-the-return-to-normalcy-after-covid-19>); and Alpha variant penetration data are published in the scientific literature (<https://pubmed.ncbi.nlm.nih.gov/33663644/>).

ETHICS APPROVAL AND CONSENT TO PARTICIPATE

Not applicable.

CONSENT FOR PUBLICATION

Not applicable.

COMPETING INTERESTS

We declare no competing interests.

REFERENCES

1. Ge, Y. et al. Untangling the changing impact of non-pharmaceutical interventions and vaccination on European COVID-19 trajectories. *Nat. Commun.* 13, 3106 (2022).
2. Flaxman, S. et al. Estimating the effects of non-pharmaceutical interventions on COVID-19 in Europe. *Nature* 584, 257–261 (2020).
3. Li, Y. et al. The temporal association of introducing and lifting non-pharmaceutical interventions with the time-varying reproduction number (R) of SARS-CoV-2: a modelling study across 131 countries. *Lancet Infect. Dis.* 21, 193–202 (2021).
4. Hsiang, S. et al. The effect of large-scale anti-contagion policies on the COVID-19 pandemic. *Nature* 584, 262–267 (2020).

5. Haug, N. et al. Ranking the effectiveness of worldwide COVID-19 government interventions. *Nat. Hum. Behav.* 4, 1303–1312 (2020).
6. Liu, Y. et al. The impact of non-pharmaceutical interventions on SARS-CoV-2 transmission across 130 countries and territories. *BMC Med.* 19, 40 (2021).
7. Di Domenico, L., Pullano, G., Sabbatini, C. E., Boëlle, P.-Y., Colizza, V. Impact of lockdown on COVID-19 epidemic in Île-de-France and possible exit strategies. *BMC Med.* 18, 240 (2020).
8. Salje, H. et al. Estimating the burden of SARS-CoV-2 in France. *Science* 369, 208–211 (2020).
9. Perra, N. Non-pharmaceutical interventions during the COVID-19 pandemic: A review. *Phys. Rep.* 913, 1–52 (2021).
10. Sharma, M. et al. Understanding the effectiveness of government interventions against the resurgence of COVID-19 in Europe. *Nat. Commun.* 12, 5820 (2021).
11. Davies, N. G. et al. Estimated transmissibility and impact of SARS-CoV-2 lineage B.1.1.7 in England. *Science* 372, (2021).
12. Volz, E. et al. Assessing transmissibility of SARS-CoV-2 lineage B.1.1.7 in England. *Nature* 1–17 (2021) doi:10.1038/s41586-021-03470-x.
13. Petherick, A. et al. A worldwide assessment of changes in adherence to COVID-19 protective behaviours and hypothesized pandemic fatigue. *Nat. Hum. Behav.* 1–16 (2021) doi:10.1038/s41562-021-01181-x.
14. Delussu, F., Tizzoni, M., Gauvin, L. Evidence of pandemic fatigue associated with stricter tiered COVID-19 restrictions. *PLOS Digit. Health* 1, e0000035 (2022).
15. Di Domenico, L. et al. Adherence and sustainability of interventions informing optimal control against the COVID-19 pandemic. *Commun. Med.* 1, 1–13 (2021).
16. Lemey, P. et al. Untangling introductions and persistence in COVID-19 resurgence in Europe. *Nature* 595, 713–717 (2021).
17. Pullano, G., Valdano, E., Scarpa, N., Rubrichi, S., Colizza, V. Evaluating the effect of demographic factors, socioeconomic factors, and risk aversion on mobility during the COVID-19 epidemic in France under lockdown: a population-based study. *Lancet Digit. Health* 2, e638–e649 (2020).
18. Valdano, E., Lee, J., Bansal, S., Rubrichi, S., Colizza, V. Highlighting socio-economic constraints on mobility reductions during COVID-19 restrictions in France can inform effective and equitable pandemic response. *J. Travel Med.* taab045 (2021) doi:10.1093/jtm/taab045.
19. Bajardi, P. et al. Human Mobility Networks, Travel Restrictions, and the Global Spread of 2009 H1N1 Pandemic. *PLOS ONE* 6, e16591 (2011).
20. Holtz, D. et al. Interdependence and the cost of uncoordinated responses to COVID-19. *Proc. Natl. Acad. Sci.* 117, 19837–19843 (2020).
21. Han, X. et al. Quantifying COVID-19 importation risk in a dynamic network of domestic cities and international countries. *Proc. Natl. Acad. Sci.* 118, e2100201118 (2021).
22. Wesolowski, A. et al. Quantifying the impact of human mobility on malaria. *Science* 338, 267–270 (2012).

23. Prosper, O., Ruktanonchai, N., Martcheva, M. Assessing the role of spatial heterogeneity and human movement in malaria dynamics and control. *J. Theor. Biol.* 303, 1–14 (2012).
24. Pullano, G., Valdano, E., Scarpa, N., Rubrichi, S., Colizza, V. Evaluating the effect of demographic factors, socioeconomic factors, and risk aversion on mobility during the COVID-19 epidemic in France under lockdown: a population-based study. *Lancet Digit. Health* 2, e638–e649 (2020).
25. Paraskevis, D. et al. A review of the impact of weather and climate variables to COVID-19: In the absence of public health measures high temperatures cannot probably mitigate outbreaks. *Sci. Total Environ.* 768, 144578 (2021).
26. Metelmann, S. et al. Impact of climatic, demographic and disease control factors on the transmission dynamics of COVID-19 in large cities worldwide. *One Health Amst. Neth.* 12, 100221 (2021).
27. Wang, J. et al. Impact of temperature and relative humidity on the transmission of COVID-19: a modelling study in China and the United States. *BMJ Open* 11, e043863 (2021).
28. Susswein, Z., Rest, E. C., Bansal, S. Disentangling the rhythms of human activity in the built environment for airborne transmission risk: An analysis of large-scale mobility data. *eLife* 12, e80466 (2023).
29. Collin, A. et al. Using a population-based Kalman estimator to model the COVID-19 epidemic in France: estimating associations between disease transmission and non-pharmaceutical interventions. *Int. J. Biostat.* (2023) doi:10.1515/ijb-2022-0087.
30. Gaymard, A. et al. Early assessment of diffusion and possible expansion of SARS-CoV-2 Lineage 20I/501Y.V1 (B.1.1.7, variant of concern 202012/01) in France, January to March 2021. *Eurosurveillance* 26, 2100133 (2021).
31. Di Domenico, L., Sabbatini, C. E., Pullano, G., Lévy-Bruhl, D., Colizza, V. Impact of January 2021 curfew measures on SARS-CoV-2 B.1.1.7 circulation in France. *Eurosurveillance* 26, 2100272 (2021).
32. Bager, P. et al. Increased Risk of Hospitalisation Associated with Infection with SARS-CoV-2 Lineage B.1.1.7 in Denmark. <https://papers.ssrn.com/abstract=3792894> (2021) doi:10.2139/ssrn.3792894.
33. data.gouv.fr. Données relatives aux personnes vaccinées contre la Covid-19 (VAC-SI). <https://www.data.gouv.fr/en/datasets/donnees-relatives-aux-personnes-vaccinees-contre-la-covid-19-1/>.
34. Dagan, N. et al. BNT162b2 mRNA Covid-19 Vaccine in a Nationwide Mass Vaccination Setting. *N. Engl. J. Med.* 384, 1412–1423 (2021).
35. Eyre, D. W. et al. Effect of Covid-19 Vaccination on Transmission of Alpha and Delta Variants. *N. Engl. J. Med.* 386, 744–756 (2022).
36. Haas, E. J. et al. Impact and effectiveness of mRNA BNT162b2 vaccine against SARS-CoV-2 infections and COVID-19 cases, hospitalisations, and deaths following a nationwide vaccination campaign in Israel: an observational study using national surveillance data. *The Lancet* 0, (2021).
37. The Economist. The global normalcy index. <https://www.economist.com/graphic-detail/tracking-the-return-to-normalcy-after-covid-19>.

38. Pullano, G. *Mobilité humaine et propagation des épidémies*. (Sorbonne université, 2021).
39. Pullano, G. et al. Underdetection of cases of COVID-19 in France threatens epidemic control. *Nature* (2020) doi:10.1038/s41586-020-03095-6.
40. Le Vu, S. et al. Prevalence of SARS-CoV-2 antibodies in France: results from nationwide serological surveillance. *Nat. Commun.* 12, 3025 (2021).
41. Carrat, F. et al. Antibody status and cumulative incidence of SARS-CoV-2 infection among adults in three regions of France following the first lockdown and associated risk factors: a multicohort study. *Int. J. Epidemiol.* 50, 1458–1472 (2021).
42. Diekmann, O., Heesterbeek, J. a. P. Metz, J. a. J. On the definition and the computation of the basic reproduction ratio R_0 in models for infectious diseases in heterogeneous populations. *Journal of mathematical biology* vol. 28 365–382 <http://localhost/handle/1874/8051> (1990).
43. Pei, S., Kandula, S. Shaman, J. Differential effects of intervention timing on COVID-19 spread in the United States. *Sci. Adv.* 6, eabd6370 (2020).
44. Paireau, J. et al. Impact of non-pharmaceutical interventions, weather, vaccination, and variants on COVID-19 transmission across departments in France. *BMC Infect. Dis.* 23, 190 (2023).
45. Islam, N. et al. Physical distancing interventions and incidence of coronavirus disease 2019: natural experiment in 149 countries. *BMJ* 370, m2743 (2020).
46. Manica, M. et al. Impact of tiered restrictions on human activities and the epidemiology of the second wave of COVID-19 in Italy. *Nat. Commun.* 12, 4570 (2021).
47. Thompson, J. Wattam, S. Estimating the impact of interventions against COVID-19: From lockdown to vaccination. *PLOS ONE* 16, e0261330 (2021).
48. Andronico, A. et al. Evaluating the impact of curfews and other measures on SARS-CoV-2 transmission in French Guiana. *Nat. Commun.* 12, 1634 (2021).
49. Tizzoni, M. et al. Addressing the socioeconomic divide in computational modeling for infectious diseases. *Nat. Commun.* 13, 2897 (2022).
50. Lai, S. et al. Effect of non-pharmaceutical interventions to contain COVID-19 in China. *Nature* 1–7 (2020) doi:10.1038/s41586-020-2293-x.
51. Alfonso Viguria, U. Casamitjana, N. Early Interventions and Impact of COVID-19 in Spain. *Int. J. Environ. Res. Public. Health* 18, 4026 (2021).
52. Binny, R. N. et al. Early intervention is the key to success in COVID-19 control. *R. Soc. Open Sci.* 8, 210488.
53. Roux, J., Massonnaud, C. R., Colizza, V., Cauchemez, S. Crépey, P. Modeling the impact of national and regional lockdowns on the 2020 spring wave of COVID-19 in France. *Sci. Rep.* 13, 1834 (2023).
54. Karatayev, V. A., Anand, M. Bauch, C. T. Local lockdowns outperform global lockdown on the far side of the COVID-19 epidemic curve. *Proc. Natl. Acad. Sci.* 117, 24575–24580 (2020).

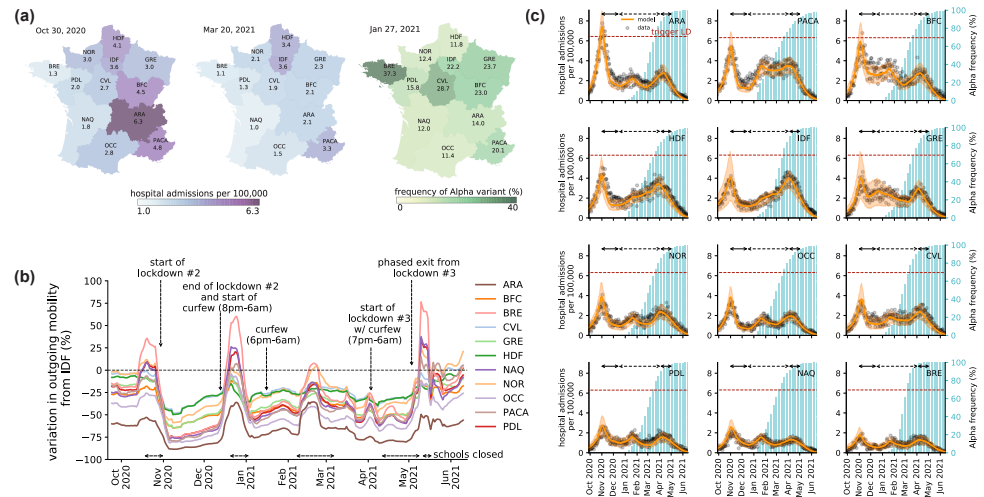
55. Guaitoli, G. Pancrazi, R. Covid-19: Regional policies and local infection risk: Evidence from Italy with a modelling study. *Lancet Reg. Health - Eur.* 8, 100169 (2021).
56. Yang, H. et al. Design of COVID-19 staged alert systems to ensure healthcare capacity with minimal closures. *Nat. Commun.* 12, 3767 (2021).
57. data.gouv.fr. Données hospitalières relatives à l'épidémie de COVID-19. <https://www.data.gouv.fr/fr/datasets/donnees-hospitalieres-relatives-a-lepidemie-de-covid-19/> (2021).

FIGURES AND TABLES

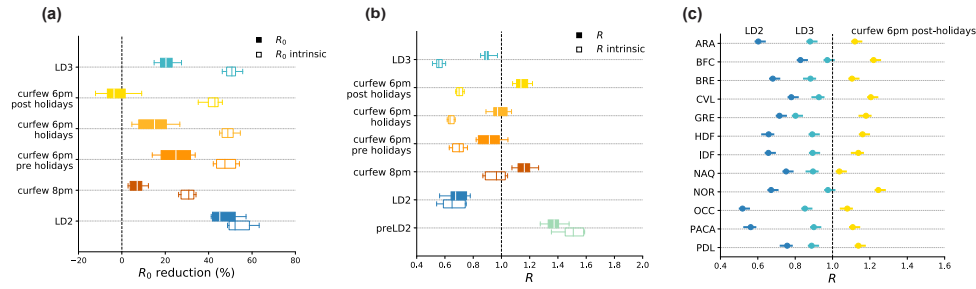
Table 1. Description of the restrictions applied in France between September 2020 and June 2021.

Period	Brief description of the applied NPIs	Abbreviation
October 17– October 29	Night-time curfew (9pm to 6am) in several French departments.	-
October 30 – December 14	Second nationwide lockdown. Primary and secondary schools remained open, subject to strict health protocols. Grocery shops and factories continued to operate; medical-related appointments remained possible. Bars, restaurants, gyms and other non-essential services were closed. Displacements were limited to a maximum radius of one kilometer from home.	LD2
December 15 – January 15	Night-time curfew in place between 8pm and 6am every day.	Curfew 8pm
January 16 – March 19	Night-time curfew hours extended to between 6pm and 6am every day.	Curfew 6pm pre-holidays / holidays / post-holidays*
March 20 – May 2	Third lockdown imposed on March 20 in 16 departments at high incidence (including the whole of Île-de-France, Hauts-de-France, one department of Normandy and one department of Provence-Alpes-Côte d'Azur). The lockdown was then extended nationwide on April 3. Schools remained closed for an extended duration, with the planned holiday closure being prolonged to one or two weeks (for primary and middle/high schools, respectively). Non-essential activities were closed. A declaration was required for travel beyond 10 km of one's place of residence. Stay-at-home orders were replaced with recommendations to encourage spending time outdoors, aiming to reduce transmission in closed spaces.	LD3

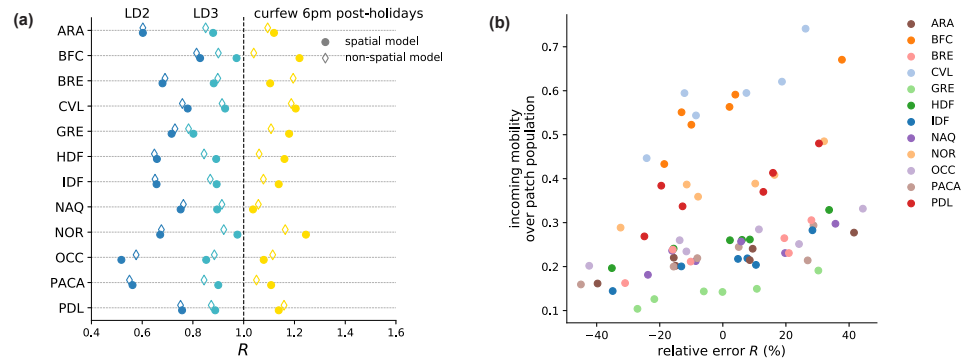
*We splitted the period of curfew 6pm into three distinct phases: before school holidays, during school holidays, and after school holidays. These three phases vary by region because the two-week school breaks are applied at different times in France (see [Table S2](#)).



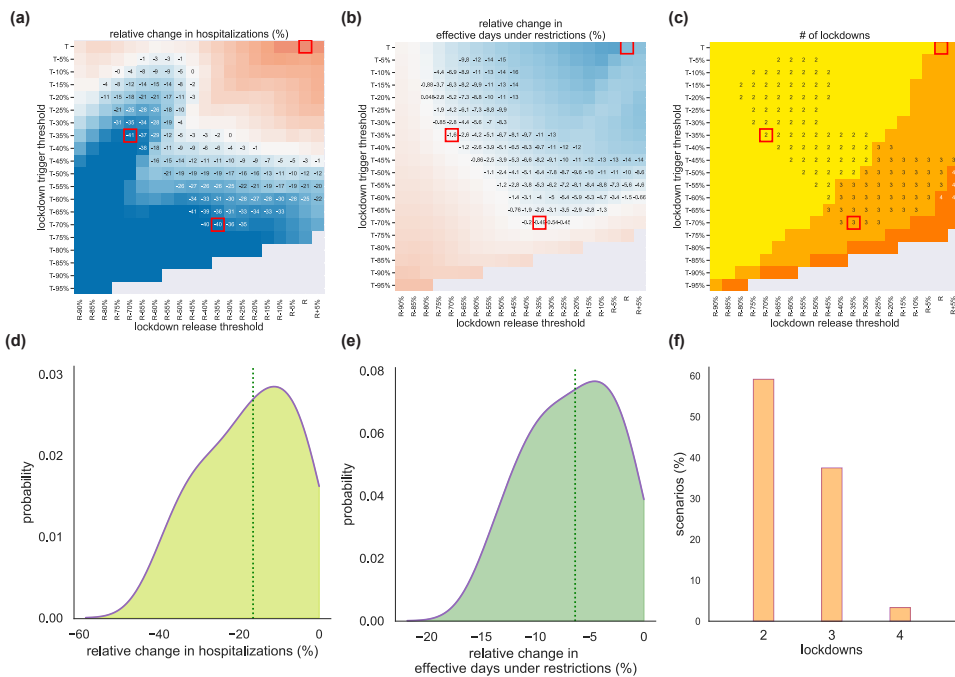
COVID-19 pandemic in French regions between September 2020 and June 2021 . (a) Regional maps of the per capita hospital admissions as of October 30, 2020 (left, start of the first lockdown) and March 20, 2021 (center, start of the third lockdown in regions IDF, HDF, in one department of NOR and one department of PACA). Hospital admissions displayed on the maps are obtained from a weekly rolling mean of the data. Regional map of the frequency of the Alpha variant (%) as of January 27, 2021 (right, date of the second genomic surveillance survey). Abbreviations refer to the regions: ARA, Auvergne-Rhône-Alpes; BFC, Bourgogne-Franche-Comté; BRE, Brittany; CVL, Centre-Val de Loire; GRE, Grand Est; HDF, Hauts-de-France; IDF, Île-de-France, the region of Paris; NAQ, Nouvelle Aquitaine; NOR, Normandy; OCC, Occitanie; PACA, Provence-Alpes-Côte d’Azur; PDL, Pays de la Loire. (b) Variation of regional outgoing mobility from Île-de-France to other regions with respect to pre-pandemic levels. The time intervals indicated over the x-axis refer to (planned or enforced) school closures. (c) For each region, the panel shows the model (orange curve and shaded area indicating the median and 95% probability range) fitted to daily hospital admissions data (gray dots). Each plot also shows the percentage of Alpha variant over time (blue histogram, right y-axis). The dashed horizontal line refers to the threshold triggering the second lockdown. Black arrows at the top of each plot correspond to social distancing measures: the second lockdown during the second wave in the fall 2020 (continuous line), followed by the curfew (dashed line) from January to March 2021, and the third lockdown during the third wave in the spring 2021 (continuous line).



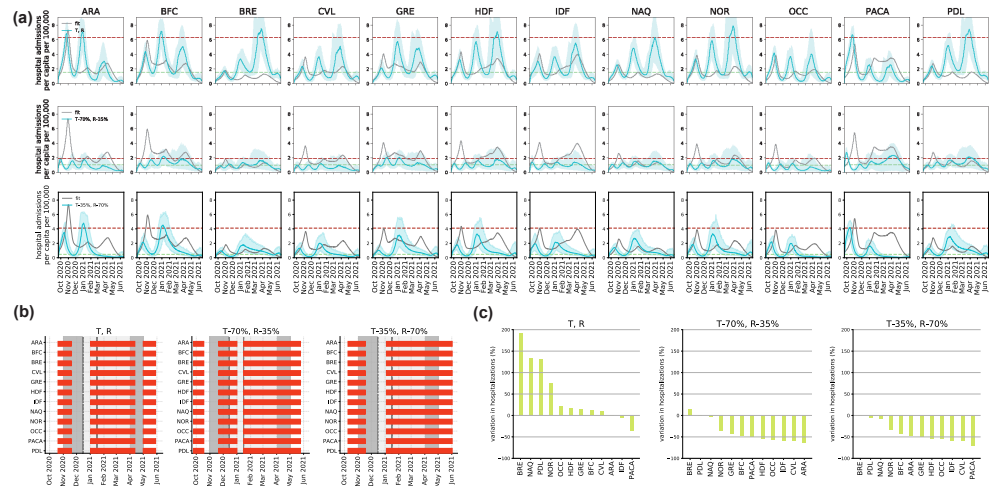
Estimated impact of implemented NPIs. a) Reduction in the estimated regional basic reproductive numbers R_0 associated to the implemented NPIs compared with the values estimated before the second lockdown. Box plots represent the median (line in the middle of the box), interquartile range (box limits) and 2.5th and 97.5th percentiles (whiskers) of the estimated values for the 12 French regions. Filled boxplots represent reductions estimated by the fit accounting for all time-varying processes (R_0); void boxplots represent the same reductions discounting the seasonal and Alpha effects ($R_0^{intrinsic}$). (b) Estimates of the regional effective reproductive numbers R for the implemented NPIs; box plots as defined in (a). Filled boxplots represent fit estimates accounting for all time-varying processes (R); void boxplots represent the same estimates discounting the seasonal and Alpha effects ($R^{intrinsic}$). (c) Regional effective reproductive numbers R for the second lockdown (LD2, dark blue dots), third lockdown (LD3, light blue dots) and the 6pm nighttime curfew in the period following the winter holidays (yellow dots). Dots represent median reproductive number values and error bars the 95% confidence interval. LD2: second lockdown in the fall 2020; curfew 8pm: nighttime curfew starting at 8pm, from mid December 2020 to mid January 2021; curfew 6pm pre-holidays: mid January 2021 to mid February 2021; curfew 6pm holidays: mid February 2021 to late February 2021; curfew 6pm post-holidays: late February 2021 to early April 2021 (see **Table S2**); LD3: third lockdown in the spring 2021.



Spatial vs. non spatial model. (a) Regional effective reproductive numbers R for the second lockdown (LD2, dark blue dots), third lockdown (LD3, light blue dots) and the 6pm nighttime curfew in the period following the winter holidays (yellow dots). Dots represent median reproductive number values. Filled symbols refer to the estimates obtained with the spatial model, void symbols represent the estimates obtained with the non-spatial model, i.e. neglecting inter-regional mobility. (b) Scattered plot between the incoming mobility divided by the patch population and the relative deviation in the estimated effective reproductive numbers obtained with the non-spatial model, for the different NPIs applied (six dots for each region, referring to six different NPIs). Colors of the dots refer to the regions. Results of a Spearman correlation test ($r=0.46$, $p\text{-value}<10^{-4}$). LD2: second lockdown in the fall 2020; curfew 8pm: nighttime curfew starting at 8pm, from mid December 2020 to mid January 2021; curfew 6pm pre-holidays: mid January 2021 to mid February 2021; curfew 6pm holidays: mid February 2021 to late February 2021; curfew 6pm post-holidays: late February 2021 to early April 2021 (see **Table S2**); LD3: third lockdown in the spring 2021.



Impact of stop-and-go lockdown scenarios on hospitalizations, effective days under restrictions, and number of lockdowns. (a-c) Heatmaps showing the relative variation in cumulative hospital admissions (a), the relative variation in effective days under restrictions (b), and the number of lockdowns (c), as functions of the thresholds for trigger (y-axis) and release (x-axis) of nationwide lockdowns. Relative changes are computed with respect to observations. The red squares indicate specific values of trigger and release threshold that are discussed in the main text and presented in detail in Figure 5. Numerical values are reported only in the area where both hospitalizations and effective days under restrictions are reduced by the lockdowns compared to observations. (d,e) Probability distributions of the relative variations in hospitalizations (d) and in effective days spent under restrictions (e) compared to observations, in the region of the trigger-release parameter space where both quantities are reduced by the lockdowns. The vertical dashed lines represent the median values of the distribution. (f) Histogram of the percentage of scenarios with a given number of lockdowns, among the scenarios that reduce both hospitalizations and effective days.



Regional trajectories of stop-and-go lockdown scenarios for specific trigger and release thresholds. (a) Trajectory of regional daily hospital admissions, model fit vs. stop-and-go lockdown scenarios for three different choices of the trigger and release thresholds, indicated by the dashed horizontal lines (top: T, R ; center: $T - 70\%, R - 35\%$; bottom: $T - 35\%, R - 70\%$). (b) Regional timeline of lockdowns, observed (gray areas) vs. lockdown scenarios (red bars). Gray shaded areas in the plots correspond to social distancing measures: the second lockdown during the second wave in the fall 2020 (darker gray), followed by the curfew (lighter gray) from January to March 2021, and the third lockdown during the third wave in the spring 2021 (darker gray). The vertical dashed line denotes the anticipation of the nighttime curfew at 6pm, on January 16, 2021. (c) Variation in hospitalizations by region under the lockdown scenario compared to observations

END

CE Sabbatini, G Pullano, L Di Domenico, S Rubrichi, S Bansal, V Colizza

The impact of spatial connectivity on NPIs effectiveness

XXXXXX

5.3 Discussion

A large number of works have addressed the impact of non-pharmaceutical interventions in the management of the COVID-19 pandemic [7, 131, 132, 133, 134, 135, 136, 137, 16, 13, 124]. Some of them also focused on the local level, evaluating, e.g., control measures in regions or departments [16, 13]. But these geographical areas were considered independently, neglecting the mobility that connects them from a spatial and epidemiological points of view. By focusing on the second and third COVID-19 waves in France, here we show that spillovers due to inter-regional mobility largely affect the effectiveness of the local NPIs, with deviations in the estimated reproductive number reductions that can be as high as 40%. Using a regionally-based epidemic metapopulation model, our study thus uncovers that:

- The third lockdown in spring 2021 was similarly effective to the second lockdown in fall 2020, despite the rather different mandates.
- The nighttime curfew starting at 6pm was considerably effective when coupled with the gastronomy sector closed. Even if kept for long, this strategy could maintain active a larger number of job sectors.
- Repeated lockdowns (instead of the curfew) could lower both the healthcare and societal impacts, but this strategy needs to be performed proactively, when hospitalization numbers are still low.

The use of a spatially-explicit regional metapopulation model with time-varying inter-regional mobility proved critical in capturing observed regional dynamics. The incorporation of spatial data enhanced the understanding of epidemic transmission processes, emphasizing the importance of mobility patterns in shaping outbreaks. Our findings are also supported by another study conducted in the United States [138], where the spillover effects of NPIs significantly impact COVID-19 transmission, explaining 61.2% of the nationally accumulated confirmed cases, and it is demonstrated that strengthening NPIs in regions with high internal human mobility can effectively reduce cumulative cases nationwide.

Our research provides a comprehensive and accurate understanding of the control measures required during the medium-term phase of a respiratory virus pandemic, from the initial alert to the mass vaccination campaign. NPI measures played overwhelming roles in mitigating the pandemic, with varied effects across space and time, in agreement with other multi-country studies [133, 135].

Lockdowns have proven highly effective in controlling transmission, reducing the virus's transmissibility by approximately 50%. Despite differences in lockdown granularity and restriction definitions between the second and the third lockdown implemented in France (impact of stay-at-home orders vs. stay-outdoor recommendations), they exhibited similar effectiveness in curbing the virus's spread. The gradient in the effectiveness of lockdown measures - the second lockdown had a larger impact compared to the third one - was primarily due to the spread of the Alpha variant, rather than variations in the stringency of restrictions or reduced population adherence.

Our research also underscores the importance of intermediate-stringency NPIs, like nighttime curfews, in controlling community transmission. Even during periods with moderate restrictions, there was a notable decrease in the effective reproductive number. This is likely attributed to the combined effects of other NPIs, such as the

closure of the gastronomy sector. This implies that less strict interventions can prove equally efficient in containing transmission, particularly when highly contagious variants are not prevalent. The 8 p.m. and 6 p.m. curfews were able to reduce the effective reproductive number by 15% and 32%, respectively (See. **Supplementary Materials**), compared to the estimates before the second national lockdown. The strengthening of restrictions was significant in reducing the reproductive number below 1 [139, 16, 124]. Similar results were found in Italy, where a tiered system of restrictions was implemented, gradually increasing the intensity of interventions based on regions' healthcare indicators [122]. In regions where NPIs were strengthened, the reproductive number dropped below one [122]. The Italian tiered system also led to comparable reductions in the effective reproductive number compared to the preceding nationwide restrictions, with reductions ranging from 15% to 52% based on the tier in place. Conversely, the reductions in the effective reproductive number induced by the tiered system in the UK were smaller, ranging from 2% to 10% [140]. The Italian tiered system, the UK tiered system and the curfews applied in France are not directly comparable because the policies in place were different, however, the national stringency index for the period assumes comparable values for France and Italy while it assumes lower values for the UK [24]. Other published work on curfews in Luxembourg [141] and Spain [142] found a relatively small or insignificant impact. However, these countries implemented curfews after 10 p.m., not as early as in France, where curfews start at 6 p.m. Over a longer period of time, however, we found that the curfew lost effectiveness in all regions. Moreover, it has been shown that even the mildest measures induce fatigue in the population and that even if effective they are not easily sustainable in the long run [12].

School holidays during the curfew period were estimated to have a negligible overall impact, despite prior work identified their contribution to further slowing down the epidemic in specific regions [12, 16]. This may be explained by the asynchronous holiday timing in France where school holidays are staggered across three geographic zones. Holidays may contribute to reduce mixing within the region, but increase inter-regional mobility potentially fueling the epidemic at destination (not under holiday). This process is inverted as the three zones enter and exit their holiday period, likely resulting in an overall balanced effect. Over a longer period of time, however, we found that curfew became less efficient in all regions, suggesting that pandemic fatigue likely settled in the population. This finding aligns with another study conducted in France [124], which showed that school closures had a limited effect on transmission.

During the period under examination, there was a race between two opposing forces: the vaccination campaigns and the spread of the Alpha variant, while the population was still subjected to a series of significant restrictions until the beginning of the summer of 2021. Without the vaccines, the Alpha wave (i.e., the third wave in France) would have been larger and would have led to an additional 255,000 hospitalized patients in the first six months; the implemented measures would not have been sufficient to prevent the collapse of the healthcare system.

Moreover, the study explores the potential of stop-and-go lockdowns as an alternative intervention strategy. Implemented early enough, stop-and-go lockdowns could achieve a substantial reduction in hospitalizations with a comparable number of days under restrictions as observed during curfew implementation. However, the longer lockdown periods required during the pandemic phase with highly transmissible variants raise concerns about sustainability and societal acceptance. Our

implementation of lockdown-only scenarios is grounded in well-defined guidelines, particularly in terms of the criteria for triggering and releasing lockdown measures [143]. However, it's in France was observed a lack of centralized guidelines based on critical epidemiological factors (hospitalization rates or incidence rates) [144]. Although France introduced a five-tiered alert system in the fall of 2020 [145], ranging from no restrictions (level 1, "zone verte") to maximum alert (level 5, "Etat d'urgence sanitaire"), these levels were not used as triggers for lockdowns. During the second and third waves of the pandemic, the incidence rates did reach the threshold for accessing level 4, however, the specific criteria employed for implementing or easing these restrictions were never made publicly available. It is crucial to emphasize that transparent communication of these criteria and objectives is of paramount importance. Such communication not only fosters public compliance but also provides the population with well-founded justifications for the policies aimed at achieving desired outcomes [143, 146].

In addition to the limitations already highlighted in the article, there are others that are worth noting. Given the specificity and granularity of the interventions, the interpretation of their effects should only be made within a specific implementation context and cannot be directly extrapolated to others. We did not consider age groups in the study; age-specific mixing is absorbed into the regional transmissibility estimate; in a country with a different age structure composition of the population, the effectiveness of the NPIS would likely be different from our prediction range. An additional reason why our results are not directly applicable to other contexts. It is worth noting that we did not extend the study period further because the dynamics of the epidemic were primarily driven by the evolution of immunity in the population induced by vaccination. We did not estimate the effect of other NPIs, such as the TTI system, as well as the use of other barrier measures like mask-wearing. Furthermore, we did not incorporate adherence loss into the measurement of intervention effectiveness and when assessing the sustainability of the interventions with effective days, we did not take into account the fatigue that these measures can induce: this is an interesting avenue of further investigation.

In our study, we have conducted a comprehensive analysis that offers valuable insights into the epidemiological impact of various NPIs in France from September 2020 to June 2021. Understanding the complex interplay between different intervention strategies, regional dynamics, and temporal aspects is essential in devising effective response plans to combat future pandemics of respiratory viruses. With the pandemic crisis behind, our findings offer an exhaustive and more accurate understanding of control measures needed in the medium-term phase of a respiratory virus pandemic, from the initial alert to the mass vaccination campaign. The specific experience of France, where interventions of different types were implemented, nourishes a portfolio of options along with their assessment to inform pandemic preparedness plans against future threats.

Conclusions and perspectives

6

The implementation of large-scale restrictive measures within a population has a significant impact on the spread of a disease [16, 13, 131, 132, 133, 133, 134, 135, 136, 137]. In this thesis, we have developed two new models to quantify some interventions' effectiveness and sustainability, aiming to provide assessment strategies applicable to different contexts and scenarios.

Our analysis underscores the crucial role played by the implementation of large-scale restrictions, including lockdowns and curfews, in containing the spread of COVID-19 in France. These measures significantly contributed to reducing infection rates and relieving pressure on healthcare systems [12]. The timing and stringency of restrictions emerged as critical factors for their effectiveness, especially in the context of the rapidly evolving European landscape in late 2020 and the first half of 2021, where new variants and vaccination campaigns altered the efficacy of interventions and our pre-existing knowledge of them.

While these restrictions proved effective in mitigating the healthcare crisis, they were not without challenges and adverse effects. Economic hardships, mental health issues, and overall population fatigue were notable consequences that continue to demand ongoing attention and further study [147].

To address the ongoing and future challenges posed by pandemics, it is essential to treat them with various approaches and models: the choice of a modeling framework should align with the specific questions and the available data [148, 149]. In the research presented in this thesis, our primary focus centered on assessing the efficacy of population-level interventions within specific regions or at the national level. Our aim did not include the examination of transmission within particular contexts (e.g., schools, workplaces, gastronomy sectors), as this would necessitate distinct frameworks and data sources [150, 151]. Furthermore, we did not incorporate the consideration of risk exposure heterogeneity, based on factors dividing the population, such as socio-economic variables. This is however possible, through, for instance, the implementation of agent-based models.

Future research should emphasize the robustness of our findings and their generalizability. This can be achieved by varying specific contexts. For example, our articles were conducted in the presence of the Alpha variant and the observed vaccination campaign pace. How would our results change in the face of a slower or faster vaccination rhythm? How would outcomes be altered by a more contagious yet less severe variant? Can we find a ballpark of results that remain consistent?

Also, vaccination campaigns have achieved widespread coverage in many countries and allowed for the relaxation of non-pharmacological interventions after several months [57, 152]. However, the management of COVID-19 has been further challenged by subsequent waves of variants such as Delta and Omicron, with vaccine protection vanishing over time [153, 154]. The need for booster doses became evident, but the optimal timing for booster administration was less clear. Further interesting studies could involve post-vaccination phase modeling, considering factors such as waning immunity, immune escape, and variant characteristics.

Modeling can also help assess the optimal spatial scales for interventions. Future research may explore how regional stop-and-go lockdowns, for instance, compare to the national-level policies adopted in France or alternative policies observed in other European countries. The diversity of national or targeted approaches taken by countries to address the COVID-19 pandemic reflects, in part, the substantial uncertainty surrounding how policies translate into outcomes. National restrictions would provide a standardized and consistent approach throughout the country but have significant economic and social consequences. Conversely, local-level restrictions enable targeted measures in regions with higher infection rates, minimizing economic and livelihood impacts. However, concerns have arisen regarding how this decision would affect healthcare indicators (e.g. hospital pressure). Additionally, transmission and implemented policies are intrinsically linked across regions, with interventions in one region producing spatial spillover effects on neighboring areas, influencing human behavior, as demonstrated by various studies [155, 156, 157].

Furthermore, future research could investigate how policies, typically defined within specific administrative areas (e.g., counties, departments, or regions), adapt to different spatial scales. While administrative boundaries represent a useful spatial scheme to define local policies, the spatial dynamics of the epidemic are inherently defined by the mobility of individuals. For example, neighboring departments that are highly connected by daily mobility also have highly coupled local epidemics, i.e. the epidemic in one department strongly impacts the epidemic in the other (e.g. in the departments of the Île-de-France region). In such situations, not representing epidemiologically independent entities, single departments would not identify the best scale of application of interventions, and a larger set of departments -defined on human mobility- could potentially represent a better choice. This research could determine the most epidemiologically-relevant spatial scale for local interventions in high-risk areas while minimizing unnecessary restrictions elsewhere.

In the first study presented, we took into account adherence to restrictions. However, we note that the observed loss of adherence is primarily fatigue-induced [158, 159]. This fatigue may be attributed to the time spent under restrictions or to the iteration of the same measures being implemented. In the context of our studies, it could be interesting to investigate how iteration, such as the stop-and-go scenarios discussed, can influence fatigue and adherence. In order to find a subset of interventions aimed at reducing such waning in adherence.

As pandemics can impact every facet of society, preparedness plans must address the emergence of new pathogens in a multidimensional manner. These plans should focus on the healthcare system and the associated direct burden of disease (e.g., hospital occupancy, mortality, healthy life years lost), the indirect burden of disease (e.g., disability and delayed unrelated care, mental well-being), the economy (e.g., productivity loss, unemployment), disruptions to essential community services, and long-term social impact. Such plans should be flexible enough to address pathogens of different types (viral, bacterial), transmitted through different routes, with varying levels of transmissibility and severity at the time of contraction. Furthermore, they should have the capability to adjust measures based on the current state and evolution of the pandemic. An important goal for future research is to provide a blueprint for making faster and better decisions for managing pandemics caused by various pathogens.

Another notable aspect to consider is the potential unlocked when collecting a huge amount of data on COVID-19 across different waves, scales and countries.

Deep learning methods are progressively finding applications in healthcare and medical fields [160, 161, 162, 163, 164]. The vast reservoir of data at our disposal opens up exciting avenues for the application of deep learning methodologies. These methodologies can serve a multitude of purposes, ranging from the analysis and prediction of time series data using recurrent neural networks (RNNs) [164] to the identification of intricate spatial patterns and high-risk regions through convolutional neural networks (CNNs) [164]. It is worth noting that these architectures are just a fraction of the deep learning techniques available. An interesting direction would be to conduct methodological research to understand how to apply these techniques to public health problems.

Furthermore, making the integration of modeling into policy decisions a standard practice can also lead to broader applications in various types of crises, including social, energy, and climate-related ones.

SUPPLEMENTARY MATERIALS

Article #1

Adherence and sustainability of interventions informing optimal control against the COVID-19 pandemic

Laura Di Domenico^{1,*}, Chiara E. Sabbatini^{1,*}, Pierre-Yves Boëlle¹, Laura Di Domenico¹, Chiara Poletto¹, Pascal Crépey², Juliette Paireau^{3,4}, Simon Cauchemez³, François Beck⁴, Harold Noel⁴, Daniel Lévy-Bruhl⁴, Vittoria Colizza^{1,5,**}

¹Sorbonne Université, INSERM, Pierre Louis Institute of Epidemiology and Public Health, Paris, France. ²Univ Rennes, EHESP, REPERES « Recherche en Pharmacologie-Epidémiologie et Recours aux Soins » – EA 7449, 35043 Rennes, France. ³Mathematical Modelling of Infectious Diseases Unit, Institut Pasteur, UMR2000, CNRS, Paris, France. ⁴Santé Publique France, French National Public Health Agency, Saint-Maurice, France. ⁵Tokyo Tech World Research Hub Initiative, Institute of Innovative Research, Tokyo Institute of Technology, Tokyo, Japan. *co-first author **corresponding author: vittoria.colizza@inserm.fr

Contents

Contents	5
0.1 Supplementary methods	6
0.1.1 SARS-CoV-2 two-strain transmission model	6
0.1.2 Stringency index	7
0.2 Supplementary Note 1: Additional results	7
0.2.1 Behavioral indicators vs risk perception and psychosocial burden	7
0.2.2 Results for different hospitalization levels triggering lockdowns	7
0.2.3 Impact of school holidays	7
0.2.4 Impact of different vaccination rhythms	8
0.2.5 Phasing out strict lockdowns	8
0.3 Supplementary Note 2: Sensitivity analysis	8
0.3.1 Sensitivity on increase in transmission due to Alpha variant	8
0.3.2 Sensitivity on the delay from implementation of the interven- tion to peak	8
0.3.3 Vaccine efficacy	8
0.4 Supplementary Tables 1-2	10
0.5 Supplementary Figures 1-14	11
0.6 Supplementaary references	18

0.1 Supplementary methods

0.1.1 SARS-CoV-2 two-strain transmission model

Compartmental model and parameters

Supplementary Figure 1 shows the compartmental scheme used to describe COVID-19 disease progression. Parameter values related to infection due to historical strains are reported in **Supplementary Table 1**. Parameter values for the Alpha variant are presented in the **Methods** section. When vaccination starts, we assumed that doses might be given to either susceptible or recovered individuals with equal probability. Efficacy of vaccination is described in the **Methods** section; such efficacy would only have an impact on the susceptible population.

Generation time distribution

The generation time distribution was computed based on the approach of Ref.¹. Let X and Y be the random variables describing the latency period and the infectious period, respectively. Then the distribution of the generation time is the result of the convolution gh_s with g being the probability density function of X and $h_s(t) = \frac{1-H(t)}{E(Y)}$ where H is the cumulative distribution function of Y , and $E(Y)$ is the mean. In the compartmental model under consideration (**Supplementary Figure S1**), we have that X is exponentially distributed with rate ϵ , and Y is the sum of two exponentially distributed random variables (prodromic phase and infectious period, with rate μ_p and μ respectively). Computations show that the corresponding generation time distribution is

$$f(t) = \frac{\epsilon\mu_p\mu}{(\mu_p + \mu)(\mu - \mu_p)} \left[\frac{\mu}{\epsilon - \mu_p} (e^{-\mu_p t} - e^{-\epsilon t}) - \frac{\mu_p}{(\epsilon - \mu)} (e^{-\mu t} - e^{\epsilon t}) \right]$$

Given the values of ϵ and μ_p informed from the literature (**Supplementary Table 1**), we chose μ so that the mean of the generation time equals to 6.6 days. The shape of the distribution is displayed in **Supplementary Figure 2** and it closely resembles a gamma distribution with mean 6.6 and shape parameter 1.87, estimated in Ref².

Frequency of the Alpha variant over time

Supplementary Figure 3 reports the proportion of infections associated with Alpha variant, from genomic (Flash surveys) and virological surveillance data (see **Methods**). Weekly data have been normalized on Alpha and historical strains for comparison with model outcomes, as the two-strains model does not account for additional variants. Model predictions agree well with observed data. Discrepancies between model and data appear in the month of April after strengthened measures were applied, and may be due to the interaction of Alpha (B.1.1.7) with Beta (B.1.351) and Gamma (P.1) variants, slowly expanding their diffusion in the region, and neglected in the model. The figure also shows the model outcomes obtained assuming that Alpha variant is 40% more transmissible than the historical variants, i.e. the lower

estimate provided in Ref³. Results show that with this hypothesis the model is not able to capture the evolution in time of frequency of the Alpha variant.

0.1.2 Stringency index

The stringency index⁴ is a quantity based on multiple indicators that include restrictions on public gatherings, stay-at-home requirements, school closures and travel bans. It provides a measure on the intensity of government policies, with a numerical value ranging from 0 to 100 (a higher value indicates a stricter response). **Supplementary Figure 4** shows the stringency index for France. If policies vary locally (e.g. at the regional level), the national index corresponds to that of the region with the strictest restrictions. The strengthened measures adopted at the end of March in Île-de-France, are of a similar intensity to the moderate lockdown implemented to curb the second wave.

0.2 Supplementary Note 1: Additional results

0.2.1 Behavioral indicators vs risk perception and psychosocial burden

Supplementary Figure 5 reports the correlation analysis between adoption of social distancing and prevalence of anxiety in the population. We observed a non-significant association between these two quantities. The figure also shows that the association found between adoption of social distancing and fear to contract the virus since the second wave (**Figure 1** of the main paper) holds when extended to the whole time period.

0.2.2 Results for different hospitalization levels triggering lockdowns

We show results for different hospitalization levels triggering interventions, i.e. interventions applied at different starting dates. **Supplementary Figure 6** and **Supplementary Figure 7** complete the results presented in **Figure 2** and **Figure 4** of the main text, referring to interventions applied at week 12, i.e. when weekly hospital admissions reached 2,900.

0.2.3 Impact of school holidays

In **Supplementary Figure 8**, we present the results obtained assuming schools to be open in w15-w16, to evaluate the effect of school holidays in those two weeks. We found that, under moderate interventions, hospitalizations would reach higher peaks and the epidemic would be less easily controlled, if schools were always in session.

0.2.4 Impact of different vaccination rhythms

Supplementary Figure 9 shows the effect of different vaccination rollouts on the scenarios presented in the main text.

0.2.5 Phasing out strict lockdowns

Supplementary Figure 10 shows the impact of a progressive transition in phasing out a 2-week strict lockdown, analogously to results of **Figure 5** of the main paper for moderate lockdowns. Results support the importance to lower the incidence level to better manage possible rebounds while reopening.

0.3 Supplementary Note 2: Sensitivity analysis

Here we present the results of our sensitivity analysis. We test a different value for the transmissibility advantage of the Alpha variant, different assumptions on the delay from the implementation of the restrictions to the peak and different vaccine efficacies.

0.3.1 Sensitivity on increase in transmission due to Alpha variant

We assessed the impact of a smaller transmissibility advantage (40% increase vs. 59% increase considered in the main text). Under this assumption, interventions are more effective in controlling the epidemic (**Supplementary Figure 11**). This assumption is however not compatible with the registered evolution of the Alpha variant in time in the region (see **Supplementary Figure 3**).

0.3.2 Sensitivity on the delay from implementation of the intervention to peak

We assessed the impact of a different delay from the implementation of the intervention to peak, which is set to 7 days in the main text, based on estimates from lockdowns implemented in 2020. Results remained robust: assuming a 10-day delay leads to differences in the ballpark of estimations (**Supplementary Figure 12**).

0.3.3 Vaccine efficacy

Supplementary Figure 13 reports the sensitivity on vaccine efficacy against transmission. We tested 40% vaccine efficacy against transmission, with respect to 65% efficacy assumed in the main text. We found no significant differences in hospital admission trajectories, owing to an already high efficacy against contracting the infection, playing a major role in reducing epidemic activity. **Supplementary Figure 14** shows the results of the sensitivity on the delay between vaccine administration

and vaccine efficacy (2 weeks vs. 3 weeks considered in the main results). As expected, a shorter delay anticipates the effect of vaccination on the epidemic evolution, but does not affect the general results presented in the main text.

0.4 Supplementary Tables 1-2

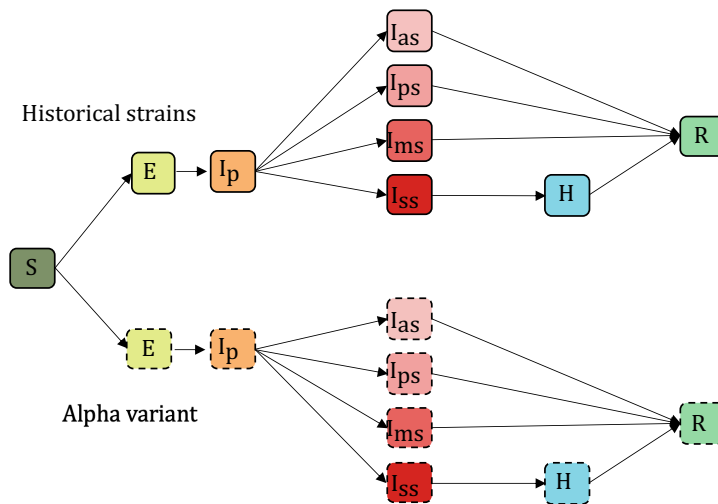
Variable	Description	Value	Source
θ^{-1}	Incubation period	5.2d	5
μ_p^{-1}	Duration of prodromal phase	1.5d, computed as the fraction of pre-symptomatic transmission events out of pre-symptomatic plus symptomatic transmission events.	6
ϵ^{-1}	Latency period	$\theta^{-1} - \mu_p^{-1}$	-
p_a	Probability of being asymptomatic	0.4	7
p_{ps}	If symptomatic, probability of being paucisymptomatic	1 for children, adolescents 0.2 for adults, seniors	8
p_{ms}	If symptomatic, probability of developing mild symptoms	0 for children, adolescents 0.7704 for adults 0.546 for seniors	8-10
p_{ss}	If symptomatic, probability of developing severe symptoms	0 for children, adolescents 0.0296 for adults 0.254 for seniors	9,10
g	Generation time	6.6d	2
μ^{-1}	Infectious period	2.3d, chosen accordingly to generation time distribution	-
τ_β	Relative infectiousness of I_{ps} , I_a , I_{ps}	0.25 for children 0.55 for adolescents, adults, seniors	Assumed, in line with available evidence ¹¹⁻¹³
s	Relative susceptibility	0.5 for children, adolescents 1 for adults, seniors	14,15

Supplementary Table 1. Parameters, values, and sources used to define the compartmental model for infection due to historical strains in absence of vaccines.

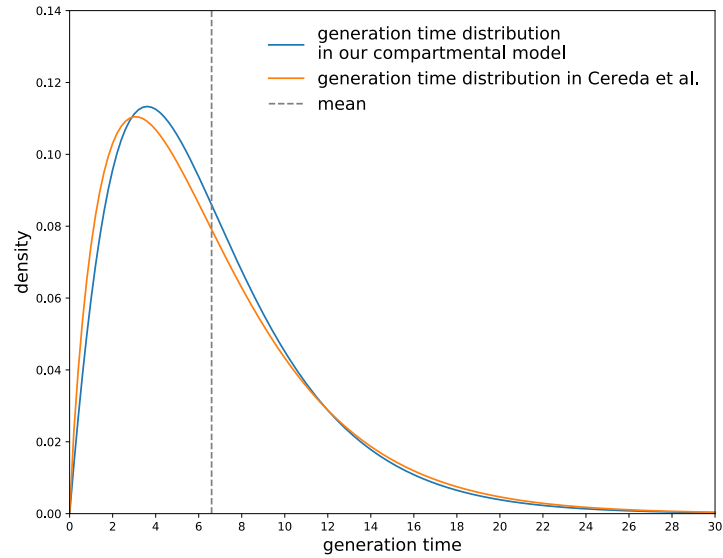
Intervention	Distress index			
	2 weeks	4 weeks	6 weeks	8 weeks
Strict LD	2.50	5.00	7.50	10.00
Strict LD w/ limited loss of adherence		4.51	6.53	8.54
Strict LD w/ continuous loss of adherence			6.14	7.45
Moderate LD	1.55	3.09	4.64	6.19
Moderate LD w/ limited loss of adherence		2.79	4.04	5.29
Moderate LD w/ continuous loss of adherence			3.80	4.61
Curfew	0.92	1.84	2.76	3.67

Supplementary Table 2. Distress index associated to lockdown scenarios with different duration, intensity and adherence. Distress index corresponding to curfew conditions lasting 2 to 8 weeks is shown for comparison.

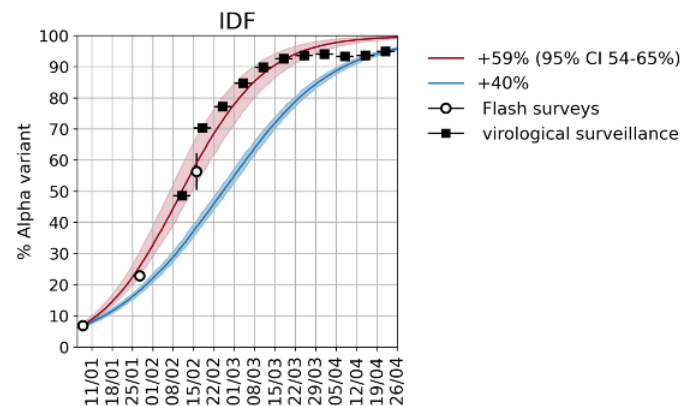
0.5 Supplementary Figures 1-14



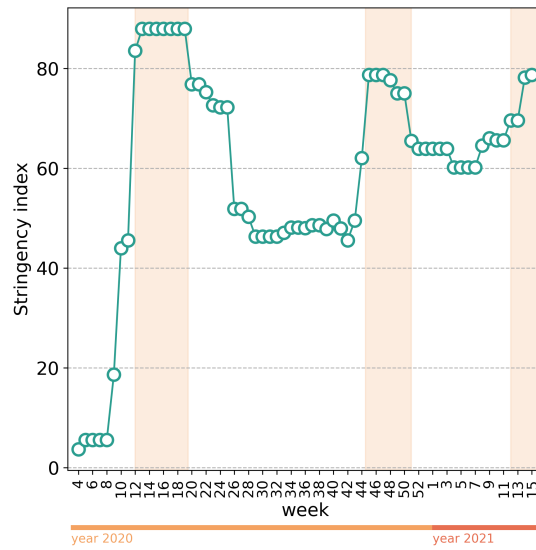
Supplementary Figure 1. Two-strains compartmental scheme with vaccination. Compartments with continuous line (top) account for infections due to historical strains, compartments with dashed line (bottom) account for infections due to the Alpha variant. Analogous compartments are considered for vaccinated individuals (not shown for the sake of visualization). S=Susceptible, E=Exposed, Ip= Infectious in the prodromic phase, Ias=Asymptomatic Infectious, Ips=Paucysymptomatic Infectious, Ims=Symptomatic Infectious with mild symptoms, Iss=Symptomatic Infectious with severe symptoms, H=severe case admitted to the hospital, R=Recovered.



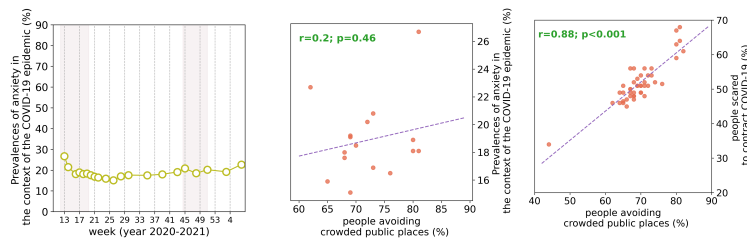
Supplementary Figure 2. Distribution of the generation time. The generation time distribution corresponding to our compartmental model (blue) in comparison with the distribution estimated in Ref.² (orange).



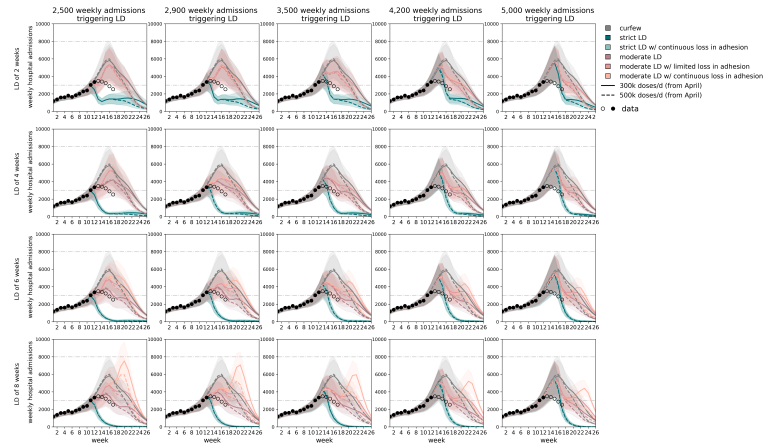
Supplementary Figure 3. Prevalence of Alpha variants over time. Estimated percentage of Alpha cases in Île-de-France over time, considering a 59% (95% CI: 54–65%) higher transmissibility (red) and a 40% higher transmissibility (blue) for the variant. Circles represent the estimates from the genomic surveillance in the Flash surveys (Flash1 on 7–8 January, Flash2 on 27 January, Flash3 on 16 February). Squares represent results from weekly virological surveillance screening allowing the detection of the N501Y mutation specific to the Alpha variant. We estimated 95% CI assuming a normal distribution. Flash3 survey estimates have larger CI as sequencing was performed on a smaller sample of viruses. Horizontal bars in weekly virological surveillance correspond to the week of reference.



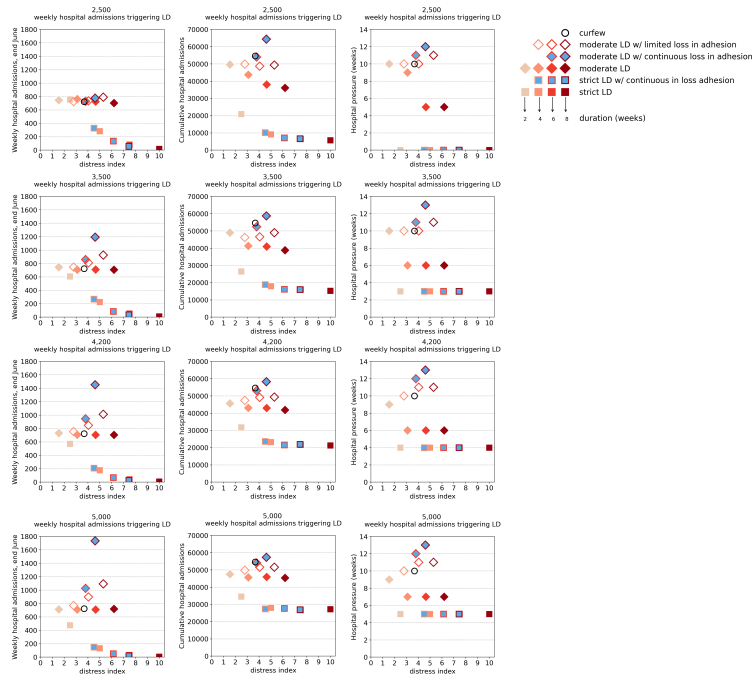
Supplementary Figure 4. Stringency index in France. Estimated stringency index for France over time. Shaded rectangles in the plot correspond to social distancing measures applied during the three waves (strict lockdown in the first wave, moderate lockdown in the second wave, strengthened measures in the third wave).



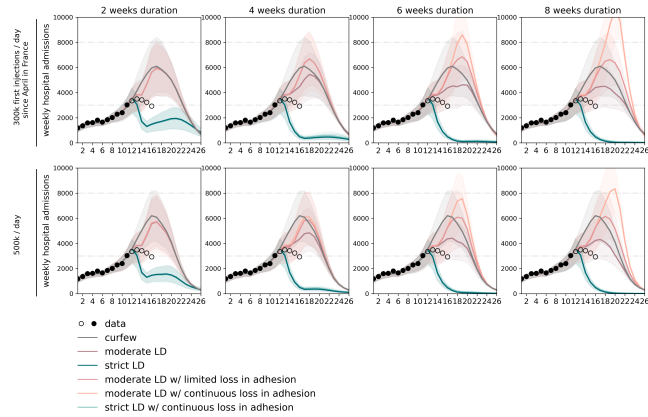
Supplementary Figure 5. Risk perception, social distancing, anxiety during COVID-19 pandemic. Prevalence of anxiety in the context of COVID-19 pandemic (left)¹⁶ as functions of time; scattered plot between the prevalence of anxiety and the percentage of individuals avoiding crowded public places¹⁷ in the time period March 2020 - April 2021, with the results of a Pearson correlation test, effect size 0.2, p-value 0.46 (center). Scattered plot between the fear to contract COVID-19 and the percentage of individuals avoiding crowded public in the time period March 2020 - April 2021, with the results of a Pearson correlation test, effect size 0.88, p-value < 10⁻³ (right). Results for these indicators refer to the national scale.



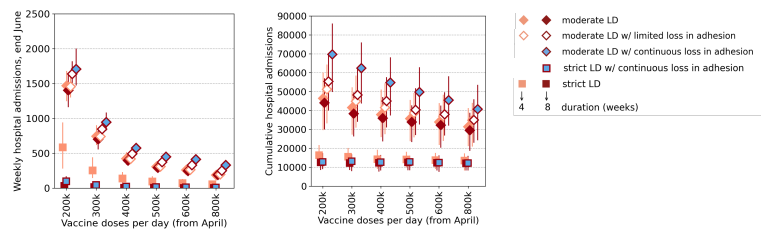
Supplementary Figure 6. Impact of timing of interventions on the timecourse of weekly hospital admissions. From left to right: increasing levels of weekly hospital admissions triggering lockdowns, corresponding to implementing interventions starting from w11 up to w15. From top to bottom: increasing lockdown duration (weeks). Solid curves refer to the median overall trajectory, obtained under the vaccination rollout of 300k first doses administered per day starting April. Dashed curves show the same for an accelerated vaccination rhythm (500k first doses/day starting April). The shaded area around the curve corresponds to the 95% probability range obtained from $n=250$ stochastic simulations. The type of intervention is coded by different line colors. Dots refer to data; filled dots correspond to the data used to fit the model and to provide the trajectory for the curfew scenario; void dots correspond to more recent data. Horizontal dashed lines refer to the peak of the first and second wave in the region. A 7-day delay is assumed from the implementation of the intervention to the peak.



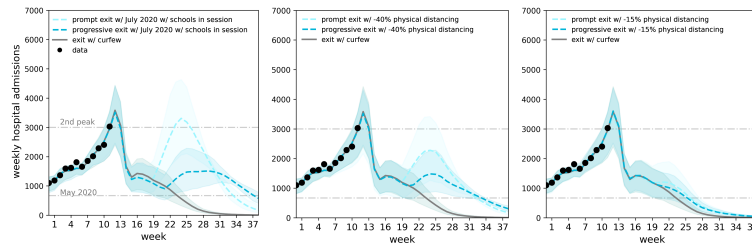
Supplementary Figure 7. Impact of timing of interventions on the intervention efficacy and associated policy-induced distress. From left to right: weekly hospital admissions at the end of June (w26), cumulative hospital admissions (computed in the time period w12-w26), hospital pressure, defined as the number of weeks in which hospital admissions remain above the peak level achieved during the second wave, in the period w12-w26 as functions of the distress index. From top to bottom: increasing levels of weekly hospital admissions triggering lockdowns corresponding to implementing interventions in w11, w13, w14 or w15. Results refer to the accelerated vaccination pace of 300,000 first doses/day since April. Color shades of the symbol contour refer to the duration (weeks) of the lockdown intervention (from the lightest shade corresponding to 2 weeks, to the darkest one corresponding to 8 weeks). Adherence to moderate and strict lockdowns is coded with the fill color (filled symbols with the color of the scenario correspond to scenarios with full adherence, void symbols represent scenarios with limited loss in adherence, blue filled-in symbols correspond to scenarios with continuous loss in adherence).



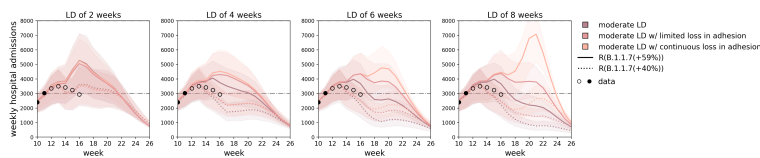
Supplementary Figure 8. Impact of school holidays on the timecourse of weekly hospital admissions in Île-de-France for interventions of varying intensity, duration, and adherence. From left to right: increasing lockdown duration, expressed in weeks. Top row: vaccination pace accelerated to 300,000 first doses/day since the start of April; bottom row: 500,000 first doses/day. Interventions are applied in w12 and assume a delay of one week to the peak in hospital admissions. Schools are assumed to be open in w15-16. Dots refer to data; filled dots correspond to the data used to fit the model and to provide the trajectory for the curfew scenario; void dots correspond to more recent data. Curves refer to the median trajectory; shaded areas around the curves correspond to the 95% probability range obtained from $n=250$ stochastic simulations. The type of intervention is coded by different line colors. Horizontal dashed lines refer to the peak of the first and second wave in the region. Results for strict lockdown scenarios with full adherence or loss of adherence overlap. For this reason, we do not show the scenario with limited loss of adherence.



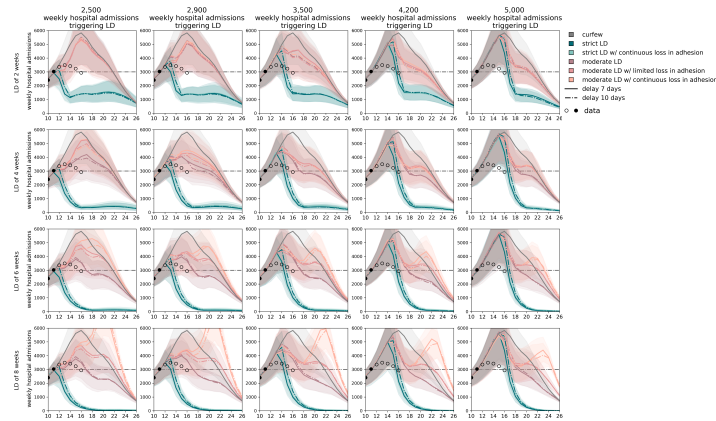
Supplementary Figure 9. Impact of accelerated vaccination. Results refer to interventions applied in w12. From left to right: weekly hospital admissions at the end on June (w26), cumulative hospital admissions (computed in the time period w12-w26). All outcomes are shown as functions of the vaccination rhythm (doses/day since April). Color shades of the symbol contour refer to the duration (weeks) of the lockdown intervention (from the lightest shade corresponding to 4 weeks, to the darkest one corresponding to 8 weeks). Adherence to moderate and strict lockdowns is coded with the fill color (filled symbols with the color of the scenario correspond to scenarios with full adherence, void symbols represent scenarios with limited loss in adherence, blue filled-in symbols correspond to scenarios with continuous loss in adherence). Plots show median values; error bars represent 95% probability obtained from $n = 250$ independent stochastic runs.



Supplementary Figure 10. Impact of different exit conditions after a 2-week strict lockdown on the timecourse of weekly hospital admission. Plots show projections of the weekly hospital admissions under different hypotheses for the reopening conditions. Progressive transition after lockdown is modeled with 4 weeks of curfew (lighter line) or 6 weeks of curfew (darker line) followed by exit conditions experienced in mid-July 2020, but with schools in session (left); curfew scenarios with 40% fewer individuals respecting physical distancing (center); curfew scenarios with 15% fewer individuals respecting physical distancing (right). Scenarios assume a 10% reduction in transmissibility due to seasonality (except for the mid-July 2020 conditions that already embed seasonal aspects) and a vaccination rhythm of 300,000 first doses per day starting April. Curves refer to the median overall trajectory and the shaded area around the curves corresponds to the 95% probability range obtained from $n=250$ stochastic simulations.



Supplementary Figure 11. Projected impact of interventions on the healthcare system, assuming a 40% transmission increase for Alpha strain. Results refer to interventions applied in w12. From left to right: increasing lockdown duration (weeks). Curves refer to the median overall trajectory, obtained under the vaccination pace of 300k first doses administered per day starting April. The shaded area around the curves corresponds to the 95% probability range obtained from $n=250$ stochastic simulations. The type of intervention is coded by different line colors. Line type indicates increase in transmission due to Alpha infection; 59% solid line vs 40% dotted line. Dots refer to data; filled dots correspond to the data used to fit the model and to provide the trajectory for the curfew scenario; void dots correspond to more recent data. Horizontal dashed line refers to the peak of the second wave in the region. A 7-day delay is assumed from the implementation of the intervention to the peak.



Supplementary Figure 12. Impact of a longer delay in peak after restriction implementation on the timecourse of weekly hospital admissions. From left to right: increasing levels of weekly hospital admissions triggering lockdowns corresponding to implementing interventions in w11 to w15. From top to bottom: increasing lockdown duration (weeks). Curves refer to the median overall trajectory, obtained under the vaccination pace of 300k first doses administered per day starting April. The shaded area around the curves corresponds to the 95% probability range obtained from $n=250$ stochastic simulations. The type of intervention is coded by different line colors. Line type indicates the assumed delay from the implementation of the intervention to the peak; solid line corresponds to a 7 day-delay, dotted-dashed line corresponds to a 10-day delay. Dots refer to data; filled dots correspond to the data used to fit the model and to provide the trajectory for the curfew scenario; void dots correspond to more recent data. Horizontal dashed line refers to the peak of the second wave in the region.

0.6 Supplementary references

1. Svensson, A. A note on generation times in epidemic models. *Math. Biosci.* 208, 300–311 (2007).
2. Cereda, D. et al. The early phase of the COVID-19 outbreak in Lombardy, Italy. *arXiv:2003.09320 [q-bio]* <http://arxiv.org/abs/2003.09320> (2020).
3. Davies, N. G. et al. Estimated transmissibility and impact of SARS-CoV-2 lineage B.1.1.7 in England. *Science* 372, (2021).
4. Hale, T. et al. A global panel database of pandemic policies (Oxford COVID-19 Government Response Tracker). *Nat. Hum. Behav.* 5, 529–538 (2021).
5. Lauer, S. A. et al. The Incubation Period of Coronavirus Disease 2019 (COVID-19) From Publicly Reported Confirmed Cases: Estimation and Application. *Ann. Intern. Med.* 172, 577–582 (2020).
6. Ferretti, L. et al. Quantifying SARS-CoV-2 transmission suggests epidemic control with digital contact tracing. *Science* 368, eabb6936 (2020).
7. Lavezzo, E. et al. Suppression of a SARS-CoV-2 outbreak in the Italian municipality of Vo'. *Nature* 584, 425–429 (2020).

8. Riccardo, F. et al. Epidemiological characteristics of COVID-19 cases and estimates of the reproductive numbers 1 month into the epidemic, Italy, 28 January to 31 March 2020. *Eurosurveillance* 25, 2000790 (2020).
9. Salje, H. et al. Estimating the burden of SARS-CoV-2 in France. *Science* 369, 208–211 (2020).
10. Lapidus, N. et al. Do not neglect SARS-CoV-2 hospitalization and fatality risks in the middle-aged adult population. *Infect. Dis. Now* (2021) doi:10.1016/j.idnow.2020.12.007.
11. Goldstein, E., Lipsitch, M., Cevik, M. On the Effect of Age on the Transmission of SARS-CoV-2 in Households, Schools, and the Community. *J. Infect. Dis.* 223, 362–369 (2021).
12. Galmiche, S. et al. Etude des facteurs sociodémographiques, comportements et pratiques associés à l’infection par le SARS-CoV-2 (ComCor). <https://hal-pasteur.archives-ouvertes.fr/pasteur-03155847> (2021).
13. Li, R. et al. Substantial undocumented infection facilitates the rapid dissemination of novel coronavirus (SARS-CoV2). *Science* (2020) doi:10.1126/science.abb3221.
14. Davies, N. G. et al. Age-dependent effects in the transmission and control of COVID-19 epidemics. *Nat. Med.* 26, 1205–1211 (2020).
15. Viner, R. M. et al. Susceptibility to SARS-CoV-2 Infection Among Children and Adolescents Compared With Adults: A Systematic Review and Meta-analysis. *JAMA Pediatr.* 175, 143 (2021).
16. Santé Publique France. CoviPrev : une enquête pour suivre l’évolution des comportements et de la santé mentale pendant l’épidémie de COVID-19. <https://www.santepubliquefrance.fr/etudes-et-enquetes/coviprev-uneenquete-pour-suivre-l-evolution-des-comportements-et-de-la-sante-mentale-pendant-l-epidemie-de-covid-19> (2020).
17. YouGov.co.uk. COVID-19 Public Monitor. <https://yougov.co.uk/covid-19> (2021).

Article #2

The impact of spatial connectivity on NPIs effectiveness

Chiara E. Sabbatini¹, Giulia Pullano², Laura Di Domenico¹, Stefania Rubrichi³,
Shweta Bansal², Vittoria Colizza^{1,*}

¹Sorbonne Université, INSERM, Pierre Louis Institute of Epidemiology and Public Health, Paris, France. ²Department of Biology, Georgetown University, Washington, DC, USA. ³Orange Labs, Sociology and Economics of Networks and Services (SENSE), Chatillon, France. *corresponding author: vittoria.colizza@inserm.fr

Contents

Contents	5
0.1 Normalcy and Stringency index	6
0.2 SARS-CoV-2 transmission model	6
0.2.1 Compartmental model and parameters	6
0.2.2 Inference framework	8
0.2.3 Parameters fitted in the MCMC procedure	10
0.2.4 Model inputs	20
0.2.5 Model validation	21
0.3 Spatial vs. Non-spatial model	23
0.4 Counterfactual scenarios	25
0.5 Additional results	26
0.5.1 Estimated impact of implemented NPIs on the reproductive number	26
0.5.2 Impact of the Alpha variant and of the vaccination rhythm on the hospitalizations	27
0.5.3 Impact of different nationwide interventions	28
0.6 Sensitivity analysis	28
0.6.1 Impact of relaxation after exiting lockdowns	28
0.6.2 Impact of transmissibility and mobility conditions during lockdowns	30
0.6.3 Impact of weekly rolling average of data	31
0.6.4 References	32

0.1 Normalcy and Stringency index

In **Figure S1**, we show two indicators, the Normalcy and the Stringency index, for France and four other European countries. The Economist's Normalcy index¹ and the Stringency index² are two measures used to evaluate the impact of the pandemic on human behavior and government policies.

The Normalcy index tracks eight different variables (sports attendance, time at home, traffic congestion, retail footfall, office occupancy, flights, film box office and public transport) to quantify an overall score. The pre-pandemic activity level was set at a Normalcy index of 100 to ease comparison. In the period including the second lockdown, the curfew, and the third lockdown, the index for France was computed to be between 37 and 64. The Stringency index quantifies the intensity of government policies. **Figure S1** shows that in the period under study Normalcy and Stringency index took complementary values, suggesting a duality between the two indicators. In the main analysis we use the Normalcy index instead of the Stringency index because it captures not only the stringency of interventions but also the behavioral response.

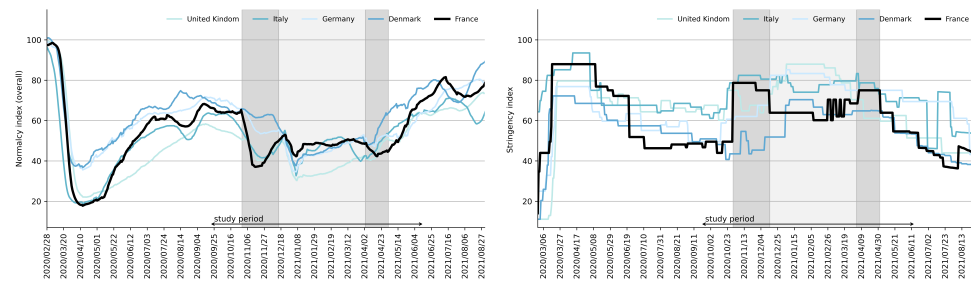


Figure S1. Indicators (left) Normalcy index over time for UK, Italy, Germany, Denmark and France. Shaded rectangle in the plot corresponds to the period of the study. (right) Stringency index over time for UK, Italy, Germany, Denmark and France. Shaded areas in the plot corresponds to the period of the second lockdown, third lockdown (dark grey) and night-time curfew in between (light grey). The horizontal arrow highlights the study period.

0.2 SARS-CoV-2 transmission model

0.2.1 Compartmental model and parameters

Figure S2 shows the compartmental scheme used to describe COVID-19 disease progression. Individuals are divided into susceptible (S), exposed (E), infectious (I), hospitalized (H) and recovered (R). Hospitalized patients are quarantined and they do not transmit the infection. Parameter values related to infection due to historical strains are reported in **Table S1**. We used estimates available in the literature to inform the average durations of the latency, infectious, and hospitalized compartments in the current work. More in detail:

We set the average latency period to $\epsilon^{-1} = 3.7$ days, based on the average length of the incubation period ($\theta^{-1} = 5.2$ days, from Ref.³) and discounting the period between onset of infectiousness and onset of symptoms ($\mu_p^{-1} = 1.5$ days, from Ref.⁴,

computed from the estimates of Ref.⁵). We set the average infectious period to $\mu^{-1} = 2.9$ days to match the estimate of the generation time (6.6 days, from Ref.⁶). We set the average time spent in the hospital to 21 days from Ref.⁴. A time lag of 3.6 days was introduced to delay the entry into the hospitalization compartment to align with the estimates on time from onset to hospital admission⁷.

The complexity of the metapopulation approach with time-varying mobility coupling the French regions required some simplifications in the compartmental structure. For example, we did not consider asymptomatic or presymptomatic transmission. Such simplifications were commonly adopted in other metapopulation models used to study the COVID-19 pandemic^{8,9}.

Parameters values for the Alpha variant are presented in the **Methods section** of the main text. When vaccination starts, we assumed doses to be distributed to either susceptible or recovered individuals with equal probability. Vaccination effectiveness is described in the **Methods section** and reported in **Table S1**.

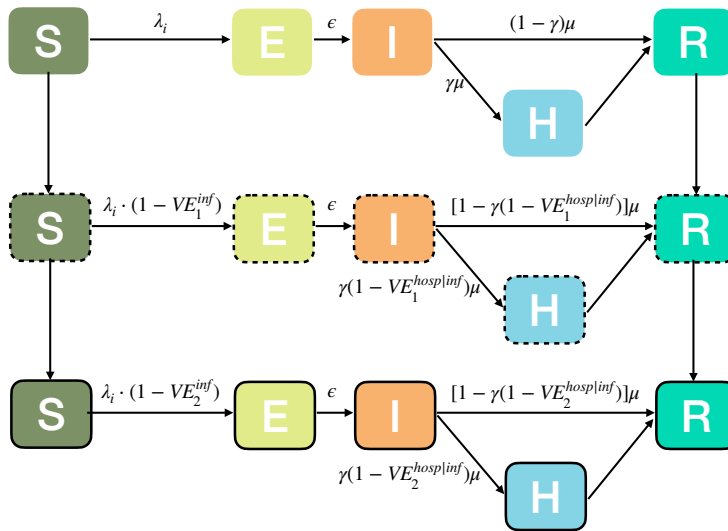


Figure S2. Compartmental scheme with vaccination. Compartments with no-lines (top) account for infections due to historical strains for non-vaccinated people. Analogous compartments are considered for vaccinated individuals (dashed and solid lines). S=Susceptible, E=Exposed, I= Infectious, H=severe case admitted to the hospital, R=Recovered. $VE^{hosp|inf}$ has been computed using the relationship: $1 - VE^{hosp} = (1 - VE^{inf}) \cdot (1 - VE^{hosp|inf})$. VE^{transm} is embedded in the force of infection. Variables are defined in **Table S1**

Table S1. Parameters, values, and sources used to define the compartmental model for infection due to historical strains.

Name	Description	Value	Source
ϵ^{-1}	Latency period	3.7 days	-
μ^{-1}	Infectious period	2.9 days	-
γ	If infected, probability of going to hospital	2.1%	¹⁰
VE_1^{inf}, VE_2^{inf}	Vaccine effectiveness in preventing infection in case of 1 or 2 doses	60%, 87.5%	11,12
VE_1^{hosp}, VE_2^{hosp}	Vaccine effectiveness in preventing hospitalization in case of 1 or 2 doses	80%, 97.2%	11,12
$VE_1^{transm}, VE_2^{transm}$	Vaccine effectiveness in preventing transmission in case of 1 or 2 doses	15%, 68%	¹³

0.2.2 Inference framework

The time windows used for the fit are defined based on the interventions applied in France (**Table 1, Table S2**), specifically: pre-second lockdown (Sept 21,2020 – region dependent date), second lockdown (region dependent date – Nov 22, 2020), curfew 8pm (Dec 15, 2020 – Jan 15, 2021), curfew 6pm pre holidays (Jan 16, 2021 – region dependent date due to school holidays), curfew 6pm during holidays (region dependent date due to school holidays), curfew 6pm post holidays (region dependent date due to school holidays – April 3, with the exception of few departments), third lockdown (April 3, with the exception of few departments – Jun 13, 2021).

Table S2. Time windows used for curfews implementation.

NPIs	Time window used	Regions
Curfew 6pm pre holidays	Jan 16, 2021 – Feb 6, 2021	ARA,BFC,NAQ
	Jan 16, 2021 – Feb 20, 2021	BRE,CVL,GRE,HDF, NOR,PACA, PDL
	Jan 16, 2021 – Feb 13, 2021	IDF,OCC
Curfew 6pm holidays	Feb 7, 2021 – Feb 21, 2021	ARA,BFC,NAQ
	Feb 21, 2021 – Mar 7, 2021	BRE,CVL,GRE,HDF, NOR,PACA, PDL
	Feb 14, 2021 – Feb 28, 2021	IDF,OCC
Curfew 6pm post holidays	Feb 22, 2021 – Apr 3, 2021	ARA,BFC,NAQ
	Mar 8, 2021 – Apr 3, 2021*	BRE,CVL,GRE,HDF, NOR,PACA, PDL
	Feb 29, 2021 – Apr 3 2021*	IDF,OCC

*third lockdown applied earlier (on Mar 20, 2021) in IDF, HDF, PACA.

The model was initialized on March 1, 2020 from estimated prevalence obtained from prior work¹⁴, which was validated against serological data. Each stochastic run

of the metapopulation model was initialized on that date by sampling the prevalence of each compartment from a Gumbel-r distribution. Its cumulative distribution function is given by:

$$F(x; \mu, \beta) = e^{-e^{-\frac{(x-\mu)}{\beta}}}$$

where β is the scale parameter, which controls the spread or dispersion of the distribution; μ is the location parameter, which represents the location of the distribution on the x -axis. In our analysis, we opted for the Gumbel distribution as it resulted to be the best distribution in terms of AIC among a set of commonly used distributions (Alpha, Gamma, Invgamma Levy, Loggamma, Lognorm, Pownorm, Norm) when fitting the prevalence estimated in our prior work¹⁴ through a maximum likelihood approach. We chose this initialization procedure as surveillance data prior to March 1, 2020 were of lower quality given that the surveillance system for hospitalizations was being developed, and this hindered the fitting procedure of the metapopulation model prior to the exponential increase of cases. In addition, fitting the early start of the pandemic requires also fitting the seeding date in each region, i.e. potentially in the month of December 2019. However, we lack mobility data for the end of 2019, therefore we were forced to use a region-specific model for the fit of the early phase, without spatial connectivity, and then use its results to initialize our metapopulation model. We expect this not to impact the successive spatial dynamics because of the small epidemic size prior to March 1, 2020 and of the time distance between the initialization (March 2020) and the period under study (starting September 2020). This is further supported by the validation of the model at subsequent dates and by the model selection analysis illustrating how the metapopulation model better describes the observed dynamics compared to a non-spatial model.

The metapopulation model fitted the epidemic trajectories of hospital admission data from March 1, 2020 to June 13, 2021.

Model parameters were estimated in a Bayesian framework by sampling the posterior parameter distribution obtained by updating prior beliefs based on a likelihood function. The likelihood function is evaluated on daily data of regional hospital admissions (**Methods** section *Inference framework and validation*). We used Markov Chain Monte Carlo (MCMC) to obtain posterior distributions, assuming a uniform prior. We used three independent chains, with each chain performing 3000 steps, to approximate the posterior distribution. We used the Metropolis-Hasting algorithm to accept or reject the set of parameters at each step. We performed 200 stochastic simulations to compute median values and associated 95% probability ranges for all quantities of interest.

To demonstrate that our model is able to estimate the parameters with the proposed inference approach and does not suffer from identifiability issues, we performed the following synthetic experiment. We parameterized the model using as priors the set of parameter values estimated with the first MCMC, and we re-calibrated the model with another MCMC procedure. By retrieving the same set of parameter values, we showed that the model was well identified and could be calibrated without bias.

0.2.3 Parameters fitted in the MCMC procedure

We used daily hospital admission data at the regional level to fit the model.

The values of the fitted transmission rates ($\beta_i^{intrinsic}(t)$) and time from lockdown implementation to hospitalization peak are reported in **Table S3**. The distributions of the fitted parameters are reported in **Figures S3-S11**.

Table S3. Values of the fitted parameters. The parameter β refers to the intrinsic transmission rate $\beta_i^{intrinsic}$ defined in the main text.

Region	β (pre-LD2)	β (LD2)	β (curfew 8pm)	β (curfew 6pm pre holidays)	β (curfew 6pm holidays)	β (curfew 6pm post holidays)	β (LD3)	Time from lockdown application to hospitalization peak, LD2	Time from lockdown application to hospitalization peak, LD3
ARA	0.573627	0.218227	0.377573	0.291390	0.292125	0.325563	0.290536	1 days	8 days
BFC	0.625011	0.315116	0.459515	0.338697	0.328621	0.386210	0.340951	2 days	5 days
BRE	0.481102	0.242640	0.328915	0.221431	0.234657	0.272123	0.239864	6 days	0 days
CVL	0.539905	0.280794	0.398681	0.298373	0.288718	0.311664	0.281231	4 days	5 days
GRE	0.576878	0.27459	0.364502	0.333694	0.316897	0.374449	0.280219	2 days	0 days
HDF	0.575018	0.250048	0.385831	0.327443	0.295461	0.323445	0.274093	2 days	6 days
IDF	0.548415	0.260598	0.394023	0.338249	0.337227	0.355278	0.320925	0 days	12 days
NAQ	0.532347	0.273099	0.385755	0.261476	0.263212	0.285782	0.267691	3 days	1 days
NOR	0.572577	0.241925	0.377648	0.259662	0.259865	0.307323	0.264029	2 days	9 days
OCC	0.567135	0.190596	0.393210	0.272494	0.258899	0.274563	0.254088	1 days	8 days
PACA	0.598687	0.217141	0.465066	0.332263	0.324089	0.340098	0.324295	2 days	8 days
PDL	0.542186	0.276619	0.374060	0.248372	0.262255	0.308712	0.269117	3 days	0 days

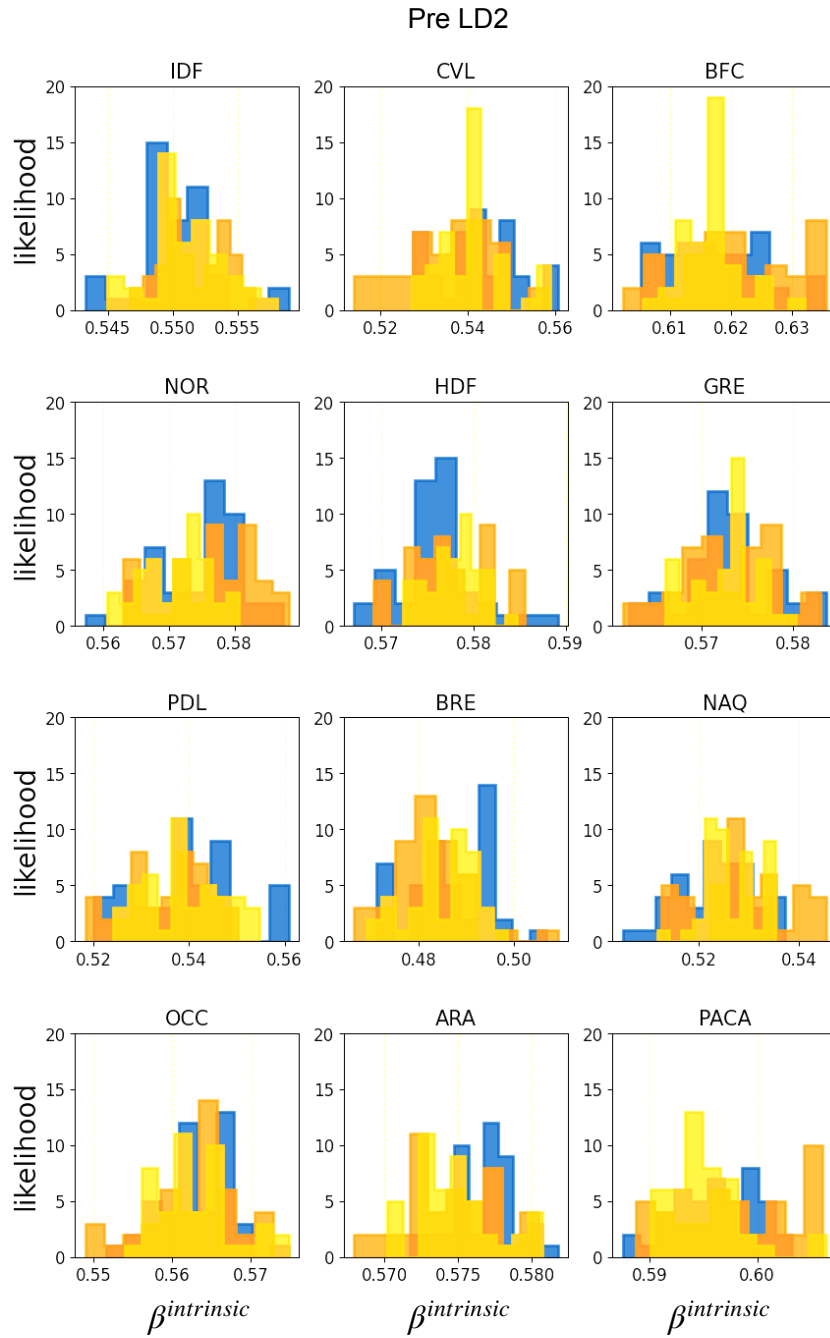


Figure S3. Histograms of samples. We reported the histograms of sampled values for the $\beta^{intrinsic}$ (*preLD2*) parameter in each region, obtained from three independent chains (yellow, orange and blue histogram), after discarding the burn-in period.

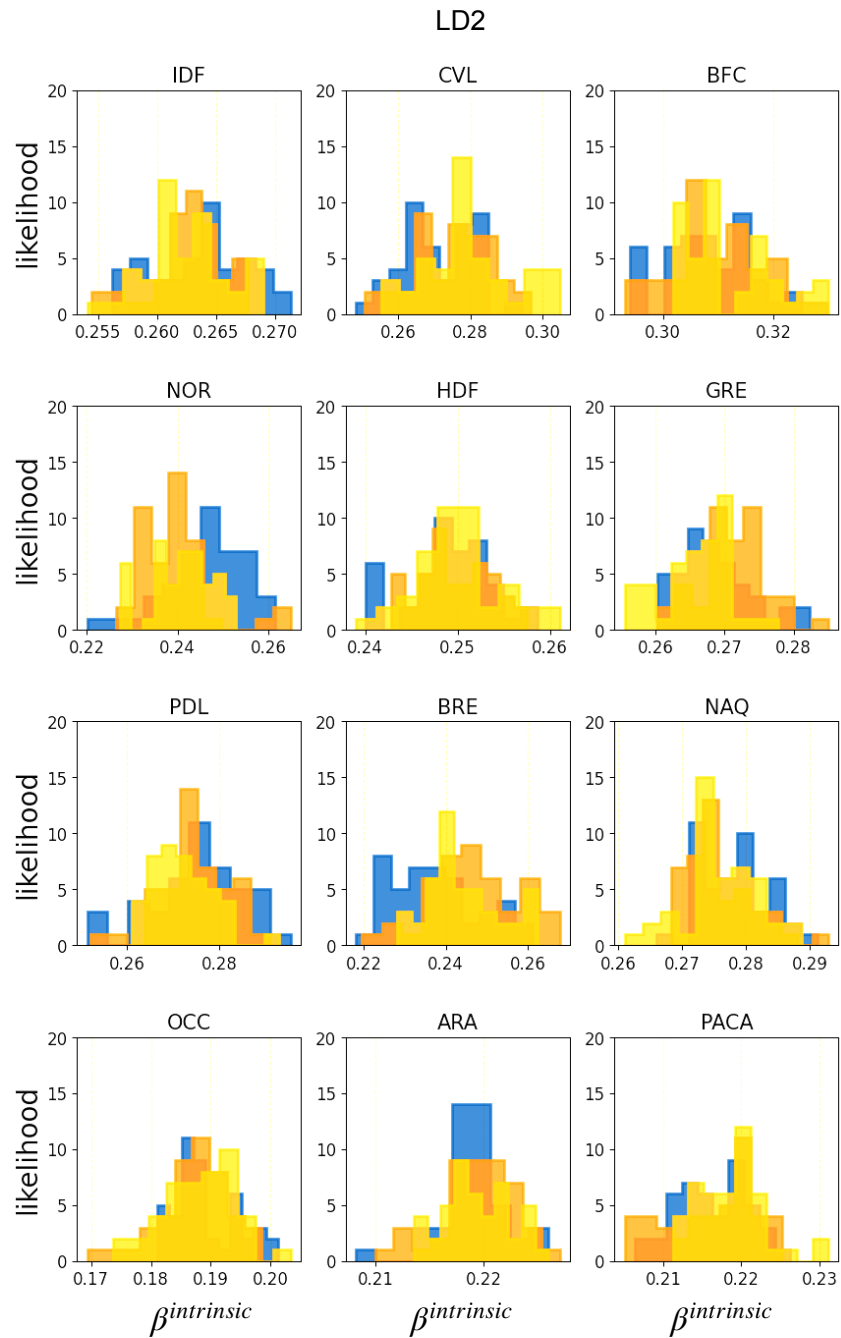


Figure S4. Histograms of samples. We reported the histograms of sampled values for the $\beta^{intrinsic}(LD2)$ parameter in each region, obtained from three independent chains (yellow, orange and blue histogram), after discarding the burn-in period.

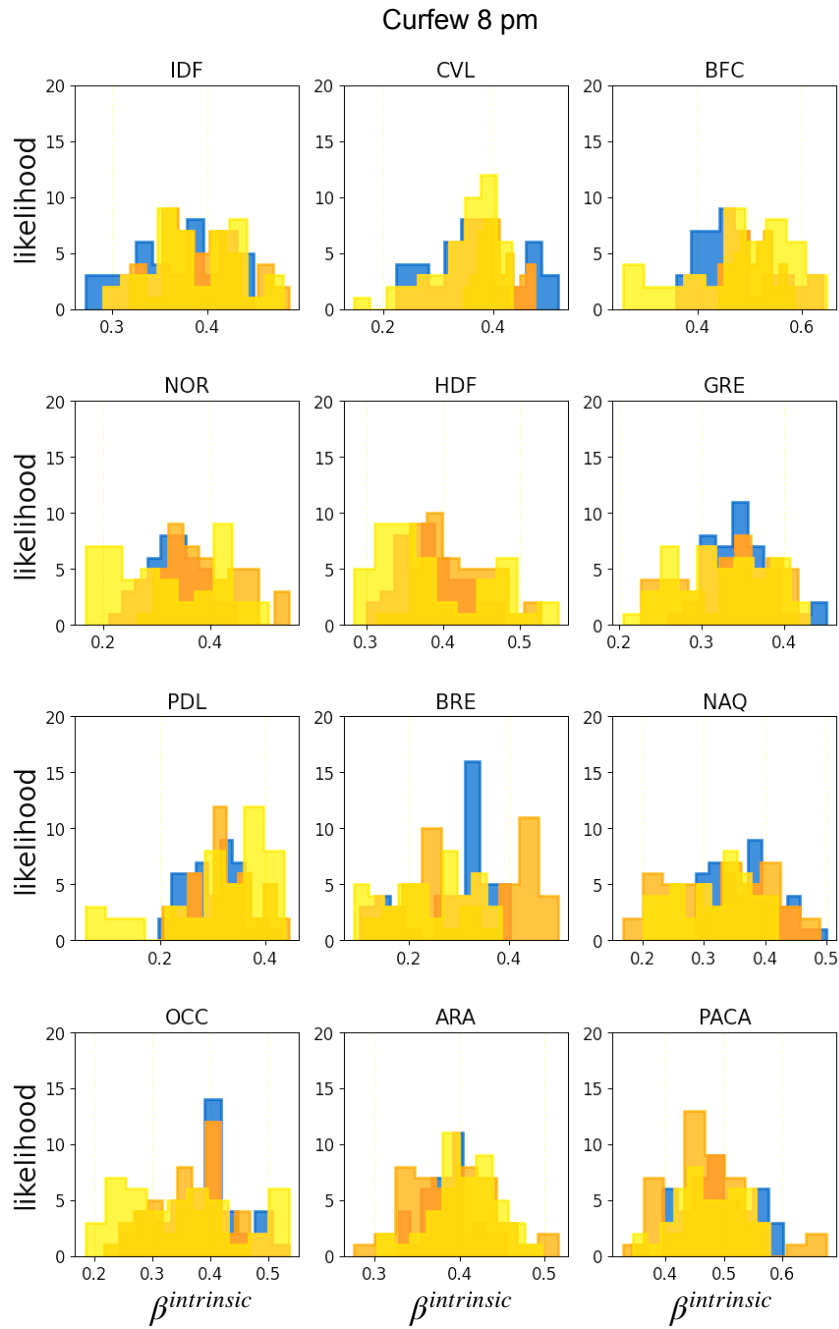


Figure S5. Histograms of samples. H We reported the histograms of sampled values for the $\beta^{intrinsic}$ (curfew 8pm) parameter in each region, obtained from three independent chains (yellow, orange and blue histogram), after discarding the burn-in period.

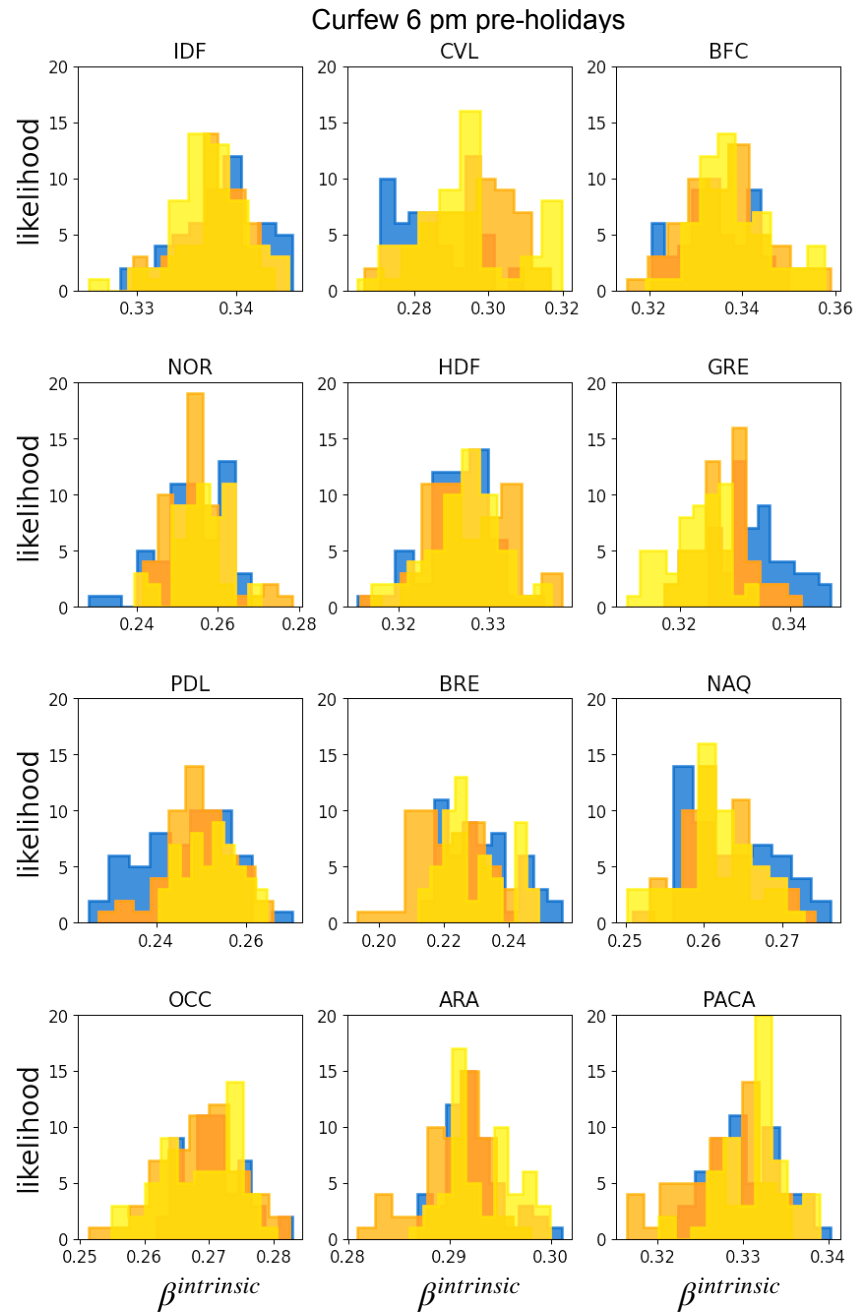


Figure S6. Histograms of samples. We reported the histograms of sampled values for the $\beta^{intrinsic}$ (curfew 6pm pre-holidays) parameter in each region, obtained from three independent chains (yellow, orange and blue histogram), after discarding the burn-in period.

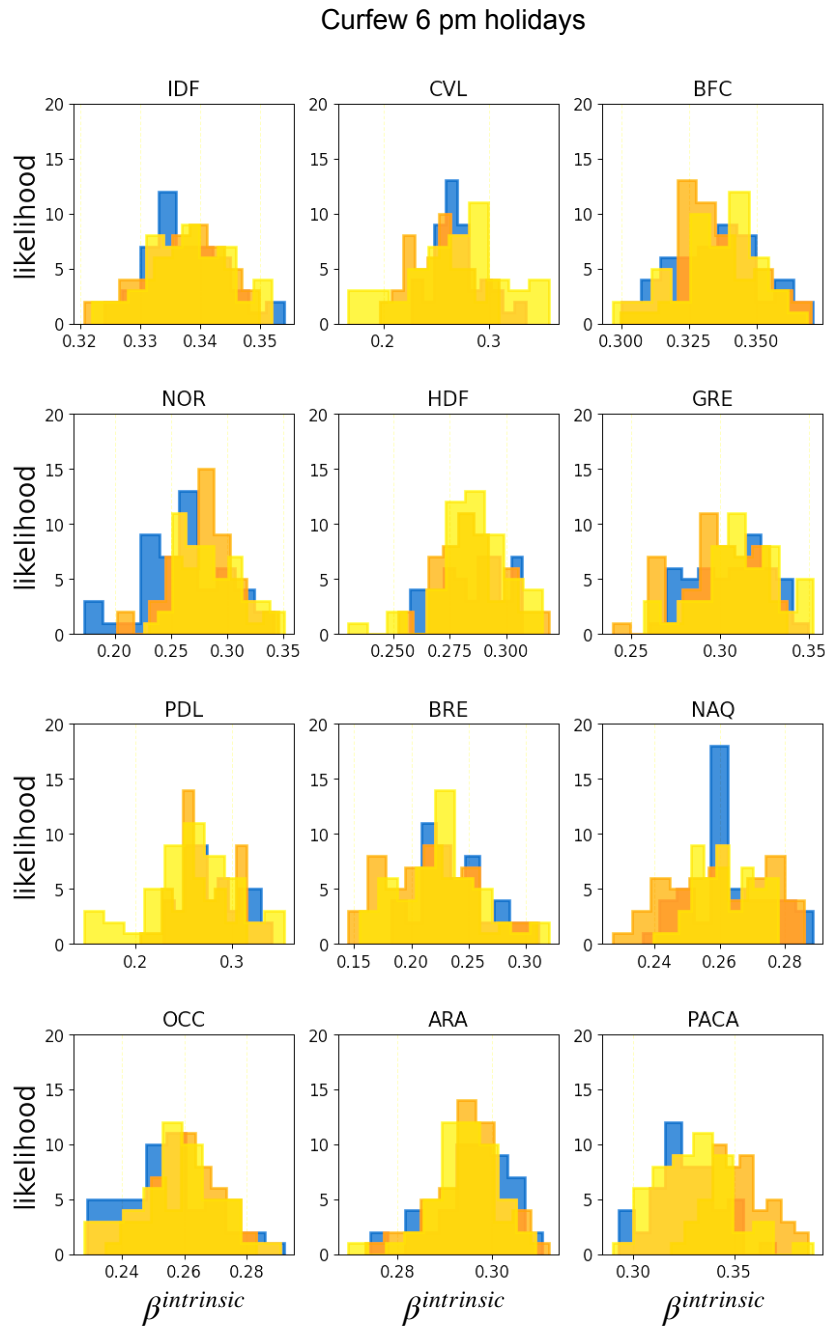


Figure S7. Histograms of samples. We reported the histograms of sampled values for the $\beta^{intrinsic}$ (curfew 6pm holidays) parameter in each region, obtained from three independent chains (yellow, orange and blue histogram), after discarding the burn-in period.

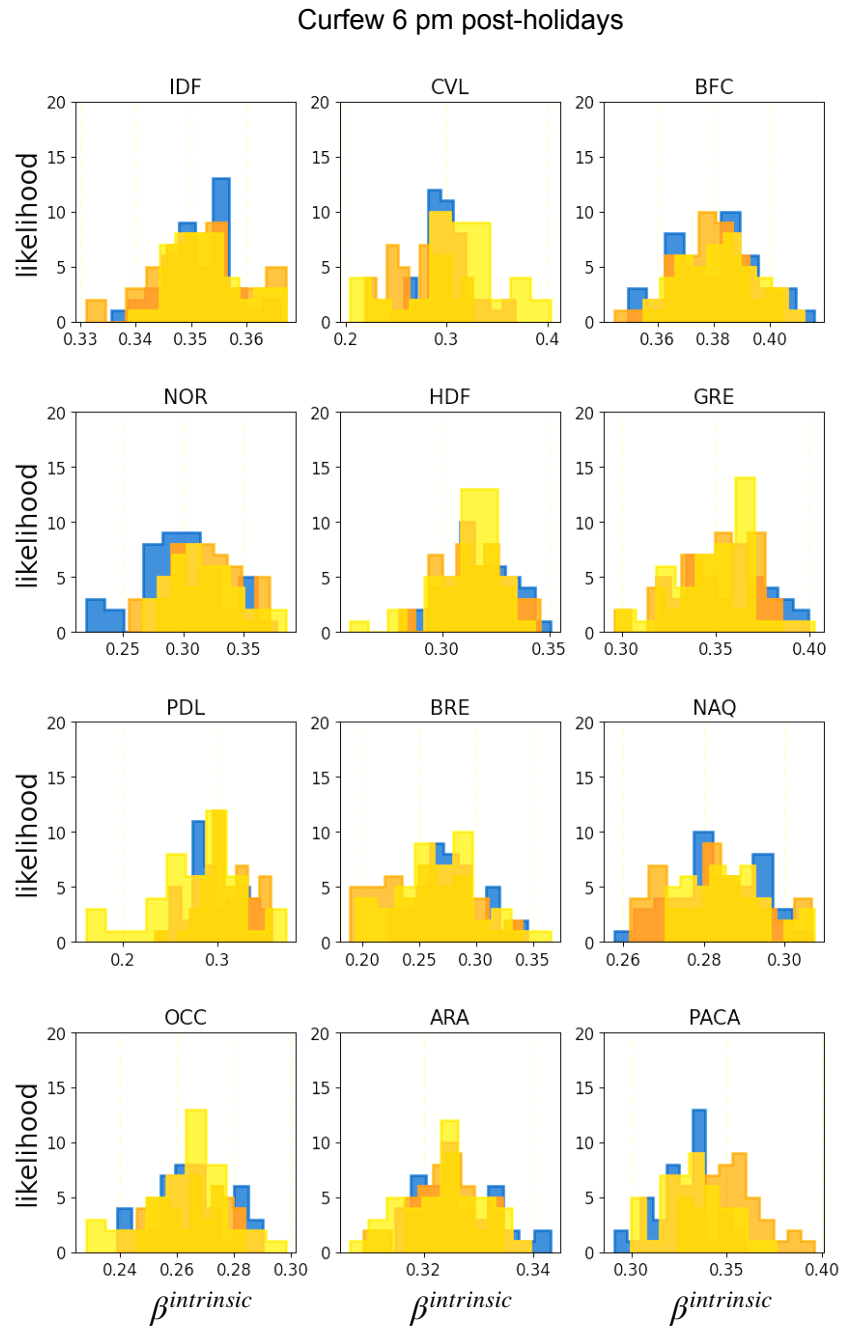


Figure S8. Histograms of samples. We reported the histograms of sampled values for the $\beta^{intrinsic}$ (curfew 6pm post-holidays) parameter in each region, obtained from three independent chains (yellow, orange and blue histogram), after discarding the burn-in period.

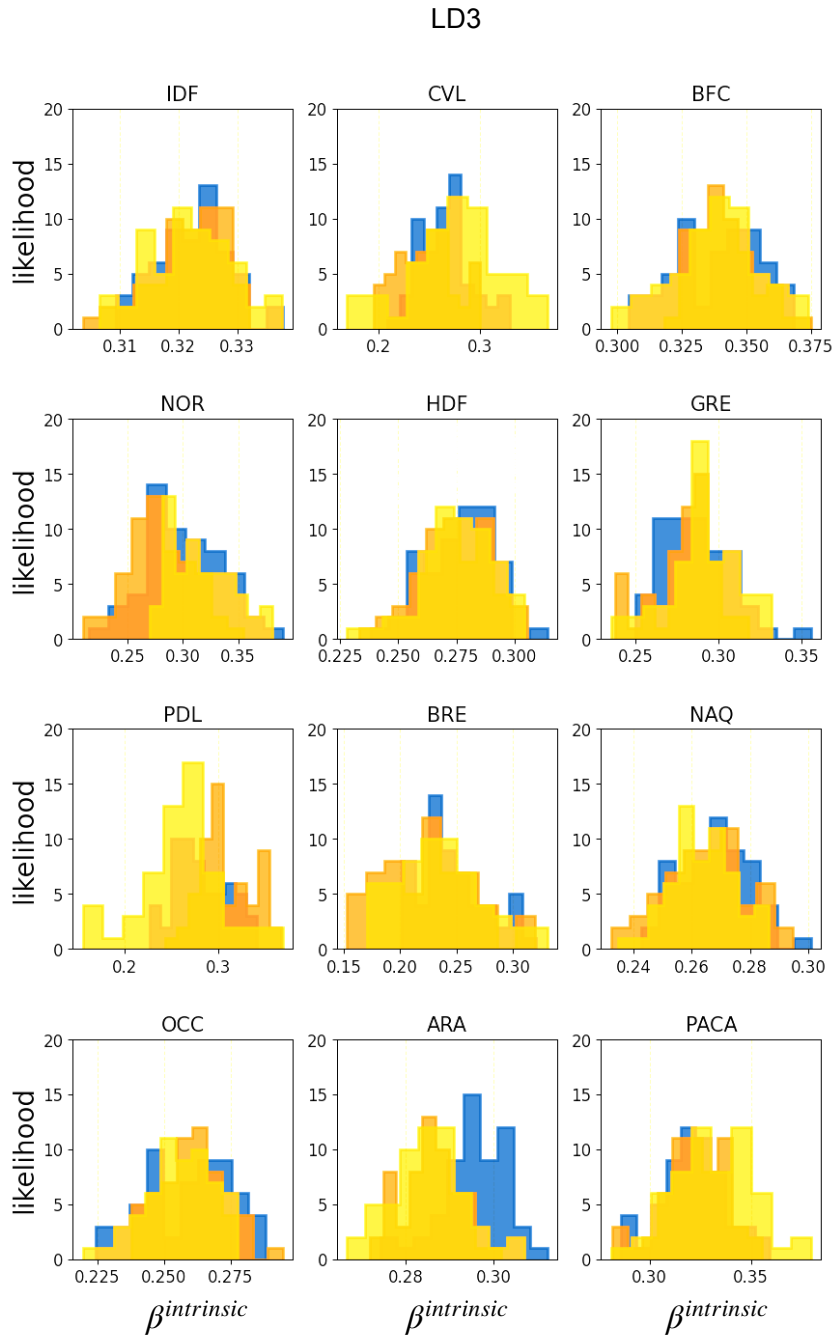


Figure S9. Histograms of samples. We reported the histograms of sampled values for the $\beta^{intrinsic}$ (LD3) parameter in each region, obtained from three independent chains (yellow, orange and blue histogram), after discarding the burn-in period.

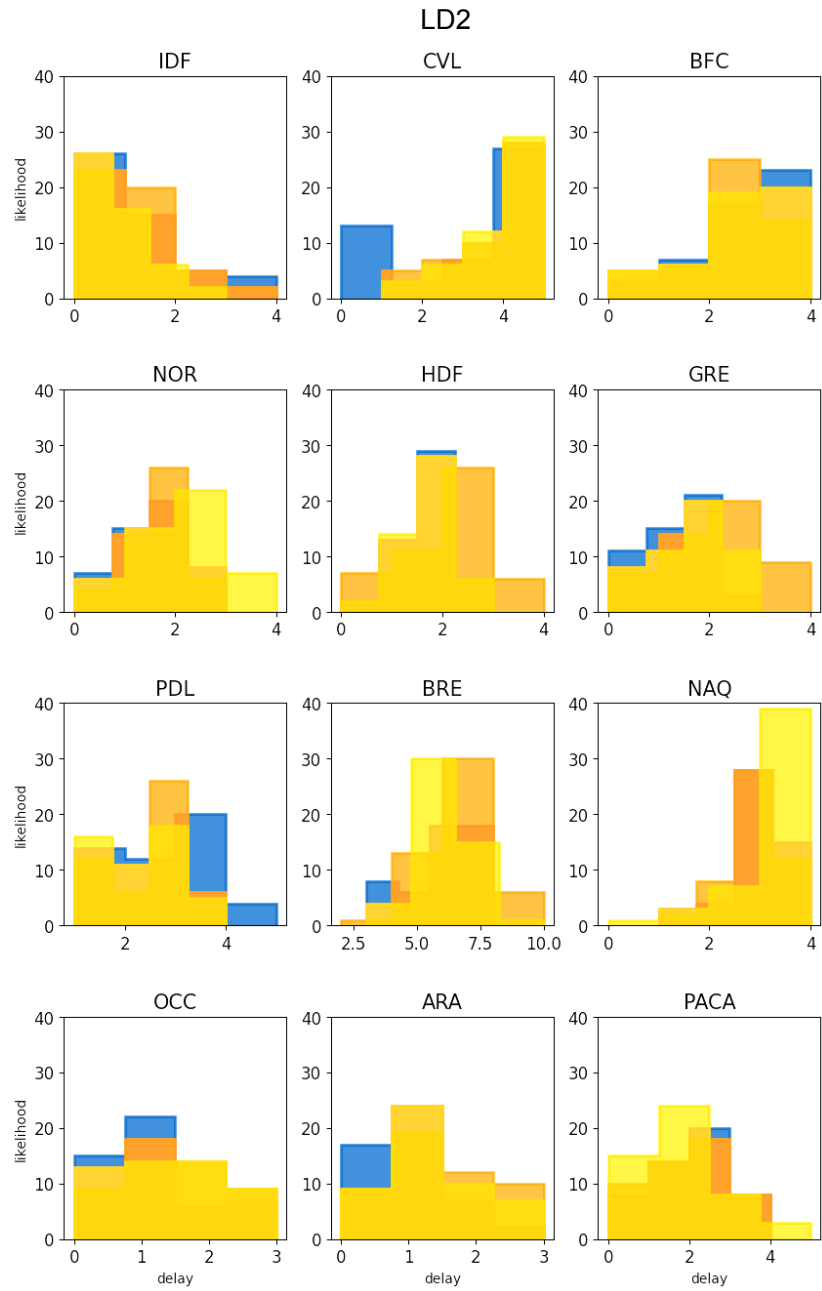


Figure S10. Histograms of samples. We reported the histograms of sampled values for the $delay(LD2)$ parameter in each region, obtained from three independent chains (yellow, orange and blue histogram), after discarding the burn-in period.

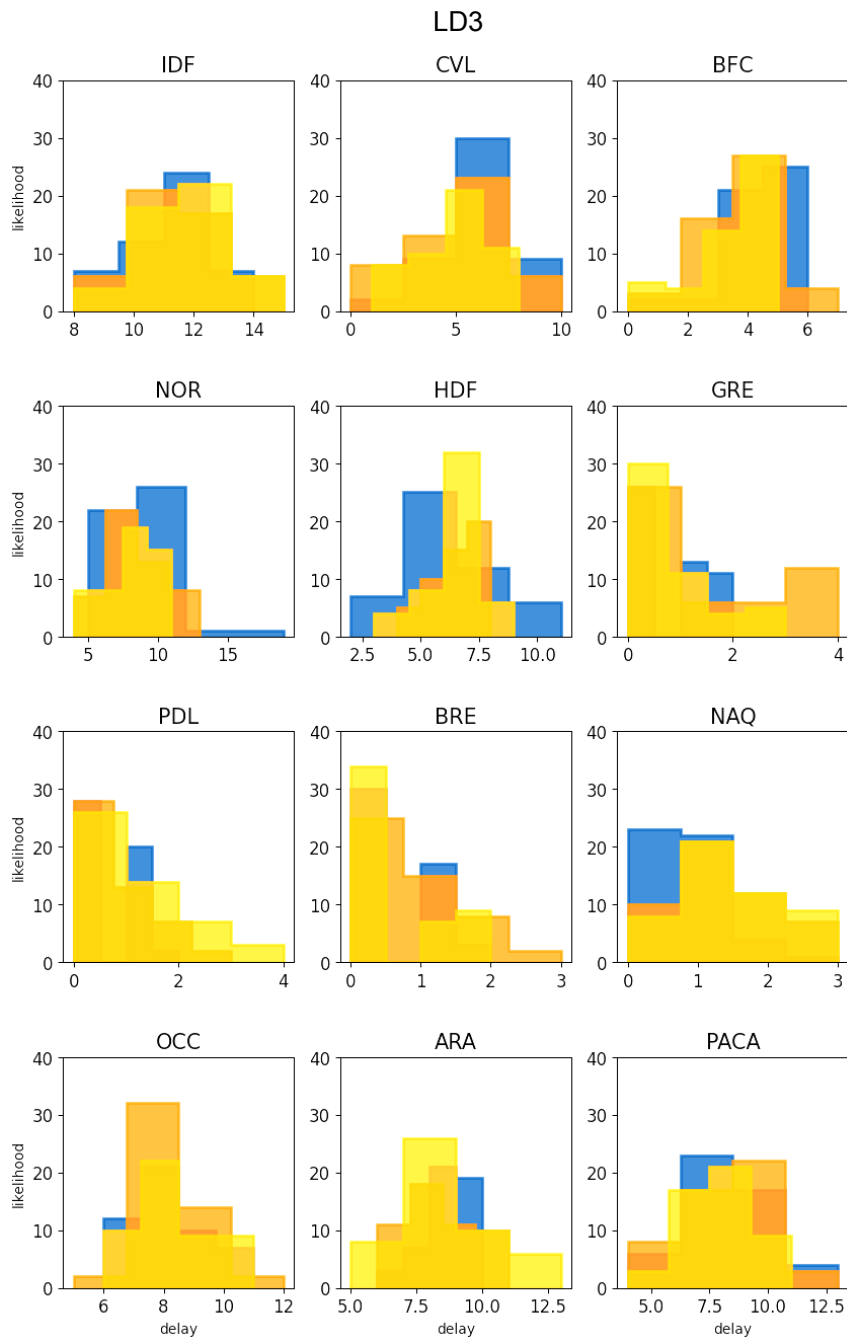


Figure S11. Histograms of samples. We reported the histograms of sampled values for the $delay(LD3)$ parameter in each region, obtained from three independent chains (yellow, orange and blue histogram), after discarding the burn-in period.

0.2.4 Model inputs

In the figure (**Figure S12**) we show the model inputs, including the change in seasonality over time, the percentage of vaccine doses administered over time, the mobility reduction, and the Alpha variant penetration over time. All these inputs were used in the model at the regional level.

Estimates from data from Ref.¹⁵ on the impact of seasonal climatic conditions on transmissibility yield an average increase of 23% of transmissibility during winter. A stronger seasonal effect is observed in northern areas with respect to the south, with a maximum difference of 17 days in the winter peak observed across regions (**Figure S12a**). We fitted the estimates with a sinusoidal curve, one for each region, using a least-squares optimization function.

A large-scale vaccination campaign started in France on December 27, 2020, prioritizing the population at risk (elderly, vulnerable individuals and healthcare personnel). Data on the number of vaccine doses administered¹⁶ included information at the regional level and by stage of vaccination (1st or 2nd dose). By June 12, 2021, around 30 million first injections had been distributed¹⁷, corresponding to 45% of the total population and 20.8% of the total population was fully vaccinated with a second dose (**Figure S12b**). For comparison, we also tested scenarios following the vaccination pace adopted in the United Kingdom¹⁸, where the fraction of population with a first dose reached 45% by April 15, 2021.

Different protocols were adopted over time for genome sequencing surveys to assess variant circulation. Flash#1 and Flash#2 surveys analyzed PCR-positive samples¹⁹. Flash#1 was conducted on Jan 8, identifying 3.3% of new cases due to Alpha. Flash#2 analyzed 10,261 samples from Jan 27, identifying 261 samples that were confirmed as Alpha variant (13.0%). Due to the need for more timely variant surveillance, a new protocol was introduced in week 6, 2021. It estimated the weekly frequency of detected viruses with specific mutations, including the N501Y mutation found in the Alpha variant, using second-line RT-PCR tests. Variant penetration was estimated by fitting the Flash surveys data¹⁹ with a logistic function (**Figure S12d**). To quantify the transmission advantage, we first estimated the daily effective reproductive numbers independently for each strain (wildtype or Alpha) at the national level starting on week 5, 2021. We then fitted the daily ratio $\frac{R_{Alpha}}{R_{wildtype}}$ with a zero-degree and a second-degree polynomial over time to allow possible variations of the transmission advantage over time. In agreement with prior estimates¹⁹, we found that initially the SARS-CoV-2 Alpha variant was 1.58 times more transmissible than the wild type. The magnitude of the transmission advantage varied over time, decreasing from 1.58 in week 5, 2021 to 1.42 in week 22, 2021, similarly to what observed in United Kingdom²⁰. These effects could be associated with vaccination, as vaccines may reduce outward transmission by reducing viral loads^{13,20}.

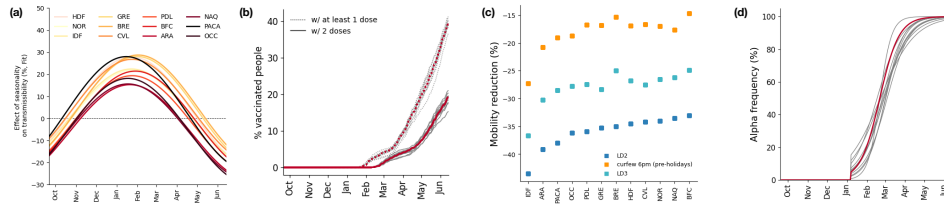


Figure S12. Model inputs and indicators. (a) Estimated effect of seasonality on the transmission over the study period. Regions are represented with solid lines of different colors: Île-de-France (IDF), Centre-Val de Loire (CVL), Bourgogne-Franche-Comté (BFC), Normandy (NOR), Hauts-de-France (HDF), Grand Est (GRE), Pays de la Loire (PDL), Brittany (BRE), Occitanie (OCC), Nouvelle Aquitaine (NAQ), Auvergne-Rhône-Alpes (ARA), Provence-Alpes-Cote d'Azur (PACA). (b) Percentage of vaccinated people with at least one dose (dotted lines) and with two doses (solid lines) according to data¹⁶. Grey lines represent the twelve French regions, red lines represent France. (c) Estimated change in mobility by region and by intervention based on Orange mobility data²¹. Dark blue squares represent the second lockdown period, light blue squares represent the third lockdown period and orange squares represent the curfew implemented at 6p.m. before the school holidays. (d) Percentage of Alpha variant over time. Grey lines represent the twelve French regions, red line represents France.

0.2.5 Model validation

By including the processes of seroconversion and seroreversion following estimates of Ref.²², we compared model projections of antibody positive people (AB+) with serological estimates^{23,24} (Figures S13, S14, Methods section). Modelling results are in good agreement with the serological estimates in the large majority of the regions and for the whole France.

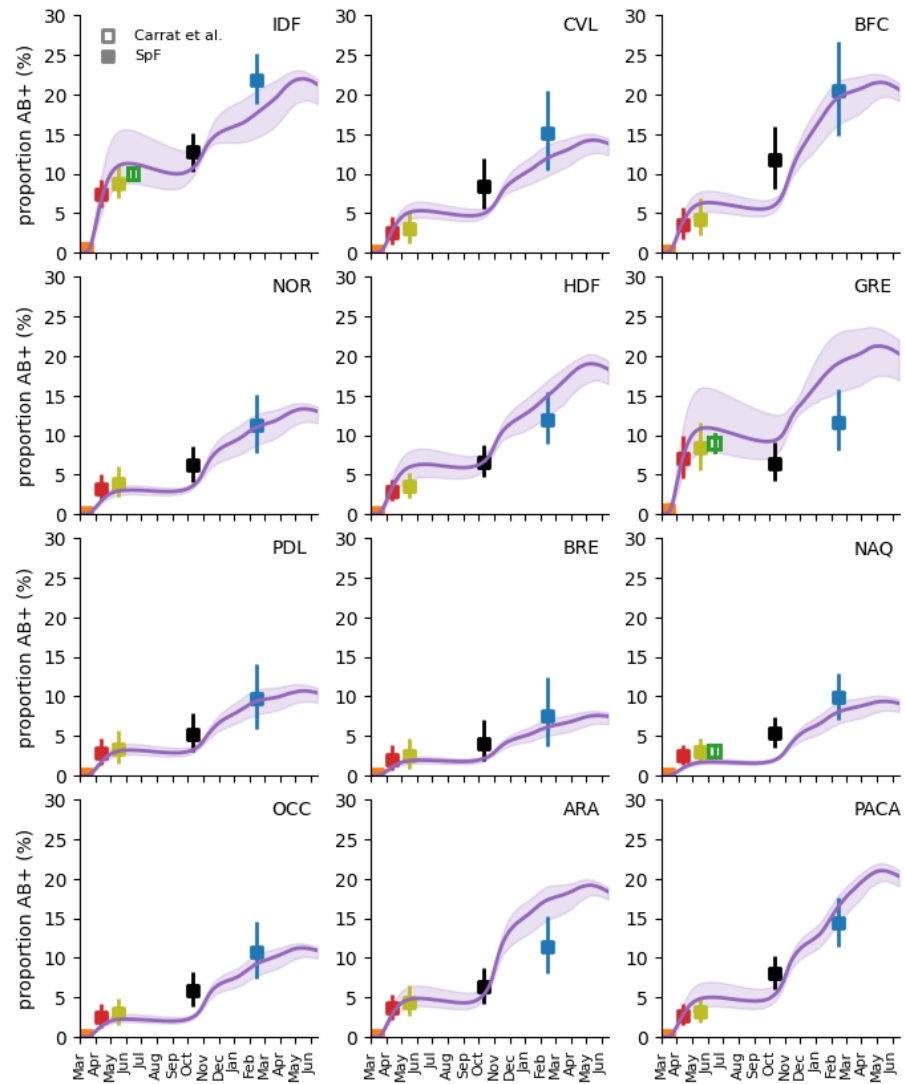


Figure S13. Model predictions versus serological estimates, french regions. For each region the panel shows the predicted percentage of antibody positive people (AB+) over time (purple curves and shaded areas for median and 95% probability range) and serological estimates of, Santé publique France (SpF)²³ (filled squares) and ref.²⁴ (void squares in IDF, GRE, NAQ). The square's colors refer to the different dates studies were conducted. Medians and 95% confidence intervals for model projections are obtained from $n = 200$ independent stochastic runs. Plots are reported for all 12 regions of mainland France : Île-de-France (IDF), Centre-Val de Loire (CVL), Bourgogne-Franche- Comté (BFC), Normandy (NOR), Hauts-de-France (HDF), Grand Est (GRE), Pays de la Loire (PDL), Brittany (BRE), Occitanie (OCC), Nouvelle Aquitaine (NAQ), Auvergne-Rhône-Alpes (ARA), Provence-Alpes-Cote d'Azur (PACA).

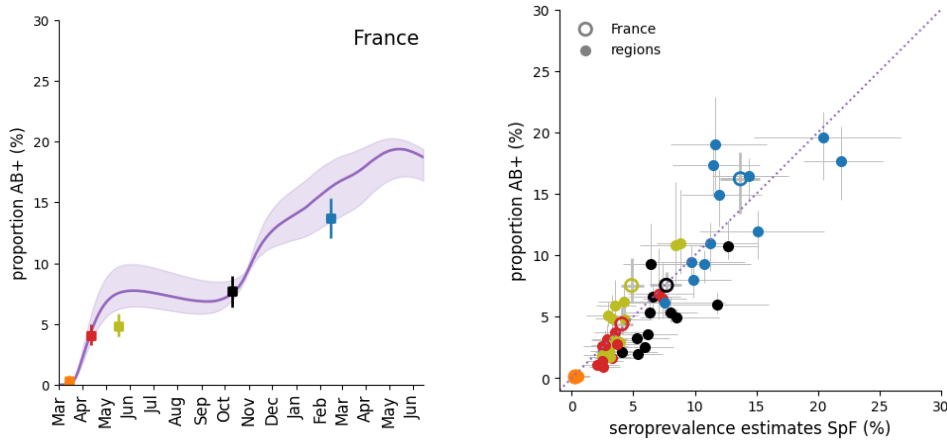


Figure S14. Model predictions versus serological estimates, nationwide estimates. (left) Model predicted percentage of antibody positive people (AB+) over time for France (purple curves and shaded areas for median and 95% probability ranges) and serological estimates of Santé publique France (SpF)²³, the square's colors refer to the different dates studies were conducted. (right) Model prediction of the percentage of antibody positive people versus the serological estimates per region (filled dots) and France (void dots) from Santé publique France (SpF)²³. Error bars correspond to 95% probability ranges. The circles's colors refer to the different dates studies were conducted.

0.3 Spatial vs. Non-spatial model

We compared our metapopulation model with a non-spatial one, by fitting the transmission rates separately for each model, with and without spatial dependence. The model without spatial dependence considers that regions are not coupled by mobility. The resulting Deviance information criterion (DIC) shows that our model better describes the observed trajectories (**Table S4, Figure S15**), thus indicating that accounting for connections between regions is important to capture the epidemic dynamics.

Table S4. Deviance information criterion (DIC) values values for the two versions of the model.

	Metapopulation model (i.e. model used in the study)	Non-spatial model
DIC	36642.16	51536.97

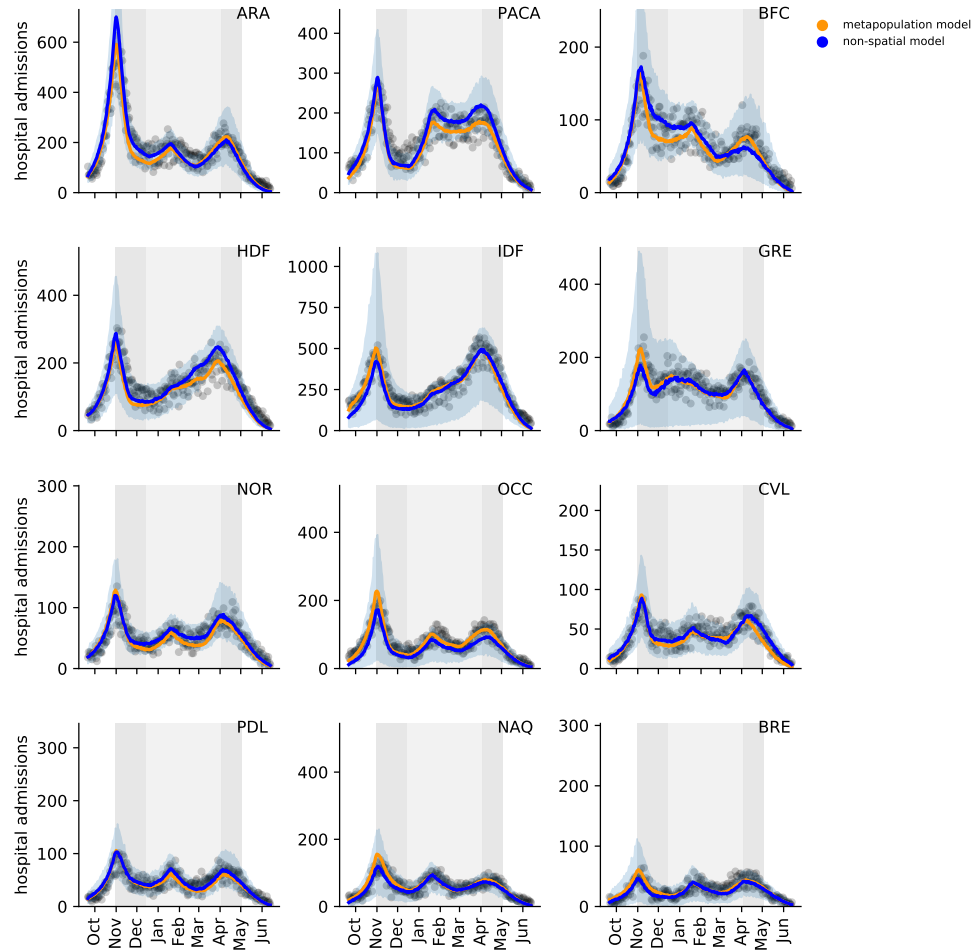


Figure S15. COVID-19 pandemic trajectory in French regions: comparison between metapopulation model used in the study and the non-spatial model. For each region, the panel shows the calibration of the model on data of daily hospital admissions with the metapopulation model (orange) and the non-spatial model (blue). Black dots indicate data, lines represent the median curve, shaded areas correspond to 95% probability ranges. Medians and 95% probability ranges for model projections are obtained from 200 independent stochastic runs. The abbreviations in the upper right corner of each plot stand for the name of the region. ARA : Auvergne-Rhône-Alpes, PACA : Provence-Alpes-Cote d’Azur, BFC : Bourgogne-Franche-Comté, HDF : Hauts-de-France, IDF: Île-de-France, GRE: Grand Est, NOR: Normandie, OCC : Occitanie, CVL: Centre-Val de Loire, PDL : Pays de la Loire, NAQ: Nouvelle Aquitaine, BRE: Bretagne. Grey areas in the plots correspond to social distancing measures: lockdown during the second wave, lockdown during the third wave, and curfew in between.

We also computed the mean absolute error (MAE) for each run of each model. We obtained a lower MAE for the spatial model in 7 regions out of 11 (64%; for IDF the errors are compatible), **Figure S16**.

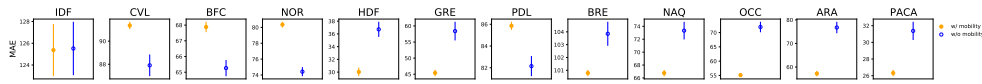


Figure S16. MAE: comparison between metapopulation model used in the study and the non-spatial model. For each region, the panel shows the mean absolute error. Circles represent the averaged MAE and its standard error estimated values for the 200 independent stochastic runs. Filled circles represent the estimates with the metapopulation model; void circles represent estimates with the non-spatial one. Plots are reported for all 12 regions of mainland France : Île-de-France (IDF), Centre-Val de Loire (CVL), Bourgogne-Franche-Comté (BFC), Normandy (NOR), Hauts-de-France (HDF), Grand Est (GRE), Pays de la Loire (PDL), Brittany (BRE), Occitanie (OCC), Nouvelle Aquitaine (NAQ), Auvergne-Rhône-Alpes (ARA), Provence-Alpes-Cote d'Azur (PACA).

0.4 Counterfactual scenarios

Table S5 and **Table S6** provided additional information on counterfactual scenarios. **Table S5** reports the values for the trigger (T) and release (R) thresholds of simulated lockdowns expressed in terms of daily hospital admissions per 100,000. **Table S6** reports the days spent under restrictions, for both the observed situation and the counterfactual scenarios discussed in the main text.

Table S5. Reference thresholds for trigger and release stop-and-go lockdowns. Values refer to daily hospital admissions per 100,000.

Trigger threshold (T)	Release threshold (R)
6.325	0.650

Table S6. Days spent under lockdowns.

	Overall days	Effective days
observed	227 (47 in LD2, 149 under curfew, 31 in LD3)	157.291
T-70%R-35%	196 (over 3 lockdowns)	156.51
T-35%R-70%	189 (over 2 lockdowns)	154.84
T, R	150 (over 3 lockdowns)	122.28

0.5 Additional results

We present in this section some additional results of our analyses not shown in the main text.

0.5.1 Estimated impact of implemented NPIs on the reproductive number

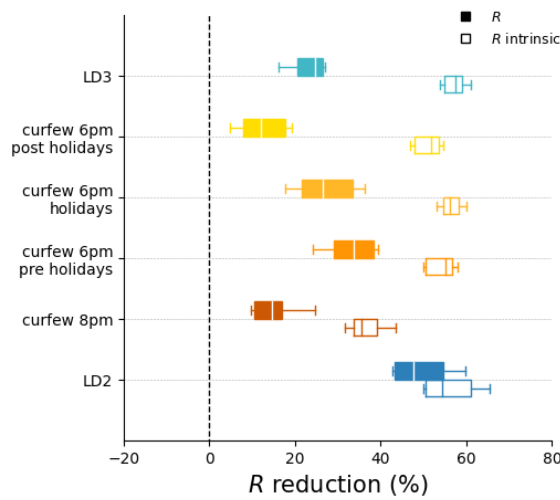


Figure S17. Estimated impact of implemented NPIs. Reduction in the estimated effective reproductive numbers R associated to the implemented social distancing interventions compared with the values estimated before the second lockdown. Box plots represent the median (line in the middle of the box), interquartile range (box limits) and 2.5th and 97.5th percentiles (whiskers) of the estimated values for the 12 French regions. Filled boxplots represent reductions estimated by the fit accounting for all time-varying processes; void boxplots represent reductions estimated in the absence of the Alpha variant and seasonality effects.

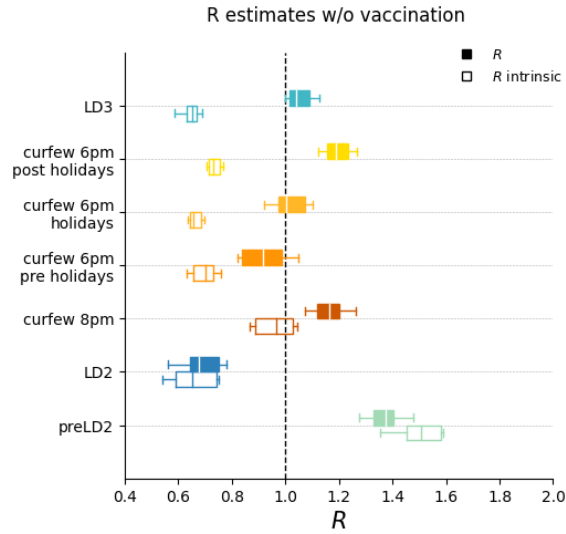


Figure S18. Estimated impact of implemented NPIs, in absence of vaccination. Estimates of the effective reproductive numbers for the implemented social distancing interventions in absence of vaccination. Box plots represent the median (line in the middle of the box), interquartile range (box limits) and 2.5th and 97.5th percentiles (whiskers) of the estimated values for the 12 French regions. Filled boxplots represent reductions estimated by the fit accounting for all time-varying processes; void boxplots represent reductions estimated in the absence of the Alpha variant and seasonality effects.

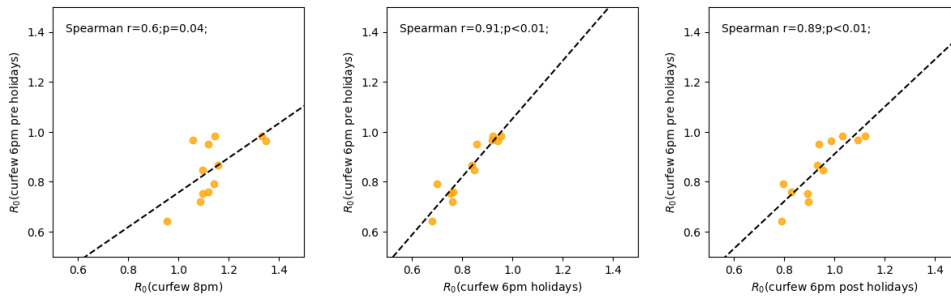


Figure S19. Correlations between basic reproductive numbers during different interventions. The panel shows the correlation of the basic reproductive number R_0 during the period with curfew at 6 p.m. before holidays and curfew at 8 p.m., curfew at 6 p.m. during holidays, curfew at 6 p.m. after holidays. Each dot represents a French region and correlation is done across regions.

0.5.2 Impact of the Alpha variant and of the vaccination rhythm on the hospitalizations

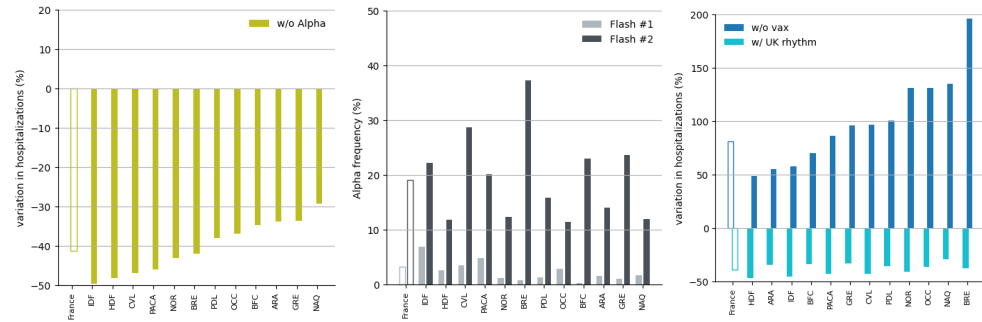


Figure S20. Impact of the Alpha variant and of the vaccination rhythm on hospitalizations. (a) Variation in the number of hospitalizations (period September 2020 - June 2021) due to the Alpha variant with respect to observations. The green bars represent a scenario without the Alpha variant. (b) Frequency of Alpha variant (%), by region according to Flash surveys. The light grey bars represent Flash #1, the dark grey bars represent Flash #2. (c) Variation in the number of hospitalizations (period September 2020 - June 2021) due to the vaccination rhythm compared to observations. The dark blue bars represent a scenario without vaccines, the light blue bars represent a context with the vaccination pace observed in the United Kingdom¹⁸. In the three panels, the empty bars represent values for France, the filled bars represent the regional values.

0.5.3 Impact of different nationwide interventions

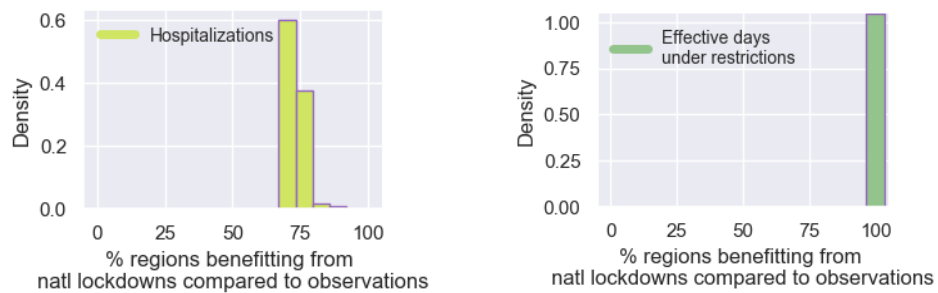


Figure S21. Regions benefiting from nationwide lockdowns compared to observations. Probability distribution of the percentage of regions benefiting from the lockdowns compared to observations, in the phase space where both effective days and hospitalizations are reduced. From left to right: hospitalizations, effective days under restrictions.

0.6 Sensitivity analysis

Here we present the results of our sensitivity analysis on some assumptions considered in the model used in the main paper. We used the value T, R of trigger and release described in the main text, as an illustrative example.

0.6.1 Impact of relaxation after exiting lockdowns

We assume that population behavior did not change immediately with policies: the population continued to adhere to public health measures being progressively lifted, such as physical distancing, during the reopening phase. We assume two weeks relaxation in the main text. Other studies²⁵ found that transmission rate during the

reopening phases following the lifting of lockdowns remained similar to the one observed during lockdowns. Here we explore one week relaxation or no relaxation (**Figure S22**), and we find that the progressive reopening helps further dampening the waves over time.

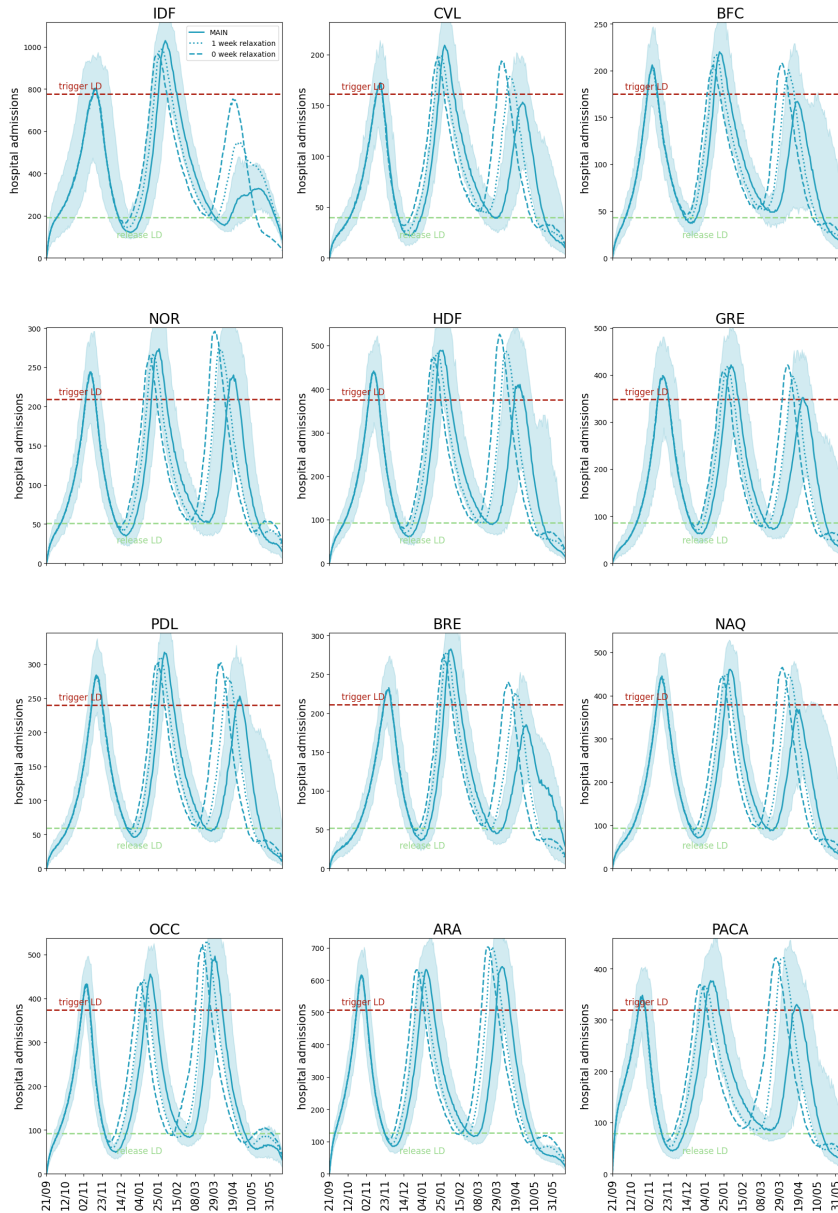


Figure S22. Impact of relaxation after exiting lockdowns on daily hospital admissions. Solid curves refer to the median trajectory, obtained under the condition of 2 weeks relaxation. Dotted and dashed curves show the same for 1 week relaxation or no relaxation, respectively. The shaded area around the curves corresponds to the 95% probability range obtained from $n=200$ stochastic simulations. The abbreviations in the upper right corner of each plot stand for the name of the region. IDF: Île-de-France, CVL: Centre-Val de Loire, BFC : Bourgogne-Franche-Comté, NOR: Normandy, HDF: Hauts-de-France, GRE: Grand Est, PDL : Pays de la Loire, BRE: Brittany, NAQ: Nouvelle Aquitaine, OCC : Occitanie, ARA: Auvergne-Rhône-Alpes, PACA: Provence-Alpes-Côte d'Azur. Dashed horizontal red lines refer to the trigger threshold relative to the second lockdown. It is estimated based on the 7-days rolling average value of the hospital admissions per capita in the Auvergne-Rhone-Alpes region, on October 30, 2020, rescaled by the regional population, the green ones to the ones observed on December 15, 2020, calculated as the average value between regions and rescaled to the region's population.

0.6.2 Impact of transmissibility and mobility conditions during lockdowns

In the main text, we simulated the stringency and mobility reductions experienced in the French second lockdown (LD2) for the initial lockdown in the stop-and-go series, and the stringency and mobility reductions experienced in the French third lockdown (LD3) for the subsequent simulated lockdowns. This was done to align with the applied policies aiming towards a larger freedom over time. Here we show the results using only the lockdown as the second phase (**Figure S23**). Assuming that all simulated lockdowns in the stop-and-go series have the same stringency and mobility reduction as the French second lockdown does not bring substantial changes to our results. This is due to the similarity of estimated effectiveness of LD2 and LD3.

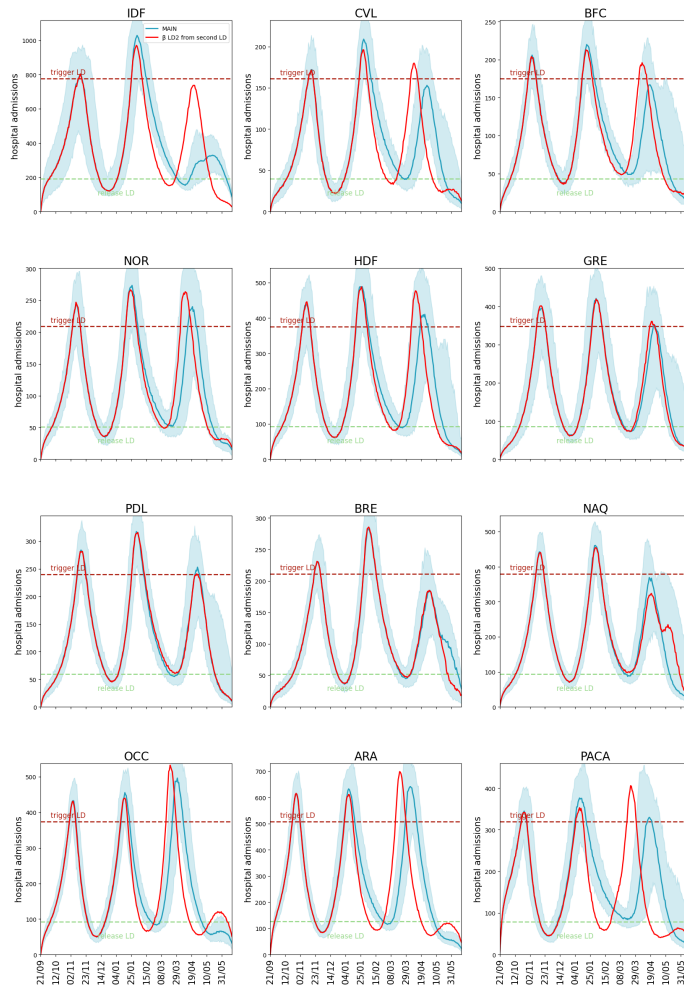


Figure S23. Impact of transmissibility and mobility conditions during lockdowns on daily hospital admissions. Blue solid curves refer to the median trajectory, obtained under the main scenario conditions. Red solid curves show the same assuming the conditions of the second lockdown for all the epidemic waves. The shaded area around the curves corresponds to the 95% probability range obtained from $n=200$ stochastic simulations. The abbreviations in the upper right corner of each plot stand for the name of the region. IDF: Île-de-France, CVL: Centre-Val de Loire, BFC : Bourgogne-Franche-Comté, NOR: Normandy, HDF: Hauts-de-France, GRE: Grand Est, PDL : Pays de la Loire, BRE: Brittany, NAQ: Nouvelle Aquitaine, OCC : Occitanie, ARA: Auvergne-Rhône-Alpes, PACA: Provence-Alpes-Côte d’Azur. Dashed horizontal lines refer to the hospitalization per capita. Dashed horizontal red lines refer to the trigger threshold relative to the second lockdown. It is estimated based on the 7-days rolling average value of the hospital admissions per capita in the Auvergne-Rhone-Alpes region, on October 30, 2020, rescaled by the regional population, the green ones to the ones observed on December 15, 2020, calculated as the average value between regions and rescaled it to the region’s population.

0.6.3 Impact of weekly rolling average of data

We show that fitting the model to the weekly rolling average to hospital admission data does not alter the estimates of the epidemiological impact of the NPIs (**Figure S24**).

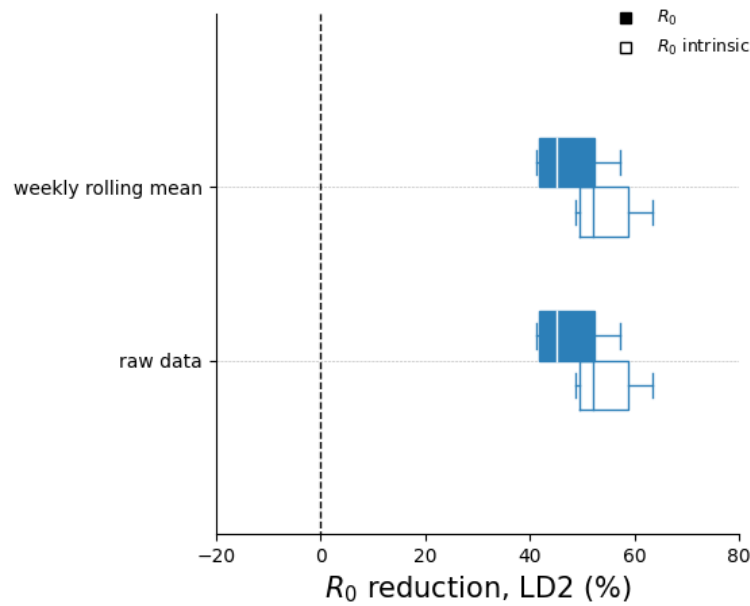


Figure S24. Impact of hospitalization data on NPI effectiveness. Reduction in the estimated regional basic reproductive numbers R_0 associated to the second lockdown (LD2) compared with the values estimated before the second lockdown using raw data and a weekly average of the data. Box plots represent the median (line in the middle of the box), interquartile range (box limits) and 2.5th and 97.5th percentiles (whiskers) of the estimated values for the 12 French regions. Filled boxplots represent reductions estimated by the fit accounting for all time-varying processes (R_0); void boxplots represent the same reductions discounting the seasonal and Alpha effects ($R_0^{intrinsic}$).

0.6.4 References

1. The Economist. The global normalcy index. <https://www.economist.com/graphic-detail/tracking-the-return-to-normalcy-after-covid-19>.
2. Our World in Data. COVID-19: Stringency Index. Our World in Data <https://ourworldindata.org/grapher/covid-stringency-index>.
3. Lauer, S. A. et al. The Incubation Period of Coronavirus Disease 2019 (COVID-19) From Publicly Reported Confirmed Cases: Estimation and Application. *Ann. Intern. Med.* 172, 577–582 (2020).
4. Di Domenico, L., Pullano, G., Sabbatini, C. E., Boëlle, P.-Y. Colizza, V. Impact of lockdown on COVID-19 epidemic in Île-de-France and possible exit strategies. *BMC Med.* 18, 240 (2020).
5. Ferretti, L. et al. Quantifying SARS-CoV-2 transmission suggests epidemic control with digital contact tracing. *Science* 368, eabb6936 (2020).
6. Cereda, D. et al. The early phase of the COVID-19 epidemic in Lombardy, Italy. *Epidemics* 37, 100528 (2021).

7. Pellis, L. et al. Challenges in control of COVID-19: short doubling time and long delay to effect of interventions. *Philos. Trans. R. Soc. B Biol. Sci.* 376, 20200264 (2021).
8. Pei, S., Kandula, S., Shaman, J. Differential effects of intervention timing on COVID-19 spread in the United States. *Sci. Adv.* 6, eabd6370 (2020).
9. Della Rossa, F. et al. A network model of Italy shows that intermittent regional strategies can alleviate the COVID-19 epidemic. *Nat. Commun.* 11, 5106 (2020).
10. Lapidus, N. et al. Do not neglect SARS-CoV-2 hospitalization and fatality risks in the middle-aged adult population. *Infect. Dis. Now* (2021) doi:10.1016/j.idnow.2020.12.007.
11. Dagan, N. et al. BNT162b2 mRNA Covid-19 Vaccine in a Nationwide Mass Vaccination Setting. *N. Engl. J. Med.* 384, 1412–1423 (2021).
12. Haas, E. J. et al. Impact and effectiveness of mRNA BNT162b2 vaccine against SARS-CoV-2 infections and COVID-19 cases, hospitalisations, and deaths following a nationwide vaccination campaign in Israel: an observational study using national surveillance data. *The Lancet* 397, 1819–1829 (2021).
13. Eyre, D. W. et al. Effect of Covid-19 Vaccination on Transmission of Alpha and Delta Variants. *N. Engl. J. Med.* 386, 744–756 (2022).
14. Pullano, G. et al. Underdetection of cases of COVID-19 in France threatens epidemic control. *Nature* 590, 134–139 (2021).
15. Collin, A. et al. Using Population Based Kalman Estimator to Model COVID-19 Epidemic in France: Estimating the Effects of Non-Pharmaceutical Interventions on the Dynamics of Epidemic. <http://medrxiv.org/lookup/doi/10.1101/2021.07.09.21260259> (2021) doi:10.1101/2021.07.09.21260259.
16. data.gouv.fr. Données relatives aux personnes vaccinées contre la Covid-19 (VAC-SI). <https://www.data.gouv.fr/en/datasets/donnees-relatives-aux-personnes-vaccinees-contre-la-covid-19-1/>.
17. France reaches 30 million Covid-19 vaccine first doses. *France 24* <https://www.france24.com/en/france/20210612-france-reaches-30-million-covid-19-vaccine-first-doses> (2021).
18. data.gov.uk. Vaccinations in England | Coronavirus in the UK. <https://coronavirus.data.gov.uk/details/vaccinations>.
19. Gaymard, A. et al. Early assessment of diffusion and possible expansion of SARS-CoV-2 Lineage 20I/501Y.V1 (B.1.1.7, variant of concern 202012/01) in France, January to March 2021. *Eurosurveillance* 26, 2100133 (2021).
20. Bhatia, S., Wardle, J., Nash, R., Nouvellet, P., Cori, A. A generic method and software to estimate the transmission advantage of pathogen variants in real-time: SARS-CoV-2 as a case-study. <http://spiral.imperial.ac.uk/handle/10044/1/92689> (2021) doi:10.25561/92689.
21. Valdano, E., Lee, J., Bansal, S., Rubrichi, S., Colizza, V. Highlighting socio-economic constraints on mobility reductions during COVID-19 restrictions in France

can inform effective and equitable pandemic response. *J. Travel Med.* taab045 (2021) doi:10.1093/jtm/taab045.

22. Peghin, M. et al. The Fall in Antibody Response to SARS-CoV-2: a Longitudinal Study of Asymptomatic to Critically Ill Patients Up to 10 Months after Recovery | *Journal of Clinical Microbiology*. <https://journals.asm.org/doi/10.1128/JCM.01138-21>.

23. Le Vu, S. et al. Prevalence of SARS-CoV-2 antibodies in France: results from nationwide serological surveillance. *Nat. Commun.* 12, 3025 (2021).

24. Carrat, F. et al. Antibody status and cumulative incidence of SARS-CoV-2 infection among adults in three regions of France following the first lockdown and associated risk factors: a multicohort study. *Int. J. Epidemiol.* 50, 1458–1472 (2021).

25. Paireau, J. et al. Impact of non-pharmaceutical interventions, weather, vaccination, and variants on COVID-19 transmission across departments in France. *BMC Infect. Dis.* 23, 190 (2023).

Bibliography

- [1] WHO announces COVID-19 outbreak a pandemic, March 2020. Library Catalog: www.euro.who.int Publisher: World Health Organization.
- [2] Epicentre. COVID-19 Epi Dashboard. Library Catalog: reports.msf.net.
- [3] Décret n° 2020-293 du 23 mars 2020 prescrivant les mesures générales nécessaires pour faire face à l'épidémie de covid-19 dans le cadre de l'état d'urgence sanitaire, March 2020.
- [4] The territorial impact of COVID-19: Managing the crisis across levels of government.
- [5] Vaccine efficacy, effectiveness and protection.
- [6] Ibrahim Mohammed, Areej Nauman, Pradipta Paul, Sanjith Ganesan, Kuan-Han Chen, Syed Muhammad Saad Jalil, Shahd H. Jaouni, Hussam Kawas, Wafa A. Khan, Ahamed Lazim Vattoth, Yasmeen Alavi Al-Hashimi, Ahmed Fares, Rached Zeghlache, and Dalia Zakaria. The efficacy and effectiveness of the COVID-19 vaccines in reducing infection, severity, hospitalization, and mortality: a systematic review. *Human Vaccines & Immunotherapeutics*, 18(1):2027160.
- [7] Sam Moore, Edward M. Hill, Michael J. Tildesley, Louise Dyson, and Matt J. Keeling. Vaccination and non-pharmaceutical interventions for COVID-19: a mathematical modelling study. *The Lancet Infectious Diseases*, 21(6):793–802, June 2021. Publisher: Elsevier.
- [8] ANIRUDDHA ADIGA, DEVDATT DUBHASHI, BRYAN LEWIS, MADHAV MARATHE, SRINIVASAN VENKATRAMANAN, and ANIL VULLIKANTI. MATHEMATICAL MODELS FOR COVID-19 PANDEMIC: A COMPARATIVE ANALYSIS. *ArXiv*, page arXiv:2009.10014v1, September 2020.
- [9] Jasmina Panovska-Griffiths. Can mathematical modelling solve the current Covid-19 crisis? *BMC Public Health*, 20(1):551, April 2020.
- [10] A contribution to the mathematical theory of epidemics | Proceedings of the Royal Society of London. Series A, Containing Papers of a Mathematical and Physical Character.
- [11] Mirjam Kretzschmar. Disease modeling for public health: added value, challenges, and institutional constraints. *Journal of Public Health Policy*, 41(1):39–51, 2020.
- [12] Laura Di Domenico, Chiara E. Sabbatini, Pierre-Yves Boëlle, Chiara Poletto, Pascal Crépey, Juliette Paireau, Simon Cauchemez, François Beck, Harold Noel, Daniel Lévy-Bruhl, and Vittoria Colizza. Adherence and sustainability of interventions informing optimal control against COVID-19 pandemic, May 2021.
- [13] Laura Di Domenico, Giulia Pullano, Chiara E. Sabbatini, Pierre-Yves Boëlle, and Vittoria Colizza. Impact of lockdown on COVID-19 epidemic in île-de-France and possible exit strategies. *BMC Medicine*, 18(1):240, July 2020.
- [14] Laura Di Domenico, Giulia Pullano, Chiara E. Sabbatini, Pierre-Yves Boëlle, and Vittoria Colizza. Modelling safe protocols for reopening schools during the COVID-19 pandemic in France. *Nature Communications*, 2021. Di d.

- [15] Giulia Pullano, Laura Di Domenico, Chiara E. Sabbatini, Eugenio Valdano, Clément Turbelin, Marion Debin, Caroline Guerrisi, Charly Kengne-Kuetche, Cécile Souty, Thomas Hanslik, Thierry Blanchon, Pierre-Yves Boëlle, Julie Figoni, Sophie Vaux, Christine Campèse, Sibylle Bernard-Stoecklin, and Vittoria Colizza. Underdetection of cases of COVID-19 in France threatens epidemic control. *Nature*, December 2020.
- [16] Laura Di Domenico, Chiara E. Sabbatini, Giulia Pullano, Daniel Lévy-Bruhl, and Vittoria Colizza. Impact of January 2021 curfew measures on SARS-CoV-2 B.1.1.7 circulation in France. *Euro-surveillance*, 26(15):2100272, April 2021. Publisher: European Centre for Disease Prevention and Control.
- [17] Etienne Jacob. Coronavirus: trois premiers cas confirmés en France, deux d’entre eux vont bien, January 2020. Library Catalog: www.lefigaro.fr Section: Sciences & Environnement.
- [18] Le Monde. « Nous sommes en guerre » : le verbatim du discours d’Emmanuel Macron. *Le Monde.fr*, March 2020.
- [19] Jonas F. Ludvigsson. How Sweden approached the COVID-19 pandemic: Summary and commentary on the National Commission Inquiry. *Acta Paediatrica*, 112(1):19–33, 2023. _eprint: <https://onlinelibrary.wiley.com/doi/pdf/10.1111/apa.16535>.
- [20] Coronavirus: Austria and Italy reopen some shops as lockdown eased. *BBC News*, April 2020.
- [21] Info Coronavirus COVID-19 - Stratégie de déconfinement. Library Catalog: www.gouvernement.fr.
- [22] Décret n° 2020-1257 du 14 octobre 2020 déclarant l’état d’urgence sanitaire, October 2020.
- [23] LOI n° 2020-1379 du 14 novembre 2020 autorisant la prorogation de l’état d’urgence sanitaire et portant diverses mesures de gestion de la crise sanitaire (1), November 2020.
- [24] Our World in Data. COVID-19: Stringency Index.
- [25] Décret n° 2020-1454 du 27 novembre 2020 modifiant le décret n° 2020-1310 du 29 octobre 2020 prescrivant les mesures générales nécessaires pour faire face à l’épidémie de covid-19 dans le cadre de l’état d’urgence sanitaire - Légifrance.
- [26] Décret n° 2021-217 du 25 février 2021 modifiant les décrets n° 2020-1262 du 16 octobre 2020 et n° 2020-1310 du 29 octobre 2020 prescrivant les mesures générales nécessaires pour faire face à l’épidémie de covid-19 dans le cadre de l’état d’urgence sanitaire - Légifrance.
- [27] Décret n° 2021-384 du 2 avril 2021 modifiant les décrets n° 2020-1262 du 16 octobre 2020 et n° 2020-1310 du 29 octobre 2020 prescrivant les mesures générales nécessaires pour faire face à l’épidémie de covid-19 dans le cadre de l’état d’urgence sanitaire - Légifrance.
- [28] LOI n° 2021-689 du 31 mai 2021 relative à la gestion de la sortie de crise sanitaire (1), 2021.
- [29] Christina Pagel and Christian A. Yates. Role of mathematical modelling in future pandemic response policy. *BMJ*, 378:e070615, September 2022. Publisher: British Medical Journal Publishing Group Section: Analysis.
- [30] Eric T. Lofgren, M. Elizabeth Halloran, Caitlin M. Rivers, John M. Drake, Travis C. Porco, Bryan Lewis, Wan Yang, Alessandro Vespignani, Jeffrey Shaman, Joseph N. S. Eisenberg, Marisa C. Eisenberg, Madhav Marathe, Samuel V. Scarpino, Kathleen A. Alexander, Rafael Meza, Matthew J. Ferrari, James M. Hyman, Lauren A. Meyers, and Stephen Eubank. Mathematical models: A key tool for outbreak response. *Proceedings of the National Academy of Sciences*, 111(51):18095–18096, December 2014. Publisher: Proceedings of the National Academy of Sciences.

- [31] C. A. K. Kwuimy, Foad Nazari, Xun Jiao, Pejman Rohani, and C. Nataraj. Nonlinear dynamic analysis of an epidemiological model for COVID-19 including public behavior and government action. *Nonlinear Dynamics*, 101(3):1545–1559, August 2020.
- [32] Matthew R. Levy and Joshua Tasoff. Exponential-growth bias and overconfidence. *Journal of Economic Psychology*, 58:1–14, February 2017.
- [33] Emily G. Simmonds, Kwaku Peprah Adjei, Christoffer Wold Andersen, Janne Cathrin Hetle Aspheim, Claudia Battistin, Nicola Bulso, Hannah M. Christensen, Benjamin Cretois, Ryan Cubero, Iván A. Davidovich, Lisa Dickel, Benjamin Dunn, Etienne Dunn-Sigouin, Karin Dyrstad, Sigurd Einum, Donata Giglio, Haakon Gjerløw, Amélie Godefroidt, Ricardo González-Gil, Soledad Gonzalo Cogno, Fabian Große, Paul Halloran, Mari F. Jensen, John James Kennedy, Peter Egge Langsæther, Jack H. Laverick, Debora Lederberger, Camille Li, Elizabeth G. Mandeville, Caitlin Mandeville, Espen Moe, Tobias Navarro Schröder, David Nunan, Jorge Sicacha-Parada, Melanie Rae Simpson, Emma Sofie Skarstein, Clemens Spensberger, Richard Stevens, Aneesh C. Subramanian, Lea Svendsen, Ole Magnus Theisen, Connor Watret, and Robert B. O’Hara. Insights into the quantification and reporting of model-related uncertainty across different disciplines. *iScience*, 25(12):105512, December 2022.
- [34] Jon Zelner, Julien Riou, Ruth Etzioni, and Andrew Gelman. Accounting for uncertainty during a pandemic. *Patterns*, 2(8), August 2021. Publisher: Elsevier.
- [35] Mircea T. Sofonea, Simon Cauchemez, and Pierre-Yves Boëlle. Epidemic models: why and how to use them. *Anaesthesia, Critical Care & Pain Medicine*, 41(2):101048, April 2022.
- [36] David M. Steinberg, Ran D. Balicer, Yoav Benjamini, Hilla De-Leon, Doron Gazit, Hagai Rossman, and Eli Sprecher. The role of models in the covid-19 pandemic. *Israel Journal of Health Policy Research*, 11(1):36, October 2022.
- [37] Ellen Brooks-Pollock, Leon Danon, Thibaut Jombart, and Lorenzo Pellis. Modelling that shaped the early COVID-19 pandemic response in the UK. *Philosophical Transactions of the Royal Society B: Biological Sciences*, 376(1829):20210001, May 2021. Publisher: Royal Society.
- [38] N Imai, I Dorigatti, A Cori, C Donnelly, S Riley, and N Ferguson. Report 2: Estimating the potential total number of novel Coronavirus cases in Wuhan City, China. Technical report, Imperial College London, January 2020.
- [39] Tracing and analysis of 288 early SARS-CoV-2 infections outside China: A modeling study | PLOS Medicine.
- [40] Virus has spread to almost every country, says WHO, July 2009. Section: science.
- [41] Giulia Pullano, Francesco Pinotti, Eugenio Valdano, Pierre-Yves Boëlle, Chiara Poletto, and Vittoria Colizza. Novel coronavirus (2019-nCoV) early-stage importation risk to Europe, January 2020. *Eurosurveillance*, 25(4):2000057, January 2020. Publisher: European Centre for Disease Prevention and Control.
- [42] COVID-19 - Report sugli spostamenti della comunità.
- [43] Hermann Pohlabein, Achim Reineke, and Walter Schill. Data Management in Epidemiology. In Wolfgang Ahrens and Iris Pigeot, editors, *Handbook of Epidemiology*, pages 979–1022. Springer, New York, NY, 2014.
- [44] Daniela De Angelis, Anne M. Presanis, Paul J. Birrell, Gianpaolo Scalia Tomba, and Thomas House. Four key challenges in infectious disease modelling using data from multiple sources. *Epidemics*, 10:83–87, March 2015.

- [45] Flavia Riccardo, Marco Ajelli, Xanthi D. Andrianou, Antonino Bella, Martina Del Manso, Massimo Fabiani, Stefania Bellino, Stefano Boros, Alberto Mateo Urdiales, Valentina Marziano, Maria Cristina Rota, Antonietta Filia, Fortunato D'Ancona, Andrea Siddu, Ornella Punzo, Filippo Trentini, Giorgio Guzzetta, Piero Poletti, Paola Stefanelli, Maria Rita Castrucci, Alessandra Ciervo, Corrado Di Benedetto, Marco Tallon, Andrea Piccioli, Silvio Brusaferrò, Giovanni Rezza, Stefano Merler, Patrizio Pezzotti, and the COVID-19 working Group. Epidemiological characteristics of COVID-19 cases and estimates of the reproductive numbers 1 month into the epidemic, Italy, 28 January to 31 March 2020. *Eurosurveillance*, 25(49):2000790, December 2020. Publisher: European Centre for Disease Prevention and Control.
- [46] Mirjam E. Kretzschmar, Ben Ashby, Elizabeth Fearon, Christopher E. Overton, Jasmina Panovska-Griffiths, Lorenzo Pellis, Matthew Quaipe, Ganna Rozhnova, Francesca Scarabel, Helena B. Stage, Ben Swallow, Robin N. Thompson, Michael J. Tildesley, and Daniel Villela. Challenges for modelling interventions for future pandemics. *Epidemics*, 38:100546, March 2022.
- [47] Henrik Salje, Cécile Tran Kiem, Noémie Lefrancq, Noémie Courtejoie, Paolo Bosetti, Juliette Paireau, Alessio Andronico, Nathanaël Hozé, Jehanne Richet, Claire-Lise Dubost, Yann Le Strat, Justin Lessler, Daniel Levy-Bruhl, Arnaud Fontanet, Lulla Opatowski, Pierre-Yves Boelle, and Simon Cauchemez. Estimating the burden of SARS-CoV-2 in France. *Science*, 369(6500):208–211, July 2020. Publisher: American Association for the Advancement of Science Section: Report.
- [48] João Viana, Christiaan H. van Dorp, Ana Nunes, Manuel C. Gomes, Michiel van Boven, Mirjam E. Kretzschmar, Marc Veldhoen, and Ganna Rozhnova. Controlling the pandemic during the SARS-CoV-2 vaccination rollout. *Nature Communications*, 12(1):3674, June 2021. Number: 1 Publisher: Nature Publishing Group.
- [49] S. Funk, S. Abbott, B. D. Atkins, M. Baguelin, J. K. Baillie, P. Birrell, J. Blake, N. I. Bosse, J. Burton, J. Carruthers, N. G. Davies, D. De Angelis, L. Dyson, W. J. Edmunds, R. M. Eggo, N. M. Ferguson, K. Gaythorpe, E. Gorsich, G. Guyver-Fletcher, J. Hellewell, E. M. Hill, A. Holmes, T. A. House, C. Jewell, M. Jit, T. Jombart, I. Joshi, M. J. Keeling, E. Kendall, E. S. Knock, A. J. Kucharski, K. A. Lythgoe, S. R. Meakin, J. D. Munday, P. J. M. Openshaw, C. E. Overton, F. Pagani, J. Pearson, P. N. Perez-Guzman, L. Pellis, F. Scarabel, M. G. Semple, K. Sherratt, M. Tang, M. J. Tildesley, E. Van Leeuwen, L. K. Whittles, CMMID COVID-19 Working Group, Imperial College COVID-19 Response Team, and Isaric4c Investigators. Short-term forecasts to inform the response to the Covid-19 epidemic in the UK, December 2020. Pages: 2020.11.11.20220962.
- [50] data.gouv.fr. Données hospitalières relatives à l'épidémie de COVID-19, 2021.
- [51] Fabrice Carrat, Xavier de Lamballerie, Delphine Rahib, Hélène Blanché, Nathanael Lapidus, Fanny Artaud, Sofiane Kab, Adeline Renuy, Fabien Szabo de Edelenyi, Laurence Meyer, Nathalie Lydié, Marie-Aline Charles, Pierre-Yves Ancel, Florence Jusot, Alexandra Rouquette, Stéphane Priet, Paola Mariela Saba Villarroel, Toscane Fourié, Clovis Lusivika-Nzinga, Jérôme Nicol, Stephane Legot, Nathalie Druésne-Pecollo, Younes Esseddik, Cindy Lai, Jean-Marie Gagliolo, Jean-François Deleuze, Nathalie Bajos, Gianluca Severi, Mathilde Touvier, Marie Zins, and for the SAPRIS and SAPRIS-SERO study groups. Antibody status and cumulative incidence of SARS-CoV-2 infection among adults in three regions of France following the first lockdown and associated risk factors: a multicohort study. *International Journal of Epidemiology*, 50(5):1458–1472, October 2021.
- [52] Stéphane Le Vu, Gabrielle Jones, François Anna, Thierry Rose, Jean-Baptiste Richard, Sibylle Bernard-Stoecklin, Sophie Goyard, Caroline Demeret, Olivier Helynck, Nicolas Escriou, Marion Gransagne, Stéphane Petres, Corinne Robin, Virgile Monnet, Louise Perrin de Facci, Marie-Noëlle Ungeheuer, Lucie Léon, Yvonnick Guillois, Laurent Filleul, Pierre Charneau, Daniel Lévy-Bruhl, Sylvie van der Werf, and Harold Noel. Prevalence of SARS-CoV-2 antibodies in France: results

from nationwide serological surveillance. *Nature Communications*, 12(1):3025, May 2021. Number: 1 Publisher: Nature Publishing Group.

- [53] A. Sarah Walker, Karina-Doris Vihta, Owen Gethings, Emma Pritchard, Joel Jones, Thomas House, Iain Bell, John I. Bell, John N. Newton, Jeremy Farrar, Ian Diamond, Ruth Studley, Emma Rourke, Jodie Hay, Susan Hopkins, Derrick Crook, Tim Peto, Philippa C. Matthews, David W. Eyre, Nicole Stoesser, and Koen B. Pouwels. Tracking the Emergence of SARS-CoV-2 Alpha Variant in the United Kingdom. *New England Journal of Medicine*, 385(27):2582–2585, December 2021. Publisher: Massachusetts Medical Society _eprint: <https://doi.org/10.1056/NEJMc2103227>.
- [54] SARS-CoV-2 Alpha variant, August 2023. Page Version ID: 1173139428.
- [55] Alexandre Gaymard, Paolo Bosetti, Adeline Feri, Gregory Destras, Vincent Enouf, Alessio Andronico, Sonia Burrel, Sylvie Behillil, Claire Sauvage, Antonin Bal, Florence Morfin, Sylvie Van Der Werf, Laurence Josset, Anrs Mie Ac43 Covid-19, French viro COVID Group, François Blanquart, Bruno Coignard, Simon Cauchemez, and Bruno Lina. Early assessment of diffusion and possible expansion of SARS-CoV-2 Lineage 20I/501Y.V1 (B.1.1.7, variant of concern 202012/01) in France, January to March 2021. *Eurosurveillance*, 26(9):2100133, March 2021. Publisher: European Centre for Disease Prevention and Control.
- [56] Coronavirus : circulation des variants du SARS-CoV-2.
- [57] data.gouv.fr. Données relatives aux personnes vaccinées contre la Covid-19 (VAC-SI).
- [58] Soeren Metelmann, Karan Pattni, Liam Brierley, Lisa Cavalerie, Cyril Caminade, Marcus S. C. Blagrove, Joanne Turner, Kieran J. Sharkey, and Matthew Baylis. Impact of climatic, demographic and disease control factors on the transmission dynamics of COVID-19 in large cities worldwide. *One Health (Amsterdam, Netherlands)*, 12:100221, June 2021.
- [59] Dimitrios Paraskevis, Evangelia Georgia Kostaki, Nikiforos Alygizakis, Nikolaos S. Thomaidis, Constantinos Cartalis, Sotirios Tsiodras, and Meletios Athanasios Dimopoulos. A review of the impact of weather and climate variables to COVID-19: In the absence of public health measures high temperatures cannot probably mitigate outbreaks. *The Science of the Total Environment*, 768:144578, May 2021.
- [60] Zachary Susswein, Eva C Rest, and Shweta Bansal. Disentangling the rhythms of human activity in the built environment for airborne transmission risk: An analysis of large-scale mobility data. *eLife*, 12:e80466, April 2023. Publisher: eLife Sciences Publications, Ltd.
- [61] Jingyuan Wang, Ke Tang, Kai Feng, Xin Lin, Weifeng Lv, Kun Chen, and Fei Wang. Impact of temperature and relative humidity on the transmission of COVID-19: a modelling study in China and the United States. *BMJ Open*, 11(2):e043863, February 2021. Publisher: British Medical Journal Publishing Group Section: Public health.
- [62] Annabelle Collin, Boris P. Hejblum, Carole Vignals, Laurent Lehot, Rodolphe Thiébaud, Philippe Moireau, and Mélanie Prague. Using a population-based Kalman estimator to model the COVID-19 epidemic in France: estimating associations between disease transmission and non-pharmaceutical interventions. *The International Journal of Biostatistics*, January 2023.
- [63] Guillaume Béraud, Sabine Kazmierczak, Philippe Beutels, Daniel Levy-Bruhl, Xavier Lenne, Nathalie Mielcarek, Yazdan Yazdanpanah, Pierre-Yves Boëlle, Niel Hens, and Benoit Dervaux. The French Connection: The First Large Population-Based Contact Survey in France Relevant for the Spread of Infectious Diseases. *PLOS ONE*, 10(7):e0133203, 2015. Publisher: Public Library of Science.

- [64] Suttikiat Changruenngam, Dominique J. Bicout, and Charin Modchang. How the individual human mobility spatio-temporally shapes the disease transmission dynamics. *Scientific Reports*, 10(1):11325, July 2020. Number: 1 Publisher: Nature Publishing Group.
- [65] Zhicheng Zheng, Zhixiang Xie, Yaochen Qin, Kun Wang, Yan Yu, and Pinde Fu. Exploring the influence of human mobility factors and spread prediction on early COVID-19 in the USA. *BMC Public Health*, 21:615, March 2021.
- [66] Baltazar Espinoza, Carlos Castillo-Chavez, and Charles Perrings. Mobility restrictions for the control of epidemics: When do they work? *PLoS ONE*, 15(7):e0235731, July 2020.
- [67] Giulia Pullano, Eugenio Valdano, Nicola Scarpa, Stefania Rubrichi, and Vittoria Colizza. Evaluating the effect of demographic factors, socioeconomic factors, and risk aversion on mobility during the COVID-19 epidemic in France under lockdown: a population-based study. *The Lancet Digital Health*, 2(12):e638–e649, December 2020.
- [68] Google.com. COVID-19 Community Mobility Report, 2021. Library Catalog: www.google.com.
- [69] Policy-Relevant Science & Technology. Point de situation sur la stratégie de lutte contre la COVID-19 | Vittoria Colizza, February 2021.
- [70] William Kermack and A.G. McKendrick. A contribution to the mathematical theory of epidemics | Proceedings of the Royal Society of London. Series A, Containing Papers of a Mathematical and Physical Character.
- [71] Herbert W. Hethcote. The Mathematics of Infectious Diseases. *SIAM Review*, 42(4):599–653, January 2000.
- [72] Giancarlo De Luca, Kim Van Kerckhove, Pietro Coletti, Chiara Poletto, Nathalie Bossuyt, Niel Hens, and Vittoria Colizza. The impact of regular school closure on seasonal influenza epidemics: a data-driven spatial transmission model for Belgium. *BMC Infectious Diseases*, 18(1):29, December 2018.
- [73] Xi He, Eric H. Y. Lau, Peng Wu, Xilong Deng, Jian Wang, Xinxin Hao, Yiu Chung Lau, Jessica Y. Wong, Yujuan Guan, Xinghua Tan, Xiaoneng Mo, Yanqing Chen, Baolin Liao, Weilie Chen, Fengyu Hu, Qing Zhang, Mingqiu Zhong, Yanrong Wu, Lingzhai Zhao, Fuchun Zhang, Benjamin J. Cowling, Fang Li, and Gabriel M. Leung. Temporal dynamics in viral shedding and transmissibility of COVID-19. *Nature Medicine*, 26(5):672–675, May 2020. Number: 5 Publisher: Nature Publishing Group.
- [74] Stephen A. Lauer, Kyra H. Grantz, Qifang Bi, Forrest K. Jones, Qulu Zheng, Hannah R. Meredith, Andrew S. Azman, Nicholas G. Reich, and Justin Lessler. The Incubation Period of Coronavirus Disease 2019 (COVID-19) From Publicly Reported Confirmed Cases: Estimation and Application. *Annals of Internal Medicine*, pages M20–0504, March 2020.
- [75] Luca Ferretti, Chris Wymant, Michelle Kendall, Lele Zhao, Anel Nurtay, Lucie Abeler-Dörner, Michael Parker, David Bonsall, and Christophe Fraser. Quantifying SARS-CoV-2 transmission suggests epidemic control with digital contact tracing. *Science*, 368(6491):eabb6936, May 2020. Publisher: American Association for the Advancement of Science Section: Research Article.
- [76] Enrico Lavezzo, Elisa Franchin, Constanze Ciavarella, Gina Cuomo-Dannenburg, Luisa Barzon, Claudia Del Vecchio, Lucia Rossi, Riccardo Manganelli, Arianna Loregian, Nicolò Navarin, Davide Abate, Manuela Sciro, Stefano Merigliano, Ettore De Canale, Maria Cristina Vanuzzo, Valeria Besutti, Francesca Saluzzo, Francesco Onelia, Monia Pacenti, Saverio G. Parisi, Giovanni Carretta, Daniele Donato, Luciano Flor, Silvia Cocchio, Giulia Masi, Alessandro Sperduti, Lorenzo Cattarino, Renato Salvador, Michele Nicoletti, Federico Caldart, Gioele Castelli, Eleonora Nieddu, Beatrice

Labella, Ludovico Fava, Matteo Drigo, Katy A. M. Gaythorpe, Alessandra R. Brazzale, Stefano Toppo, Marta Trevisan, Vincenzo Baldo, Christl A. Donnelly, Neil M. Ferguson, Ilaria Dorigatti, and Andrea Crisanti. Suppression of a SARS-CoV-2 outbreak in the Italian municipality of Vo'. *Nature*, 584(7821):425–429, August 2020. Number: 7821 Publisher: Nature Publishing Group.

- [77] Robert Verity, Lucy C. Okell, Ilaria Dorigatti, Peter Winskill, Charles Whittaker, Natsuko Imai, Gina Cuomo-Dannenburg, Hayley Thompson, Patrick G. T. Walker, Han Fu, Amy Dighe, Jamie T. Griffin, Marc Baguelin, Sangeeta Bhatia, Adhiratha Boonyasiri, Anne Cori, Zulma Cucunubá, Rich FitzJohn, Katy Gaythorpe, Will Green, Arran Hamlet, Wes Hinsley, Daniel Laydon, Gemma Nedjati-Gilani, Steven Riley, Sabine van Elsland, Erik Volz, Haowei Wang, Yuanrong Wang, Xiaoyue Xi, Christl A. Donnelly, Azra C. Ghani, and Neil M. Ferguson. Estimates of the severity of coronavirus disease 2019: a model-based analysis. *The Lancet Infectious Diseases*, 20(6):669–677, June 2020. Publisher: Elsevier.
- [78] D Cereda, M Tirani, F Rovida, V Demicheli, M Ajelli, Poletti P, Trentini F, Guzzetta G, Marziano V, Barone A, Magoni M, Deandrea S, Diurno G, Lombardo M, Faccini M, Pan A, Bruno R, Pariani E, Grasselli G, Piatti A, Gramegna M, Baldanti F, Melegaro A, and Merler S. The early phase of the COVID-19 outbreak in Lombardy, Italy, March 2020. arXiv: 2003.09320.
- [79] Ruiyun Li, Sen Pei, Bin Chen, Yimeng Song, Tao Zhang, Wan Yang, and Jeffrey Shaman. Substantial undocumented infection facilitates the rapid dissemination of novel coronavirus (SARS-CoV2). *Science*, 368(6490):489–493, March 2020. Publisher: American Association for the Advancement of Science Section: Research Article.
- [80] Nicholas G. Davies, Petra Klepac, Yang Liu, Kiesha Prem, Mark Jit, and Rosalind M. Eggo. Age-dependent effects in the transmission and control of COVID-19 epidemics. *Nature Medicine*, 26(8):1205–1211, June 2020. Publisher: Nature Publishing Group.
- [81] Anne-Laure Frémont. Emmanuel Macron annonce la fermeture des écoles, March 2020. Library Catalog: www.lefigaro.fr Section: Politique.
- [82] Ministère de l'Éducation Nationale de la Jeunesse et des Sports. Déconfinement phase 2 : point de situation au 28 mai. Library Catalog: www.education.gouv.fr.
- [83] Santé publique France. Covid-19 : une enquête pour suivre l'évolution des comportements et de la santé mentale pendant l'épidémie, 2021. Library Catalog: www.santepubliquefrance.fr.
- [84] Kim Van Kerckhove, Niel Hens, W. John Edmunds, and Ken T. D. Eames. The impact of illness on social networks: implications for transmission and control of influenza. *American Journal of Epidemiology*, 178(11):1655–1662, December 2013.
- [85] Adam J. Kucharski, Petra Klepac, Andrew J. K. Conlan, Stephen M. Kissler, Maria L. Tang, Hannah Fry, Julia R. Gog, W. John Edmunds, Jon C. Emery, Graham Medley, James D. Munday, Timothy W. Russell, Quentin J. Leclerc, Charlie Diamond, Simon R. Procter, Amy Gimma, Fiona Yueqian Sun, Hamish P. Gibbs, Alicia Rosello, Kevin van Zandvoort, Stéphane Hué, Sophie R. Meakin, Arminde K. Deol, Gwen Knight, Thibaut Jombart, Anna M. Foss, Nikos I. Bosse, Katherine E. Atkins, Billy J. Quilty, Rachel Lowe, Kiesha Prem, Stefan Flasche, Carl A. B. Pearson, Rein M. G. J. Houben, Emily S. Nightingale, Akira Endo, Damien C. Tully, Yang Liu, Julian Villabona-Arenas, Kathleen O'Reilly, Sebastian Funk, Rosalind M. Eggo, Mark Jit, Eleanor M. Rees, Joel Hellewell, Samuel Clifford, Christopher I. Jarvis, Sam Abbott, Megan Auzenbergs, Nicholas G. Davies, and David Simons. Effectiveness of isolation, testing, contact tracing, and physical distancing on reducing transmission of SARS-CoV-2 in different settings: a mathematical modelling study. *The Lancet Infectious Diseases*, 20(10):1151–1160, October 2020. Publisher: Elsevier.

- [86] Peter Bager, Jan Wohlfahrt, Jannik Fonager, Mads Albertsen, Thomas Yssing Michaelsen, Camilla Holten Møller, Steen Ethelberg, Rebecca Legarth, Mia Sara Fischer Button, Sophie Madeleine Gubbels, Marianne Voldstedlund, Kåre Mølbak, Robert Leo Skov, Anders Fomsgaard, and Tyra Grove Krause. Increased Risk of Hospitalisation Associated with Infection with SARS-CoV-2 Lineage B.1.1.7 in Denmark, March 2021.
- [87] Erik Volz, Swapnil Mishra, Meera Chand, Jeffrey C. Barrett, Robert Johnson, Lily Geidelberg, Wes R. Hinsley, Daniel J. Laydon, Gavin Dabrera, Áine O'Toole, Roberto Amato, Manon Ragonnet-Cronin, Ian Harrison, Ben Jackson, Cristina V. Ariani, Olivia Boyd, Nicholas J. Loman, John T. McCrone, Sónia Gonçalves, David Jorgensen, Richard Myers, Verity Hill, David K. Jackson, Katy Gaythorpe, Natalie Groves, John Sillitoe, Dominic P. Kwiatkowski, Seth Flaxman, Oliver Ratmann, Samir Bhatt, Susan Hopkins, Axel Gandy, Andrew Rambaut, and Neil M. Ferguson. Assessing transmissibility of SARS-CoV-2 lineage B.1.1.7 in England. *Nature*, pages 1–17, March 2021. Publisher: Nature Publishing Group.
- [88] Tjede Funk, Anastasia Pharris, Gianfranco Spiteri, Nick Bundle, Angeliki Melidou, Michael Carr, Gabriel Gonzalez, Alejandro Garcia-Leon, Fiona Crispie, Lois O'Connor, Niamh Murphy, Joël Mossong, Anne Vergison, Anke K. Wienecke-Baldacchino, Tamir Abdelrahman, Flavia Riccardo, Paola Stefanelli, Angela Di Martino, Antonino Bella, Alessandra Lo Presti, Pedro Casaca, Joana Moreno, Vítor Borges, Joana Isidro, Rita Ferreira, João Paulo Gomes, Liidia Dotsenko, Heleene Suija, Jevgenia Epstein, Olga Sadikova, Hanna Sepp, Niina Ikonen, Carita Savolainen-Kopra, Soile Blomqvist, Teemu Möttönen, Otto Helve, Joana Gomes-Dias, Cornelia Adlhoch, and on behalf of COVID study Groups. Characteristics of SARS-CoV-2 variants of concern B.1.1.7, B.1.351 or P.1: data from seven EU/EEA countries, weeks 38/2020 to 10/2021. *Eurosurveillance*, 26(16):2100348, April 2021. Publisher: European Centre for Disease Prevention and Control.
- [89] O. Diekmann, J. a. P. Heesterbeek, and J. a. J. Metz. On the definition and the computation of the basic reproduction ratio R_0 in models for infectious diseases in heterogeneous populations, 1990. Accepted: 2006-03-14T16:48:21Z ISSN: 0303-6812 Issue: 4 Library Catalog: dspace.library.uu.nl Pages: 365-382 Publisher: Springer Verlag Volume: 28.
- [90] Vittoria Colizza, Alain Barrat, Marc Barthélemy, and Alessandro Vespignani. The role of the airline transportation network in the prediction and predictability of global epidemics. *Proceedings of the National Academy of Sciences*, 103(7):2015–2020, February 2006. Publisher: Proceedings of the National Academy of Sciences.
- [91] C. Poletto, C. Pelat, D. Lévy-Bruhl, Y. Yazdanpanah, P. Y. Boëlle, and V. Colizza. Assessment of the Middle East respiratory syndrome coronavirus (MERS-CoV) epidemic in the Middle East and risk of international spread using a novel maximum likelihood analysis approach. *Eurosurveillance*, 19(23):20824, June 2014. Publisher: European Centre for Disease Prevention and Control.
- [92] Moritz U. G. Kraemer, Chia-Hung Yang, Bernardo Gutierrez, Chieh-Hsi Wu, Brennan Klein, David M. Pigott, Open COVID-19 Data Working Group, Louis du Plessis, Nuno R. Faria, Ruoran Li, William P. Hanage, John S. Brownstein, Maylis Layan, Alessandro Vespignani, Huaiyu Tian, Christopher Dye, Oliver G. Pybus, and Samuel V. Scarpino. The effect of human mobility and control measures on the COVID-19 epidemic in China. *Science*, 368(6490):493–497, May 2020. Publisher: American Association for the Advancement of Science.
- [93] Lisa Sattenspiel and Klaus Dietz. A structured epidemic model incorporating geographic mobility among regions. *Mathematical Biosciences*, 128(1):71–91, July 1995.
- [94] Matt J. Keeling and Pejman Rohani. Estimating spatial coupling in epidemiological systems: a mechanistic approach. *Ecology Letters*, 5(1):20–29, 2002. [_eprint: https://onlinelibrary.wiley.com/doi/pdf/10.1046/j.1461-0248.2002.00268.x](https://onlinelibrary.wiley.com/doi/pdf/10.1046/j.1461-0248.2002.00268.x).

- [95] B. Bolker and B. Grenfell. Space, persistence and dynamics of measles epidemics. *Philosophical Transactions of the Royal Society of London. Series B, Biological Sciences*, 348(1325):309–320, May 1995.
- [96] DJ Earn, P Rohani, and BT Grenfell. Persistence, chaos and synchrony in ecology and epidemiology. *Proceedings of the Royal Society B: Biological Sciences*, 265(1390):7–10, January 1998.
- [97] B. T. Grenfell, O. N. Bjørnstad, and J. Kappey. Travelling waves and spatial hierarchies in measles epidemics. *Nature*, 414(6865):716–723, December 2001.
- [98] I. M. HALL, R. GANI, H. E. HUGHES, and S. LEACH. Real-time epidemic forecasting for pandemic influenza. *Epidemiology and Infection*, 135(3):372–385, April 2007.
- [99] Giulia Pullano. *Human mobility and epidemics*. phdthesis, Sorbonne Université, September 2021.
- [100] Sen Pei, Sasikiran Kandula, and Jeffrey Shaman. Differential effects of intervention timing on COVID-19 spread in the United States. *Science Advances*, 6(49):eabd6370, 2020.
- [101] Fabio Della Rossa, Davide Salzano, Anna Di Meglio, Francesco De Lellis, Marco Coraggio, Carmela Calabrese, Agostino Guarino, Ricardo Cardona-Rivera, Pietro De Lellis, Davide Liuzza, Francesco Lo Iudice, Giovanni Russo, and Mario di Bernardo. A network model of Italy shows that intermittent regional strategies can alleviate the COVID-19 epidemic. *Nature Communications*, 11(1):5106, October 2020. Number: 1 Publisher: Nature Publishing Group.
- [102] Vadim A. Karatayev, Madhur Anand, and Chris T. Bauch. Local lockdowns outperform global lockdown on the far side of the COVID-19 epidemic curve. *Proceedings of the National Academy of Sciences*, 117(39):24575–24580, September 2020. Publisher: Proceedings of the National Academy of Sciences.
- [103] Lorenzo Pellis, Francesca Scarabel, Helena B. Stage, Christopher E. Overton, Lauren H. K. Chappell, Elizabeth Fearon, Emma Bennett, Katrina A. Lythgoe, Thomas A. House, Ian Hall, and null null. Challenges in control of COVID-19: short doubling time and long delay to effect of interventions. *Philosophical Transactions of the Royal Society B: Biological Sciences*, 376(1829):20200264, July 2021. Publisher: Royal Society.
- [104] Nathanael Lapidus, Juliette Paireau, Daniel Levy-Bruhl, Xavier de Lamballerie, Gianluca Severi, Mathilde Touvier, Marie Zins, Simon Cauchemez, Fabrice Carrat, and SAPRIS-SERO study group. Do not neglect SARS-CoV-2 hospitalization and fatality risks in the middle-aged adult population. *Infectious Diseases Now*, 51(4):380–382, June 2021.
- [105] S Bhatia, J Wardle, R Nash, P Nouvellet, and A Cori. A generic method and software to estimate the transmission advantage of pathogen variants in real-time : SARS-CoV-2 as a case-study. Technical report, Imperial College London, November 2021.
- [106] David W. Eyre, Donald Taylor, Mark Purver, David Chapman, Tom Fowler, Koen B. Pouwels, A. Sarah Walker, and Tim E.A. Peto. Effect of Covid-19 Vaccination on Transmission of Alpha and Delta Variants. *New England Journal of Medicine*, 386(8):744–756, February 2022. Publisher: Massachusetts Medical Society _eprint: <https://doi.org/10.1056/NEJMoa2116597>.
- [107] Annabelle Collin, Boris P. Hejblum, Carole Vignals, Laurent Lehot, Rodolphe Thiébaud, Philippe Moireau, and MéLanie Prague. Using Population Based Kalman Estimator to Model COVID-19 Epidemic in France: Estimating the Effects of Non-Pharmaceutical Interventions on the Dynamics of Epidemic. preprint, *Epidemiology*, July 2021.
- [108] The Economist. The global normalcy index.

- [109] Sharon K. Inouye, Sidney T. Bogardus, Jr, Christianna S. Williams, Linda Leo-Summers, and Joseph V. Agostini. The Role of Adherence on the Effectiveness of Nonpharmacologic Interventions: Evidence From the Delirium Prevention Trial. *Archives of Internal Medicine*, 163(8):958–964, April 2003.
- [110] L. E. Smith, R. Amlt, H. Lambert, I. Oliver, C. Robin, L. Yardley, and G. J. Rubin. Factors associated with adherence to self-isolation and lockdown measures in the UK: a cross-sectional survey. *Public Health*, 187:41–52, October 2020.
- [111] Jonathan A. Polonsky, Sangeeta Bhatia, Keith Fraser, Arran Hamlet, Janetta Skarp, Isaac J. Stopard, Stéphane Hugonnet, Laurent Kaiser, Christian Lengeler, Karl Blanchet, and Paul Spiegel. Feasibility, acceptability, and effectiveness of non-pharmaceutical interventions against infectious diseases among crisis-affected populations: a scoping review. *Infectious Diseases of Poverty*, 11(1):14, January 2022.
- [112] Marlena Klavic, Suzanne Kapp, Peter Hudson, Wendy Chapman, Linda Denehy, David Story, and Jill J. Francis. Implementability of healthcare interventions: an overview of reviews and development of a conceptual framework. *Implementation Science : IS*, 17:10, January 2022.
- [113] Enhancing public trust in COVID-19 vaccination: The role of governments.
- [114] Juan Yang, Valentina Marziano, Xiaowei Deng, Giorgio Guzzetta, Juanjuan Zhang, Filippo Trentini, Jun Cai, Piero Poletti, Wen Zheng, Wei Wang, Qianhui Wu, Zeyao Zhao, Kaige Dong, Guangjie Zhong, Cécile Viboud, Stefano Merler, Marco Ajelli, and Hongjie Yu. Despite vaccination, China needs non-pharmaceutical interventions to prevent widespread outbreaks of COVID-19 in 2021. *Nature Human Behaviour*, 5(8):1009–1020, August 2021. Number: 8 Publisher: Nature Publishing Group.
- [115] Sharon Guerstein, Victoria Romeo-Aznar, Ma’ayan Dekel, Oren Miron, Nadav Davidovitch, Rami Puzis, and Shai Pilosof. The interplay between vaccination and social distancing strategies affects COVID19 population-level outcomes. *PLoS Computational Biology*, 17(8):e1009319, August 2021.
- [116] WHO Director-General’s opening remarks at the media briefing on COVID-19 - 4 November 2021.
- [117] Soeren Metelmann, Karan Pattni, Liam Brierley, Lisa Cavalerie, Cyril Caminade, Marcus S. C. Blagrove, Joanne Turner, Kieran J. Sharkey, and Matthew Baylis. Impact of climatic, demographic and disease control factors on the transmission dynamics of COVID-19 in large cities worldwide. *One Health (Amsterdam, Netherlands)*, 12:100221, June 2021.
- [118] Jingyuan Wang, Ke Tang, Kai Feng, Xin Lin, Weifeng Lv, Kun Chen, and Fei Wang. Impact of temperature and relative humidity on the transmission of COVID-19: a modelling study in China and the United States. *BMJ Open*, 11(2):e043863, February 2021. Publisher: British Medical Journal Publishing Group Section: Public health.
- [119] Anna Petherick, Rafael Goldszmidt, Eduardo B. Andrade, Rodrigo Furst, Thomas Hale, Annalena Pott, and Andrew Wood. A worldwide assessment of changes in adherence to COVID-19 protective behaviours and hypothesized pandemic fatigue. *Nature Human Behaviour*, 5(9):1145–1160, September 2021. Number: 9 Publisher: Nature Publishing Group.
- [120] Andrea Gurmankin Levy, Alistair Thorpe, Laura D. Scherer, Aaron M. Scherer, Frank A. Drews, Jorie M. Butler, Nicole Burpo, Holly Shoemaker, Vanessa Stevens, and Angela Fagerlin. Misrepresentation and Nonadherence Regarding COVID-19 Public Health Measures. *JAMA Network Open*, 5(10):e2235837, October 2022.
- [121] Policy Responses to COVID19.

- [122] Mattia Manica, Giorgio Guzzetta, Flavia Riccardo, Antonio Valenti, Piero Poletti, Valentina Marziano, Filippo Trentini, Xanthi Andrianou, Alberto Mateo-Urdiales, Martina del Manso, Massimo Fabiani, Maria Fenicia Vescio, Matteo Spuri, Daniele Petrone, Antonino Bella, Sergio Iavicoli, Marco Ajelli, Silvio Brusaferro, Patrizio Pezzotti, and Stefano Merler. Impact of tiered restrictions on human activities and the epidemiology of the second wave of COVID-19 in Italy. *Nature Communications*, 12(1):4570, July 2021. Number: 1 Publisher: Nature Publishing Group.
- [123] Mrinank Sharma, Sören Mindermann, Charlie Rogers-Smith, Gavin Leech, Benedict Snodin, Janvi Ahuja, Jonas B. Sandbrink, Joshua Teperowski Monrad, George Altman, Gurpreet Dhaliwal, Lukas Finnveden, Alexander John Norman, Sebastian B. Oehm, Julia Fabienne Sandkühler, Laurence Aitchison, Tomáš Gavenčíak, Thomas Mellan, Jan Kulveit, Leonid Chindelevitch, Seth Flaxman, Yarin Gal, Swapnil Mishra, Samir Bhatt, and Jan Markus Brauner. Understanding the effectiveness of government interventions against the resurgence of COVID-19 in Europe. *Nature Communications*, 12:5820, October 2021.
- [124] Impact of non-pharmaceutical interventions, weather, vaccination, and variants on COVID-19 transmission across departments in France | BMC Infectious Diseases | Full Text.
- [125] Andrew J. Shattock, Epke A. Le Rutte, Robert P. Dünner, Swapnoleena Sen, Sherrie L. Kelly, Nakul Chitnis, and Melissa A. Penny. Impact of vaccination and non-pharmaceutical interventions on SARS-CoV-2 dynamics in Switzerland. *Epidemics*, 38:100535, March 2022.
- [126] Badrah S. Alghamdi, Yasser Alatawi, Fahad S. Alshehri, Haythum O. Tayeb, Hanin AboTaleb, and Amal Binsalman. Psychological Distress During COVID-19 Curfews and Social Distancing in Saudi Arabia: A Cross-Sectional Study. *Frontiers in Public Health*, 9:792533, January 2022.
- [127] Guillaume Spaccaferri, Sophie Larrieu, Jérôme Pouey, Clémentine Calba, Thomas Benet, Cécile Sommen, Daniel Lévy-Bruhl, Sabira Smaili, Didier Che, Laurent Filleul, Céline Caserio-Schönemann, Fatima Ait-El-Belghiti, Sylvie Haeghebaert, Jean-Claude Desenclos, Laëtitia Huiart, Anne Laporte, and Patrick Rolland. Early assessment of the impact of mitigation measures to control COVID-19 in 22 French metropolitan areas, October to November 2020. *Eurosurveillance*, 25(50):2001974, December 2020. Publisher: European Centre for Disease Prevention and Control.
- [128] Alessio Andronico, Cécile Tran Kiem, Juliette Paireau, Tiphonie Succo, Paolo Bosetti, Noémie Lefrancq, Mathieu Nacher, Félix Djossou, Alice Sanna, Claude Flamand, Henrik Salje, Cyril Rousseau, and Simon Cauchemez. Evaluating the impact of curfews and other measures on SARS-CoV-2 transmission in French Guiana. *Nature Communications*, 12(1):1634, March 2021. Number: 1 Publisher: Nature Publishing Group.
- [129] David García-García, Rafael Herranz-Hernández, Ayelén Rojas-Benedicto, Inmaculada León-Gómez, Amparo Larrauri, Marina Peñuelas, María Guerrero-Vadillo, Rebeca Ramis, and Diana Gómez-Barroso. Assessing the effect of non-pharmaceutical interventions on COVID-19 transmission in Spain, 30 August 2020 to 31 January 2021. *Eurosurveillance*, 27(19):2100869, May 2022. Publisher: European Centre for Disease Prevention and Control.
- [130] James Thompson and Stephen Wattam. Estimating the impact of interventions against COVID-19: From lockdown to vaccination. *PLOS ONE*, 16(12):e0261330, December 2021. Publisher: Public Library of Science.
- [131] Jonathan Stokes, Alex James Turner, Laura Anselmi, Marcello Morciano, and Thomas Hone. The relative effects of non-pharmaceutical interventions on wave one Covid-19 mortality: natural experiment in 130 countries. *BMC Public Health*, 22(1):1113, June 2022.
- [132] Francisco Pozo-Martin, Heide Weishaar, Florin Cristea, Johanna Hanefeld, Thurid Bahr, Lars Schaade, and Charbel El Bcheraoui. The impact of non-pharmaceutical interventions on COVID-19

epidemic growth in the 37 OECD member states. *European Journal of Epidemiology*, 36(6):629–640, 2021.

- [133] Yang Liu, Christian Morgenstern, James Kelly, Rachel Lowe, James Munday, C. Julian Villabona-Arenas, Hamish Gibbs, Carl A. B. Pearson, Kiesha Prem, Quentin J. Leclerc, Sophie R. Meakin, W. John Edmunds, Christopher I. Jarvis, Amy Gimma, Sebastian Funk, Matthew Quaife, Timothy W. Russell, Jon C. Emory, Sam Abbott, Joel Hellewell, Damien C. Tully, Rein M. G. J. Houben, Kathleen O'Reilly, Georgia R. Gore-Langton, Adam J. Kucharski, Megan Auzenbergs, Billy J. Quilty, Thibaut Jombart, Alicia Rosello, Oliver Brady, Katherine E. Atkins, Kevin van Zandvoort, James W. Rudge, Akira Endo, Kaja Abbas, Fiona Yueqian Sun, Simon R. Procter, Samuel Clifford, Anna M. Foss, Nicholas G. Davies, Yung-Wai Desmond Chan, Charlie Diamond, Rosanna C. Barnard, Rosalind M. Eggo, Arminder K. Deol, Emily S. Nightingale, David Simons, Katharine Sherratt, Graham Medley, Stéphane Hué, Gwenan M. Knight, Stefan Flasche, Nikos I. Bosse, Petra Klepac, Mark Jit, and CMMID COVID-19 Working Group. The impact of non-pharmaceutical interventions on SARS-CoV-2 transmission across 130 countries and territories. *BMC Medicine*, 19(1):40, February 2021.
- [134] Paul R Hunter, Felipe J Colón-González, Julii Brainard, and Steven Rushton. Impact of non-pharmaceutical interventions against COVID-19 in Europe in 2020: a quasi-experimental non-equivalent group and time series design study. *Eurosurveillance*, 26(28):2001401, July 2021.
- [135] Seth Flaxman, Swapnil Mishra, Axel Gandy, H. Juliette T. Unwin, Thomas A. Mellan, Helen Coupland, Charles Whittaker, Harrison Zhu, Tresnia Berah, Jeffrey W. Eaton, Mélodie Monod, Azra C. Ghani, Christl A. Donnelly, Steven Riley, Michaela A. C. Vollmer, Neil M. Ferguson, Lucy C. Okell, and Samir Bhatt. Estimating the effects of non-pharmaceutical interventions on COVID-19 in Europe. *Nature*, 584(7820):257–261, August 2020. Number: 7820 Publisher: Nature Publishing Group.
- [136] Nicholas G. Davies, Adam J. Kucharski, Rosalind M. Eggo, Amy Gimma, W. John Edmunds, Thibaut Jombart, Kathleen O'Reilly, Akira Endo, Joel Hellewell, Emily S. Nightingale, Billy J. Quilty, Christopher I. Jarvis, Timothy W. Russell, Petra Klepac, Nikos I. Bosse, Sebastian Funk, Sam Abbott, Graham F. Medley, Hamish Gibbs, Carl A. B. Pearson, Stefan Flasche, Mark Jit, Samuel Clifford, Kiesha Prem, Charlie Diamond, Jon Emery, Arminder K. Deol, Simon R. Procter, Kevin van Zandvoort, Yueqian Fiona Sun, James D. Munday, Alicia Rosello, Megan Auzenbergs, Gwen Knight, Rein M. G. J. Houben, and Yang Liu. Effects of non-pharmaceutical interventions on COVID-19 cases, deaths, and demand for hospital services in the UK: a modelling study. *The Lancet Public Health*, 5(7):e375–e385, July 2020. Publisher: Elsevier.
- [137] Nikolaos Askitas, Konstantinos Tatsiramos, and Bertrand Verheyden. Estimating worldwide effects of non-pharmaceutical interventions on COVID-19 incidence and population mobility patterns using a multiple-event study. *Scientific Reports*, 11(1):1972, January 2021. Number: 1 Publisher: Nature Publishing Group.
- [138] Quantifying the spatial spillover effects of non-pharmaceutical interventions on pandemic risk | International Journal of Health Geographics | Full Text.
- [139] Is Curfew Effective in Limiting SARS-CoV-2 Progression? An Evaluation in France Based on Epidemiokinetic Analyses | SpringerLink.
- [140] Association of tiered restrictions and a second lockdown with COVID-19 deaths and hospital admissions in England: a modelling study - The Lancet Infectious Diseases.
- [141] Estimating the impact of interventions against COVID-19: From lockdown to vaccination | PLOS ONE.

- [142] David García-García, Rafael Herranz-Hernández, Ayelén Rojas-Benedicto, Inmaculada León-Gómez, Amparo Larrauri, Marina Peñuelas, María Guerrero-Vadillo, Rebeca Ramis, and Diana Gómez-Barroso. Assessing the effect of non-pharmaceutical interventions on COVID-19 transmission in Spain, 30 August 2020 to 31 January 2021. *Eurosurveillance*, 27(19):2100869, May 2022. Publisher: European Centre for Disease Prevention and Control.
- [143] Haoxiang Yang, Özge Sürer, Daniel Duque, David P. Morton, Bismark Singh, Spencer J. Fox, Remy Pasco, Kelly Pierce, Paul Rathouz, Victoria Valencia, Zhanwei Du, Michael Pignone, Mark E. Escott, Stephen I. Adler, S. Claiborne Johnston, and Lauren Ancel Meyers. Design of COVID-19 staged alert systems to ensure healthcare capacity with minimal closures. *Nature Communications*, 12(1):3767, June 2021. Number: 1 Publisher: Nature Publishing Group.
- [144] Zeynep Or, Coralie Gandré, Isabelle Durand Zaleski, and Monika Steffen. France's response to the Covid-19 pandemic: between a rock and a hard place. *Health Economics, Policy, and Law*, pages 1–13.
- [145] discours O.VERAN -Point presse lutte contre COVID-19 _ 23 septembre 2020.pdf.
- [146] OECD. REDUCING THE RISK OF POLICY FAILURE: CHALLENGES FOR REGULATORY COMPLIANCE.
- [147] Tackling the mental health impact of the COVID-19 crisis: An integrated, whole-of-society response.
- [148] Glenn Marion, Liza Hadley, Valerie Isham, Denis Mollison, Jasmina Panovska-Griffiths, Lorenzo Pellis, Gianpaolo Scalia Tomba, Francesca Scarabel, Ben Swallow, Pieter Trapman, and Daniel Villela. Modelling: Understanding pandemics and how to control them. *Epidemics*, 39:100588, June 2022.
- [149] Pascal Crépey, Harold Noël, and Samuel Alizon. Challenges for mathematical epidemiological modelling. *Anaesthesia, Critical Care & Pain Medicine*, 41(2):101053, April 2022.
- [150] Screening and vaccination against COVID-19 to minimise school closure: a modelling study - The Lancet Infectious Diseases.
- [151] Agent-based modelling of reactive vaccination of workplaces and schools against COVID-19 - Google Search.
- [152] data.gov.uk. Vaccinations in England | Coronavirus in the UK.
- [153] J. M. Heffernan and M. J. Keeling. Implications of vaccination and waning immunity. *Proceedings. Biological Sciences*, 276(1664):2071–2080, June 2009.
- [154] Toon Braeye, Lucy Catteau, Ruben Brondeel, Joris A.F. van Loenhout, Kristiaan Proesmans, Laura Cornelissen, Herman Van Oyen, Veerle Stouten, Pierre Hubin, Matthieu Billuart, Achille Djiena, Romain Mahieu, Naima Hammami, Dieter Van Cauteren, and Chloé Wyndham-Thomas. Vaccine effectiveness against transmission of alpha, delta and omicron SARS-COV-2-infection, Belgian contact tracing, 2021–2022. *Vaccine*, 41(20):3292–3300, May 2023.
- [155] David Holtz, Michael Zhao, Seth G. Benzell, Cathy Y. Cao, Mohammad Amin Rahimian, Jeremy Yang, Jennifer Allen, Avinash Collis, Alex Moehring, Tara Sowrirajan, Dipayan Ghosh, Yunhao Zhang, Paramveer S. Dhillon, Christos Nicolaidis, Dean Eckles, and Sinan Aral. Interdependence and the cost of uncoordinated responses to COVID-19. *Proceedings of the National Academy of Sciences*, 117(33):19837–19843, August 2020. Publisher: Proceedings of the National Academy of Sciences.
- [156] Xiaoyi Han, Yilan Xu, Linlin Fan, Yi Huang, Minhong Xu, and Song Gao. Quantifying COVID-19 importation risk in a dynamic network of domestic cities and international countries. *Proceedings of the National Academy of Sciences*, 118(31):e2100201118, August 2021. Publisher: Proceedings of the National Academy of Sciences.

- [157] Paolo Bajardi, Chiara Poletto, Jose J. Ramasco, Michele Tizzoni, Vittoria Colizza, and Alessandro Vespignani. Human Mobility Networks, Travel Restrictions, and the Global Spread of 2009 H1N1 Pandemic. *PLOS ONE*, 6(1):e16591, January 2011. Publisher: Public Library of Science.
- [158] Barry Smyth. The fading impact of lockdowns: A data analysis of the effectiveness of Covid-19 travel restrictions during different pandemic phases. *PLOS ONE*, 17(6):e0269774, June 2022. Publisher: Public Library of Science.
- [159] Zhanwei Du, Lin Wang, Songwei Shan, Dickson Lam, Tim K. Tsang, Jingyi Xiao, Huizhi Gao, Bingyi Yang, Sheikh Taslim Ali, Sen Pei, Isaac Chun-Hai Fung, Eric H. Y. Lau, Qiuyan Liao, Peng Wu, Lauren Ancel Meyers, Gabriel M. Leung, and Benjamin J. Cowling. Pandemic fatigue impedes mitigation of COVID-19 in Hong Kong. *Proceedings of the National Academy of Sciences of the United States of America*, 119(48):e2213313119, November 2022.
- [160] Sijie Yang, Fei Zhu, Xinghong Ling, Quan Liu, and Peiyao Zhao. Intelligent Health Care: Applications of Deep Learning in Computational Medicine. *Frontiers in Genetics*, 12, 2021.
- [161] Riccardo Miotto, Fei Wang, Shuang Wang, Xiaoqian Jiang, and Joel T Dudley. Deep learning for healthcare: review, opportunities and challenges. *Briefings in Bioinformatics*, 19(6):1236–1246, May 2017.
- [162] George A. Truskey. The Potential of Deep Learning to Advance Clinical Applications of Computational Biomechanics. *Bioengineering*, 10(9):1066, September 2023.
- [163] Pratik Shah, Francis Kendall, Sean Khozin, Ryan Goosen, Jianying Hu, Jason Laramie, Michael Ringel, and Nicholas Schork. Artificial intelligence and machine learning in clinical development: a translational perspective. *npj Digital Medicine*, 2(1):1–5, July 2019. Number: 1 Publisher: Nature Publishing Group.
- [164] Stylianos Serghiou and Kathryn Rough. Deep Learning for Epidemiologists: An Introduction to Neural Networks. *American Journal of Epidemiology*, page kwad107, May 2023.

ACKNOWLEDGEMENTS

I would like to conclude this thesis trying to express my gratitude to the people that have accompanied me in the last years. A first thanks goes to Vittoria, my supervisor, for having shaped my research work in a significant way. I owe my professional growth to the passion and dedication she passed on to me daily. She managed to make me become a bit more meticulous (just a bit) when I've always been accused of being sloppy.

I would like to thank all the members of the jury, especially the reviewers, for investing their time and contributing to the defense of my doctoral thesis. I want also to thank Pierre-Yves for the valuable advice he gave me during all my work.

I am deeply grateful to all my colleagues. GP, LDD - for the endless pandemic days spent correcting each other's mistakes and supporting each other. All the time with a sincere smile on our faces. You have been equally and in a complementary way my mentors. EC - for going through this journey together, in parallel. AR the best near-far desk neighbor. MM, DM, FP - the canteen team- always up for small talks, AH and LC last arrived but that quickly have found a place in our traditions and rituals. Thank you for all the coffees and ice creams you've offered me; I believe I have significant debts to all of you. Thanks also to everyone from 802.

From Tuscany I think I have to thank a bunch of people, but particularly those who emigrated to Turkey and Spain: GB, SR you are one of the most intense things that ever happened to me, thank you for having grown up by my side.

There is a chance that if you are an Italian living abroad, you'll be surrounded by plenty of other Italian people. This has definitely been the case for me here in Paris. My warmest appreciation goes to the clique of people who have been a part of my daily life these years, without you my summers would not have been filled with love.

Thank ME, wild and carefree spirit - having the opportunity to steal your socks in the morning always gave me great satisfaction. FC and GA - you are a persistent and consistent presence in my life, thank you for bearing with me during these years ...! I want to thank MB, unstoppable narcoleptic hurricane, this is the second time you ended up in my acknowledgments, I hope I can keep thanking you all the time. RD, cherished friend, sister and soul, perché le giornate passate con te sono un toccasana per lo spirito. FPP, beloved sun-filled creature, every now and then we share colorful and bright emotions, and emotions are all that matter.

Voglio ringraziare tanto la mia famiglia, per aver reso possibile questo lavoro, come conseguenza di piu' cinque lustri di formazione, sostegno e amore incondizionato. Ringrazio il mio babbo, per l'inamovibile coerenza tra la sua vita e il suo lavoro; la mia mamma per il suo senso del dovere e la sua curiosità; G, perché quando ho bisogno c'è e spero ci sarà sempre.

And thanks to myself, for keeping it up.

